Springer Theses
Recognizing Outstanding Ph.D. Research

María Jesús Lerma García

Characterization and Authentication of Olive and Other Vegetable Oils

New Analytical Methods

Springer

Springer Theses

Recognizing Outstanding Ph.D. Research

For further volumes:
http://www.springer.com/series/8790

Aims and Scope

The series "Springer Theses" brings together a selection of the very best Ph.D. theses from around the world and across the physical sciences. Nominated and endorsed by two recognized specialists, each published volume has been selected for its scientific excellence and the high impact of its contents for the pertinent field of research. For greater accessibility to non-specialists, the published versions include an extended introduction, as well as a foreword by the student's supervisor explaining the special relevance of the work for the field. As a whole, the series will provide a valuable resource both for newcomers to the research fields described, and for other scientists seeking detailed background information on special questions. Finally, it provides an accredited documentation of the valuable contributions made by today's younger generation of scientists.

Theses are accepted into the series by invited nomination only and must fulfill all of the following criteria

- They must be written in good English.
- The topic should fall within the confines of Chemistry, Physics, Earth Sciences, Engineering and related interdisciplinary fields such as Materials, Nanoscience, Chemical Engineering, Complex Systems and Biophysics.
- The work reported in the thesis must represent a significant scientific advance.
- If the thesis includes previously published material, permission to reproduce this must be gained from the respective copyright holder.
- They must have been examined and passed during the 12 months prior to nomination.
- Each thesis should include a foreword by the supervisor outlining the significance of its content.
- The theses should have a clearly defined structure including an introduction accessible to scientists not expert in that particular field.

María Jesús Lerma García

Characterization and Authentication of Olive and Other Vegetable Oils

New Analytical Methods

Doctoral Thesis accepted by
the Universitat de València, Spain

Springer

Author
Dr. María Jesús Lerma García
Department of Analytical Chemistry
Faculty of Chemistry
Universitat de València
Spain

Supervisors
Prof. Dr. Guillermo Ramis Ramos
Department of Analytical Chemistry
Faculty of Chemistry
Universitat de València
Spain

Prof. Dr. Ernesto Fco. Simó Alfonso
Department of Analytical Chemistry
Faculty of Chemistry
Universitat de València
Spain

ISSN 2190-5053 ISSN 2190-5061 (electronic)
ISBN 978-3-642-31417-9 ISBN 978-3-642-31418-6 (eBook)
DOI 10.1007/978-3-642-31418-6
Springer Heidelberg New York Dordrecht London

Library of Congress Control Number: 2012941415

Printed on acid-free paper

Springer is part of Springer Science+Business Media (www.springer.com)

Parts of this thesis have been published in the following journal articles (permission to reproduce or to adapt these articles in this thesis has been obtained by courtesy of American Chemical Society, Elsevier Ltd., Springer–Verlag, and Wiley-VCH Verlag)

1. M. J. Lerma-García; E. F. Simó-Alfonso, G. Ramis-Ramos, J. M. Herrero-Martínez, "*Determination of tocopherols in vegetable oils by CEC using methacrylate ester-based monolithic columns*" Electrophoresis 28 (2007) 4128–4135.

2. M. J. Lerma-García, G. Ramis-Ramos, J. M. Herrero-Martínez, E. F. Simó-Alfonso, "*Classification of vegetable oils according to their botanical origin using amino acid profiles established by direct infusion mass spectrometry*" Rapid Commun. Mass Spectrom. 21 (2007) 3751–3755.

3. M. J. Lerma-García, J. M. Herrero-Martínez, G. Ramis-Ramos, E. F. Simó-Alfonso, "Evaluation of the quality of olive oil using fatty acid profiles by direct infusion electrospray ionization mass spectrometry" Food Chem. 107 (2008) 1307–1313.

4. M. J. Lerma-García, J. M. Herrero-Martínez, G. Ramis-Ramos, E. F. Simó-Alfonso, "*Prediction of the genetic variety of Spanish extra virgin olive oils using fatty acid and phenolic compound profiles established by direct infusion mass spectrometry*" Food Chem. 108 (2008) 1142–1148.

5. M. J. Lerma-García, G. Ramis-Ramos, J. M. Herrero-Martínez, E. F. Simó-Alfonso, "*Classification of vegetable oils according to their botanical origin using sterol profiles established by direct infusion mass spectrometry*" Rapid Commun. Mass Spectrom. 22 (2008) 973–978.

6. M. J. Lerma-García, E. F. Simó-Alfonso, G. Ramis-Ramos, J. M. Herrero-Martínez, "*Rapid determination of sterols in vegetable oils by CEC using methacrylate ester-based monolithic columns*" Electrophoresis 29 (2008) 4603–4611.

7. M. J. Lerma-García, G. Ramis-Ramos, J. M. Herrero-Martínez, J. V. Gimeno-Adelantado, E. F. Simó-Alfonso, "*Characterization of the alcoholic fraction of vegetable oils by derivatization with diphenic anhydride followed by high-performance liquid chromatography with spectrophotometric and mass spectrometric detection*" J.Chromatogr. A 1216 (2009) 230–236.

8. M. J. Lerma- García, E. F. Simó-Alfonso, A. Bendini, L. Cerretani, "*Metal oxide semiconductor sensors for monitoring of oxidative status evolution*

and sensory analysis of virgin olive oils with different phenolic content" Food Chem. 117 (2009) 608–614.

9. M. J. Lerma-García, E. F. Simó-Alfonso, E. Chiavaro, A. Bendini, G. Lercker, L. Cerretani, "*Study of chemical changes produced in virgin olive oils with different phenolic content during an accelerated storage treatment*" J. Agric. Food Chem. 57 (2009) 7834–7840.

10. M. J. Lerma-García, C. Lantano, E. Chiavaro, L. Cerretani, J. M. Herrero-Martínez, E. F. Simó-Alfonso, "*Classification of extra virgin olive oils according to their geographical origin using phenolic compound profiles obtained by capillary electrochromatography*" Food Res. Int. 42 (2009) 1446–1452.

11. M. J. Lerma-García, J. M. Herrero-Martínez, E. F. Simó-Alfonso, G. Lercker, L. Cerretani, "*Evaluation of the oxidative status of virgin olive oils with different phenolic content by direct infusion atmospheric pressure chemical ionization mass spectrometry*" Anal. Bioanal. Chem. 395 (2009) 1543–1550.

12. V. Concha-Herrera, M. J. Lerma-García, J. M. Herrero-Martínez, E. F. Simó-Alfonso, "*Prediction of the genetic variety of extra virgin olive oils produced at La Comunitat Valenciana, Spain, by Fourier-transform infrared spectroscopy*" J. Agric. Food Chem. 57 (2009) 9985–9989.

13. M. J. Lerma-García, E. F. Simó-Alfonso, A. Bendini, L. Cerretani, "*Rapid evaluation of oxidized fatty acid concentration in virgin olive oils using metal oxide semiconductor sensors and multiple linear regression*" J. Agric. Food Chem. 57 (2009) 9365–9369.

14. M. J. Lerma-García, V. Concha-Herrera, J. M. Herrero-Martínez, E. F. Simó-Alfonso, "*Classification of extra virgin olive oils produced at La Comunitat Valenciana according to their genetic variety using sterol profiles established by high performance liquid chromatography with mass spectrometry detection*" J. Agric. Food Chem. 57 (2009) 10512–10517.

15. M. J. Lerma-García, G. Ramis-Ramos, J. M. Herrero-Martínez, E. F. Simó-Alfonso, "*Authentication of extra virgin olive oils by Fourier-transform infrared spectroscopy*" Food Chem. 118 (2010) 78–83.

16. L. Cerretani, M. J. Lerma-García, J. M. Herrero-Martínez, T. Gallina-Toschi, E. F. Simó-Alfonso, "*Determination of tocopherols and tocotrienols in vegetable oils by nanoliquid chromatography with ultraviolet-visible*

detection using a silica monolithic column" J. Agric. Food Chem. 58 (2010) 757–761.

17. V. Concha-Herrera, M. J. Lerma-García, J. M. Herrero-Martínez, E. F. Simó-Alfonso, "*Classication of vegetable oils according to their botanical origin using amino acid profiles established by high performance liquid chromatography with UV-vis detection: A first approach*" Food Chem. 120 (2010) 1149–1154.

18. M. J. Lerma-García, E. F. Simó-Alfonso; A. Méndez, J. L. Lliberia, J. M. Herrero-Martínez, "*Fast separation and determination of sterols in vegetable oils by ultraperformance liquid chromatography with atmospheric pressure chemical ionization mass spectrometry detection*" J. Agric. Food Chem. 58 (2010) 2771–2776.

19. M. J. Lerma-García, L. Cerretani, C. Cevoli, E. F. Simó-Alfonso, A. Bendini, T. Gallina-Toschi, "*Use of electronic nose to determine defect percentage in oils. Comparison with sensory panel results*" Sensor Actuat. B-Chem. 147 (2010) 283–289.

20. M. J. Lerma-García, L. Cerretani, J. M. Herrero-Martínez, A. Bendini, E. F. Simó-Alfonso. "*Methacrylate ester-based monolithic columns for nano-LC separation of tocopherols in vegetable oils*". J. Sep. Sci. 33 (2010) 2681–2687.

21. M. J. Lerma- García, E. F. Simó-Alfonso, A. Bendini, L. Cerretani. "*Rapid evaluation of oxidized fatty acid concentration in virgin olive oil using Fourier-transform infrared spectroscopy and multiple linear regression*". Food Chem. 124 (2011) 679–684.

22. M. J. Lerma-García, E. F. Simó-Alfonso, A. Méndez, J. L. Lliberia, J. M. Herrero-Martínez. "*Classification of extra virgin olive oils according to their genetic variety using linear discriminant analysis of sterol profiles established by ultra-performance liquid chromatography with mass spectrometry detection*". Food Res. Int. 44 (2011) 103–108.

Supervisors' Foreword

I have the pleasure of presenting María Jesús Lerma-García who developed this PhD thesis under the supervision of Prof. Ernesto F. Simó-Alfonso and me. This was an extensive, long, varied, pleasant, and exciting task. Almost 30 articles in high rated scientific journals were published. Aside from the huge amount of work, of upmost relevance is the wide variety of analytical techniques, complemented with chemometric tools, which were applied. This, together with the tasks of hypothesis formulation, planning of experiments, result interpretation, and writing resulted in a solid well-founded scientific training. This was complemented by stays abroad and by the current work of María Jesús in another university. All this was possible because the following two conditions were always met: pressure applied day-after-day by María Jesús on their supervisors (and not the reverse), and her prompt response to the demands of the new literature searching, new experiments to do, or new text to write, or to amend after an extensive waste of red ink. Following the Tolstoy's Anna Karenina principle (happy families are all alike; every unhappy family is unhappy in its own way), I should conclude that success was the consequence of avoiding as much as possible every deficiency.

Prof. Guillermo Ramis-Ramos

Contents

Abbreviations

3,4-DHPAA	3,4-dihydroxyphenyl acetic acid
3,4-DHPEA	3,4-dihydroxyphenyl etanol
α-T-AcO	α-tocopherol acetate
ACN	Acetonitrile
AcPIN	1-acetoxypinoresinol
AIBN	α,α'-azobisisobutyronitrile
Ala	Alanine
ANN	Artificial neural network
APCI	Atmospheric pressure chemical ionization
API	Apigenin
APPI	Atmospheric pressure photoionization
Arg	Arginine
Asn	Asparagine
Asp	Aspartic acid
ATR	Attenuated total reflectance
BDDA	1,3-butanediol diacrylate
BHT	Butylated hydroxytoluene
CE	Capillary electrophoresis
CEC	Capillary electrochromatography
Cys	Cysteine
CZE	Capillary zone electrophoresis
DAD	Diode array detector
DEA	Decarboxymethylated form of elenolic acid
DLA	Decarboxymethyl ligstroside aglycon
DOA	Decarboxymethyl oleuropein aglycon
EA	Elenolic acid
EC	European Community
EDMA	Ethylene dimethacrylate
EEC	European Economic Community
EIC	Extracted ion chromatogram
ELSD	Evaporative light scattering detector

EOF	Electroosmotic flow
ESI	Electrospray ionization
EtOH	Ethanol
EVOO	Extra virgin olive oil
FID	Flame ionization detector
FTIR	Fourier transform infrared
GC	Gas chromatography
Gln	Glutamine
Glu	Glutamic acid
Gly	Glycine
HCl	Hydrochloric acid
His	Histidine
HPLC	High performance liquid chromatography
HYTY	Hydroxytyrosol
ID	Internal diameter
Ile	Isoleucine
IOC	International olive council
IR	Infrared
KOH	Potassium hydroxide
LAg	Ligstroside aglycon
LA	Lauryl acrylate
LC	Liquid chromatography
LDA	Linear discriminant analysis
Leu	Leucine
LMA	Lauryl methacrylate
LOD	Limit of detection
LOQ	Limit of quantification
LPO	Lauroyl peroxide
LUT	Luteolin
LVOO	Lampante virgin olive oil
Lys	Lysine
MeOH	Methanol
Met	Methionine
META	[2-(methacryloyloxy)ethyl]trimethyl ammonium chloride
MLP	Multilayer perceptron
MLR	Multiple linear regression
MOS	Metal oxide semiconductor
MOSFET	Metal oxide semiconductor field effect transistor
MS	Mass spectrometry
MW	Molecular weight
m/z	Mass-charge ratio
NAC	N-acetyl-cysteine
NaCl	Sodium chloride
NaOH	Sodium hydroxide
NMR	Nuclear magnetic resonance

NP	Normal phase
OA	Oleuropein aglycon
ODMA	Octadecyl methacrylate
OFA	Oxidized fatty acid
OLEA	Italian organization of olive oil tasters
OPA	*o*-phthaldialdehyde
OPO	Olive pomace oil
OSI	Oxidative stability instrument
OxDEA	Oxidized form of decarboxymethyl elenolic acid
OxDLA	Oxidized form of decarboxymethyl ligstroside aglycon
OxDOA	Oxidized form of decarboxymethyl oleuropein aglycon
OxEA	Oxidized form of elenolic acid
OxLAg	Oxidized form of ligstroside aglycon
OxOA	Oxidized form of oleuropein aglycon
PCR	Principal component regression
Phe	Phenylalanine
PDO	Protected designation of origin
PLSR	Partial least squares regression
Pro	Proline
QCM	Quartz crystal microbalance
r	Linear regression coefficient
ROPO	Refined olive pomace oil
RP	Reverse phase
RSD	Relative standard deviation
SAW	Surface acoustic wave
sccm	Standard cubic centimetres per min
SEM	Scanning electron microscope
Ser	Serine
SIR	Selected ion recording
T	Tocopherol
T_3	Tocotrienol
THF	Tetrahydrofurane
Thr	Threonine
TIC	Total ion chromatogram
TLC	Thin layer chromatography
t_R	Retention time
Tris	Tris(hydroxymethyl)amino ethane
Trp	Tryptophan
TY	Tyrosol
Tyr	Tyrosine
UPLC	Ultra performance liquid chromatography
Val	Valine
VOO	Virgin olive oil

Chapter 1
Introduction

1.1 Edible Oils

1.1.1 Introduction

Edible oils are mainly vegetable oils which have been subjected to several processes to removed undesirable constituents. In order to make them suitable for human consumption, most edible oils are subjected to refining processes, such as neutralization, bleaching and deodorization. Among edible oils, only virgin olive oil (a natural juice obtained by olive pressing), can be consumed without refining.

Edible oils are characterized by a wide range of physical and chemical properties, since their composition depend on the type of oil (Rossell 1991).

Oil suitability for most uses depends on its quality and chemical composition. Several tests can be used to determine oil purity, such as the determination of triacylglycerols, Ts, sterols and other constituents of the unsaponifiable fraction of oil.

1.1.2 Constituents of Edible Oils

The constituents of edible oils can be grouped into the saponifiable (triacylglycerols, free fatty acids, phosphatides) and the unsaponifiable (hydrocarbons, fatty alcohols, etc.) fractions. The unsaponifiable fraction accounts, in general, 0.5–1.5 % of the oils.

1.1.2.1 Saponifiable Fraction

The saponifiable fraction accounts for 98.5–99.5 % of oils. The major part of this fraction are triacylglycerols and free fatty acids, although other fatty acid

M. J. Lerma García, *Characterization and Authentication of Olive and Other Vegetable Oils*, Springer Theses, DOI: 10.1007/978-3-642-31418-6_1,

derivatives such as mono- and diacylglycerols, phospholipids, waxes and sterol esters are also found.

Triacylglycerols. These compounds comprise 98–99 % of the oils. They are esters derived from the union of glycerol (1,2,3-propanetriol) and fatty acids. Generally, the fatty acids at the central position of the glycerol molecule are generally unsaturated, although saturated acids can be found at this position when the total concentration of saturated fatty acids in the oil is very high. The most abundant triacylglycerols found in olive oil are OOO (43.5 %), POO (18.4 %), OOL (6.8 %), POL (5.9 %) and SOO (5.1 %) (being O = oleic acid; P = palmitic acid; S = stearic acid and L = linoleic acid) (Fedeli 1977).

Mono- and diacylglycerols. Jointly with triacylglycerols, edible oils also contain partial glycerols such as mono- and diacylglycerols, comprising 0.2 and 1.3 % of total fatty acids, respectively. Their present in an olive oil is an index of low quality (Mariani and Fedeli 1985). For this reason, their determination is often used as an oil quality marker.

Free fatty acids. Their proportion in the oil depends on the hydrolysis degree of triacylglycerols, being their composition variable according to the botanical variety of oil, or, in the case of olive oil, according to the genetic variety, climatic conditions, fruit maturity and geographical origin of olives (Aparicio et al 1994; Boskou 2002; D'Imperio et al. 2007; Stefanoudaki Kotsifaki and Koutsaftakis 1999; Torres and Maestri 2006). Major fatty acids in olive oils are oleic (55–85 %), palmitic (7.5–20 %), linoleic (7.5–20 %), stearic (0.5–5 %), palmitoleic (0.3–3.5 %) and linolenic (0.0–1.5 %) acids, although traces of myristic, arachidic and margaric acids could be also found.

Phospholipids. Phospholipids are found in small quantities in freshly produced olive oils (40–135 mg/kg) (Tiscornia et al. 1982), being their concentration lower with oil aging. The most important phospholipids in olive oil are phosphatidylcholine, phosphatidylethanolamine, phosphatidylinositol and phosphatidylserine (Alter and Gutfinger 1982; Boskou 2002).

Waxes. These compounds are esters of fatty alcohols with fatty acids. The main waxes detected in olive oils have a high and even carbon number, in particular, C_{36}–C_{46} esters. Their amount is very low, not exceeding 35 mg/100 g (Boskou 2002).

Sterol esters. These compounds are combinations of fatty acids with different types of sterols (sterols will be discussed below).

1.1.2.2 Unsaponifiable Fraction

The unsaponifiable fraction of edible oils contain different compounds which are not chemically related to fatty acids, such as hydrocarbons, fatty alcohols, free sterols (common sterols, 4-α-methylsterols, 4,4-dimethylsterols or triterpene alcohols and triterpene dialcohols), Ts and T_3s, pigments, different volatile compounds and aromatic hydrocarbons, phenolic compounds and proteins.

Hydrocarbons. The most important hydrocarbon found in both virgin and refined olive oils is squalene. Squalene contents comprised between 2,500 and

9,250 μg/g has been found in olive oils, which are widely larger in comparison to those found in other edible oils, which ranged from 16 to 370 μg/g, according to Gutfinger and Letan 1974. Other hydrocarbons also present in olive oil are C_{14}–C_{30} *n*-alkanes, some *n*-alkenes and terpene hydrocarbons such as α-farnesene. The concentration of these hydrocarbons is approximately 150–200 μg/g (Lanzon et al. 1994). β-carotene, which could be included in the family of terpene hydrocarbons due to its chemical structure, will be discussed in the pigment section.

Fatty alcohols. These minor compounds are also important constituents of edible oils, and, in the case of olive oil, they can be used to distinguish different olive oil types (Regulation (EEC) N° 2568/91). Fatty alcohols can be linear (aliphatic) o triterpene (see sterol section). Other alcohols, such as diterpene alcohols or acyclic diterpene alcohols are also found in olive oils.

Aliphatic alcohols are compounds of linear structure. On the other hand, they are precursors of the formation of waxes. The main linear alcohols present in olive oil, whose concentrations are usually lower than 35 mg/g, are docosanol (C22), tetracosanol (C24), hexacosanol (C26) and octacosanol (C28). Other alcohols with an odd atom number, present at trace levels, are tricosanol (C23), pentacosanol (C25) and heptacosanol (C27).

Olive oil also contains two important diterpene alcohols: phytol (found at concentrations ranging from 120 to 180 mg/kg) and geranylgeraniol (Paganuzzi 1979).

Sterols. There different types of sterols in vegetable oils: common sterols or 4-α-desmethylsterols, 4-α-methylsterols, 4,4-dimethyl sterols or triterpene alcohols and triterpene dialcohols.

4-α-desmethylsterols are the most abundant sterols in oils, and its content in olive oil ranged from 100 to 200 mg/g. The main sterols in olive oil are β-sitosterol (75–90 %), Δ^5-avenasterol (5–36 %) and campesterol (which accounts approximately 3 % of the total sterol fraction). However, other sterols such as cholesterol, campestanol, stigmasterol, Δ^7-campesterol, chlerosterol, sitostanol, $\Delta^{5,24}$- stigmastadienol, Δ^7- stigmasterol and Δ^7-avenasterol have been also found at trace levels (Boskou 2002).

4-α-methylsterols are found in low concentrations, which normally ranged between 20 and 70 mg/g (Boskou 1996) as a consequence of sterol biosynthesis. The most abundant 4-α-methylsterols found in olive oil are obtusifoliol, cycloeucalenol, gramisterol and citrostadienol.

On the other hand, major triterpene alcohols present in olive oil, whose content ranged between 100 and 150 mg/100 g oil (Kiosseoglou et al. 1987), are α- and β-amyrin, cycloartenol, butyrospermol, 24-methylenecycloartanol, taraxerol, dammaradienol and 24-methylene-24-dihydroparkeol (Boskou 2002; Kiritsakis et al. 2003; Paganuzzi 1982).

The main triterpene dialcohols are erythrodiol and uvaol. Their total content in olive oil ranged from 1 to 20 mg/g, although a content up to 280 mg/g could be found in β-residual oils (Boskou 2002; Mariani et al. 1987).

Ts and T_3s. Ts and T_3s are important fat-soluble vitamins. Both series of compounds contribute to the stability of oils protecting them from oxidation (Blekas et al. 1995; Manzi et al. 1998; Psomiadou and Tsimidou 1998) preventing

lipid peroxidation in biological membranes (Panfili et al. 2003; Solomon 1998), having also a beneficial biological role as antioxidants (Mateos et al. 2005). While Ts are found in all oils, T_3s are mainly found in palm oil (Choo et al. 1996) and in oils obtained from cereals. The relative concentrations of Ts and T_3s vary with the type of oil, being α-T the most abundant in olive oil, representing 95 % of Ts (Gimeno et al. 2000; Tasioula-Margari and Okogeri 2001). The other 5 % are mainly β- and γ-Ts.

Pigments. The main pigments present in edible oils are carotenoids (Serani and Piacenti 1992). The main carotenoids present in olive oil are β-carotene and lutein, although small quantities of xanthophylls such as violaxanthin and/or neoxanthin have been also reported (Boskou 2002). The total pigment content ranged from 1 to 20 mg/kg, although in most cases its quantity does not exceed 10 mg/kg. Other pigments also found in olive oils (10–30 mg/kg) are chlorophylls. Olive oil green colour is a consequence of the presence of these pigments. Pheophytin α is the most abundant chlorophyll found in packed oils, although the occurrence of other chlorophylls such as chlorophyll α, chlorophyll β, pheophytin α and pheophytin β have been also reported in fresh oils (Miguez-Mosquera et al. 1990).

Volatile and aromatic compounds. They are responsible of the aroma and flavor of virgin olive oils. There are more than one hundred components directly related to the aroma and flavor, such as hydrocarbons, alcohols, aldehydes, esters, phenols, terpenes and furan derivates (Boskou 1996; Morales and Aparicio 1999 and 2003; Reiners and Grosch 1998). The most important constituents of olive oil aroma are 6-carbon aldehydes and the alcohols formed in the fruit from polyunsaturated fatty acids.

Phenolic compounds. These compounds, more commonly known as polyphenols, are minor constituents of olive oil. Their antioxidant potential has attracted great interest, since they are supposed to have chemoprotective properties in human beings (Bendini et al. 2007; Caponio et al. 1999; Vissers et al. 2001) and also for being one of the most important olive oil antioxidants (Caponio 1999; Tsimidou 1998; Tura 2007; Velasco 2002). Their antioxidant activity has been related to the protection against chronic and degenerative diseases such as heart disease, diseases of neuro-degenerative aging and tumors located in various parts of the human body (Franceschi 1999; Hodge 2004). In addition, polyphenols also contribute to the sensorial properties of virgin olive oils (Servili 2002) by conferring bitterness, pungency, and astringency (Gutiérrez-Rosales 1992 and 2003; Tsimidou 1998).

Phenolic compounds can be mainly grouped into the following categories (Harborne 1989):

- Simple phenols, such as TY, the HYTY, p-hydroxyphenylacetic acid and homovanillic acid.
- Phenolic acids, with the basic structure C6–C1 (benzoic acids), such as gallic, gentisic, benzoic, vanillic, protocatechuic, *p*-hidroxybenzoic and syringic acid, or with the basic structure C6–C3 (cinnamic acids), such as caffeic, *p*-coumaric, *o*-coumaric, ferulic, cinnamic and sinapic acids.

- Phenolic alcohols, such as 3,4-DHPEA and 2-(4-hydroxyphenyl)ethyl acetate.
- Secoiridoids such as oleuropein, ligstroside, OA, LAg, deacetoxy oleuropein aglycon, deacetoxy ligstroside aglycon, dialdehydic form of oleuropein and dialdehydic form of ligstroside.
- Flavonoids, such as API, LUT and taxifolin.
- Lignans, such as AcPIN, pinoresinol and 1-hydroxypinoresinol.

Proteins. Finally, the presence of proteins in vegetable oils has been described (Hidalgo et al. 2001a, b, 2002). The total protein content varies widely depending on the type of oil and its extraction method (Hidalgo 2006). On the other hand, it has been shown that there are significant differences in protein content in olive oils depending on the crop and the maturity of the fruit (Zamora 2001).

1.1.3 Methods of Analysis of Main Edible Oil Constituents

1.1.3.1 Determination of Triacylglycerols

Different LC techniques have been used for the analysis of triacylglycerols in vegetable oils, such as TLC (Christie 1992), RP-HPLC (Carelli 1993; Cunha and Oliveira 2006a; Holčapek 2005; Parcerisa 1995) and high-temperature-capillary GC (Aparicio 2000; Carelli 1993). Columns packed with silver ions have been the most commonly used in RP-HPLC, since silver presence in the stationary phase promotes the selective retention of unsaturated compounds (Macher 2001). On the other hand, comprehensive two-dimensional chromatography using both a C18 column with a second column load with silver ions have been also employed to achieve selectivity and high peak capacities (Dugo 2006; Robison 1985; van der Klift 2008). Among these techniques, the most widely employed methodology for triacylglycerol analysis has been RP-HPLC. The official method of analysis involves the use of an HPLC coupled with a refractive index detector (Parcerisa 1995), but, since this detector is not compatible with the use of gradient elution (desirable to reduce analysis times and to improve chromatographic resolution), other detectors have been also used, such as UV at low wavelengths (Carelli 1993; Holčapek 2005; Van der Klift 2008), ELSD (Holčapek 2005; Macher 2001; Perona 2001; Van der Klift 2008) or MS (Holčapek 2005; Van der Klift 2008).

1.1.3.2 Determination of Fatty Acids

Analysis of free fatty acids has been usually carried out by GC-FID, being this technique that proposed by the official method of analysis (Hajimahmoodia 2005; Regulation (EEC) N° 2568/91, annex X; Sakouhia 2008). However, other analytical methods, such as HPLC (Kotani 2002), CEC (Dermaux 1999) or NMR (Sacchi 1997) have been also developed for this purpose.

1.1.3.3 Determination of Alcohols

Aliphatic and triterpene alcohols present in vegetable oils have been usually determined by GC-FID (Abou Hadeed 1990; Azadmard-Damirchi 2005; Benitez-Sánchez 2003; Lazzez 2008; Ntsourankoua 1994; Ranalli 2002; Rivera del Álamo et al. 2004; Sindhu-Kanya 2007) o GC–MS (Abou Hadeed 1990; Azadmard-Damirchi 2005; Cunha et al. 2006b; Ntsourankoua 1994; Sindhu-Kanya 2007). Only some studies have described the use of HPLC after derivatization of alcohols with 3,5-dinitrobenzoyl chloride (Cortesi 1987).

1.1.3.4 Determination of Sterols

The analysis of sterols have been usually carried out by GC-FID (Cercaci 2007; Galeano 2005; Parcerisa 2000; Ranalli 2002; Rivera del Álamo et al. 2004) or GC–MS (Cercaci 2007; Cunha et al. 2006b; Parcerisa 2000; Thanh 2006; Medvedovici 1997), after extraction of the sterol fraction by TLC followed by derivatization, as indicated by the official method (Regulation (EEC) N° 2568/91, annex V). The major disadvantage of GC is the requirement of thermally stable columns and the need of chemical derivatization prior to analysis. For this reason, alternative methods have been described based on the use of HPLC–MS (Cañabate-Díaz 2007; Martínez-Vidal 2007; Segura-Carretero 2008) and CEC (Abidi 2004).

1.1.3.5 Determination of Ts and T_3s

Ts and T_3s analysis has been mainly carried out by GC (Melchert 2002) and HPLC using several detectors (Abidi 2000; Cunha et al. 2006c; Gruszka and Kruk 2007). Both, NP-HPLC, which is capable of separating β and γ isomers (Abidi 2000), and RP-HPLC, which shows higher column stability, better reproducibility, and shorter analysis times, have been used (Abidi 2000; Gimeno et al. 2000b). On the other hand, Ts have also been determined by FTIR spectroscopy (Silva et al. 2009), synchronous fluorescence spectroscopy (Sikorska et al. 2005) and by CEC using packed columns (Aturki et al. 2005).

1.1.3.6 Determination of Volatile Compounds

Many efforts have been made to develop instrumental methods capable of determining the components responsible for flavor and aroma of olive oils, and to remove the subjectivity and other disadvantages coming from the sensory evaluation by tasting panels. Traditionally, volatile compounds were determined by GC–MS (Baccouri et al. 2008a, b; Guth and Grosch 1993; Tateo et al. 1993). Later, another approach was proposed for the determination of volatiles, based on the use of sensor arrays (electronic nose), which is able to assess the basic

perceptions produced by the oil (Aparicio 1995; Tena 2007). In some cases, the results obtained by the electronic nose have been compared with those provided by a tasting panel (Camurati 2006). On the other hand, GC has been also used in combination of sensor arrays (Cimato et al. 2006; García-Gónzalez 2010; López-Feria 2008; Morales 1994; Tena 2007).

1.1.3.7 Determination of Phenolic Compounds

Several methods have been described for the analysis of phenolic compounds in olive oil. The most used technique has been LC, coupled to UV–Vis (Allalout 2009; Baccouri et al. 2008a, b; Bendini 2003; Bonoli 2004; Cerretani 2006; Gutierrez-Rosales 2003; Ocakoglu 2009), electrochemical (Brenes 2000), fluorimetric (Cartoni 2000; García 2003) or MS detectors (Baccouri 2008b; Bendini 2003; Bonoli 2004; Carrasco-Pancorbo 2007a; Gutierrez-Rosales 2003; Suárez 2008). Other techniques, such as GC (Carrasco-Pancorbo 2005; Liberatore 2001; Ríos 2005; Saitta 2009) and CE (Bendini 2003; Bonoli 2004; Carrasco-Pancorbo 2004, 2006,2007; Gómez-Caravaca 2005) coupled to different detectors, have been also widely used. In addition, and more recently, voltammetric sensors (Rodríguez-Méndez 2008) and high-resolution NMR (Christophoridou 2009) have also been used for this purpose.

1.1.3.8 Determination of Proteins

Due to the recent description of proteins as trace components of vegetable oils, only one method for their determination has been described (Hidalgo 2001). This method involves, in first place, protein hydrolysis followed by derivatization of the amino acids obtained with diethyl ethoxymethyl malonate, and subsequent analysis of the derivatives by HPLC–UV-Vis.

1.1.4 Detection of Adulteration

EVOO is often illegally adulterated with cheaper vegetable oils such as corn, peanut, sunflower and soybean oils (Kiritsakis 1998), although the most common adulteration is performed with hazelnut oil, due to the difficulty of its detection by the great similarity between hazelnut and olive oil chemical compositions. EVOO is also adulterated with other olive oils of lower quality, such as olive pomace (Kiritsakis 1998).

To analyze and detect adulteration different physical and chemical tests (Comission of Codex Alimentarius 1993; Fedeli 1977; Kiritsakis 1991), and chromatographic (Fasciotti 2010; Marcos Lorenzo et al. 2002; Maryam 2009; Saba 2005), spectroscopic (Agiomyrgianaki 2010; Fragaki et al. 2005; Fronimaki et al. 2002; Maryam et al. 2009; Poulli et al. 2006; Vlachos et al. 2006) and termic

(Chiavaro et al. 2008; Maryam et al. 2009) methods, among others, have been applied.

On the other hand, the analysis of the unsaponifiable fraction is an alternative and powerful tool to detect adulteration and to increase reliability to differentiate between vegetable oils from different botanical origins, or between olive oils of different quality. Among the constituents of the unsaponifiable fraction, the sterol family, which composition in EVOOs is very characteristic, provides excellent adulteration tracers, both to distinguish between vegetable oils from different botanical origin (Ballesteros et al. 1995; Cañabate-Díaz et al. 2007; Cercaci et al. 2003; Mariani et al. 2006) or to differentiate olive oils of different quality (Martínez-Vidal et al. 2007; Philips et al. 2002), which explains why this family of compounds has been widely used in oil authentication.

1.2 Olive Oil

Olive oil is an olive juice directly obtained from *Olea europaea* fruits. This oil could present excellent organoleptic properties depending on the quality of the fruits used for its elaboration (fresh fruits free of defects, adequate maturation degree, etc.).

1.2.1 Legal Classification of Olive Oil

There are several quality levels in olive oil, which can be classified as virgin olive oils and olive–pomace oils. Their characteristics, within the European Union, were established in the Commission Regulation (EEC) No. 2568/91, as amended by EEC 796/2002.

1.2.1.1 Virgin Olive Oil

Virgin olive oil is that obtained only by mechanical or physical methods that do not involve any alteration, particularly thermal. Virgin olive oil must have not undergone any treatment other than washing, decantation, centrifugation and filtration. However, not all virgin olive oils are characterized by an excellent quality. For this reason, virgin olive oils could be classified into several categories according to their acidity, organoleptic score and the absence of defects. These categories are:

- *Extra virgin olive oil or EVOO.* It is considered the best olive oil. Its organoleptic score (set of aromas and flavours) must be equal to or greater than 6.5, and its free acidity (percentage of oleic acid) can not exceed 0.8 g/100 g. EVOOs can present different characteristics, depending on several factors ranging from the olive genetic variety to the cultivation conditions. According to these

factors, EVOOs could be subdivided into at least three major groups: monovarietal oils, made with a single variety of olives; coupages, prepared from different olive varieties to always get the same standards of taste and aroma; and PDO oils, prepared from olives from one geographical area, which are officially recognized.

- *Virgin olive oil or VOO*. It is the virgin olive oil that can be slightly altered, either in their analytical indexes or in their sensory characteristics, but always at a small scale. These alterations, especially sensory, may be almost imperceptible, but depreciated in relation to quality EVOO. In this case, the organoleptic score should be equal to or greater than 5.5, and maximum free acidity of 2° (2 g of oleic acid per 100 g of oil).
- *Ordinary virgin olive oil.* It features sensitive alterations in their physicochemical parameters or in their sensory characteristics. Its organoleptic score must be equal or superior to 3.5, and its maximum acidity of 3.3°. It is used as a component of the so-called olive oil (defined below) but only when its organoleptic characteristics are not significantly altered, being then used to be refined.
- *Lampante virgin olive oil or LVOO*. It is not intended in any way for direct consumption, and must be necessarily subject to a refining process to make it edible. Free acidity is greater than 3.3° and its organoleptic score lessthan 3.5.
- *Refined olive oil*. It is the resulting oil when the previous two oils are subjected to a refination process. Refined olive oil must have a free acidity not higher than 0.3°, and should present almost neutral sensory characteristics (without taste or smell), so it is used as the basis for the manufacturement of other olive oils.

1.2.1.2 Crude Olive–Pomace Oil

Crude olive–pomace oil is the one extracted with organic solvents from the solid waste of mills. It is necessarily subjected to refinement since it is not directly suitable for human consumption. It is commercialized, as explained below, mixed with virgin olive oil.

1.2.1.3 Other Commercial Olive Oils

- *Olive oil*. It is another commercial product obtained by mixing different proportions of VOO or common virgin olive oil with refined olive oil. Its maximum acidity is 1°.
- *Olive–pomace oil or OPO*. It is that obtained by mixing VOO with refined pomace oil or ROPO.

Table 1.1 Discriminant tests in sensory analysis

Test	Short description
Paired	Two labeled samples. Assessor must indicate the differences between them
Duo–trio	Three samples, two identical and one different. One of the two identical samples is identified as reference. Assessor must recognize which sample is identical to the one used as reference
Triangle	Three samples, two identical and one different. The judge must indicate which sample is different
Classification	Assessor must order a set of samples according to the intensity of a certain attribute
Threshold	A series of samples with decreasing concentrations of an attribute is presented. Assessor must indicate for each sample if the attribute is detected

1.2.2 Sensory Assessment of Virgin Olive Oils

As it can be deduced from Sect. 1.2.1, sensory analysis is, jointly with the chemical analysis of olive oils, an excellent marker of oil quality.

Sensory analysis is a discipline that uses human senses to evaluate food products. With sight, product appearance, colour and shape is evaluated, while smell evaluated food aromas. Consistency and other characteristics such as fluidity and/or viscosity are evaluated by both touch and hearing. Finally, food flavour is evaluated through a combination of smell, taste and touch.

1.2.2.1 Methods for Evaluating Sensory Characteristics

Various sensory tests have been developed to provide the evaluation of organoleptic characteristics of foods, including oils. Some of these tests are planned to give information about the overall acceptability of a product or to determine the preference of assessors or consumers between two products or among samples of the same food (preference tests). Other tests are used to evaluate qualitative and quantitative sensory differences between two products (discriminant tests), or to identify, describe, and quantify each sensory quality perceived in an assessment (descriptive tests). Discriminatory tests (which are the ones used in this thesis) are summarized in Table 1.1.

1.2.2.2 Organoleptic Assessment of Virgin Olive Oil

The purpose of this international method (IOC, COI/T.20/Doc. No 15/Rev. 4 November 2011; Regulation (EC) No. 796/2002) is to determine the procedure for assessing the organoleptic characteristics of virgin olive oil and to establish the method for its classification on the basis of those characteristics. This method can be used only for grading virgin oils on the basis of fruitiness and intensity of

Table 1.2 Specific vocabulary for olive oil described in Annex XII of the Commission Regulation (EC) No. 796/2002, Off. J. Eur. Commun. (2002)

Positive attributes	
Fruity	Range of smells (dependent on variety) characteristic of oil from healthy fresh fruit, green or white, perceived directly or retronasally
Bitter	Characteristic taste of oil from green olives or olives turning colour
Pungent	Tingling sensation characteristic of oil made at the beginning of the season mainly from olives that are still green
Negative attributes	
"Atrojado" (fusty)	Characteristic flavour of oil from piled olives in advanced anaerobic fermentation
Mustiness/ humidity	Characteristic flavour of oil from olives in which large numbers of fungi and yeasts had developed as a result of storage for several days in humid conditions
Muddy sediment	Characteristic flavour of oil that has remained in contact with sediment in vats and tanks
Winey/vinegary	Characteristic flavour of certain oils reminiscent of wine or vinegar, due basically to formation of acetic acid, ethyl acetate and ethanol by fermentation of the olives
Metallic	Flavour reminiscent of metal, characteristic of oil that has been in prolonged contact with metal surfaces during crushing, mixing, pressing or storage.
Rancid	Flavour of oil that has become oxidised
Heated or burnt	Characteristic flavour caused by excessive and/or prolonged heating during production, particularly by thermo-mixing of the paste in unsuitable conditions
Hay/wood	Characteristic flavour of certain oils from dry olives
Rough	Thick and pasty mouthfeel produced by some oils
Greasy	Flavour reminiscent of diesel, grease or mineral oil
Vegetable water	Flavour acquired by oil through prolonged contact with the vegetable water
Brine	Flavour of oil from olives preserved in salt solution
Esparto	Characteristic flavour of oil from olives pressed in new esparto mats. It can vary according to whether the mats are of green or dried esparto
Earthy	Flavour of oil from olives collected with earth or mud on them and not washed
Grubby	Flavour of oil from olives heavily attacked by grubs of the olive fly (*Bactrocera oleae*)
Cucumber	Characteristic flavour of oil kept too long in hermetically sealed containers, notably in tins, attributed to formation of 2,6-nonadienal

defects by a group of selected trained tasters operating as a panel. Candidates shall be selected, trained and monitored by the panel leader in accordance with their skills in distinguishing between similar samples; it should be borne in mind that their accuracy will improve with training. Tasters must act like real sensory observers, setting aside their personal tastes and solely reporting the sensations they perceive. Between 8 and 12 tasters are required for each test. The selection of a group of people can average the differences that exist in some odour thresholds depending on the person, probably related to genetic, cultural and environmental factors, thus providing a final result that represents all consumers. To solve this

problem, assessors must use the same vocabulary. One part of this vocabulary, common to all foods, is the "general vocabulary", which included terms such aspect, attribute, panel, sensitivity, taster, response, fatigue, sensory stimulation, aroma, flavour, texture, etc. The "specific vocabulary" for the analysis of virgin olive oil was developed by experts from the IOC. A summary of this vocabulary is shown in Table 1.2.

However, and as published by the IOC (COI/T.20/Doc. No 15/Rev. 4 November 2011), other measures must be taken into consideration to assess olive oil quality. Thus, the dimensions, form and colour of the tasting glass have been established. Glasses should have a narrow mouth which helps to concentrate the odours and facilitates their identification, and should be made of dark-coloured glass to prevent the taster from perceiving the colour of the oil, thus eliminating any prejudices and impeding the possible formation of biases or tendencies that might affect the objectiveness of the determination. The glass shall contain 14–16 ml of oil, or between 12.8 and 14.6 g if the samples are to be weighed, and shall be covered with a watch-glass. Moreover, the oil samples shall be kept in the glasses at 28 °C ± 2 °C throughout the test. This temperature has been chosen because it makes it easier to observe organoleptic differences than at ambient temperature and because at lower temperatures the aromatic compounds peculiar to these oils volatilise poorly while higher temperatures lead to the formation of volatile compounds peculiar to heated oils. For this purpose, a heating device (IOC, COI/T.20/Doc. No 5/Rev. 1 September 2007) shall be installed in each booth within the taster's reach.

On the other hand, when organoleptically assessing a virgin olive oil, it is recommended that four samples are the most be evaluated in each session with a maximum of three sessions per day, to avoid the contrast effect that could be produced by immediately tasting other samples.

Assessors use a profile sheet (Fig. 1.1) that contains the sensory defects normally found in virgin olive oils. Among the positive perceptions, only the attributes fruity, bitter and pungent are evaluated. Fruity perception is assessed by direct inhalation, while the rest of sensations are perceived via retronasal. It is appropriate to adopt a scale, which is easy to use both by experts and amateurs, to quantify the different stimuli and to process statistical data. It uses a linear scale of 10 cm length to measure the intensity of sensory notes defined in the vocabulary. The intensity data provided by the tasters, expressed in centimeters, are treated statistically.

1.2.3 Genetic Varieties

EVOO consumption has increased considerably in the last years when compared to the consumption of olive oils of lower quality. This increase has been attributed to the excellent organoleptic and nutritional properties of EVOOs. For this reason, more monovarietal EVOOs are being produced to respond at this growing demand,

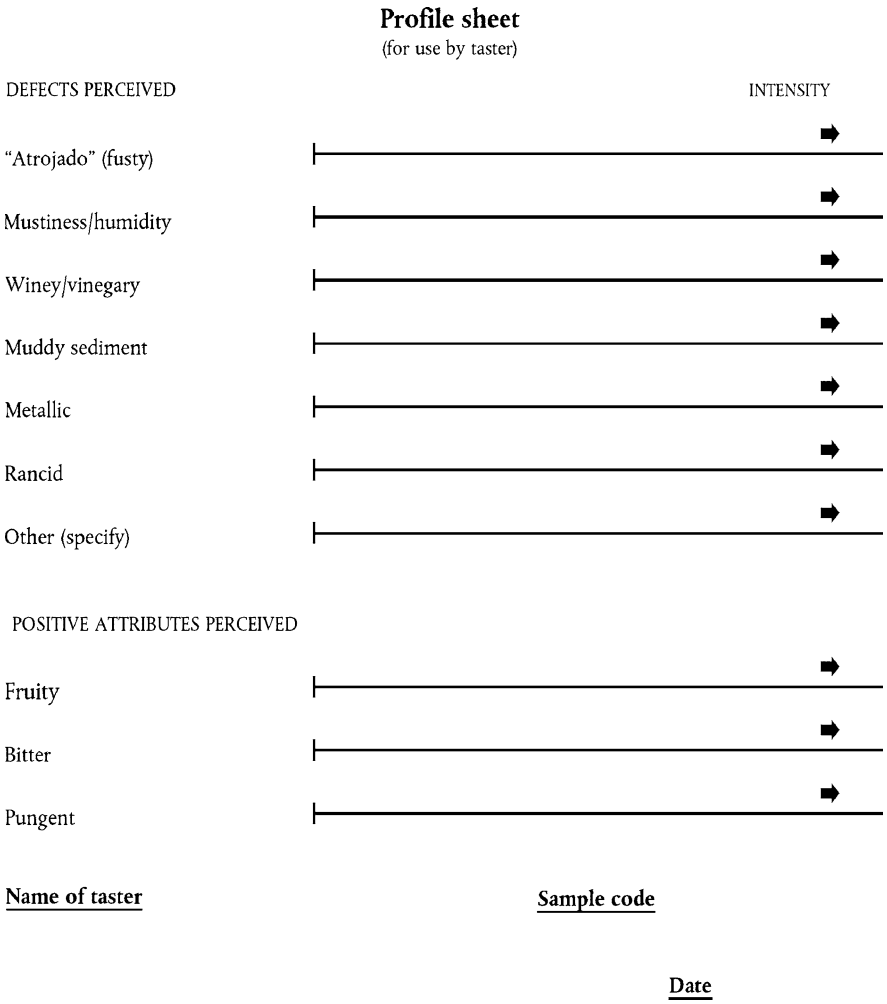

Fig. 1.1 Oil tasting sheet of virgin olive oil adopted by Regulation (EC) N° 640/2008

since chemical composition and organoleptic properties of EVOOs vary depending on the genetic variety of the olive used in its preparation (Baccouri et al. 2008b; Tura et al. 2007).

EVOOs are produced from very different genetic varieties (Barranco et al. 2001). The most widespread varieties in Spain, which accounts 95 % of the produced olives, are Arbequina, Hojiblanca and Picual varieties, although the number of other varieties cultivated in Spain is also high and very diverse, depending on the geographic region where the crop is located. The cultivar Picual, also know as Marteña, is the most important and widespread, mainly cultivated in Andalucía, Castilla-La Mancha and Extremadura. Its production is approximately 50 % of the total Spanish olives,

and about 20 % of world production. On the other hand, Hojiblanca variety is mainly cultivated in Málaga, but it is also very abundant in Sevilla and Córdoba (Andalucía). Finally, Arbequina variety is mainly grown in Lérida, Tarragona and Córdoba. Among the other varieties cultivated in Spain, Cornicabra Lechín, Picuda and Verdial are the most important, among others.

Other genetic varieties of particular interest in the development of this thesis are those grown in the Comunidad Valenciana, Spain, including Serrana de Espadán and Borriolenca (mainly grown in the provinces of Castellón and Valencia), and the varieties Farga and Canetera (mainly grown in the province of Castellón).

1.2.4 Geographical Origin

In addition to the genetic variety of olives, EVOOs may present very different characteristics depending on the geographical origin of the cultivar (Cerretani et al. 2006). Only in Spain, there are 32 PDOs, which are distributed along the country (Ministerio de Medio Ambiente y Medio Rural y Marino (ed.): Aceites de oliva virgen con denominación de origen) (see Table 1.3). Each PDO is governed by its own rules, which have been established in order to preserve olive oil quality. These rules are committed to the final product quality through rigorous quality controls, setting patterns of cultivation, harvesting, processing, bottling and labeling. As it can be observed in Table 1.3, most PDOs are located in Andalucía, which is the main olive oil producing area in the world.

1.2.5 Oxidation Compounds from Olive Oil

Olive oil is characterized by a high oxidative stability compared to other edible oils, which is due to its fatty acid composition, with high concentrations of oleic acid and low in polyunsaturated fatty acids, as well as the presence of natural antioxidants as α-T and phenolic compounds (Tsimidou et al. 1992; Bendini et al. 2007). However, olive oil is susceptible to be oxidized, like other edible oils. Oxidation processes depend on several factors, being the presence of oxygen and trace metals, temperature and light (Al-Ismail et al. 1998, 1999) some of the causes of oil deterioration. The oxidative deterioration may be due to enzymatic oxidation processes (occurring when oil is still in the fruit, or during the extraction process itself), or chemical oxidation processes, such as photo-oxidation (which occurs when the oil is exposed to light) or autoxidation (produced mainly during processing or storage of oil in contact with oxygen) (Bendini et al. 2009; Frankel 1985).

Oil oxidation produces hydroperoxides, which are very unstable primary products, which could decompose or react with other molecules present in the lipid matrix, producing a wide range of secondary oxidation products that derive from fatty acids and other minor compounds, such as oxidised fatty acids (OFAs), oxidised polymers and volatile compounds among others (Choe and Min 2006).

Table 1.3 Name of the Spanish virgin olive oil PDOs and their geographical distribution in Spain

No.	Name of the PDO	Geographical area
1	Sierra de Cádiz	Andalucía
2	Antequera	Andalucía
3	Estepa	
4	Lucena	Andalucía
5	Priego de Córdoba	Andalucía
6	Poniente de Granada	Andalucía
7	Baena	Andalucía
8	Jaén Sierra Sur	Andalucía
9	Montes de Granada	Andalucía
10	Sierra Mágina	Andalucía
11	Sierra de Cazorla	Andalucía
12	Sierra de Segura	Andalucía
13	Campiñas de Jaén	Andalucía
14	Montoro-Adamuz	Andalucía
15	Monterrubio	Extremadura
16	Gata-Hurdes	Extremadura
17	Aceite Campo de Montiel	Castilla-La Mancha
18	Campo de Calatrava	Castilla-La Mancha
19	Aceite Montes de Alcaraz	Castilla-La Mancha
20	La alcarria	Castilla-La Mancha
21	Montes de Toledo	Castilla-La Mancha
22	Aceite de Mallorca	Mallorca
23	Baix Ebre-Montsià	Catalunya
24	Oli de Terra Alta	Catalunya
25	Siurana	Catalunya
26	Les Garrigues	Catalunya
27	Oli de l'Empordà	Catalunya
28	Aceite de La Rioja	La Rioja
29	Aceite de Navarra	Navarra
30	Aceite del Bajo Aragón	Aragón
31	Aceite de la Comunitat Valenciana	Comunitat Valenciana
32	Aceite de Madrid	Comunidad de Madrid

All these compounds affect negatively oil flavor and aroma. Therefore, the study of the oxidative stability of oils is important in determining both the quality and shelf life (Hamilton 1994).

1.2.5.1 Evaluation of Primary Oxidation Products

The analytical tests typically used to evaluate oil primary oxidation products are peroxide value, and the measurement of conjugated diene and triene absorptivity in the UV.

Peroxide value is one of the most used parameter to evaluate oil oxidative deterioration. It has been traditionally determined by iodometric titration (official method Regulation (EEC No 2568/91), although other methods that use enzymes,

HPLC and colorimetry, have been also developed. However, and despite the good estimation that peroxide index provided about the oxidative state of oils, its determination must be done jointly with the determination of secondary oxidation products, in order to have a more complete knowledge of oxidation evolution (Gordon 2001).

On the other hand, during the formation of peroxide and hydroperoxide radicals, there is a change in the position of the double bonds, which modifies its conjugation. The diene and triene test is based on conjugation changes affecting these molecular structures. The conjugated dienes show an absorption band at 232 nm and trienes at 268 nm. However, there are also other products derived from hydroperoxides, which have the same or similar conjugation, which may contribute to the absorption, making the measurement of conjugated dienes and trienes less specific than the peroxide one.

1.2.5.2 Evaluation of the Secondary Oxidation Products

Several approaches have been attempted to find a reliable oxidation index that, combined with the evaluation of primary oxidation products, would provide a realistic idea about the oxidation status of the fatty matrix (Farhoosh and Pazhouhanmehr 2009). The secondary oxidation indices more widely applied to fat and vegetable oils are the p-anisidine value and thiobarbituric acid reactive substances (Frankel 1998) as well as the content of hexanal or nonanal or their ratio (Frankel 1998; Vichi et al. 2003). Among the chemical methods, the measurements of total polar compounds and polymerized triglycerides (Caponio et al. 2002; Melton et al. 1994), measurement of OSI time, and more recently the determination of OFAs by HPLC (Cortesi et al. 1991), have been also used. Among them, OSI time and OFA determination, which are the methods used in this thesis, will be discussed below.

OSI is an instrument that works under standardized conditions of air flow and temperature (90–110 °C). One advantage of this instrument is that, working under controlled conditions, thermo-oxidation was reduced, which is important for assessing the amount of volatile byproducts. In an OSI, a stream of purified air was passed through the oil sample that is heated to 90–110 °C, and the effluent air for the oil sample was then bubbled through a vessel containing deionized water. The effluent air contains especially volatile organic acids as formic acid (Jebe et al. 1993) and other volatile compounds formed during thermal oxidation of the oil, which increased the conductivity of the water. The results, expressed as induction time in hours, allow a comparative evaluation between different lipid matrices, although the measurement of OSI time can not be applied to predictive studies of oxidation, or to know a priori the oil life. In fact, heat stress conditions jointly with the air flow, accelerate the oxidation of oil promoting kinetics of reaction between oxygen and fatty acids that differ from those occurring in normal conditions of oil storage.

On the other hand, the use of HPLC, according to the method developed by Cortesi et al. (1991), allows the identification and quantification of the main OFAs (hydroxy,

keto, epoxy, and epidioxy) after a simple derivatization step with sodium benzyl oxide of the triglycerides. As these latter compounds are more stable than peroxides, OFAs seem to be a good index of oxidative changes in lipids.

1.3 Analytical Techniques

1.3.1 CEC

CEC is a separation technique in which the flow of the mobile phase or buffer is driven through a chromatographic column by an electric field. Thus, this technique combines the high selectivity and reproducibility of HPLC and the high efficiency of CZE, which is originated from the plug-like flow profile. As in CZE, EOF in CEC is generated by an electric field, in which EOF is an interfacial phenomenon generated as a consequence of the surface charge on the interior wall of the column.

In CEC the separation mechanism is double (Rathore and Horváth 1996). There is a chromatographic mechanism, since there is a distribution of solutes between mobile and stationary phases. On the other hand, the ionic solutes are also separated by an electrophoretic mechanism, which is based on the differences in electrophoretic mobility, so the nature of the stationary phase of the column determines the EOF and influences the quality of the separation.

1.3.1.1 Instrumentation in CEC

A CEC instrument (see Fig. 1.2) consists basically of a high voltage source, a system to provide solvent and/or sample to the inlet and outlet vials of the column, a capillary column, an isothermal compartment for the column and a detection system capable of recording the concentration profiles of the analytes in the eluent.

The instrumentation used in CEC is basically the same as in CE, although CE systems are frequently modified for CEC by applying pressure (2–15 bar) at the inlet and outlet vials (without providing a net pressure drop across the column). This pressure is necessary to avoid bubble formation, which could interrupt current. The formation of bubbles can be attributed to local differences in EOF rate (Rathore 1998), local differences in the electric field due to the loss of gas trapped in the pores of the stationary phase or by electrochemically formed gas (Carney et al. 1999), by heating (Knox 1988; Tsuda 1987) or in the case of packed columns, by the presence of the retaining frits that maintain the structural integrity of the stationary phase (Rebscher 1994). Pressurization could be applied to the inlet or outlet vials, but is usually performed in both vials to ensure a reproducible flow. An inert gas, usually N_2, is used to pressurize the vials.

The quality of a separation technique is characterized by efficiency, selectivity, sensitivity and reproducibility. To obtain reproducible results in CEC, it is

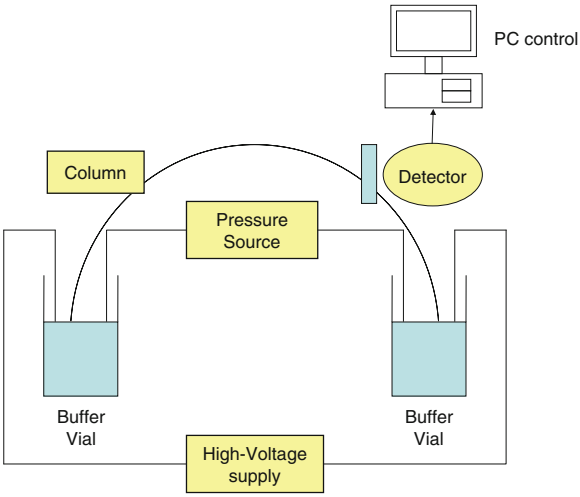

Fig. 1.2 Scheme of a CEC instrument

necessary to control different parameters such as column temperature, applied voltage and pressure. In CE commercial equipments, these parameters are controlled automatically, leading to significant improvements in separation reproducibility.

The UV–Vis spectrophotometric detection is the most commonly used in CEC (Choudhary 2000; Rozing 2001; Devowsky 2002; Cahours 2002) with both direct and indirect modes. Other detection techniques widely used are laser-induced fluorescence (Wall 2002; Horstkötter 2002; Liu 2001), and most recently, MS (Shamsi 2004; Klampfl 2004; Barceló-Barrachina 2004).

1.3.1.2 Columns Used in CEC

CEC columns are usually prepared using fused silica capillaries with internal diameters between 100 and 200 μm. Based on the differences in the chromatographic supports used in their preparation, three types of columns could be distinguished: open-tubular, packed and monolithic columns.

Monolithic columns consist of a continuous porous bed which allows their use on HPLC at high flow rates, providing fast separations without incurring in an excessive pressure increase. This is one of the advantages of these columns when compared to packed ones.

In CEC, monolithic columns also represent an alternative to packed columns due to: (1) the easy preparation, (2) no need of frits, (3) the nearly total exclusion of bubble formation during operation, (4) adjustable porosity and pore size (which allows the use of long columns that could achieve highly efficient separations) and (5) the wide variety of monomers available for the synthesis of stationary phases with many different functionalities. Moreover, monolithic columns could be

prepared in situ, so that the preparation of monolithic beds is relatively simple when compared to the particle packing techniques.

Monolithic materials can be classified into two main categories, organic polymer- and silica-based monoliths. Polymeric stationary phases are usually prepared by in situ polymerization of a mixture composed of functional monomer/s, cross-linker, porogens and a radical initiator. The hydrophobicity of the resulting monolith can be controlled by selecting the nature of the monomer (Liao 1996; Palm 1997). In all cases, EOF is ensured by the addition of monomers derived from acrylic acid or sulfonic acid, or by the addition of quaternary ammonium salts in the polymerization mixture (Ericson 1999). Polymerization reaction is commonly initiated thermally, chemically or by UV irradiation.

In order to enable covalent attachment of the monolith to the wall, a surface modification of the inner wall of the fused-silica capillaries is performed. For this purpose, the wall is silanized using, in most cases, 3-(trimethoxysilyl)propyl methacrylate, also called *silane binding*.

Different types of polymers, such as acrylamide, styrene, methacrylate and acrylate esters, have been employed as stationary phases in CEC. The first monolithic columns described were prepared using acrylamide and methacrylamide (Hjertén 1989; Fujimoto 1995; Hoegger 2001). These polymers are prepared by polymerization of acrylamide or methacrylamide in the presence of methylenebisacrylamide or piperazine diacrylamide as crosslinkers. Polystyrene-based monolithic columns (Gusev 1999; Petro 1996) are obtained by polymerization of styrene or its derivatives using divinylbenzene as crosslinker. Monoliths based on methacrylate esters (Merthar 2003; Zhang 2003; Peters et al. 1998a, b) are prepared by polymerization of butylmethacrylate or other methacrylate esters using ethylene glycol dimethacrylate as crosslinker.

1.3.1.3 Polymerization of Monolithic Columns Based on Methacrylate and Acrylate Esters

Polymethacrylate-based monolithic columns are the most widespread and best characterized columns, being mainly developed by Svec et al. (Peters et al. 1998a , b), who have described several applications in both HPLC and CEC. Methacrylate and acrylate polymers present several advantages such as easily adjustable polarity, fine control of pore characteristics and high stability under extreme pH conditions (2–12).

The polymerization is carried out through a radical reaction, usually initiated by a high temperature, by UV irradiation, or by chemical agents at room temperature. For thermal initiation AIBN (Peters 1998a, b; Chirica 2001), benzoyl peroxide (Xie 1997) or other peroxides (Cantó-Mirapeix 2008) are usually added to the polymerization mixture.

Svec et al. (Peters 1998a and b) have demonstrated that the chromatographic properties (efficiency, selectivity, permeability, etc.) of these materials can be altered by varying the composition of the polymerization mixture, which is

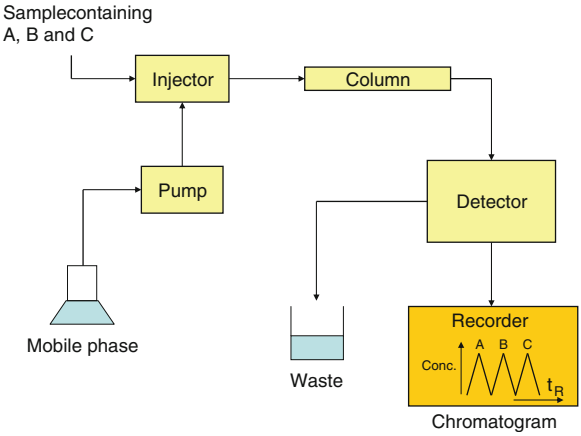

Fig. 1.3 Block diagram of the components of a liquid chromatograph

interesting not only for the development and optimization of chromatographic separations, but also for environmental, biochemical and industrial applications.

1.3.2 LC

Chromatography is a physical separation method in which the components to be separated are distributed between two phases, called stationary and mobile phases. A chromatographic system (see Fig. 1.3) comprises at least one pump system, a device for sample introduction or injector, a column, a detector and a system for data acquisition and control.

According to the different mechanisms of chromatographic retention, different column types could be found:

- Partition chromatography, in which columns with a bonded liquid phase are used. Depending on the relative polarities of the mobile and stationary phases, there are two modes: RP, where the stationary phase is apolar and the mobile phase is polar, or NP, where the stationary phase is polar and the mobile phase is apolar.
- Ion chromatography, in which the stationary phase is an ion (cationic or anionic) exchange resin.
- Size exclusion chromatography, in which the pores of a microporous solid or gel are used as stationary phase.

On the other hand, it is important to degas solvents to prevent the formation of bubbles in the system. To this end, liquid chromatographs typically include an online degasser.

The most employed detection techniques in LC are UV–Vis spectrophotometry and MS. However, other detectors, such as refractive index and different evaporative detectors are also commonly used. Amperometric and fluorimetric detectors

Table 1.4 Representative characteristics of the different miniaturization techniques

Parameter	Classic LC	Micro-LC	Capilar-LC	Nano-LC
Internal diameter	4.6 mm	1–2,1 mm	0.1–1 mm	25–100 μm
Length	1.5–25 cm	1.5–20 cm	1.5–20 cm	1.5–20 cm
Particle diameter	1.8–5 μm	1.8–5 μm	1.8–5 μm	1.8–3 μm
Injection volume	5–100 μL	1–5 μL	0.03–0.3 μL	0.03–0.3 μL
Typical flow rate	< 1 mL min^{-1}	10–100 μL min^{-1}	1–10 μL min^{-1}	0.1–1 μL min^{-1}

are also used for specific applications. Finally, conductivity detection is commonly used in ion chromatography.

In UV–Vis spectrophotometry, the signal is proportional to the solute molar concentration, which molar absorptivity depends on the nature of the absorbent group/s. There are two different types of UV–Vis detectors: variable wavelength detector and DAD. In the first type, a fixed wavelength is measured, while in a DAD all spectral range is measured several times per second.

In MS, the detector is an instrument that provides high-level information about analyte molecular structures, distinguishing between functional groups, chemical elements and isotopes, separating the fragments according to their *m/z* ratio. A MS detector coupled to a liquid chromatograph is able to differentiate compounds with similar retention characteristics, being also possible the identification and/or the quantification of compounds that are only partially resolved or even unresolved. More information about MS is given in Sect. 1.3.5.

More recently, different chromatographic modalities has been introduced involving miniaturization, either in the column size or the particle diameter. Miniaturization is one of the present trends in science and technology, especially in the field of analytical chemistry. The use of these miniaturized techniques offers several advantages over the classical ones, such as better separation efficiencies, increase in sensitivity, shorter analysis times, and lower sample and reagent consumption. However, there are also some disadvantages, such as major instrumental requirements (use of micro-pumps, micro/nano-nebulizers, miniaturized connections, etc.).

Considering column diameter and other related features, a distinction between micro-LC, capillary LC and nano-LC should be performed. The following table shows some of the representative characteristics of these modalities (Table 1.4).

On the other hand, there is another chromatographic method, the UPLC, which enables the use of columns packed with smaller particle sizes, which were able to deliver mobile phases at higher pressures (up to 1,000 bar) than those provided by a conventional chromatography system. With these improvements, higher speed of analysis, peak capacity, resolution and sensitivities are obtained.

1.3.3 Chromatographic Parameters

To successfully carry out a chromatographic separation, analyst must determine if the analytes of interest can be accurately separated from other sample components,

and if this separation is enough to correctly detect and/or determine them. The time elapsed between the injection of the sample components into the column and their detection is known as retention time (t_R). t_R is longer when the solute has higher affinity to the stationary phase due to its chemical nature. A non retained substance passes through the column at a time t_0, called void time. The retention factor or capacity factor (k) measures the degree of retention of an analyte:

$$k_i = \frac{t_{R,i} - t_0}{t_0} \tag{1.1}$$

where $t_{R,i}$ is the retention time of the analyte i. The optimum k value ranged from 1 to 5, being values between 0.2 and 20 also acceptable. k values below 0.2 indicate poor retention, while k values above 20 indicate a high retention caused by an excessive preference of the solute for the stationary phase. This high retention provides very long analysis times and broad and low height peaks, which are difficult to detect and to accurately measure.

The ability of a chromatographic system to distinguish between two solutes is expressed by the selectivity factor $\alpha_{i,j}$, which is calculated as the ratio between the relative retention of both solutes:

$$\alpha_{i,j} = \frac{k_j}{k_i} \tag{1.2}$$

being i and j two adjacents peaks, and i the less retained one.

The degree of separation between two solutes is measured by resolution, R:

$$R = \frac{t_{R,i} - t_{R,j}}{0,5(w_i + w_j)} \tag{1.3}$$

where w_i and w_j are the widths at the base of peaks i and j.

On the other hand, efficiency is a measure of the capacity of the column to restrain peak dispersion and thus, provide high resolution. The higher the efficiency, the more the peak dispersion is restrained, and the better the column. Column efficiency is measured in theoretical plates (N):

$$N = 16 \cdot \left(\frac{t_R}{w}\right)^2 \text{ and } N = 5,54 \cdot \left(\frac{t_R}{w_{1/2}}\right)^2 \tag{1.4}$$

where t_R is solute retention time and w and $w_{1/2}$ are the width of the base peak and its width at half height, respectively.

The height equivalent to the theoretical plate or the variance per unit length of a column (H) is calculated as the ratio of the column length to the column efficiency:

$$N = \frac{L}{H} \tag{1.5}$$

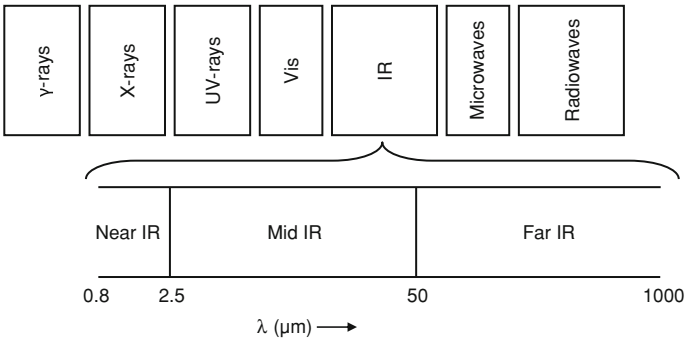

Fig. 1.4 IR region of the electromagnetic spectrum

Van Deemter equation describes which parameters contribute to H, that is, indicates how the different factors of column construction and operation affect its effectiveness. In the case of microparticulate columns both in HPLC and in CEC:

$$H = A + \frac{B}{\bar{u}} + C \cdot \bar{u} \tag{1.6}$$

where $\bar{u}$ is the mean of the linear velocity of the mobile phase.

In this equation the parameters that influence the overall peak width, are expressed in three terms:

- A-term, also known as eddy diffusion. This diffusion is due to the different lengths of the flow paths and the different velocities of the analytes that travel along the chromatographic bed. This contribution to H is a function only of the geometry of the stationary phase, that is, it does not depends on $\bar{u}$.
- B-term, which represents longitudinal diffusion: This diffusion is proportional to the diffusivity of the solutes and the time that sample passed into the column. As this time increases, diffusion is higher, and therefore the term B becomes important only at low flow rates. This dependence with time is reflected in the inverse of this contribution with respect to $\bar{u}$.
- C-term, which is the resistance against mass transfer between mobile and stationary phases. This term is proportional to $\bar{u}$ due to the slow mass transfer of solute between both phases. Thus, the contribution of C-term increases with mobile phase velocity as the equilibration time between the two phases is lower. The slow or delay with which mass transfers are made after each mobile phase movement leads to an additional peak broadening.

1.3.4 IR Spectroscopy

The IR region of the electromagnetic spectrum is that located between visible and microwave regions, as shown in Fig. 1.4.

The section of the IR region that provides more structural information at molecular level ranged between 4,000 and 650 cm^{-1}. This region is called mid-IR. However, the use of far-IR (between 650 and 200 cm^{-1}) has expanded considerably in recent decades, especially for the study of organometallic and inorganic compounds. The near-IR region, between 12,500 and 4,000 cm^{-1}, has been widely used for sample authenticity and classification purposes, although its used for structural purposes is limited. It could be said that the IR spectrum characterizes a molecular structure, since two different molecules, with the exception of optical isomers, should show different IR spectra. This property has been extensively used in the characterization of organic compounds. The existence of large databases of IR spectra allows the use of this technique coupled to chromatographic systems in the identification and rapid determination of components of organic mixtures. Moreover, IR spectroscopy could be applied for quantitative purposes using the Beer-Lambert law.

1.3.4.1 IR Spectrophotometers

According to the measurement technique used, IR spectrophotometers could be classified in dispersive and FTIR. The dispersive IR spectrophotometer emerged in the 1940s, while FTIR were developed for commercial use in the 1960s. The main difference between both types is that a dispersive IR spectrometer measures intensity over a narrow range of wavelengths at a time, while an FTIR spectrophotometer simultaneously collects spectral data in a wide spectral range. For this reason, and also by the speed, sensitivity, resolution and signal/noise ratio obtained with the FTIR spectrophotometer when compared with the dispersive one, FTIR is nowadays the most widely spectrophotometer used.

1.3.4.2 *Reflection Techniques in the IR* (© 2005–2012 PerkinElmer, Inc. All Rights Reserved. Adapted with Permission)

One of the strengths of IR spectroscopy is its ability as an analytical technique to obtain spectra from a very wide range of solids, liquids and gases. However, in many cases some form of sample preparation is required in order to obtain a good quality spectrum. Sample preparation is easier for liquid transmission studies when compared to solid transmission sampling but both suffer from inevitable reproducibility issues given the complexity of the sample preparation methods. In addition, preparation can be very messy and time consuming and is further complicated by difficulties in getting sample to matrix ratios correct and homogenous throughout the sample. The materials involved are fragile and hydroscopic and the quality of measurements can be adversely affected if handled or stored incorrectly. In these cases, reflection techniques address these issues. Among them, the ATR technique, which is used in this thesis, is discussed below.

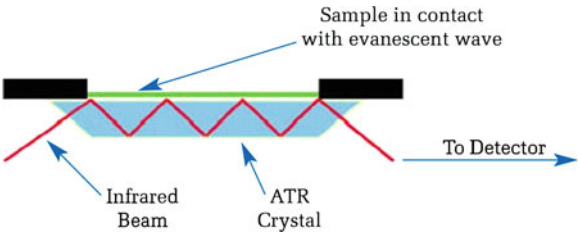

Fig. 1.5 A multiple reflection ATR system (© 2005–2012 PerkinElmer, Inc. All rights reserved. Reprinted with permission)

An ATR accessory operates by measuring the changes that occur in a totally internally reflected infrared beam when the beam comes into contact with a sample (indicated in Fig. 1.5). An infrared beam is directed onto an optically dense crystal with a high refractive index at a certain angle. This internal reflectance creates an evanescent wave that extends beyond the surface of the crystal into the sample held in contact with the crystal. It can be easier to think of this evanescent wave as a bubble of infrared that sits on the surface of the crystal. This evanescent wave protrudes only a few microns (0.5–5 μ) beyond the crystal surface and into the sample. Consequently, there must be good contact between the sample and the crystal surface. In regions of the IR spectrum where the sample absorbs energy, the evanescent wave will be attenuated or altered. The attenuated energy from each evanescent wave is passed back to the IR beam, which then exits the opposite end of the crystal and is passed to the detector in the IR spectrometer. The system then generates an infrared spectrum.

For the technique to be successful, the following two requirements must be met: (1) sample must be in direct contact with the ATR crystal and (2) the refractive index of the crystal must be significantly greater than that of the sample or else internal reflectance will not occur—the light will be transmitted rather than internally reflected in the crystal. Typically, ATR crystals have refractive index values between 2.38 and 4.01 at 2,000 cm^{-1}. It is safe to assume that the majority of solids and liquids have much lower refractive indices.

The traditional ATR design in which a thin sample was clamped against the vertical face of the crystal has been now been replaced by a horizontal design. In horizontal ATR units, the crystal is a parallel-sided plate with the upper surface exposed (Fig. 1.5). The number of reflections at each surface of the crystal is usually between five and ten, depending on the length and thickness of the crystal and the angle of incidence.

The issue of solid sample/crystal contact has been overcome to a great extent by the introduction of ATR accessories with very small crystals. The most frequently crystal is diamond because it has the best durability and chemical inertness. However, there are other materials available for ATR, such as zinc selenide (ZnSe) and germanium. ZnSe, which is the one employed in this thesis, is a relatively low cost ATR crystal material and is ideal for analyzing liquids and non-abrasive pastes and gels.

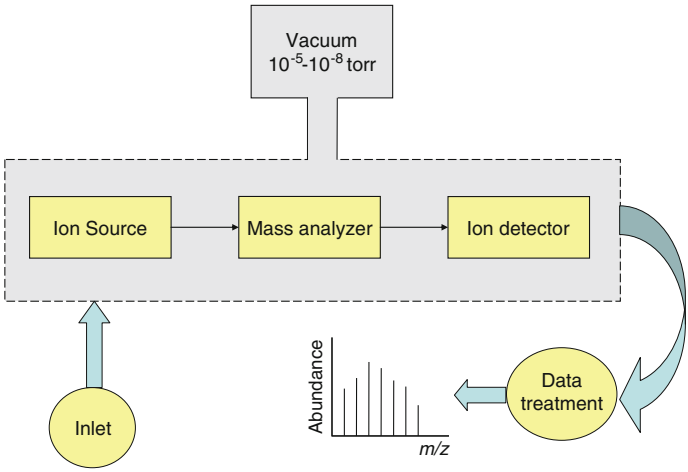

Fig. 1.6 Components of a mass spectrometer

1.3.5 MS

MS is a technique of wide application able to provide information about qualitative and quantitative composition of both organic and inorganic analytes in complex samples. Mass spectra are obtained by conversion of sample components into their gas-phase ions, which are separated according to their *m/z* ratio, being the analytical signal the abundance or intensity for each *m/z* value. The diagram showing the main components of a mass spectrometer is represented in Fig. 1.6.

As illustrated in this figure, a mass spectrometer is composed by an entry system that allows the introduction of a small amount of sample into the mass spectrometer. There are different entry systems depending on the type of sample to be analyzed (solid, liquid or gaseous). Sample can be introduced in a discrete manner using a syringe or continuously by coupling mass spectrometer with flow injection or with chromatographic or electrophoretic systems.

Jointly with the entry system, the ion source is the responsible of converting sample components into ions by bombardment with electrons, molecules, photons, etc. In many cases, such as the spectrometers used in this thesis, the entry system and the ion source are combined into a single component. Once the ions are produced, they pass into the mass analyzer, which is responsible of separating the various fragment ions produced in the ion source according to their ratio *m/z*. These fragments arrive at detector, which is responsible of converting the ion beam into an electrical signal which is amplified and recorded. These four components are usually found under a vacuum atmosphere at pressures of 10^{-7}–10^{-10} atm, to avoid collisions with background gas and other molecules, although in some cases, vacuum is

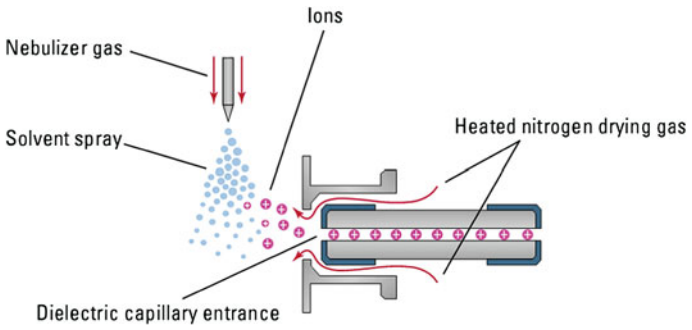

Fig. 1.7 ESI source scheme (Copyright 2001 Agilent Technologies, Inc. reproduced with permission)

only applied on mass analyzer and detector. Finally, once the analytical signal is registered, it is processed and analyzed providing a mass spectrum.

1.3.5.1 Ion Sources

The most commonly used ion sources, especially in the LC–MS coupling, are ESI, APCI and APPI, which are also used in the studies described below.

In an ESI source (see Fig. 1.7), the sample in solution was passed through a capillary nebulizer jointly with a coaxial N_2 flow. A high electric potential is applied at the exit of nebulizer that, jointly with N_2 flow, creates a fine spray of charged particles. The gas present at atmospheric pressure in the spray chamber carries the ions into capillary entrance, where the pressure is reduced to about 3 mbar by a vacuum pump.

APCI source (see Fig. 1.8) uses the heat provided by a vaporizer, which usually works at temperatures of 250–400 °C, and a coaxial N_2 flow, to convert the sample solution into a fine spray. With solvent evaporation, the resulting gas phase molecules are ionized by accelerated electrons which are formed by in an electrode by a corona discharge. This electrode is composed by a metal needle at which a high potential is applied.

In an APPI source (see Fig. 1.9), as in the APCI, the nebulization and ionization processes occur independently. For the correct used of this source, a certain concentration of a solvent that absorbs UV radiation (doping agent), such as a 1 % acetone, has to be added in the mobile phase. Also in this source, the heat provided by a vaporizer and a coaxial N_2 flow are used to convert the eluate into a fine spray, which passes through and area lit by a krypton lamp. The UV radiation produced by krypton lamp ionize dopant agent, which in turn ionizes solutes, being the ionization wavelength is short enough to not ionize common solvents such as

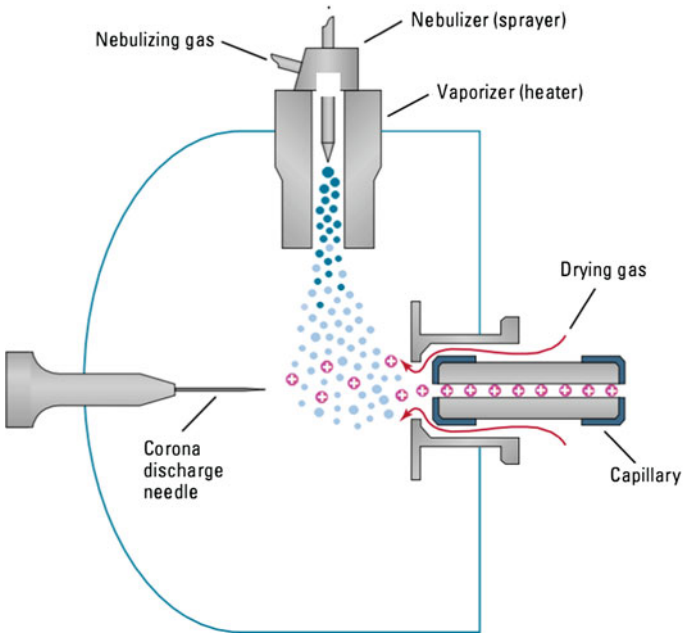

Fig. 1.8 APCI source scheme (Copyright 2001 Agilent Technologies, Inc. reproduced with permission)

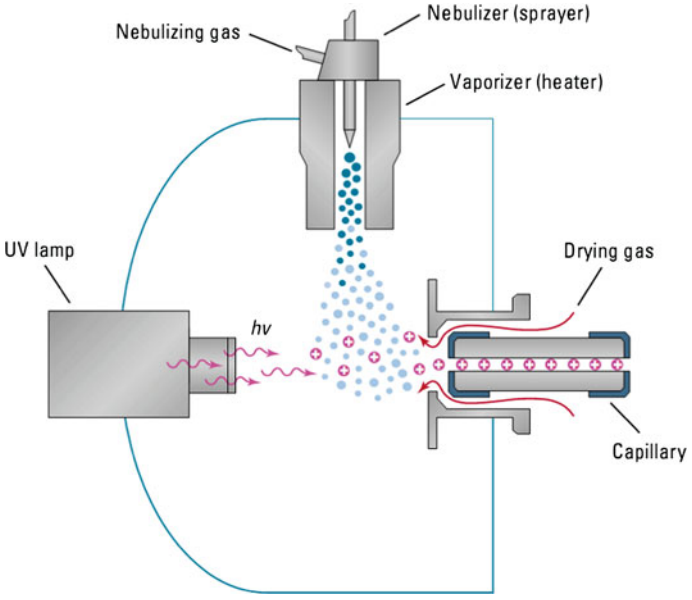

Fig. 1.9 APPI source scheme (Copyright 2001 Agilent Technologies, Inc. reproduced with permission)

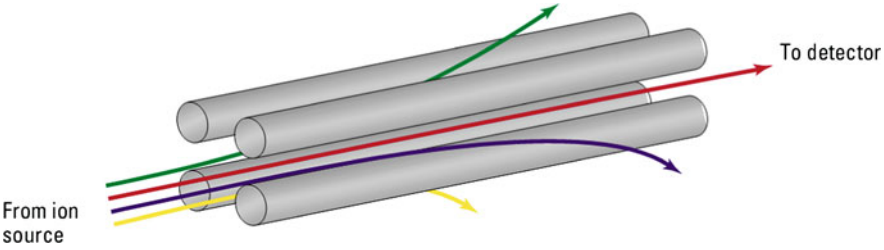

Fig. 1.10 Scheme of a quadrupole mass analyzer (Copyright 2001 Agilent Technologies, Inc. reproduced with permission)

water, MeOH and ACN. Finally, the ions produced by the solutes are attracted to the capillary and solvents are discarded.

1.3.5.2 Mass Analyzers

The most widely used mass analyzers are quadrupole (single or triple), ion trap and time of flight.

A quadrupole mass analyzer or quadrupole mass filter use oscillating electrical fields to selectively stabilize or destabilize the paths of ions passing through a radio frequency quadrupole field created between 4 parallel rods (see Fig. 1.10). Only the ions in a certain range of *m/z* ratio are passed through the system at any time, but changes to the potentials on the rods allow a wide range of *m/z* values to be swept rapidly, either continuously or in a succession of discrete hops.

A common variation of the transmission quadrupole is the triple quadrupole mass spectrometer. The "triple quad" has three consecutive quadrupole stages, the first acting as a mass filter to transmit a particular incoming ion to the second quadrupole, a collision chamber, wherein that ion can be broken into fragments. The third quadrupole also acts as a mass filter, to transmit a particular fragment ion to the detector. If a quadrupole is made to rapidly and repetitively cycle through a range of mass filter settings, full spectra can be reported. Likewise, a triple quad can be made to perform various scan types characteristic of tandem MS.

On the other hand, in an ion trap mass analyzer ions are trapped and analyzed, following the scheme described in Fig. 1.11, in a space defined by a ring electrode (usually connected to the main radio frequency potential) and between two endcap electrodes (typically connected to DC or auxiliary AC potentials).

The ions formed in the ionization source enter the analyzer, where different voltages are applied, generating a three-dimensional electric field in the cavity of the trap. During the storage phase, this field captures and focuses the ions into stable oscillation paths, depending on these potentials and the *m/z* of the ions. During the scanning or detection stage, the electrode potentials are altered to cause instability in ion trajectories and ejected them in the axial direction. The expulsion or withdrawal of the trap is made based on ion *m/z*, resulting in a mass spectrum. One of the characteristics of the quadrupole ion trap is its ability to isolate an ion

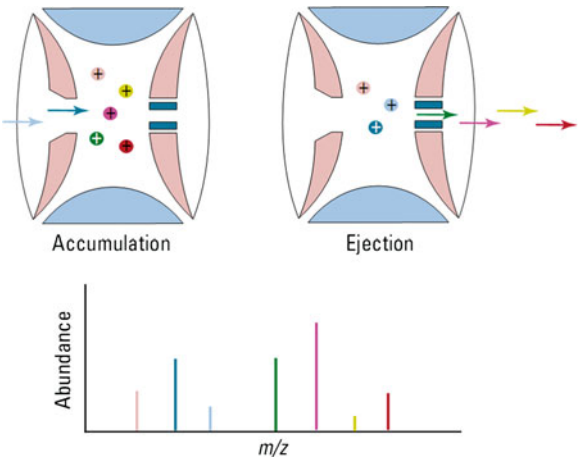

Fig. 1.11 Scheme of operation of an ion trap (Copyright 2001 Agilent Technologies, Inc. reproduced with permission)

and fragment it, thus obtaining the so-called "fragmentation spectrum" or MS/MS or MS^2 spectrum. The fragmentation is induced by collisions with helium atoms, making it possible to control the energy of collisions by controlling the speed of the ions in the trap.

1.3.5.3 Resolution

The ability of a mass spectrometer to distinguish between similar masses is usually expressed as resolution, R, defined as:

$$R = m/\Delta m \tag{1.7}$$

being m the nominal mass of the first peak, and Δm the difference between two adjacent peaks that are resolved.

The resolution that is needed in a mass spectrometer depends largely on the application. For example, to distinguish between ions of the same nominal mass but different exact masses, a high resolution equipment is needed.

1.3.6 Electronic Olfactometry

Although several approaches of an experimental "electronic nose" were made in the late 50s, it was in 1982 when Dodd et al. (1982) announced the beginning of a new technology: electronic olfactometry. These authors reported the design of an electronic nose based on a set of reversible and semi-selective sensors with different chemical properties. Selectivity was achieved by applying the pattern recognition techniques to the responses obtained with these sensors.

In 1993, Gardner and Bartlett (Gardner 1993) defined the electronic nose as an instrument composed by a set of electrochemical sensors with partial specificity associated with a pattern recognition system capable of recognizing both simple and complex odours. Compared to the human olfactory system, this is also composed by a system capable of detecting odours (human olfactory receptors) and by a data processing system (the brain), which requires training or learning and memory storage. In fact, in both cases, the goal is to relate the perceived aroma with a response that, once stored in the memory, will act as a model for further analysis. In the case of the electronic nose, that memory are databases which has been created from samples previously analyzed by the instrument and from external information that allows the identification of the sample. In this way the recognition system is "trained" to obtained optimal classifications that allow odour identification. Another similarity with biological systems is that the perceived aroma is processed in a global form, without identifying each constituent, so that the classification is based on the perceived aromatic similarity when the pattern is recognized.

1.3.6.1 Components of an Electronic Nose

Electronic noses include three major parts: a sample delivery system, a sensing system and a data analysis system, where both signal pre-processing and pattern recognition techniques are included.

The sample delivery system enables the generation of the headspace (volatile compounds) of a sample, which is the fraction analyzed. The system then injects this headspace into the sensing system of the electronic nose. The sample delivery system is essential to guarantee constant operating conditions.

On the other hand, the sensing system is the "reactive" part of the instrument. When in contact with volatile compounds, the sensors react, which means they experience a change of electrical properties. The main difference between electronic nose systems is the nature of the sensors used. Then, the main goal is to find sensor arrays with broad selectivity profiles but similar at the same time. This sensor array should generate a pattern recognition model capable of distinguishing between different samples. On the other hand, the sensor array responses to a specific compound should be as independent as possible (in a statistical sense) to gather as much information as possible about the compound. Depending on the type of measures in which sensor response is based, sensors can be classified as (1)conductivity sensors, such as MOS, conducting polymers and MOSFET, (2) piezoelectric sensors, such as QCM and SAW and (3) optical sensors.

MOS sensors are based on conductance changes induced by the absorption or reaction of gases on their surface. These sensors are formed by depositing a thick film of the metallic oxide into a ceramic piece that is electrically heated. They are mainly produced using SnO_2, ZnO, In_2O_3, WO_3, Fe_2O_3, Ga_2O_3 and TiO_2, being SnO_2 the oxide most widely used. In most cases, and in order to change sensor sensitivity, doping materials such as Pd or Pt are added. An example of a one of

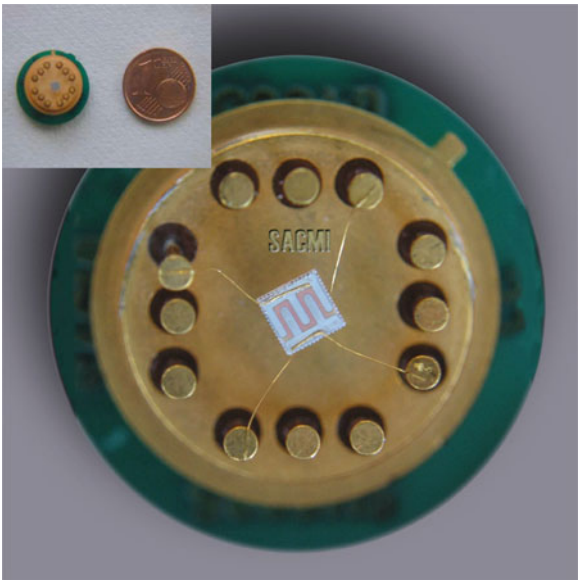

Fig. 1.12 Example of a MOS sensor used in this study (reprinted from M.J. Lerma-García et al., Ingredienti Alimentari 45 (2009) 12 by courtesy of Chiriotti Editori srl)

the MOS sensors used in this thesis is shown in Fig. 1.12. Metal oxides are an intrinsically *n*-type bulk semiconductors. Oxygen is always present in the eluent of the sensor arrays and upon exposure to oxygen, the oxygen is physi- or chemisorbed onto lattice vacancies in the semiconductor. The loss of the electron results in a decrease in conductance thus increasing resistance. When an odorant is present, the adsorbed oxygen species reacts and is removed from the surface allowing the electron to flow back into the conduction band thereby increasing the conductance (and decresing resistance). These sensors are capable of working at high temperatures (200–400 °C) and its sensitivity is quite high (5–5,000 ppm), but they usually present significant drift and contamination problems.

Finally, data analysis system treats all data provided by sensor arrays. The chemometric techniques used can be classified into two groups: signal pre-processing and pattern recognition techniques.

Signal pre-processing techniques are used to compensate possible deviations from sensor signals, and also to reduce variations between the measure of different samples. The techniques applied in these cases include:

- Handling of the baseline, which is a transformation based on the initial values of the sensors.
- Normalization of responses. Scaling is able to adjust the values of the responses of the sensors to prevent that some variables have more weight than others in the result obtained. The normalization methods are able to avoid experimental variations and reduce computational errors when applying pattern recognition techniques (Gardner 1993).

- Selection of the areas of the sensor response that provide discriminatory information without eliminating essential information. If all the data extracted from a sensor array was used, large matrices will be obtained; for this reason it is convenient to reduce them. Many authors have used different algorithms for this purpose (Hermle 1999), although commercial equipments normally used one data per sensor.

On the other hand, the automated pattern recognition system is the pattern recognition algorithm, which is created to extract useful information from sensors. There are a variety of pattern recognition methods available. The choice of the method depends on available data and the type of result that is required. Data treatment by multivariate techniques is one of the most employed methodologies to analyze electronic nose signals, as multivariate analysis generally involves data reduction. It reduces high dimensionality in a multivariate problem where variables are partly correlated, allowing the information to be displayed in a smaller dimension. Typical multivariate techniques include principal component analysis, feature weighting, ANN, cluster analysis, and discriminant function analysis. In a supervised pattern recognition technique input patterns are learned and associated with an odor class. In an unsupervised pattern recognition technique, the multidimensional configuration space from the preprocessor is converted into a feature space. The unknown chemical is identified by comparison to a knowledge base, from a previous learning scheme. More information on pattern recognition techniques can be found in the Sect. 1.3.7.

1.3.7 Data Statistical Treatment

1.3.7.1 Supervised Classification Analysis[1]

In the supervised classification analysis, models capable of predicting if an object belongs to a determine category are constructed. For this purpose, a data matrix that contains at least one variable that indicates the category to which each object belongs (categorical variable) is constructed. This categorical variable constitutes the variable to be predicted. Data matrix also contains one or more scale variables that describe object characteristics. These variables are used as predictors.

To construct a model, it is necessary to have a data set with known information of both, category and predictors (although data belonging to a category could be assumed). The object assignment to the categories should be exhaustive (all objects belong to a category) and mutually exclusive (any object belongs to more than one category). These objects form the training set, which is used to construct

[1] This section has been adapted and translated with permission from Editorial Síntesis, S.A from "G. Ramis Ramos and M. Celia García Álvarez-Coque, Quimiometría, Chap. 8: Análisis Clasificatorio".

the classification model. Once constructed, the model is used to predict the category of new objects from the measurement of predictors. The prediction of an evaluation set allows the validation of the model, which will be applied to predict the category of unknown samples (Ramis Ramos 2001).

There are different supervised classification techniques, such as discriminant analysis, which can be linear (LDA) or quadratic, and the ANN technique.

LDA. In LDA, an algorithm that searches functions or discriminant vectors, i.e, linear combinations of the manifest variables that maximize the variance between categories, while minimizing the intra-category variance, is used. To construct the model, it is necessary to assign the objects of the training set to a given category. To do this, a categorical variable is added to the data matrix containing as many categories as needed. The LDA estimates the coefficients a_1, a_2, …, a_m of the linear discriminant function, f, which is able to predict the object belonging s to one or another category:

$$f = a_1x_1 + a_2x_2 + \ldots + a_mx_m \tag{1.8}$$

The discriminant functions are constructed one at a time, looking for directions in space that maximize the expression:

$$\lambda' = \frac{SC_D}{SC_I} \tag{1.9}$$

where SC_D is the sum of squares of the Euclidean distances between objects belonging to different categories in the direction of the discriminant function, and SC_I is the sum of squared Euclidean distances between objects belonging to the same category, also in the direction of the discriminant function. From the q categories, $q - 1$ discriminant functions are obtained (although if the number of predictor variables, N, is lower than q, $N - 1$ discriminant functions will be obtained). The discriminant functions are obtained in decreasing order of their value λ' and maintaining orthogonality between them.

The λ' function varies widely with the number of objects and the separation between them. Therefore, instead of maximizing λ', is often minimized Wilks' lambda, which is defined as:

$$\lambda_W = \frac{1}{1 + \lambda'} = \frac{SC_I}{SC_I + SC_D} \tag{1.10}$$

This function takes values between 0 and 1. Categories with a clear separation gave λ_w values close to 0, while largely overlapping categories gave λ_w values close to unity (Ramis Ramos 2001).

ANN. An ANN is a systematic procedure of data processing. On a very simplified and abstract level, ANN is based on the cognitive process of the human brain, and is able to accurately predict categorical and scale variables. An ANN is not based on an explicit algebraic model, as LDA. It is based in a set of activation units, called nodes, perceptrons or artificial neurons, which are connected together in a network.

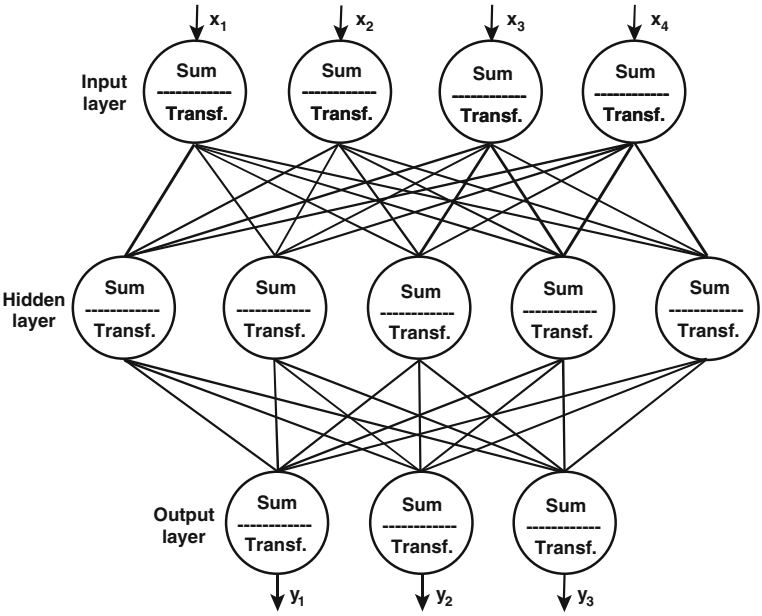

Fig. 1.13 Scheme of a neural network designed to predict three responses from four predictor variables (adapted with permission from Editorial Síntesis, S.A from G. Ramis Ramos and M. Celia García Álvarez-Coque, Quimiometría, from Fig. 8.12 of p. 192)

An artificial neuron contains two algorithms, one of them calculates the weighted sum of the values that come through the inlet connexions, and the other, called transfer function, generates a response or output that is communicated to other neurons. The network is able to "learn" mainly by adjusting the "weights" of the connections between neurons, until the network as a whole provides sufficiently precise predictions.

A diagram of a simple network, with neurons arranged in three rows or layers, called input layer, hidden layer and output layer, is shown in Fig. 1.13.

The input layer has as many entries as manifest variables, generating as many outputs as nodes in the output layer. The hidden layer has usually one or two more neurons than the input layer. Finally, the output layer has as many neurons as categorical variables to predict.

To get the network to function properly, it is necessary to subject it to a learning or training phase. When the network is trained, the neurons in the input layer obtained information of the values of the manifest variables for the new object. The results of the input layer are processed again in the hidden layer, and the results generated by it are reprocessed in the output layer. The results of the output layer are the probabilities that the new object belongs to each the categories for each of the categorical variables (Ramis Ramos 2001).

1.3.7.2 Linear Regression[2]

Linear regression is an explanatory model which aims to "explain" the P value of dependent variables (response variables) from the information provided by Q independent variables (predictors). Once the model is obtained, expressed as algebraic equations, the final objective is to predict future values of the dependent variables from the independents (Mongay 2005).

Univariate models. The simplest model is "simple linear regression," with a dependent variable and an independent, and which is reduced to:

$$y = b_0 + b_1 x + e \tag{1.11}$$

being $\hat{y} = b_0 + b_1 x$ the adjust linear function, where b_0 and b_1 are sample regression coefficients.

However, Q independent variables could be needed to explain the experimental data. In this case, the model corresponds to a multiple linear regression or MLR, which fits a simple equation with Q independent variables:

$$y = b_0 + b_1 x_{i1} + b_2 x_{i2} + b_3 x_{i3} + \ldots + b_Q x_{iQ} + e_i = b_0 + \sum_{q=1}^{Q} b_q x_{iq} + e_i \tag{1.12}$$

which is the general expression of the univariate linear model, where e_i is the error associated with the i-th observation when the model is accepted, x_{iq} is the i-th observation of the independent variable X_q, and b_0, b_1, …, b_Q are the Q + 1 parameters to be determined (Mongay 2005).

Multivariate models. In these models, there are P dependent variables ($P > 1$). These models do not pose major problems than the transformation of all vectors of the model matrices (Mongay 2005).

MLR is next described, since is the regression model used in this thesis.

One of the critical operations in MLR is the selection of predictor variables to be included in the model. The model should include a single predictor variable to represent each of the sources of variance of data, that being relevant, are also correlated with the response. If all significant sources of variance are not taken into account, "underfitted" models, which made predictions affected by systematic error, will be obtained. In the opposite case, when the model included more sources of variance than those strictly necessary, "overfitted" models are obtained. In this case, model predicions will be affected by an excessive error (Ramis Ramos 2001).

[2] The information included in this section has been obtained and translated with permission from Editorial Síntesis, S.A from "G. Ramis Ramos and M. Celia García Álvarez-Coque, Quimiometría, Chap. 9: Calibración y regresión múltiple y multivariante" and from the Servei de Publicacions de la Universitat de València from "C. Mongay Fernández, Quimiometría, Chap. 15 : Regresión lineal múltiple.

A simple procedure for variable selections is to initially include in the model all variables that have some probability of influencing the response. Regression coefficients are obtained, and then the variable associated to the lowest regression coefficient is eliminated. The process is repeated until all variables have non-negligible values of the regression coefficient. However, this technique should be applied with caution, since the presence in the model correlated variables reduces its regression coefficient. Therefore, when there is a group of strongly correlated variables, only one variable should be selected to represent the group.

On the other hand, there are more rigorous selection procedures known as "forward", "backward" and "stepwise". These procedures are usually found in statistical packages, and are very helpful when a large number of variables are handled, and when it is not easy to assign the variables to specific sources of variance. In the three methods, the variables are entered or removed from the model following a criterion of "in–out". Thus, in the "forward" algorithm, linear correlations of all variables with the response are calculated, and it is chosen as candidate the variable with the highest r^2 value. The variable is only introduced if it exceeds the entrance threshold of the following F-test:

$$F = \frac{SC'_{exp} - SC_{exp}}{\frac{SC'_{res}}{n-p}} \tag{1.13}$$

where SC'_{exp} and SC_{exp} are the sums of squares of the variance explained by the models constructed including and excluding the variable candidate, respectively, and SC'_{res} is the sum of squares of the residual variance of the model constructed including the candidate variable. If the first variable entered the model, it is considered as the next candidate the variable that has a higher correlation with the model residuals, that is, the variable which is more correlated with response after removing the variance due to the first variable. The second variable entered the model if it also exceeds the entrance threshold. The process continues with a third candidate, and ends when there are no variables with a partial correlation with the response significantly different from zero, and that also exceeds the entrance threshold. In the "backwards" algorithm, all variables are initially introduced in the model, and then are sequentially eliminated according to the F test. The first variable to be eliminated is the variable that has the lowest correlation with the response. The process ends when there are no variables in the model that satisfy the rejection threshold. Finally, in "stepwise" algorithm, variables are sequentially introduced, as in the "forward" algorithm. However, the entrance of a new variable modifies the significance of those variables which are already present in the model. For this reason, after the inclusion of a new variable, a rejection threshold is used to decide if one of the other variables should be removed from the model. The process terminates when there are no variables entering or being eliminated from the model (Ramis Ramos 2001).

Once the model is obtained, it is necessary to evaluate the goodness of fit. This can be estimated based on the coefficient of multiple determination, R^2, and also

by the sum of squared residuals. However, if the sum of squares is calculated considering only the objects of the calibration set, the ability of the model to accurately predict new objects, not included in this set, could be excessively optimistic. To solve this problem, cross-validation techniques are used, such as leave-one-out, which is the most common used. Leave-one-out validation involves the use of a single object from the original sample matrix as the validation set, and the remaining objects as the training set. This is repeated such that each object in the sample matrix is used once as the validation set. In addition to this, the prediction capability of a model could be also evaluated using an independent evaluation set, which will determine the percentage of correctly predicted objects (Ramis Ramos 2001).

References

Abidi SL (2000) J Chromatogr A 881:197
Abidi SL (2004) J Chromatogr A 1059:199
Abou Hadeed AMF, Kotb AR, Daniels CEJ (1990) Food Chem 35:167
Agiomyrgianaki A, Petrakis PV, Dais P (2010) Talanta 80:2165
Al-Ismail K, Caboni MF, Lercker G (1998) Riv Ital Sost Grasse 75:175
Al-Ismail K, Caboni MF, Rodríguez-Estrada MT, Lercker G (1999) Grasas Aceites 50:448
Allalout A, Krichène D, Methenni K, Taamalli A, Oueslati I, Daoud D, Zarrouk M (2009) Sci Hort 120:77
Alter M, Gutfinger T (1982) Riv Ital Sost Grasse 59:14
Aparicio R, Aparicio-Ruíz R (2000) J Chromatogr A 881:93
Aparicio R, Morales MT (1995) J Sci Food Agric 67:247
Aparicio R, Alonso V, Morales MT (1994) Grasas Aceites 45:241
Aturki Z, D'Orazio G, Fanali S (2005) Electrophoresis 26:798
Azadmard-Damirchi S, Savage GP, Dutta PC (2005) J Am Oil Chem Soc 82:717
Baccouri O, Bendini A, Cerretani L, Guerfel M, Baccouri B, Lercker G, Zarrouk M, Miled DDB (2008a) Food Chem 111:322
Baccouri O, Guerfel M, Baccouri B, Cerretani L, Bendini A, Lercker G, Zarrouk M, Daoud Ben Miled D (2008b) Food Chem 109:743
Ballesteros E, Gallego M, Valcárcel M (1995) Anal Chim Acta 308:253
Barceló-Barrachina E, Moyano E, Galceran MT (2004) Electrophoresis 25:1927
Barranco D, Cimato A, Florino P, Rallo L, Touzani A, Castañeda C, Sefarini F, Trujillo I (2001) Catálogo mundial de variedades de olivo. Ed. Consejo Oleícola Internacional
Bendini A, Bonoli M, Cerretani L, Biguzzi B, Lercker G, Gallina-Toschi T (2003) J Chromatogr A 985:425
Bendini A, Cerretani L, Carrasco-Pancorbo A, Gómez-Caravaca AM, Segura-Carretero A, Fernández-Gutiérrez A, Lercker G (2007) Molecules 12:1679
Bendini A, Cerretani L, Salvador MD, Fregapane G, Lercker G (2009) Ital J Food Sci 21:389
Benitez-Sánchez PL, León-Camacho M, Aparicio R (2003) Eur Food Res Technol 218:13
Blekas G, Tsimidou M, Bouskou D (1995) Food Chem 52:289
Bonoli M, Bendini A, Cerretani L, Lercker G, Gallina-Toschi T (2004) J Agric Food Chem 52:7026
Boskou D (1996) Olive oil, chemistry and technology. AOCS Press, Champaign
Boskou D (2002) Olive oil. In: Gunstone FD (ed) Vegetable oils in food technology. CRC Press, Blackwell Publishing Ltd., Oxford, pp 244–277

Brenes M, García A, García P, Garrido A (2000) J Agric Food Chem 48:5178
Cahours X, Cherkaoui S, Rozing GP, Veuthey JL (2002) Electrophoresis 23:2320
Camurati F, Tagliabue S, Bresciani A, Sberveglieri G, Zaganelli P (2006) Riv Ital Sost Grasse 83:205
Cañabate-Díaz B, Segura Carretero A, Fernández-Gutiérrez A, Belmonte Vega A, Garrido Frenich A, Martínez Vidal JL, Duran Martos J (2007) Food Chem 102:593
Cantó-Mirapeix A, Herrero-Martínez JM, Mongay-Fernández C, Simó-Alfonso EF (2008) Electrophoresis 29:4399
Caponio F, Alloggio V, Gomes T (1999) Food Chem 64:203
Caponio F, Pasqualone A, Gomes T (2002) Eur Food Res Technol 215:114
Carelli AA, Cert A (1993) J Chromatogr A 630:213
Carney RA, Robson MM, Bartle KD, Myers P (1999) J High Resolut Chromatogr 22:29
Carrasco-Pancorbo A, Cruces-Blanco C, Segura-Carretero A, Fernández-Gutiérrez A (2004) J Agric Food Chem 52:6687
Carrasco-Pancorbo A, Cerretani L, Bendini A, Segura-Carretero A, Gallina Toschi T, Fernández-Gutiérrez A (2005) J Sep Sci 28:837
Carrasco-Pancorbo A, Gómez-Caravaca AM, Cerretani L, Bendini A, Segura-Carretero A, Fernández-Gutiérrez A (2006) J Agric Food Chem 54:7984
Carrasco-Pancorbo A, Neusúβ C, Pelzing M, Segura-Carretero A, Fernández-Gutiérrez A (2007a) Electrophoresis 28:806
Carrasco-Pancorbo A, Cerretani L, Bendini A, Segura-Carretero A, Lercker G, Fernández-Gutiérrez A (2007b) J Agric Food Chem 55:4771
Cartoni GP, Coccioli F, Jasionowska R, Ramires D (2000) Ital J Food Sci 12:163
Cercaci L, Rodríguez-Estrada MT, Lercker G (2003) J Chromatogr A 985:211
Cercaci L, Passalacqua G, Poerio A, Rodriguez-Estrada MT, Lercker G (2007) Food Chem 102:66
Cerretani L, Bendini A, Del Caro A, Piga A, Vacca V, Caboni MF, Gallina Toschi T (2006) Eur Food Res Technol 222:354
Chiavaro E, Vittadini E, Rodriguez-Estrada MT, Cerretani L, Bendini A (2008) Food Chem 110:248
Chirica GS, Remcho VT (2001) J Chromatogr A 924:223
Choe E, Min DB (2006) Compr Rev Food Sci 5:169
Choo YM, Yap SC, Ooi CK, Ma AN, Goh SH, Ong ASH (1996) J Am Oil Chem Soc 73:599
Choudhary G, Apffel A, Yin H, Hancock W (2000) J Chromatogr A 887:85
Christie WW (1992) Advances in lipid methodology. The Oily Press, Ayr, pp 239–271
Christophoridou S, Dais P (2009) Anal Chim Acta 633:283
Cimato A, Dello Monaco D, Distante C, Epifani M, Siciliano P, Taurino AM, Zuppa M, Sani G (2006) Sens Actuat B 114:674
Codex Alimentarius Commission (1993) Proposed draft standard for named vegetable oils, CX 1993/16, issued by the Joint FAO/WHO Food standards program. Rome, Italy
Commission Regulation (EC) (2002) No. 796/2002 of 6 May 2002 amending Regulation (EEC) No 2568/91 on the characteristics of olive oil and olive-pomace oil and on the relevant methods of analysis and the additional notes in the Annex to Council Regulation (EEC) No 2658/87 on the tariff and statistical nomenclature and on the Common Customs Tariff. Off J Eur Commun
Commission Regulation (EC) (2008) No. 640/2008 of 4 July 2008 amending Regulation (ECC) No. 2568/91 on the characteristics of olive oil and olive-residue oil and on the relevant methods of analysis. Off J Eur Commun L178
Commission Regulation (EEC) (1991) No. 2568/91 of 11 July 1991 on the characteristics of olive oil and olive-residue oil and on the relevant methods of analysis. Off J Eur Union L128
Cortesi N, Fusetti MG, Fedeli E (1987) Riv Ital Sost Grasse 64:513
Cortesi N, Rovellini P, Fedeli E (1991) Riv Ital Sost Grasse 68:511
Cunha SC, Oliveira MBPP (2006) Food Chem 95:518
Cunha SC, Amaral JS, Fernandes JO, Oliveira MBPP (2006a) J Agric Food Chem 54:3351

Cunha SC, Fernandes JO, Beatriz M, Oliveira PP (2006b) J Chromatogr A 1128:220
Dermaux A, Sandra P, Ferraz V (1999) Electrophoresis 20:74
Devowsky JK (2002) J Liq Chromatogr Relat Tech 25:1875
D'Imperio M, Dugo G, Alfa M, Mannina L, Segre AL (2007) Food Chem 102:956
Dood GH, Persaud KC (1982) Nature 299:352
Dugo P, Kumm T, Crupi ML, Cotroneo A, Mondello L (2006) J Chromatogr A 1112:269
Ericson C, Hjertén S (1999) Anal Chem 71:1621
Farhoosh R, Pazhouhanmehr S (2009) Food Chem 114:1002
Fasciotti M, Pereira N, Annibal D (2010) Talanta 81:1116
Fedeli E (1977) Lipids of olives. In: Ralph E, Holman T (eds) Progress on chemistry of fats and other lipids. Pergamon Press, Paris, pp 15–74
Fragaki G, Spyros A, Siragakis G, Salivaras E, Dais P (2005) J Agric Food Chem 53:2810
Franceschi S, Favero A, Conti E, Salamini R, Volpe R, Negri E, Barman L, La Vecchia C (1999) British J Cancer 80:614
Frankel EN (1985) Chemistry of autoxidation: mechanism, products and flavor significance. In: Min DB, Smouse TH (eds) Flavor chemistry of fats and oils. AOCS Press, Champaign, pp 1–37
Frankel EN (1998) Lipid oxidation. The Oily Press, Dundee
Fronimaki P, Spyros A, Christophoridou S, Dais P (2002) J Agric Food Chem 50:2207
Fujimoto C, Kino J, Sawada H (1995) J Chromatogr A 716:107
Galeano Diaz T, Durán Merás I, Sánchez Casas J, Alexandre Franco MF (2005) Food Control 16:339
García A, Brenes M, García P, Romero C, Garrido A (2003) Eur Food Res Technol 216:520
García-González D, Aparicio R (2010) Food Chem 120:572
Gardner JW, Bartlett PN (1993) Sens Actuators B 18:211
Gimeno E, Castellote AI, Lamuela-Raventós RM, De la Torre MC, López-Sabater MC (2000a) J Chromatogr A 881:255
Gimeno E, Calero E, Castellote AI, Lamuela-Ravento's RM, De La Torre MC, Lo'pez-Sabater MC (2000) J Chromatogr A 881
Gómez-Caravaca AM, Carrasco-Pancorbo A, Cañabate-Díaz B, Segura-Carretero A, Fernández-Gutiérrez A (2005) Electrophoresis 26:3538
Gordon MH (2001) Measuring antioxidant activity. In: Pokorný J, Yanishlieva N, Gordon MH (eds) Antioxidants in foods. Woodhead Publishing Ltd., Oxford
Gruszka J, Kruk J (2007) Chromatographia 66:909
Gusev I, Huang X, Horváth C (1999) J Chromatogr A 855:273
Gutfinger J, Letan A (1974) Lipids 9:658
Guth H, Grosch W (1993) J Am Oil Chem Soc 70:513
Gutiérrez-Rosales F, Perdiguero S, Gutiérrez R, Olías JM (1992) J Am Oil Chem Soc 69:394
Gutiérrez-Rosales F, Ríos JJ, Gómez-Rey ML (2003) J Agric Food Chem 51:6021
Hajimahmoodia M, Vander Heydenb Y, Sadeghia N, Jannata B, Oveisia MR, Shahbaziana S (2005) Talanta 66:1108
Hamilton RJ (1994) The chemistry of rancidity in foods. In: Allen JC, Hamilton RJ (eds) rancidity in foods. Blackie Academic & Professional, London, pp 1–21
Harborne JB, Dey PM (1989) Methods in plant biochemistry. Academic Press, London
Hermle T, Weimar U, Mitrovics J, Rosenmistiel W, Göpel W (1999) Sens Actuators B 65:253
Hidalgo FJ, Zamora R (2006) Trends Food Sci Technol 17:56
Hidalgo FJ, Alaiz M, Zamora R (2001a) Anal Chem 73:698
Hidalgo FJ, Alaiz M, Zamora R (2001b) J Agric Food Chem 49:4267
Hidalgo FJ, Alaiz M, Zamora R (2002) J Am Oil Chem Soc 79:685
Hjertén S, Liao JL, Zhang R (1989) J Chromatogr 473:273
Hodge E, English DR, McCredie MRE, Severi G, Boyle P, Hopper JL, Giles GG (2004) Cancer Cause Control 15:11
Hoegger D, Freitag R (2001) J Chromatogr A 914:211
Holčapek M, Lísa M, Jandera P, Kabátová N (2005) J Sep Sci 28:1315

Horstkötter C, Jiménez-Lozano E, Barrón D, Barbosa J, Blaschke G (2002) Electrophoresis 23:3078
Jebe TA, Matlock MG, Sleeter RT (1993) J Am Oil Chem Soc 70:1055
Kiosseoglou B, Vlachopoulou L, Boskou D (1987) Grasas Aceites 38:102
Kiritsakis A (1998) Olive oil, 2nd edn. Food and Nutrition Press, Inc., Trumbull
Kiritsakis A, Christie WW (2003) Análisis de aceites comestibles. In: Aparicio R, Hardwood J (eds) Manual del aceite de oliva. Ed. Mundi-Prensa, Madrid, pp 135–162
Kiritsakis AK, Markakis P (1991) Olive oil analysis. In: Linskens HF, Jackson JF (eds) Modern methods of plant analysis: essential oils and waxes. Springer, Berlin, pp 1–20
Klampfl CW (2004) J Chromatogr A 1044:131
Knox JH (1988) Chromatographia 26:329
Kotani A, Kusu F, Takamura K (2002) Anal Chim Acta 465:199
Lanzon A, Albi T, Cert A, Gracian J (1994) J Am Oil Chem Soc 71:285
Lazzez A, Perri E, Caravita MA, Khlif M, Cossentini M (2008) J Agric Food Chem 56:982
Liao JL, Chen N, Ericson C, Hjertén A (1996) Anal Chem 68:3468
Liberatore L, Procida G, D'Alessandro N, Cichelli A (2001) Food Chem 73:119
Liu X, Takahashi LH, Fitch WL, Rozing G, Bayle C, Couderc F (2001) J Chromatogr A 924:323
López-Feria S, Cardenas S, García-Mesa JA, Valcárcel M (2008) J Chromatogr A 1188:308
Macher MB, Holmqtvist A (2001) J Sep Sci 24:179
Manzi P, Panfili G, Esti M, Pizzoferrato L (1998) J Sci Food Agric 77:115
Marcos Lorenzo I, Pérez Pavón JL, Fernández Laespada ME, García Pinto C, Moreno Cordero B (2002) J Chromatogr A 945:221
Mariani C, Fedeli E (1985) Riv Ital Sost Grasse 62:3
Mariani C, Fedeli E, Morchio G (1987) Riv Ital Sost Grasse 64:359
Mariani C, Bellan G, Lestini E, Aparicio R (2006) Eur Food Res Technol 223:655
Martínez-Vidal JL, Garrido-Frenich A, Escobar-García MA, Romero-González R (2007) Chromatographia 65:695
Maryam J, Mahdi K, Javad K (2009) J Am Oil Chem Soc 86:103
Mateos R, Trujillo M, Pérez-Camino MC, Moreda W, Cert A (2005) J Agric Food Chem 53:5766
Medvedovici A, David F, Sandra P (1997) Chromatographia 44:37
Melchert HU, Pollock D, Pabel E, Ruback K, Stan HJ (2002) J Chromatogr A 976:215
Melton SL, Jafra S, Sykes D, Trigiano MK (1994) J Am Oil Chem Soc 71:1301
Merthar M, Podgornik A, Žigon M, Štrancar A (2003) J Sep Sci 26:322
Miguez-Mosquera I, Gandul-Rojas B, Garrido-Fernandez J, Gallardo-Guerrero L (1990) J Am Oil Chem Soc 67:192
Mongay Fernández C (2005) Quimiometría. Servei de Publicacions de la Universitat de València, Spain pp 322–323 (chapter 15: Regresión lineal múltiple)
Morales MT, Aparicio R (1999) J Am Oil Chem Soc 76:295
Morales MT, Tsimidou M (2003) El papel de los compuestos volátiles y polifenoles en la calidad sensorial del aceite de oliva. In: Aparicio R, Harwood J (eds) Manual del aceite de oliva. Ed. Mundi-Prensa, Madrid, Spain, pp 381–442
Morales MT, Aparicio R, Rios JJ (1994) J Chromatogr A 668:455
Ntsourankoua H, Artaud J, Guerere M (1994) Fr Ann Fals Expert Chim Toxicol 87:91
Ocakoglu D, Tokatli F, Ozen B, Korel F (2009) Food Chem 113:401
Paganuzzi V (1979) J Am Oil Chem Soc 56:925
Paganuzzi V (1982) Riv Ital Sost Grasse 59:415
Palm A, Novotny MV (1997) Anal Chem 69:4499
Panfili G, Fratianni A, Irano M (2003) J Agric Food Chem 51:3940
Parcerisa J, Boatella J, Codony R, Rafecas M, Castellote AI, García J, López A, Romero A (1995) J Agric Food Chem 43:13
Parcerisa J, Casals I, Boatella J, Codony R, Rafecas M (2000) J Chromatogr A 881:149
Perona JS, Barrón LJR, Ruiz-Gutierrez V (2001) J Chromatogr A 706:173
Peters EC, Petro M, Svec F, Fréchet JMJ (1998a) Anal Chem 70:2288
Peters EC, Petro M, Svec F, Fréchet JMJ (1998b) Anal Chem 70:2296

Petro M, Svec F, Fréchet JMJ (1996) J Chromatogr A 752:59
Philips KM, Ruggio DM, Toivo JI, Swank MA, Simpkins AH (2002) J Food Compos Anal 15:123
Poulli KI, Mousdis GA, Georgiou CA (2006) Anal Bioanal Chem 386:1571
Psomiadou E, Tsimidou M (1998) J Agric Food Chem 46:5132
Ramis Ramos G, García Álvarez-Coque MC (2001) Quimiometría.In: Síntesis SA (ed) Madrid, Spain (2001) pp 184–192 and 213–218
Ranalli A, Pollastri L, Contento S, Di Loreto G, Lannucci E, Lucera L, Russi F (2002) J Sci Food Agric 82:854
Rathore AS (1998) Horváth. Anal Chem 70:3271
Rathore AS, Horváth C (1996) J Chromatogr A 743:231
Rebscher H, Pyell U (1994) Chromatographia 38:737
Reiners J, Grosch W (1998) J Agric Food Chem 46:2754
Ríos JJ, Gil MJ, Gutiérrez-Rosales F (2005) J Chromatogr A 1903:167
Rivera del Álamo RM, Fregapane G, Aranda F, Gómez-Alonso S, Salvador MD (2004) Food Chem 84:533
Robison JL, Tsimidou M, Macrae R (1985) J Chromatogr A 324:35
Rodríguez-Méndez ML, Apetrei C, de Saja JA (2008) Electrochim Acta 53:5867
Rossell JB (1991) Vegetable oils and fats. In: Rossell JB, Pritchard JLR (eds) Analysis of oilseeds, fats and fatty foods. Elsevier Science, London, pp 261–327
Rozing GP, Dermaux A, Sandra P (2001) J Chromatogr Library Ser, No. 62, Elsevier Science B.V., Amsterdam, p 39
Saba A, Mazzini F, Raffaelli A, Mattei A, Salvadori P (2005) J Agric Food Chem 53:4867
Sacchi R, Addeo F, Paolillo L (1997) Magn Reson Chem 35:S133
Saitta M, Salvo F, Di Bella G, Dugo G, La Torre GL (2009) Food Chem 112:525
Sakouhia F, Harrabia S, Absalonb C, Sbeia K, Boukhchinaa S, Kallela H (2008) Food Chem 108:833
Segura-Carretero A, Carrasco-Pancorbo A, Cortacero S, Gori A, Cerretani L, Fernández-Gutiérrez A (2008) Eur J Lipid Sci Technol 110:1142
Serani A, Piacenti D (1992) J Am Oil Chem Soc 69:469
Servili M, Montedoro G (2002) Eur J Lipid Sci Technol 104:602
Shamsi SA, Miller BE (2004) Electrophoresis 25:3927
Sikorska E, Gliszczyńska-Świgło A, Khmelinskii I, Sikorski M (2005) J Agric Food Chem 53:6988
Silva SD, Rosa NF, Ferreira AE, Boas LV, Bronze MR (2009) Food Anal Method 2:120
Sindhu-Kanya TC, Jaganmohan-Rao L, Shamanthaka-Sastry MC (2007) Food Chem 101:1552
Solomon NW (1998) Nutr Rev 56:309
Stefanoudaki E, Kotsifaki F, Koutsaftakis A (1999) J Am Oil Chem Soc 76:623
Suárez M, Macià A, Romero MP, Motilva MJ (2008) J Chromatogr A 1214:90
Tasioula-Margari M, Okogeri O (2001) Food Chem 74:377
Tateo E, Brunelli N, Cucurachi S, Ferillo A (1993) New trends in the study of the merits and shortcoming of olive oil in organoleptic terms in correlation with GC/MS analysis of aromas. In: Charalampous G (ed) Food flavors, ingredients and composition. Elsevier Science B. V., Amsterdam, pp 301–311
Tena N, Lazzez A, Aparicio-Ruiz R, García-González DL (2007) J Agric Food Chem 55:7852
Thanh TT, Vergnes MF, Kaloustian J, El-Moselhy TF, Amiot-Carlin MJ, Portugal H (2006) J Sci Food Agric 86:220
Tiscornia E, Fiorina N, Evangelisti F (1982) Riv Ital Sost Grasse 59:519
Torres MM, Maestri DM (2006) Food Chem 96:507
Tsimidou M (1998) Ital J Food Sci 10:99
Tsimidou M, Papadopoulos G, Boskou D (1992) Food Chem 44:53
Tsuda T (1987) Anal Chem 59:521
Tura D, Gigliotti C, Pedo S, Failla O, Bassi D, Serraiocco A (2007) Sci Hort 112:108

Van der Klift EJC, Vivó-Truyols G, Claassen FW, van Holthoon FL, van Beek TA (2008) J Chromatogr A 1178:43
Velasco J, Dobarganes C (2002) Eur J Lipid Sci Technol 104:661
Vichi S, Pizzale L, Conte LS, Buxaderas S, López-Tamames E (2003) J Agric Food Chem 51: 6564
Vissers MN, Zock PL, Leenen R, Roodenburg AJC, van Putte KPAM, Katan MB (2001) Free Radical Res 35:619
Vlachos N, Skopelitis Y, Psaroudaki M, Konstantinidou V, Chatzilazarou A, Tegou E (2006) Anal Chim Acta 573–574:459
Wall W, Li J, el Rassi Z (2002) J Sep Sci 25:1231
Xie S, Svec F, Fréchet JMJ (1997) J Chromatogr A 775:65
Zamora R, Alaiz M, Hidalgo FJ (2001) J Agric Food Chem 49:4267
Zhang L, Ping G, Zhang L, Zhang W, Zhang Y (2003) J Sep Sci 26:331

Chapter 2
Objectives and Work Plan

The objective of this PhD thesis was the development of fast and sensitive methods for the characterization of vegetable oils according to their botanical origin, and for the characterization and authentication of olive oils in relation to their quality, genetic variety and geographical origin. For this purpose, oils selected considering each and every one of the factors discussed in the introduction section will be used.

First, methods based on the determination of Ts and T_3s in oils of different botanical origin will be established. For this purpose, different techniques such as CEC and nano-LC will be employed. In turn, the sterol content in oils of different botanical origin will be established by UPLC and CEC. For nano-LC and CEC analysis, packed columns (porous silica) and methacrylate monolithic columns will be used. The latter, which are not commercial, will be developed in the laboratory.

On the other hand, the application of different chemometric tools, such as LDA, will allow the development of methods of high discriminatory power to classify vegetable oils according to their botanical origin. For this purpose, FTIR spectra obtained by depositing the oils directly on the ATR prism, the profile of the alcoholic fraction established by HPLC–MS and the profiles of amino acids and sterols obtained either by direct infusion MS or by HPLC, using both UV and MS detection, will be used.

Later, work will be focused on the study of olive oil. In first place, a method capable of assessing olive oil quality will be developed. For this purpose, free fatty acid profiles established by direct infusion MS will be used. These profiles will be employed to classify olive oils according to their quality.

On the other hand, an olfactometry method using MOS sensor arrays will be also developed to classify different oils according to the sensory threshold of the typical organoleptic defects of olive oil (fusty, mouldy, muddy, rancid and winey). The sensory threshold will be previously established by a tasting panel. Moreover,

M. J. Lerma García, *Characterization and Authentication of Olive and Other Vegetable Oils*, Springer Theses, DOI: 10.1007/978-3-642-31418-6_2,

the data obtained by the electronic nose will be used to quantify the percentage of defect present in several oil samples.

Next, different methods will be developed to classify EVOOs according to their genetic variety by constructing LDA models. For this purpose, free fatty acid and phenolic compound profiles established by direct infusion MS, sterol profiles established by HPLC–MS and UPLC-MS and ATR-FTIR spectra obtained by depositing oils directly on the prism of the ATR, will be used as predictors. Also, methods to classify EVOOs according to their geographical origin will be developed, using in this case phenolic compound profiles established by CEC as predictors.

Finally, the oxidation products of olive oils will be studied, being methods for its evaluation proposed. In first place, the changes produced during storage in two aliquots of a same olive oil sample, which differ in their content of phenolic compounds (since one of the aliquots will have undergone a prior process of phenolic content extraction), will be studied. Both aliquots will be subjected to an accelerated aging for seven weeks, analyzing a portion of each of them once a week. The differences obtained in free acidity, absorbance in the UV, peroxide value, oxidative stability, fatty acids and Ts depending on the content of phenols in the starting sample, and the evolution of these values with accelerated aging time, will be studied. Moreover, the transformation undergone by phenolic compounds during the oxidation process will be monitored by HPLC–MS. These same samples will be also analyzed by direct infusion MS, and by using an array of MOS sensors so that they can be classified according to their oxidative status.

Finally, MLR models will be constructed to predict OFA content through analysis of different olive oil samples, either by FTIR spectroscopy and MOS sensors.

Chapter 3
Materials and Methods

3.1 Reagents and Materials

3.1.1 Standards

The following standards were used: α-, γ-, δ-T y α-T-AcO (Sigma, St. Louis, MO, USA), erythrodiol (Fluka, Buchs, Suiza), β-sitosterol (mixture of 75 % β-sitosterol and 10 % campesterol), ergosterol, stigmasterol (Acros Organics, Morris Plains, NJ, USA), cholesterol (Aldrich, Milwaukee, WI, USA) and lanosterol (Maybridge Chemical Co., Cornwall, UK).

On the other hand, the following aliphatic alcohol standards were used: 1-octadecanol (C18, Fluka), 1-hexadecanol (C16), 1-docosanol (C22), 1-tetracosanol (C24) and 1-hexacosanol (C26, Sigma), and also the following amino acids: Ala, Asp, Cys, Glu, Gly, Gln, Leu, Val, Trp, Phe, Pro (Aldrich), Arg, Asn, His, Lys, Thr (Fluka), Met, Tyr (Merck, Darmstadt, Germany), Ile (Guinama, Valencia, Spain) and Ser (Scharlau, Barcelona, Spain). Moreover, API, LUT, tricaproin, triheptadecanoin (Sigma) and 3,4-DHPAA (Fluka) were also used.

3.1.2 Solvents

The following analytical grade solvents were used: 1,4-butanediol (Aldrich), acetone, EtOH, 1-propanol, 2-propanol, ACN, MeOH, THF, 1,4-dioxane anhydrous, dichloromethane (Scharlau), diethyl ether, chloroform (J.T. Baker, Deventer, Países Bajos), iso-octane (Fluka) and *n*-hexane (Riedel-de-Haën, Seelze, Germany).

M. J. Lerma García, *Characterization and Authentication of Olive and Other Vegetable Oils*, Springer Theses, DOI: 10.1007/978-3-642-31418-6_3,

3.1.3 Monomers, Crosslinkers and Initiators

For monolithic column preparation the following reagents were used: LMA, ODMA, LA, EDMA, BDDA, META (75 % water), 3-(trimethoxysilyl)propyl methacrylate (*silane binding*), AIBN and LPO (Aldrich).

3.1.4 Other Reagents

Diphenic anhydride (98 %) (Aldrich), Sylon HTP (mixture of 3:1:9 hexamethyldisilazane, trimethylchlorosilane and pyridine, Supelco, Bellefonte, PA, USA), BHT, Tris, urea (99.5 %), potassium iodide, OPA, NAC (Fluka), KOH (Probus, Barcelona), boric acid, HCl (37 %), acetic acid (Panreac Química, Barcelona), NaOH, sodium sulphate anhydrous, ammonium hydroxide (Scharlau), NaCl (Carlo Erba, Milán, Italia), citric acid, sodiumbenzyl oxide in benzyl alcohol, 2,7-dichlorofluorescein (Sigma), thiourea (Riedel-de-Haën), formic acid, phenolphthalein, sodium thiosulphate and starch (Merck).

Deionized water was obtained with a Barnstead deionizer (Sybron, Boston, MA, USA).

Glass plates for TLC, coated with silica gel without fluorescent indicator (0.25 mm plate thickness; Merck, Darmstadt, Germany), were also used.

To obtain monolithic columns, fused-silica capillaries with 375 μm OD and 100 μm ID, both uncoated and with UV-transparent external coating, were used (Polymicro Technologies (Phoenix, AZ, USA).

3.2 Samples

The vegetable oils samples used in each work are specified in its corresponding chapter. All samples used are of botanical and geographical origin, quality and genetic variety guaranteed by the producers. In most cases, the samples were purchased in supermarkets in the area or provided by the same producers and/or commercial brands, such as Coosur (Vilches, Jaén, Spain), Borges (Tàrrega, Lleida, Spain), Grupo Hojiblanca (Antequera, Málaga, Spain), Intercoop Olival (Almassora, Castellón, Spain) Cooperativa de Altura (Altura, Castellón) and OLEA. Only in some cases, the olives were collected from the trees, being oil obtained by an Oliomio 150 extraction machine (Tem, Tavarnelle Val di Pesa, Florence, Italy).

3.3 Sample Preparation[1]

3.3.1 Ts

According to Aturki et al. (2005), vegetable oil samples (4 g) were extracted twice with 10 mL of MeOH containing 0.1 % w/v BHT as antioxidant, and once again with 10 mL of a MeOH/2-propanol mixture 80:20 v/v. All extractions were performed by shaking during 30 s followed by centrifugation at 8,000 g for 10 min. The combined extracts were evaporated to dryness using a rotary evaporator at 40 °C. The residue was dissolved in 1 mL of MeOH and stored at −20 °C in amber vials. In all cases, three replicates for each sample were performed. These solutions were properly diluted with the mobile phase and injected.

3.3.2 Sterols and Alcohols

The sterol and alcohol bands of the vegetable oils were obtained following the procedure established by the Official Journal of the European Union (Regulation (EEC) N° 2568/91, annex V and XIX). Accordingly, 5 g of oil was saponified by refluxing with 2 M ethanolic KOH for 20 min; 50 mL of distilled water was added, and the non-saponifiable fraction was extracted three times with diethyl ether. The three ether extracts were introduced into a separating funnel and washed with distilled water (50 mL each time) until neutral reaction. The organic extracts were dried with anhydrous sodium sulfate and filtered. These extracts were evaporated to dryness using a rotatory evaporator. The remaining unsaponifiables were dissolved in 2 mL of chloroform, and then the sterol and alcohol fractions were separated by TLC using a plate-developing chamber, which contained *n*-hexane/diethyl ether 60:40 (v/v). After TLC separation, the silica plate was sprayed lightly and uniformly with 2,7-dichlorofluorescein. The sterol and alcohol bands (see Fig. 3.1) were removed from the silica plate using a spatula.

Sterol band was dissolved in 10 mL of diethyl ether and filtered through a Whatman no. 1 paper using a Büchner funnel. A rotatory evaporator was used to remove this solvent. When sample was analyzed by CEC or by direct infusion MS, the residue was dissolved in 200 μL of 2-propanol (with a 1 % acetone for MS), while in the analysis by UPLC-MS and HPLC–MS it was dissolved in 500 μL of 2-propanol. In all cases, solutions were stored at −20 °C in amber vials. These solutions were properly diluted with the mobile phase and injected two times. When sterol samples were analyzed by GC, the residue was derivatized with 200 μL of Sylon HTP and injected.

[1] The information included in this section has been obtained and adapted with permission from the articles listed at the beginning of this thesis with copyright from American Chemical Society, Elsevier Ltd., Springer –Verlag and Wiley–VCH Verlag

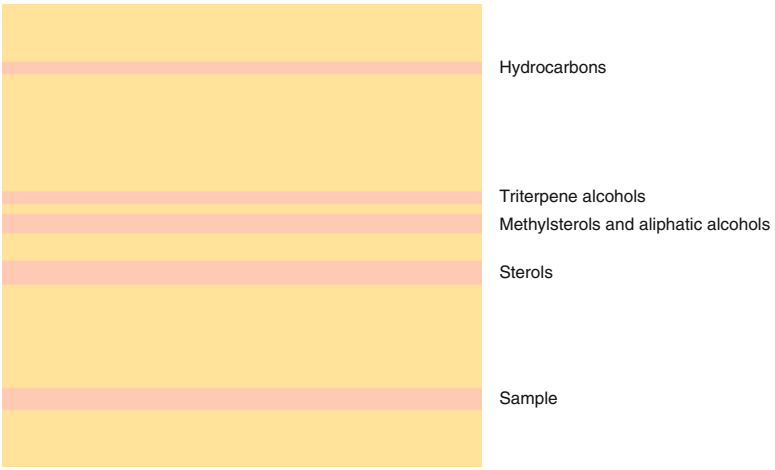

Fig. 3.1 Unsaponifiable fraction of an oil purified by TLC

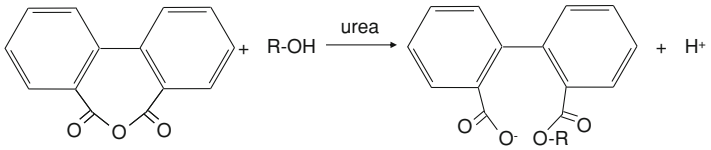

Fig. 3.2 Esterification reaction with diphenic anhydride (Adapted with permission from Lerma-García et al. (2009a). Copyright 2008 Elsevier B.V)

On the other hand, the two bands containing, respectively, the aliphatic and triterpene alcohols were jointly suspended in 4 mL THF and introduced in a screw-cap tube (15 mL, 15 cm long) also containing 0.45 g diphenic anhydride and 0.25 g finely grinded urea. The esterification reaction is illustrated in Fig. 3.2. The tube was shaken and introduced in a thermostatic bath at 60 °C for 120 min. After cooling, 2 mL of a 2:1 (v/v) MeOH/water mixture containing 0.1 M NH_3 was added. The suspension was sonicated for 15 min and passed through a 0.45 μm pore-size nylon filter (Albet, Barcelona). The solution was immediately injected in the chromatograph or stored in a freezer.

3.3.3 Amino Acids

The procedure for the isolation of proteins was taken from Hidalgo et al. (2001). Briefly, to precipitate the proteins, 40 g oil were weighed and cooled at 18 °C for at least 90 min prior to the addition of 98 mL acetone, which had also previously been cooled at 4 °C. The mixture was kept at 4 °C for 30 min and filtered through

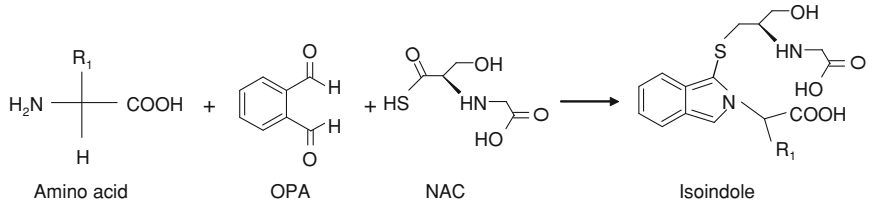

Fig. 3.3 Reaction of formation of isoindoles

a Whatman no. 1 filter paper using a Buchner funnel. The filter paper was extracted by shaking with 5 mL THF followed by 5 mL 1,4-dioxane. The extracts were combined and evaporated to dryness under a nitrogen stream. The residue was dissolved in 100 μL concentrated HCl and hydrolyzed for 24 h at 110 °C (Gimeno-Adelantado 2002; Peris-Vicente 2005). After being allowed to cool, 1 mL aqueous 0.1 M HCl and 1 mL EtOH were added. Direct infusion MS was performed using this extract after filtered through a 0.45 mm Nylon filter. On the other hand, for the determination of amino acids by HPLC–UV-Vis, this mixture was derivatized (see Fig. 3.3).

For this purpose, 100 μL of the amino acid mixture were disolved in 1 mL of derivatization reagent, containing 1.25×10^{-2} M OPA and 2.5×10^{-2} M NAC, which was buffered with 1 M boric acid at pH 9.5 (Concha-Herrera et al., 2005), giving place to their corresponding isoindoles. This mixture, protected from light with aluminium foil, was stored at 4 °C and renewed weekly.

3.3.4 Oil Treatment for Direct Infusion MS

For direct infusion into the mass spectrometer, both olive oil samples of different quality and EVOOS from different genetic varieties were prepared by weighing the proper amount of oil, which was diluted in a ratio 1:50 (v/v) with a mixture 1-propanol/MeOH 85:15 (v/v) containing 40 mM KOH. On the other hand, EVOO samples previously oxidized were diluted in a ratio 1:4 (v/v) with 1-propanol/MeOH 85:15 (v/v), alkalized in this case with 40 mM ammonium hydroxide.

3.3.5 Phenolic Compounds

The liquid–liquid procedure used was adapted from Carrasco-Pancorbo et al. (2004). Briefly, 50 g of oil were dissolved in 50 mL of *n*-hexane containing, when necessary, 200 μL of 3,4-DHPAA (1000 mg L^{-1}, used as internal standard). The resulting solution was extracted successively with four portions of 20 mL of MeOH/water (60:40, v/v). The combined extracts of the hydrophilic layer were

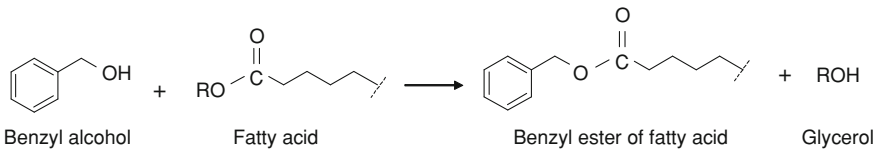

Fig. 3.4 Transesterification of fatty acids

brought to dryness in a rotary evaporator under pressure at 40 °C. Finally, the residue was redissolved in 1 mL of MeOH/water (50:50, v/v) and filtered through a 0.45 μm filter.

3.3.6 Elimination of EVOO Phenolic Compounds

Phenolic compounds were removed from EVOO according to the procedure described by Bonoli-Carbognin et al. (2008). Briefly, 35 g of EVOO was washed with several aliquots of 0.5 M NaOH (4 × 15 mL). To eliminate the aqueous phase, the mixture was centrifuged (1000 *g*, 5 min) after each washing. Combined olive oil fractions were then washed with 0.5 M HCl (2 × 10 mL) and saturated NaCl solution (5 × 10 mL), centrifuged at 1000 *g* for 5 min, dried with anhydrous sodium sulfate, and finally filtered under vacuum. Dried EVOO was then obtained.

3.3.7 Fatty Acids

Fatty acid analysis by GC-FID was performed according to the method described in Bendini et al. (2006), in which the methyl esters of fatty acids were obtained after a cold basic transmethylation procedure.

3.3.8 OFAs

OFAs were determined according to Rovellini and Cortesi (2004). OFAs, obtained after transesterification with 1.0 M sodium benzyloxide in benzyl alcohol (see Fig. 3.4), were determined by HPLC using both UV–vis and MS as detection systems Tricaproin and triheptadecanoin were used as internal standards (results were reported in percentages as g of total OFA expressed as benzyl heptadecanoate per 100 g of oil). On the other hand, benzyl caproate was used as a control for the derivatization reaction.

3.3.9 Other Analytical Parameters

Acidity and peroxide indexes have been also determined. Oil UV spectrophotometric measurement has been also carried out by measuring the absorbance at 232 and 270 nm (k_{232}, k_{270}). All these tests were conducted following the methods described in the Journal of the European Communities (Commission Regulation (EEC) 1991, Annexes II, III and IX, respectively).

3.4 Column Treatment

3.4.1 Column Conditioning

Before filling the columns with the polymerization mixtures, surface modification of the inner wall of the fused-silica capillaries is necessary to enable covalent attachment of the monolith to the wall. For this purpose, the following solutions (Peters 1997) were passed through 4 m of capillary [by using Hamilton syringe connected to a syringe pump (kd Scientific, Holliston, MA, USA)] at a flow rate of 200 μL min^{-1} (unless otherwise specified):

1. Acetone until few drops are observed at the exit of the capillary to assure the cleanliness of the inner wall.
2. Nanopure water until complete elimination of acetone.
3. 0.2 M NaOH until basic pH was observed at the exit of the capillary.
4. Nanopure water until removal of NaOH, to avoid sudden changes in pH by applying the next treatment.
5. 0.2 M HCl until acidic pH was observed at the exit of the capillary.
6. Nanopure water until neutral pH was obtained at the exit of the capillary.
7. EtOH until persistent odor, to remove water and to prevent hydrolysis of the *silane-binding* that is added in the next stage.
8. Solution of *silane-binding* at 20 % (w/v) in EtOH, acidified with acetic acid to pH 5. This solution was passed through the capillary at a flow rate of 0.25 μL min^{-1} for 60 min.
9. Acetone to remove the excess of *silane-binding*.

After this treatment, a stream of nitrogen was applied to dry the capillary, which was maintained under these conditions for 24 h to complete the condensation reaction of silanol groups with *silane-binding*. After 24 h, nitrogen stream was removed and the ends of the capillary were sealed in order to avoid the hydrolysis of siloxane bonds.

3.4.2 Monolithic Column Preparation

Monoliths were prepared using polymerization mixtures containing a monomer (LMA, ODMA o LA), a crosslinker (EDMA o BDDA) and a binary pore-forming solvents constituted by 1,4-butanediol and 1-propanol. These mixtures are prepared by weighing each component in an analytical balance.

Mixtures were polymerized by using different initiators with both thermal and photoionization. The initiators used were AIBN and LPO, both at 1 wt % with respect to the monomers. After mixing and to obtain a clear solution, sonication for 10 min followed by deaeration with nitrogen for more 10 min were applied.

The preconditioned capillary (33.5 cm) was filled with the polymerization mixture to a total length of 8.5 or 25 cm. Once filled, the ends are sealed and polymerization took place.

Finally, in the case of thermal polymerization, the filled capillaries were introduced in an oven at 70 °C for 24 h, while in the photopolymerization, capillaries underwent irradiation of 0.9 J/cm^2 for 10 min in a UV chamber (see Sect. 3.5.1 for specifications).

Next, the columns were flushed with MeOH to remove the pore-forming solvents and possible unreacted monomers by using an HPLC pump. A detection window adjacent to the monolithic material was made by burning off the polyimide coating (in the columns started with UV radiation it was not necessary to practice the detection window, as their construction requires the use of a UV–Vis transparent capillary). Then, portions of capillary were cut to adjust the position of the optical window to 8.5 cm of one end, and also to adjust the total length of the capillary to 33.5 cm. Cutting the endings also guarantees a monolith cross section perpendicular to the longitudinal axis of the capillary. Finally, before the injection of standards or samples, mobile phase is passed through the capillary for 30 min.

3.5 Instrumentation and Working Conditions[2]

3.5.1 CEC

CEC experiments were performed on an HP^{3D} CE instrument (Agilent Technologies, Waldbronn, Germany) equipped with a DAD and external nitrogen pressure. The pressurization of the capillary is important to avoid the appearance of bubbles that would cut the electric current passing through it. Data acquisition was performed with ChemStation Software (Rev.A.10.01, Agilent).

[2] the information included in this section has been obtained and adapted with permission from the articles listed at the beginning of this thesis with copyright from American Chemical Society, Elsevier Ltd., Springer—Verlag and Wiley–VCH Verlag

The monolithic column was placed in the instrument, and equilibrated with the mobile phase at 25 °C as follows. A pressure of 10 bar (1 MPa) was applied to both ends of the column, and the voltage was stepwise raised, in 5 kV increments, up to 25 kV. Each voltage was maintained until a constant current and a stable baseline were achieved. This stage lasted 45–60 min, depending on the flow characteristics of each column. For the CEC tests was used, when necessary, a sample of thiourea as EOF marker, in addition to relevant standards (Ts, sterols or phenols).

For T determination, separations were performed at +15 kV. The sample extracts and standard solutions were injected electrokinetically under +20 kV for 3 s. Detection was performed at 205 and 295 nm (450 ± 80 nm as reference). In this case, monolithic columns of 8.5 cm length were used.

For sterol determination, separations were performed at +20 kV The sample extracts and standard solutions were injected electrokinetically under +10 kV for 2 s. Detection was performed at 210 nm (450 ± 80 nm as reference). In this case, monolithic columns of 8.5 cm length were also used.

Finally, for phenolic compound determination, separations were performed at − 10 kV The sample extracts and standard solutions were injected electrokinetically under −20 kV for 3 s. Detection was performed at 280 nm (450 ± 80 nm as reference). In this case, monolithic columns of 25 cm length were used.

To photoinitiate polymerization, capillaries were placed into an UV crosslinker (model CL1000) from UVP Inc. (Upland, CA, USA) equipped with five UV lamps (5 × 8 W, 254 nm).

SEM photographs of monolithic materials were taken with a SEM model S-4100 (Hitachi, Ibaraki, Japan) provided with a field emission gun, a BSE AUTRATA detector and an EMIP 3.0 image data acquisition system.

3.5.2 Nano-LC

A 1,200 series liquid chromatograph provided with a degasser, a nanopump, and a DAD with a micro flow cell (Agilent) were used in all studies. The column was directly coupled to a 10 nL injector equipped with a microelectric actuator (Valco, Schenkon, Switzerland). UV–vis detection was performed at 295 ± 16 nm (360 ± 100 nm taken as reference). In all cases, flow rate was 0.5 μL min^{-1}. T separation was carried out with two different monolithic columns, with a Chromolith CapRod RP-18 capillary column (150 × 0.1 mm, Merck) and with a laboratory-made methacrylate column of 20 cm.

3.5.3 UPLC-MS

An AcQuity ultraperformance liquid chromatograph using a binary pump system (Waters, Mildford, MA) was used. Separation was carried out with an AcQuity UPLC BEH C18 column (50 × 2.1 mm, 1.7 μm, Waters). Mobile phases were

prepared by mixing ACN/acetic acid (100:0.01, v/v) (phase A) with water/acetic acid (100:0.01, v/v) (phase B). Elution was performed using a linear gradient from 80 to 100 % A for 0.5 min followed by an isocratic elution with 100 % A for 4.5 more min. The column temperature was kept at 10 °C, and the flow rate was 0.8 mL min^{-1}. The injection volume was 15 μL. The UPLC was coupled to the APCI ion source of a SQD mass spectrometer (Waters Corporation). Ionization was performed in APCI positive-ion mode, and data were collected in SIR mode. Optimization of the source parameters was performed automatically by the Waters Intellistar software (Waters). The ionization source parameters were as follows: corona, 4 kV; source temperature, 120 °C; desolvation gas temperature, 400 °C, with a flow rate of 750 L/h. Nitrogen, supplied by a gas generator (Dominick Hunter generator, Gateshead, England), was used as desolvation gas. The individual cone voltage for each sterol standard was evaluated between 10 and 60 V, by infusing 1 μg mL^{-1} of each compound to obtain the best instrumental conditions, which corresponded to 30 V to each of them.

3.5.4 FTIR Spectroscopy

FTIR spectra were obtained using a Nicolet Nexus FTIR spectrophotometer (Thermo Electron Corporation, Waltham, MA, USA) with a resolution of 4 cm^{-1} at 32 scans. A small quantity of the oil samples ($\approx$2 μL) was directly deposited between two well-polished KBr disks, creating a thin film. Spectra were scanned in the absorbance mode from 4000 to 500 cm^{-1} and the data were handled with the EZ OMNIC 7.3 software (Thermo Electron Corporation).

On the other hand, FTIR spectra of EVOOs from different genetic varieties was carried out using a Jasco 4100 type A spectrophotometer (Jasco, Easton, MD) fitted with an ATR accessory. The ATR accessory (ATRPRO410-S, Jasco) was equipped with a ZnSe reflection crystal. All analyses were carried out at room temperature. Measurements were obtained using 15 scans at 2 cm^{-1} resolution. Spectra were recorded in the absorbance mode from 4000 to 600 cm^{-1}. For each sample (ca. 20 μL were put on the crystal surface), the absorbance spectrum was collected against a background obtained with a dry and empty ATR cell. Two spectra were recorded for each sample. Before each spectrum was acquired, the ATR crystal was cleaned with a cellulose tissue soaked in *n*-hexane, rinsed with acetone, and dried. Data handling was performed with the Spectra Manager version 2.07.00 software (Jasco).

Finally, for FTIR spectra of olive oils previously oxidized, a Tensor 27™ FTIR spectrometer system (Bruker Optics, Milan, Italy), fitted with a Rocksolid™ interferometer and a DigiTect™ detector system coupled to an ATR accessory, was used. The ATR accessory (Specac Inc., Woodstock, GA, USA) was equipped with a ZnSe 11 reflection crystal. All analyses were carried out at room temperature. Spectra were acquired (32 scans/sample or background) in the range of 4000–700 cm^{-1} at a resolution of 4 cm^{-1}, using OPUS r. 6.0 (Bruker Optics) software.

For each sample (1–1.5 mL uniformly spread throughout the crystal surface), the absorbance spectrum was collected against a background obtained with a dry and empty ATR cell. Three spectra were recorded for each sample. Before acquiring each spectrum, the ATR crystal was cleaned with a cellulose tissue soaked in *n*-hexane and then rinsed with acetone.

3.5.5 Direct Infusion MS

The studies for the analysis of samples by direct infusion MS were performed using an ion trap mass spectrometer (HP 1100 series, Agilent), as well as the three most common interfaces: ESI, APPI and APCI. The interface used is selected depending on the type of analyte to be analyzed. A syringe pump (kdScientific, Holliston, MA, USA) was used to infuse the samples at 0.3 mL h^{-1} (5 μL min^{-1}). In all cases, nitrogen was used as the nebulizer and drying gas (Gaslab NG LCMS 20 generator; Equcien, Madrid, Spain). The maximum loading of the ion trap was 3×10^4 counts, and the maximum collection time was 300 ms.

For sterol determination, two interfaces, ESI and APPI, were used. The working conditions for the ESI source were: nebulizer gas pressure, 15 psi; drying gas flow rate, 12 L min^{-1} at 365 °C; capillary voltage, −4.5 kV; voltages of skimmers 1 and 2, 25.9 and 6.0 V, respectively. The working conditions for the APPI were: nebulizer gas pressure, 15 psi; drying gas flow rate, 12 L min^{-1} a 350 °C; vaporizer temperature, 275 °C; capillary voltage, −4.4 kV; voltages of skimmers 1 and 2, 24.0 and 7.4 V, respectively. The mass spectrometer was scanned within the *m/z* 200–500 range in the positive ion mode. The ion trap target mass was set at *m/z* 397 ($[M + H - H_2O]^+$ ion of *β*-sitosterol).

On the other hand, the ESI–MS working conditions for the determination of amino acids were: nebulizer gas pressure, 25 psi; drying gas flow rate, 8 L min^{-1} at 250 °C; capillary voltage, 3.5 kV; voltages of skimmers 1 and 2, −26.8 and −6.0 V, respectively. The mass spectrometer was scanned within the *m/z* 50–300 range in the positive ion mode. The ion trap target mass was set at *m/z* 122 ($[M\text{-}H]^+$ of Cys).

For the study of fatty acid profiles of olive oils of different quality, and also for the study of fatty acid and phenolic profiles of EVOOs from different genetic varieties, the experimental conditions were the same as for amino acid analysis, except temperature and drying gas flow that were 200 °C and 5 L min^{-1}, respectively. In this case, the spectrum was recorded in the range of *m/z* 100–800 in negative ion mode, being ion trap target mass was set at *m/z* 181 ($[M\text{-}H]^-$ ion o oleic acid).

Finally, for the study of oxidized EVOOs, an APCI interface was used. The MS working conditions were: nebulizer gas pressure, 25 psi; drying gas flow, 5 L min^{-1} at 200 °C; vaporizer temperature, 400 °C; capillary voltage, 2.6 kV; voltages of skimmers 1 and 2, −41.5 and −7.6 V, respectively. In this case, the spectrum was recorded in the range of *m/z* 100–800 in negative ion mode, being ion trap target mass was set at *m/z* 181 ($[M\text{-}H]^-$ ion of oleic acid).

3.5.6 GC

For sterol determination, an HP-5890 gas chromatograph provided with a FID (Agilent Technologies) was used. Separation was carried out with an HP-5 capillary column (30 m × 0.32 mm ID, 0.25 μm; J&W Scientific, Folsom, CA, USA). The operation conditions, adapted from the official method (Commission Regulation (EEC) 1991, annex V) were as follows: oven temperature, 263 °C for 30 min; split ratio, 1:10; injector temperature, 290 °C; detector temperature, 320 °C. Hydrogen was used as the carrier gas at a flow rate of 30 mL min^{-1}.

On the other hand, fatty acid composition was established using a Clarus 500 gas chromatograph (Perkin-Elmer, Waltham, MA, USA), also with FID. Separation was carried out using a fused silica capillary column BPX70 (50 m × 0.22 mm ID, 0.25 μm) from SGE Forte (Palo Alto, CA). The operation conditions were as follows: temperature was kept at 140 °C for 5 min, then was increased 4 °C min^{-1} until reaches 240 °C, keeping this temperature 5 more min; oven and injector temperature, 250 °C. Helium was used as the carrier gas at a flow rate of 0.8 mL min^{-1}.

3.5.7 HPLC–UV–Vis and HPLC–MS

A 1100 series liquid chromatograph provided with a degasser, a quaternary pump, thermostated column compartment, automatic sampler and DAD (Agilent), was used. In some cases, a mass spectrometer was also used, alone or connected in series as detection system. In all cases, data treatment was performed using ChemStation v.10.02 software (Agilent).

For alcohol analysis, separation was carried out with a C8 fused-core type column (Ascentis-Express, 150 × 4.6 mm ID, 2.7 μm, Supelco, Bellefonte, PA, USA). The chromatographic conditions selected were: injection volume, 40 μL; column temperature, 25 °C; flow rate, 1 mL min^{-1}. Mobile phases were prepared by mixing ACN and water, both containing 0.01 % acetic acid. Elution was performed isocratically with 90 % ACN for 25 min, followed by a linear gradient from 90 to 100 % ACN for 10 min, and by isocratic elution with 100 % ACN for 10 more min. UV–Vis detection was performed at 200 ± 10 nm (360 ± 60 nm as reference). The liquid chromatograph was also coupled (in series with the UV–Vis detector) to the ESI source of an HP 1100 series ion trap mass spectrometer (ITMS) (Agilent). The ITMS working conditions were: nebulizer gas pressure,35 psi; drying gas flow, 7 L min^{-1} at 300 °C; capillary voltage, 2.5 kV; voltages of skimmers 1 and 2, −41.0 and −6.0 V, respectively. The mass spectrometer was scanned within the *m/z* 300–800 range in the negative-ion mode. The ion trap target mass was set at *m/z* 605 ($[M - H]^-$ peak of the diphenic hemiester of C26). As in direct infusion MS, nitrogen was used as nebulizer and drying gas, being also the maximum loading of the ion trap 3 × 10^4 counts, and the maximum collection time 300 ms.

To enhance sensitivity in the detection of the $[M - H]^-$ ions of the hemiesters, the pH of the eluate was increased For this purpose, a T union located after the UV–vis detector and before the ESI source, and an auxiliary isocratic HPLC pump set at 0.1 mL min^{-1}, were used to mix the eluate with a 0.01 M ammonium hydroxide stream.

For amino acid analysis, separation was carried out with a Kromasil C18 column (250 × 4 mm ID, 5 μm, Análisis Vínicos, Tomelloso, Spain). The HPLC conditions were adapted from Beneito-Cambra et al. (2009) and Concha-Herrera et al. (2005). Briefly, mobile phases were prepared by mixing ACN and water, both containing 5 mM citric acid adjusted at pH 6.5 with sodium hydroxide. A gradient elution from 5 to 30 % ACN in 30 min, followed by an increase from 30 to 50 % ACN in another 5 min, was used. Detection was performed at 335 ± 10 nm (450 ± 30 nm as reference). In all cases, 20 μL was injected, being the flow rate 1 mL min^{-1} and column temperature 25 °C.

For sterol determination, separation was carried out with a dC18 column (Atlantis, 100 × 3 mm ID, 3 μm, Waters). Mobile phases were prepared by mixing ACN and water, both containing 0.01 % acetic acid. A linear gradient at a flow rate of 1 mL min^{-1} from 90 to 100 % ACN for 10 min, followed by isocratic elution with 100 % ACN for 2 more min, was used. In all cases, 20 μL was injected. A HP 1100 series ion trap mass spectrometer (Agilent), equipped with an APPI source was used as detection system. The MS working conditions were as follows: nebulizer gas pressure, 15 psi; drying gas flow, 12 L min^{-1} at 350 °C; vaporizer temperature, 275 °C; capillary voltage,-1.9 kV; voltages of skimmers 1 and 2, 25.9, and 6.0 V, respectively. The mass spectrometer was scanned within the *m/z* 200–500 range in the positive ion mode. The ion trap target mass was set at *m/z* 397 ($[M + H-H_2O]^+$ peak of *β*-sitosterol). The other experimental conditions were the same previously employed for alcohol analysis.

For OFA determination, separation was carried out with a Luna C18 column (250 × 4.6 mm ID, 5 μm, Phenomenex, Torrance, CA, USA). Mobile phases were prepared by mixing ACN and water in gradient mode. The gradient elution was performed as follows: from 0 to 50 min, the ACN percentage was increased from 60 to 100 %; and finally an isocratic elution at 100 % ACN was carried out from 50 to 70 min. UV–Vis detection was performed at 255 ± 10 nm (reference 500 ± 50 nm). In all cases, 20 μL was injected at a flow rate of 1 mL min^{-1}. These conditions were adapted from the NGD C-88 official method published by Norme Grassi e Derivati (Method NGD C-88, 2007). The liquid chromatograph was also coupled (in series with the DAD) to an APCI source from an HP 1100 series quadrupole mass analyzer (Agilent). The MS working conditions were as follows: nebulizer gas pressure, 50 psi; drying gas flow, 9 L min^{-1} at 350 °C; vaporizer temperature, 300 °C; capillary voltage, 3 kV; corona current, 4 μA; and fragmentor voltage, 60 V. The mass spectrometer was scanned within the *m/z* 300–500 range in the positive-ion mode.

For phenolic compound determination, separation was carried out with a reverse phase C18 Luna column (250 × 3 mm, 5 μm) and with a C18 precolumn, both from Phenomenex. Mobile phases were prepared by mixing water containing

0.5 % formic acid and ACN. A gradient elution was performed according to the conditions described by Carrasco- Pancorbo et al. (2007). UV–Vis detection was set at 240, 280, and 330 nm. In all cases, 10 μL was injected, the flow rate being 0,5 mL min^{-1}. The liquid chromatograph was also coupled (in series with the DAD) to the ESI source from an HP 1100 series quadrupole mass analyzer. The MS working conditions were as follows: nebulizer gas pressure, 50 psi; drying gas flow, 9 L min^{-1} at 350 °C; capillary voltage, 3 kV. The MS was scanned within the *m/z* 50–800 range in the positive-ion mode.

For T determination, separation was performed using a CN Luna 100A column (150 × 4.6 mm ID, 5 μm, Phenomenex). Ts were determined using isocratic conditions with *n*-hexane/dichloromethane (95:5, v/v). UV–Vis detection was performed at 295 nm. In all cases, 10 μL was injected, the flow rate being 1.0 mL min^{-1}.

3.5.8 Electronic Nose

Both for the analysis of oil samples containing reference defects provided by IOC, and for the analysis of previously oxidized olive oils, an electronic olfactory system (EOS 507, Sacmi Imola S·C., Imola, Bologna, Italy) composed of a measuring chamber with 6 metal oxide sensors and a personal computer, was used for the acquisition and analysis of the data generated by the EOS 507. The sensors used were: sensor 1 (SnO_2), sensor 2 (SnO_2 + SiO_2), sensor 3, 4 and 5 (catalyzed SnO_2 with Au, Ag and Pd, respectively) and sensor 6 (WO_3). During the analysis, sensors were maintained at a temperature range of 350–450 °C. The EOS 507 was controlled by an integrated PDA equipped with proprietary software, and was connected to an automatic sampling apparatus (Model HT500H) which had a carousel of 10 sites for loading samples. Samples were kept at controlled temperature (37 °C) and placed in a chamber provided by a system that removes humidity from the surrounding environment.

The experimental conditions were adapted from Camurati et al. (2006). For each sample, 15 g were placed in 100 mL Pyrex vials equipped with a pierceable silicon/Teflon cap. Figure 3.5 represents the response of the six sensors for an olive oil sample. For each sensor, the signal is divided in four parts:

A. conditioning phase, constituted by a 25 min period employed to obtain a constant baseline.
B. before injection phase, in which samples were incubated at 37 °C for 7 min before injection.
C. measurement cycle, in which the oil headspace, sampled with an automatic syringe, was then pumped over the sensor surfaces for 2 min during which the sensor signals were recorded; in this phase sensors were exposed to filtered air at a constant flow rate of 50 sccm to obtain the baseline.

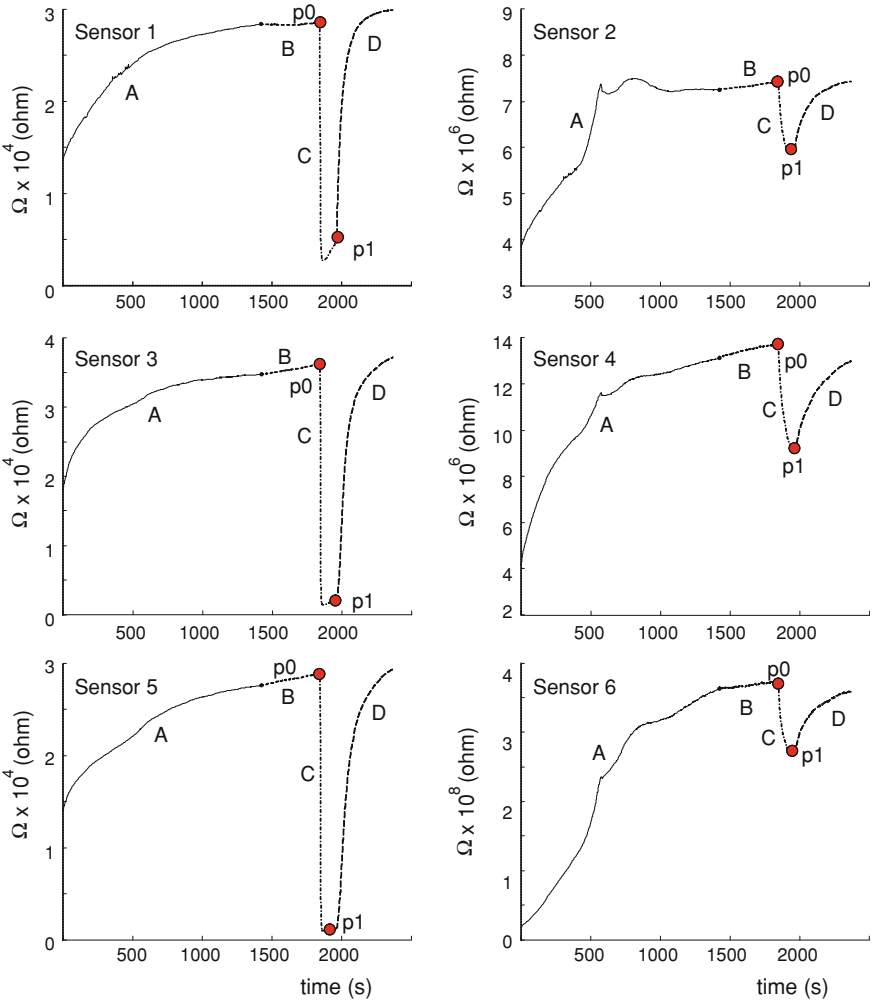

Fig. 3.5 Response of the 6 sensors for an olive oil sample obtained with the algorithm "classical feature": (*A*) conditioning phase; (*B*) before injection phase; (*C*) measurement cycle; (*D*) recovery phase (Reprinted with permission from Lerma-García et al (2009b). Copyright 2009 American-Chemical Society)

D. recovery phase, another 7 min period applied to restore the original MOS conditions.

The data from the electronic nose were extracted and analyzed with the statistical package "Nose Pattern Editor" (Sacmi Imola S·C.). This program allows data extraction with different algorithms, such as "classical feature" and "classical feature after".

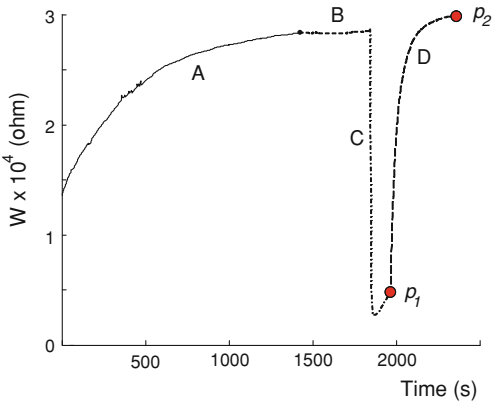

Fig. 3.6 Response of the 6 sensors for an olive oil sample obtained with the algorithm "classical alter feature": (*A*) conditioning phase; (*B*) before injection phase; (*C*) measurement cycle; (*D*) recovery phase (Reprinted with permission from Lerma-García et al (2010). Copyright 2010 Elsevier B.V)

In the extraction algorithm called "classical feature", the response extracted by each sensor, X, was defined by:

$$X = p_1/p_0 \tag{3.1}$$

where p_0 was the initial resistance of the sensor balanced in the air (see Fig. 3.5) and p_1 was the resistance (see Fig. 3.5) of a sensor in the presence of the volatile compounds emitted from the headspace (which decreased respect to p_0).

On the other hand, in the extraction algorithm called "classical after feature", the response extracted by each sensor, X, was defined by:

$$X = p_1/p_2 \tag{3.2}$$

where p_1 was the resistance (see Fig. 3.6) of a sensor in the presence of the volatile compounds emitted from the headspace and p_2 was the resistance of the sensor after the measurement (see Fig. 3.6).

3.5.9 OSI

To measure the oxidative status of olive oils, an eight-channel OSI instrument was used (Omnion, Decatur, IL, USA). As explained in Sect. 1.2.5.2, a stream of purified air (120 mL min^{-1} air flow rate) was passed through a 5 g oil sample, and the effluent air for the oil sample was then bubbled through a vessel containing deionized water. The effluent air contains especially volatile organic acids as formic acid and other volatile compounds formed during thermal oxidation of the oil, which increased the conductivity of the water. The temperature at which this test was carried out was 110 °C. The OSI (or OSI time) was expressed in hours.

3.6 Sensory Analysis

Sensory analysis was performed according to the European normative reported in Commission Regulation (EEC) 1991 (Annex XII). Ten trained assessors working as a professional panel from the Dipartimento di Scienze degli Alimenti (panel recognized by Italian Ministry-Mipaaf on 20 July 2006) used a scorecard to provide a quantitative descriptive analysis (Cerretani 2007) of orthonasal perceptions. A set of positive (green or ripe fruity and other pleasant attributes such as leaf, grass, artichoke, tomato, almond, apple, others) and negative (winey-vinegary, fusty, mouldy, muddy, rancid, others) sensory attributes were evaluated. Oil samples were graded for each positive and negative attribute using a numerical scale from 0 to 5 related to the perception of flavor stimuli, according to the judgement of assessors. The median, mean, and robust standard deviation (Commission Regulation (EC) No. 640/2008) were calculated for each attribute. If the value of the robust standard deviation was higher than 20 %, the analysis was repeated.

On the other hand, the assessors also established sensory thresholds of the following defects (fusty, mouldy, muddy, rancid and winey). For this purpose, the panel leader has used as reference defected oils those provided by IOC. A series of 12–15 samples of each of the defected oils were performed at descending concentrations by making successive dilutions in sunflower oil until the defect is not perceived. Then, paired comparison tests were carried out between these defected samples and a blank to establish the mean threshold of the panel. Up to a total of 8 pairs (the 8 samples with lower defect and 8 blanks) were randomly presented in successive independent tastings. After each tasting, the assessors were asked whether the two samples are identical or different. Upon completion of the test, the panel leader noted down the correct answers of the tasters for each concentration and expressed them as a percentage. The leader plotted the concentrations tested along the x-axis and the percentages of correct answers along the y-axis and then, by interpolation of the curve, shall determine the detection threshold which is the concentration corresponding to 75 % correct answers.

3.7 Treatment of Variables for Statistical Analysis

Due to the variability associated with sample treatment prior to injection and/or to other possible sources of variance that can also affect the experimental variables, two different normalization procedures were tried. In the normalization procedure A, the value of the original variable (area, peak intensity, etc.) was divided by the sum of the values of all the original variables. In the normalization procedure B, the value of each original variable was divided by the value of all the other original variables to obtained ratios of variable pairs, avoiding duplicates in all cases. For example, for a spectrum with 12 peaks used as variables, the value of each one of

the 12 areas was divided by the value of the remaining 11 areas, obtaining in this case a total of $(12 \times 11)/2 = 66$ normalized variables.

After obtaining the normalized variables, and depending on the objective (classify, quantify, explore), different statistical techniques such as LDA, ANN, MLR and PLSR were applied. The data processing was performed using Microsoft Excel, SPSS statistical software (v. 12.0.1, SPSS Inc., Chicago, IL, USA), The Unscrambler (v. 7.6, CAMO Technologies Inc., Bergen, Norway) and STATISTICA Neural Networks (v. 4.0, Statsoft Inc., Tulsa, USA). In all cases, the models constructed were validated by leave-one-out. Unless explicitly stated, the LDA and MLR models were constructed using the stepwise variable selection model, being the probability values of F_{in} and F_{out} of 0.05 and 0.1, respectively.

In the case of ANN, the network is constructed with three layers of nodes or perceptrons, trained with a learning algorithm of back-propagation. On the other hand, in all regression models residual analysis was performed, being an heteroskedasticity study performed.

References

Aturki Z, D'Orazio G, Fanali S (2005) Electrophoresis 26:798

Bendini A, Cerretani L, Vecchi S, Carrasco-Pancorbo A, Lercker G (2006) J Agric Food Chem 54:4880

Beneito-Cambra M, Bernabé-Zafón V, Herrero-Martínez JM, Simó-Alfonso EF, Ramis-Ramos G (2009) Talanta 79:275

Bonoli-Carbognin M, Cerretani L, Bendini A, Almajano MP, Gordon MH (2008) J Agric Food Chem 56:7076

Camurati F, Tagliabue S, Bresciani A, Sberveglieri G, Zaganelli P (2006) Riv Ital Sost Grasse 83:205

Carrasco-Pancorbo A, Cruces-Blanco C, Segura-Carretero A, Fernández-Gutiérrez A (2004) J Agric Food Chem 52:6687

Carrasco-Pancorbo A, Cerretani L, Bendini A, Segura-Carretero A, Lercker G, Fernández-Gutiérrez A (2007) J Agric Food Chem 55:4771

Cerretani L, Biasini G, Bonoli-Carbognin M, Bendini A (2007) J Sens Stud 22:403

Commission Regulation (EEC) (1991) No. 2568/91 of 11 July 1991 on the characteristics of olive oil and olive-residue oil and on the relevant methods of analysis, Off J Eur Union. p L128

Commission Regulation (EC) (2008) No. 640/2008 of 4 July 2008 amending Regulation (ECC) No. 2568/91 on the characteristics of olive oil and olive-residue oil and on the relevant methods of analysis. Off J Eur Commun. p L178

Concha-Herrera V, Vivó-Truyols G, Torres-Lapasió JR, García-Álvarez-Coque MC (2005) J Chromatogr A 1063:79

Gimeno-Adelantado JV, Mateo-Castro R, Doménech-Carbó MT, Bosch-Reig F, Doménech-Carbó A, De la Cruz-Cañizares J, Casas-Catalán MJ (2002) Talanta 56:71

Hidalgo FJ, Alaiz M, Zamora R (2001) Anal Chem 73:698

Lerma-García MJ, Ramis-Ramos G, Herrero-Martínez JM, Gimeno-Adelantado JV, Simó-Alfonso EF (2009a) J Chromatogr A 1216:230. Copyright 2008 Elsevier B.V

Lerma-García MJ, Simó-Alfonso EF, Bendini A, Cerretani L (2009b) J Agric Food Chem 57: 9365. Copyright 2009 American Chemical Society

Lerma-García MJ, Cerretani L, Cevoli C, Simó-Alfonso EF, Bendini A, Gallina-Toschi T (2010) Sensor Actuat B-Chem 147:283. Copyright 2010 Elsevier B.V

Norme Grassi e Derivati (NGD). Method NGD C-88 (2007) Stazione Sperimentali degli Oli e dei Grassi, Milano, Italy
Peris-Vicente J, Simó-Alfonso E, Gimeno-Adelantado JV, Doménech-Carbó MT (2005) Rapid Commun Mass Spectrom 19:3463
Peters EC, Petro M, Svec F, Fréchet JMJ (1997) Anal Chem 69:3646
Rovellini P, Cortesi N (2004) Ital J Food Sci 16:333

Chapter 4
Development of Methods for the Determination of Ts, T_3s and Sterols in Vegetable Oils

4.1 Determination of Ts by CEC Using Methacrylate Monolithic Columns[1]

In this work, a CEC method using methacrylate ester-based monolithic columns was developed to determine Ts and T_3s present in edible oils. The potential of this method to evaluate olive oil adulteration with lower-cost oils of a different botanical origin was also investigated. For these purposes, the following vegetable oils were used: soybean, sunflower, grapeseed, EVOO (Coosur), hazelnut (Guinama), corn (Hacendado) and red palm (Blue Bay).

Stock solutions of 2000 μg mL^{-1} of the T standards described in Sect. 3.1.1 were prepared in MeOH containing 0.1 % w/v BHT, and stored at −20 °C in amber vials. Working solutions were prepared daily by dilution of the stock solutions with the mobile phase. Thiourea was also added as EOF marker.

Methacrylate ester-based capillary monolithic columns were prepared from polymerization mixtures constituted by LMA, EDMA, 1,4-butanediol, 1-propanol and AIBN as thermal initiator. META was also added to generate the EOF.

4.1.1 Influence of Pore Size

As both monolith pore size and surface area were highly dependent on the 1,4-butanediol content present in the monolith, different polymerization mixtures were prepared in order to examine the influence of pore size on the separation of Ts. For this purpose, the content of 1,4-butanediol in the polymerization mixture

[1] Parts of the text of this section have been adapted with permission from Lerma-García et al. (2007). Copyright 2007 WILEY–VCH Verlag GmbH & Co. KGaA, Weinheim.

M. J. Lerma García, *Characterization and Authentication of Olive and Other Vegetable Oils*, Springer Theses, DOI: 10.1007/978-3-642-31418-6_4,

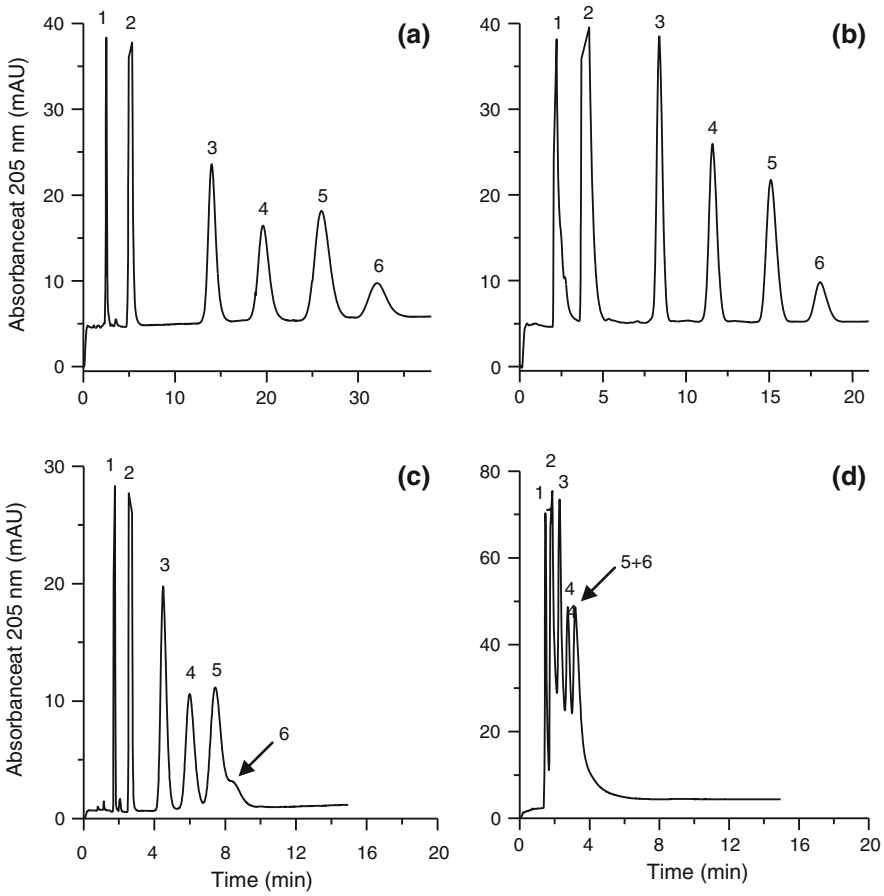

Fig. 4.1 Influence of the percentage of 1,4-butanediol in the polymerization mixture on the CEC separation of Ts: **a** 10, **b** 12, c 15 and **d** 20 wt % 1,4-butanediol. Working conditions: Mobile phase, 95:5 (v/v) MeOH - 5 mM Tris at pH 8.0; electrokinetic injection, 20 kV for 3 s; separation voltage, 15 kV. Peak identification: 1, thiourea; 2, BHT; 3, δ-T; 4, γ-T; 5, α-T and 6, α-T-AcO (Reprinted with permission from Lerma-García et al. (2007). Copyright 2007 WILEY–VCH Verlag GmbH & Co. KGaA, Weinheim)

was varied from 10 to 25 wt %, keeping the proportion of monomers to pore-forming solvents fixed at 40:60 wt %. When 1,4-butanediol content was below 10 wt %, small pore sizes (<125 nm), which were clearly unsuitable for any flow-through applications, were obtained, whereas with contents higher than 25 wt %, the components of the polymerization mixture were not completely dissolved.

Therefore, a monolith constructed using 10 wt % 1,4-butanediol was first used. The mobile phase composition used in these experiments was 95:5 (v/v) MeOH—5 mM Tris at pH 8.0. As shown in Fig. 4.1, the monolithic column produced with

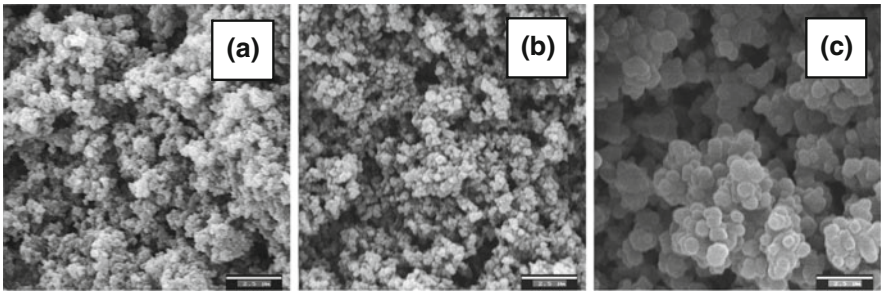

Fig. 4.2 SEM micrographs of the LMA monolithic materials prepared with **a** 10, **b** 12, and **c** 20 wt % 1,4-butanediol in the polymerization mixture, respectively. The bar lengths stand for 2.5 μm (Reprinted with permission from Lerma-García et al. (2007). Copyright 2007 WILEY–VCH Verlag GmbH & Co. KGaA, Weinheim)

10 wt % 1,4-butanediol showed the highest resolution of the analytes; however, separation times were too long (>35 min).

With 12 wt % 1,4-butanediol (see Fig. 4.1b), all T pairs were resolved within 19 min. When the content was increased up to 15 wt % 1,4-butanediol, the α-T/α-T-AcO pair was poorly resolved (Fig. 4.1c). Finally, monolithic columns prepared with 20 wt % 1,4-butanediol or higher contents were unable to resolve all the analyte pairs, even when the MeOH percentage in the mobile phase was reduced from 95 to 90 % (data not shown). When these phases were examined by SEM (Fig. 4.2), an increase of both the macropore size and the dimensions of the globules at increasing 1,4-butanediol percentages was observed. Thus, the best resolution was obtained with the lowest 1,4-butanediol content. This monolithic phase also showed the smallest pore size and the highest surface area. Then, the monolithic column obtained with 12 wt % 1,4-butanediol was selected as the best compromise between resolution and analysis time.

4.1.2 Influence of Mobile Phase Composition

The influence of the MeOH concentration in the mobile phase was also studied. For this purpose, 90:10, 95:5 and 99:1 (v/v) mixtures of MeOH-aqueous buffer at pH 8 were tried. As observed in Fig. 4.1b and in Fig. 4.3, resolution decreased when MeOH concentration was increased; however, resolution of all the peak pairs was still higher than 1.5 with the 99:1 mixture, except for the α-T/α-T-AcO pair which gave $R = 1.3$. Efficiencies also increased, and analysis time largely decreased, when the MeOH content in the mobile phase increased from 90 to 99 % (see Fig. 4.3). With 99:1, efficiencies within the 4,200–65,000 plates/m were obtained. Thus, this mobile phase was selected as the best compromise between resolution and analysis time (less than 10 min).

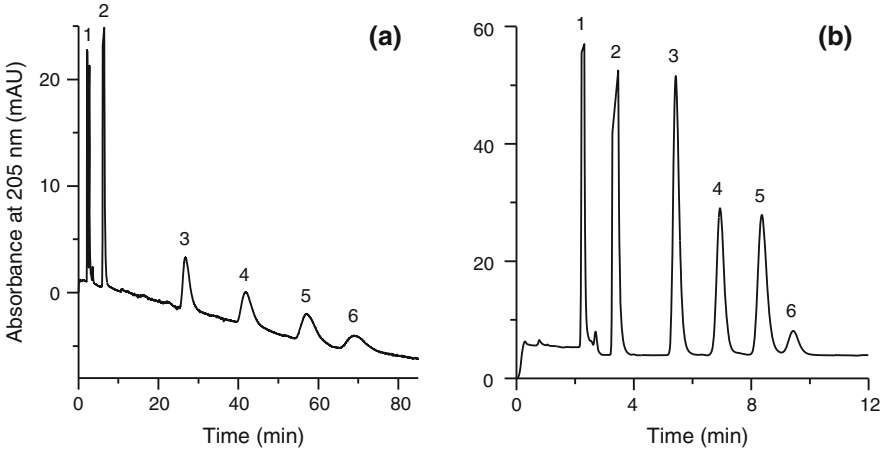

Fig. 4.3 Influence of the MeOH content in the mobile phase on the separation of Ts: **a** 90:10 and **b** 99:1 MeOH-aqueous buffer (5 mM Tris at pH 8). The monolithic capillary column was prepared with 12 wt % 1,4-butanediol in the polymerization mixture. Other experimental conditions as in Fig. 4.1 (Reprinted with permission from Lerma-García et al. (2007). Copyright 2007 WILEY–VCH Verlag GmbH & Co. KGaA, Weinheim)

4.1.3 Quantitation Studies and Application to Real Samples

Under these optimum experimental conditions, the method was tested in terms of repeatability. Intra- and inter-day repeatabilities were calculated by analyzing a standard mixture at a concentration level of 25 μg mL^{-1} of each T (Table 4.1). The mixture was injected eight times in order to obtain the repeatability (intra-day precision) of the method in terms of retention times and peak areas. The same mixture was analyzed over three consecutive days to evaluate the inter-day precision. Three monolithic columns were prepared from the same polymerization mixture and were tested by repeating the same number of injections in order to verify the column-to-column reproducibility. The reproducibility of EOF, retention times and peak areas are summarized in Table 4.1. As observed, the column-to-column reproducibilities of the retention times and peak areas were better than 4.5 and 5.6 %, respectively. About 100 injections of the standard mixture and 60 injections of vegetable oil extracts were performed without the need of replacing the column, therefore, the stability of the columns was satisfactory.

External calibration curves of peak areas were constructed by injecting six standard solutions of each solute within 5–100 μg mL^{-1} range. Straight lines with $r > 0.995$ were obtained. The LODs, calculated for a signal-to-noise ratio of 3, are also summarized in Table 4.1.

The optimized method was applied to the determination of Ts in several oil samples (Table 4.2). α-T-AcO was not detected in any of the samples analyzed.

Table 4.1 Repeatability and column-to-column reproducibility of retention times and peak areas (Reprinted with permission from Lerma-García et al. (2007). Copyright 2007 WILEY–VCH Verlag GmbH & Co. KGaA, Weinheim)

Compounds	Intra-day repeatability ($n = 8$) RSD, %		Inter-day repeatability (3 days) RSD, %		Column-to-column reproducibility ($n = 3$) RSD, %		LOD, μg mL^{-1}
	t_R	Peak area	t_R	Peak area	t_R	Peak area	
α-T	1.34	2.23	2.15	4.00	4.29	5.60	2.00
γ-T	1.19	1.76	1.92	3.30	3.64	5.20	1.80
δ-T	0.93	1.47	1.68	2.50	2.74	4.52	1.50
α-T-AcO	1.65	2.54	2.76	4.20	4.56	6.20	2.30
BHT	1.02	1.24	1.54	2.76	3.21	3.70	–
EOF	0.64	0.96	1.22	2.35	2.28	3.20	–

Table 4.2 Contents of Ts in vegetable oils (mg/100 g) (Reprinted with permission from Lerma-García et al. (2007). Copyright 2007 WILEY–VCH Verlag GmbH & Co. KGaA, Weinheim)

Oil	α-T	β-T + γ-T	δ-T
EVOO	12.2	1.12	ND [a]
Refined corn	31.2	128	7.1
Refined hazelnut	32.1	3.20	0.80
Refined sunflower	60.0	3.83	1.50
Crude red palm [b]	14.2	ND [a]	ND [a]
Refined grapeseed [b]	4.60	ND [a]	ND [a]
Refined soybean	23.1	162	80.4

[a] ND = Not detected

[b] Quantitation performed with a mobile phase containing 93:7 MeOH-aqueous buffer (5 mM Tris, pH 8.0); the other results were obtained with 99:1 MeOH aqueous buffer

Peak identification was performed by comparing the retention times and absorption spectra with those of the standards, and when necessary also by spiking the sample extracts with the standards. Additionally, standard addition calibration curves were obtained by adding to the extracts at least four solutions with increasing concentrations (up to 100 μg mL^{-1}). The curves were linear with $r > 0.992$, and in all cases the slope of calibration curve did not differ significantly from that obtained with the external calibration method. Therefore, no matrix effect was observed.

Representative electrochromatograms of EVOO, corn and soybean oil extracts are shown in Fig. 4.4, where different fingerprints were obtained according to the botanical origin of the oil. Since the monolithic columns used in this work were unable to resolve β-T and γ-T isomers, it could be concluded that this monolith showed RP characteristics. This behaviour has been previously observed by other authors (Abidi 1997 and Abidi 2000; Gimeno 2000). Thus, the sum of the concentrations of the two isomers is given in Table 4.2. I all cases, the found concentrations of Ts were consistent with those reported for oils of the same botanical origins (Dionisi 1995; Jee 2002; Rovellini 1997).

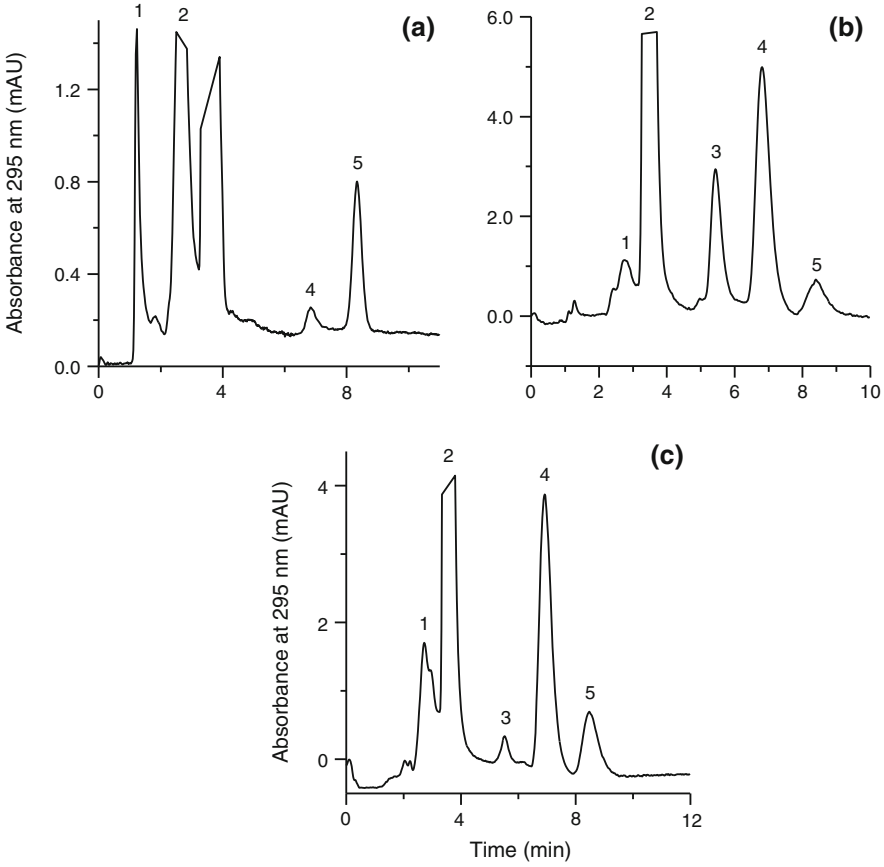

Fig. 4.4 Electrochromatograms of **a** EVOO, **b** soybean and c corn oils. Mobile phase: 99:1 MeOH-aqueous buffer (5 mM Tris, pH 8.0). Other conditions as in Fig. 4.1, except the peak labeled as 4 which accounts for the sum of the β-T and γ-T isomers (adapted with permission from Lerma-García et al. (2007). Copyright 2007 WILEY–VCH Verlag GmbH & Co. KGaA, Weinheim)

From the data indicated in Table 4.2 and Fig. 4.4a, α-T was the major T present in EVOO, while the presence of δ-T was not detected. However, large quantities of β-T + γ-T and δ-T were observed in soybean oil (Table 4.2 and Fig. 4.4b). Thus, the presence of this Ts could be used to detect EVOO adulteration with soybean oil (Dionisi 1995). Thus, several mixtures of EVOO-soybean oils were prepared and injected. Using the δ-T peak area as an adulteration marker, the presence of 10 % soybean oil in EVOO was clearly evidenced. Regarding corn oil, large quantities of β-T + γ-T and small amounts of α-T and δ-T were obtained (see Table 4.2 and Fig. 4.4c). In hazelnut and sunflower oils, the content of α-T was higher than the amounts found for the other isomers; however, since α-T also predominates in EVOO, this T is not a good tracer for the presence of these two vegetable oils in EVOO.

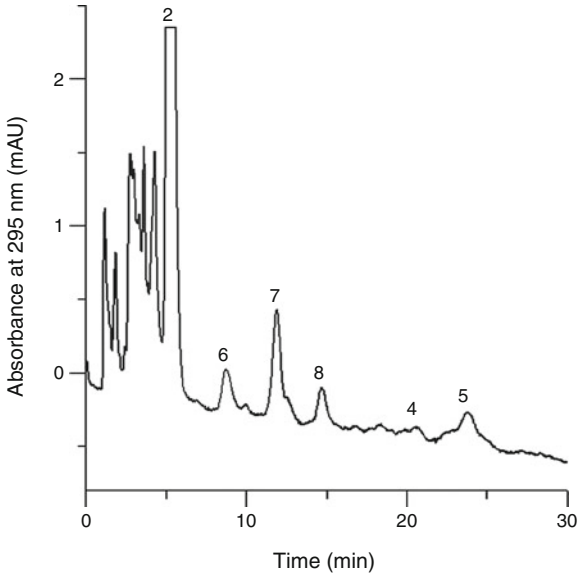

Fig. 4.5 Electrochromatogram of an EVOO containing 10 % red palm oil. Peak identification: 6, δ-T_3; 7, β-T_3 + γ-T_3; 8, α-T_3. Mobile phase: 93:7 MeOH-aqueous buffer (5 mM Tris, pH 8.0). Other peaks and working conditions as in Fig. 4.1 (Reprinted with permission from Lerma-García et al. (2007). Copyright 2007 WILEY–VCH Verlag GmbH & Co. KGaA, Weinheim)

Red palm and grapeseed oils constitute important sources of T_3s in edible oils (Choo 1996; Jee 2002). Thus, these samples were analyzed to provide reference retention times and spectra for the identification of T_3s. Using the RP mode, T_3s eluted following the same order observed for the Ts (Abidi 1999, 2001 and 2002). In addition, the double bonds of the side-chain of T_3s are not conjugated, thus, Ts and T_3s have closely similar UV spectra. These features were employed to assign the additional peaks observed with the grapeseed and palm oils to T_3s. Additionally, injections of these two oils, after spiking with the T standards, were performed. However, using a 99:1 MeOH-aqueous buffer mobile phase, T and T_3 peaks partially overlapped. For this purpose, mobile phase MeOH content was decreased up to 93 %, where both T and T_3 peaks were resolved (data not shown). Since T_3s are not found in olive oil, their presence in a sample clearly indicate its adulteration with T_3s-rich oils, such as grapeseed or palm oils. An electrochromatogram of an EVOO spiked with 10 % palm oil is shown in Fig. 4.5. As in can be observed in this figure, several T_3 peaks are observed (although the β-T_3 + γ-T_3 pair was not resolved).

Table 4.3 Botanical origin, number of samples and brand of the oil samples used in this work (Reprinted with permission from Cerretani et al. (2010) . Copyright 2009 American Chemical Society)

Origin	No. of samples	Brand
Avocado	1	Guinama
	1	Marnys
Corn	1	Guinama
	1	Gloria
Extra virgin olive	1	Intercoop Olival[a]
	1	Tenuta Pennita[b]
Grapeseed	1	Guinama
	1	Coosur
Hazelnut	1	Guinama
	1	Percheron
Peanut	1	Guinama
	1	Maurel
Red Palm	2	Blue Bay
Soybean	1	Guinama
	1	Coosur

[a] Oil produced in Spain from Serrana cultivar
[b] Oil produced in Italy from Brisighella cultivar

4.2 Determination of Ts and T_3s by Nano-LC Using a Silica Monolithic Column[2]

The aim of this study was to develop a nano-LC method, using UV–Vis detection, to determine Ts and T_3s in vegetable oils. For this purpose, a commercial C18 silica monolithic column was used. The vegetable oils employed in this study are specified in Table 4.3.

Stock solutions of ca. 1500 μg mL^{-1} of T standards were also prepared in MeOH with 0.1 % BHT (w/v) and stored at −20 °C in amber vials. Working solutions were prepared daily by dilution of the stock solutions with the mobile phase. As indicated in Sect. 3.3.1, three extracts were performed for each sample, being each injected three times.

4.2.1 Optimization of the Separation Conditions

Mobile phase composition was first optimized. For this purpose, a T standard mixture containing ca. 300 μg mL^{-1} of α-, γ- and δ-T was used. An 89:10:1 ACN/MeOH/water mixture (v/v/v) containing 0.2 % acetic acid was first tried as mobile phase (Gruszka 2007) using isocratic elution mode with a flow rate of 0.5 μL min^{-1}. Using this mobile phase, all peak pairs overlapped (see Fig. 4.6a). Thus,

[2] Parts of the text of this section have been adapted with permission from Cerretani et al. (2010). Copyright 2009 American Chemical Society

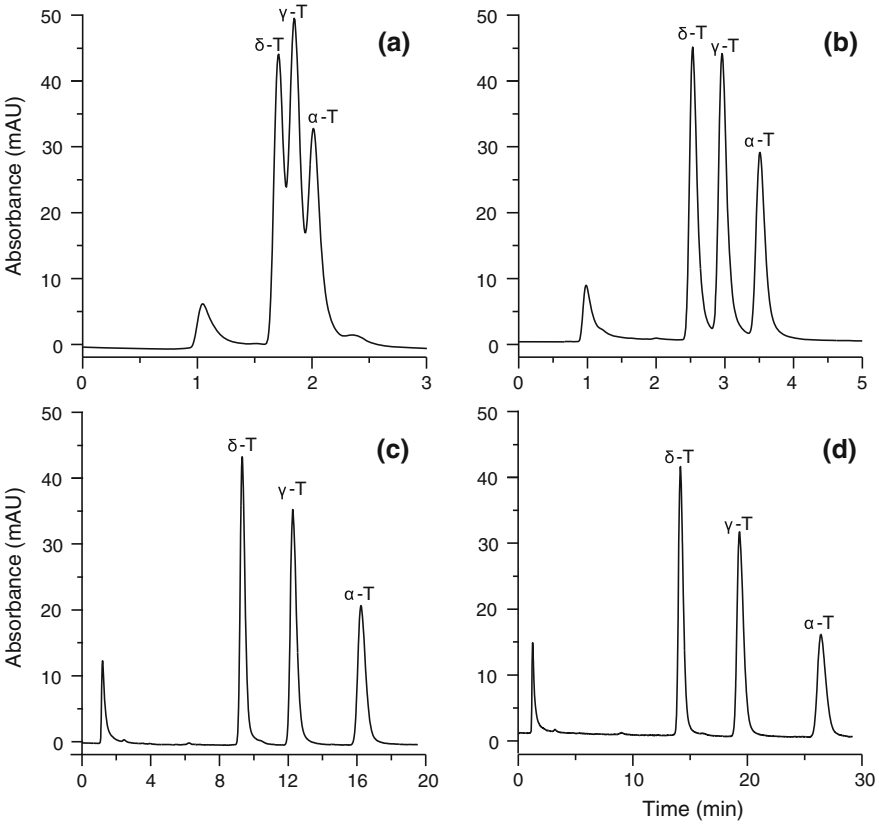

Fig. 4.6 Influence of water content in the mobile phase composition on the separation of T standards: **a** 89:10:1, **b** 84:9:7, **c** 75:8:17 and **d** 71:8:21 ACN/MeOH/water (v/v/v) with 0.2 % acetic acid. Other conditions: flow rate, 0.5 μL min^{-1}; wavelength detection, 295 nm (Reprinted with permission from Cerretani et al. (2010). Copyright 2009 American Chemical Society)

water content was increased, from 1 to 21 % (keeping constant the acetic acid percentage) in order to improve resolution. As shown in Fig. 4.6, an increase in water content led to higher analysis times.

In addition to this, efficiency and resolution were calculated to evaluation the quality of T separation (see Fig. 4.7). As observed, both efficiency and resolution were highly dependent on the water content in the mobile phase. When the water content was increased, efficiency values progressively increased (Fig. 4.7a), reaching a maximum at 19 % water and decreasing at higher water contents. At all water percentages, theoretical plate values followed the order: α-T > γ-T > δ-T. Regarding resolution, its values also increased when the water percentage was increased, reaching a maximum at 17 % (Fig. 4.7b), also decreasing its values when the water percentage was decreased. Therefore, a mobile phase containing

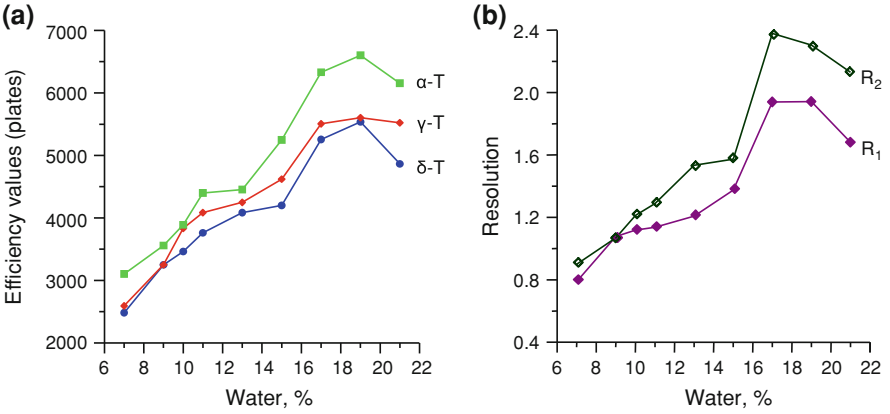

Fig. 4.7 **a** Efficiency and **b** resolution values of T pairs at several water contents in the mobile phase (R_1 = resolution between δ- and γ-T; R_2 = resolution between γ- and α-T) (adapted with permission from Cerretani et al. (2010). Copyright 2009 American Chemical Society)

75:8:17 ACN/MeOH/water (v/v/v) was selected as the best compromise between efficiency, resolution and analysis time (ca. 18 min, see Fig. 4.6c).

4.2.2 Quantitation Studies and Application to Real Samples

Under the proposed chromatographic conditions, external calibration curves were obtained by injecting six standard solutions of each solute within its linearity range (5–500 mg mL^{-1}). Each solution contained the three T standards. Straight lines with $r > 0.999$ were obtained. The proposed method was also evaluated in terms of precision, linearity, and LODs and LOQs (see Table 4.4).

Precision was obtained by testing the repeatabilities of peak areas and retention time obtained by injecting ten times the same 50 mg mL^{-1} solution for all analytes. The LODs and LOQs of the solutes were obtained for signal-to-noise ratio of 3 and 10, respectively. In all cases, these values were lower than others reported in literature (Lerma-García 2007; Waseem 2009). The repeatability values for retention times and peak areas were in all cases below 0.2 and 4.2 %, respectively. Similar sensitivities were obtained for δ- and γ-T, this value being lower for α-T. Therefore, a higher LOD was obtained for α-T with respect to the other two isomers. These results are in agreement with those reported in the literature (Fanali 2004).

The recommended method was applied to the determination of Ts in several oils from different botanical origin (Table 4.3). The monolithic column used in this study worked also in the RP mode, and as indicated in the previous section, was unable to resolve the β-T and γ-T isomers present in the oil samples. Consequently, the sum of the concentrations of both isomers is given in Table 4.3. Representative chromatograms of corn, grapeseed, hazelnut and soybean oil extracts are shown in Fig. 4.8, while the found concentrations of Ts, expressed as mg kg^{-1} oil, are

Table 4.4 Analytical figures of merit for the determination of Ts by nano-LC (Reprinted with permission from Cerretani et al. (2010). Copyright 2009 American Chemical Society)

Analyte	Repeatability[a], RSD, %		LOD	LOQ	Relative
	area	t_R	(μg mL^{-1})		sensitivity[b]
δ-T	2.8	0.1	0.07	0.2	1.81
γ-T	3	0.1	0.07	0.2	1.92
α-T	4.2	0.2	0.16	0.5	1.00

[a] For a T concentration of 50 μg mL^{-1} (n = 30)
[b] As the ratio of the slopes of calibration curves of Ts (respect to α-T)

reported in Table 4.5. Different fingerprints of Ts were obtained according to the botanical origin of the oil. In general, the levels of Ts found in these samples are in good agreement with the data reported for these compounds in edible oils of the same origin (Dionisi 1995; Jee 2002; Rovellini 1997). On the other hand, and as indicated above, each extract was injected three times. In all cases, the RSD of the peak areas was below 2.3 %. As deduced from Table 4.5 and Fig. 4.8, corn oil showed large quantities of β-T + γ-T and small amounts of α-T and δ-T, while hazelnut oil showed α-T concentrations higher than those of the other Ts. In soybean oil, large quantities of β-T + γ-T and δ-T were observed. Thus, the presence of these Ts could be used as an adulteration marker to detect EVOO adulteration with soybean oil (Dionisi 1995), since EVOO major isomer was α-T (Table 4.5).

As previously indicated in Sect. 4.1.3, several vegetable oils are rich in T_3s; then, the T_3 concentration was also determined in these oils (see Table 4.5). Each T_3 was quantified using the calibration curve of its corresponding T. The found T_3 contents were also consistent with those reported in literature (Choo 1996; Jee 2002). Since T_3s are not found in olive oil, their presence in a sample clearly indicate its adulteration with T_3s-rich oils.

4.3 Methacrylate Monolithic Columns for Nano-LC Determination of Ts and T_3s[3]

In this work, the content of Ts and T_3s present in vegetable oils from different botanical origins was determined by a nano-LC-UV–Vis method using a methacrylate ester-based monolithic column The vegetable oils employed in this study, which were the same used in Sect. 4.2, are indicated in Table 4.3. As in this section, stock solutions of ca. 1500 μg mL^{-1} were prepared and used to optimize T separation. Three extracts were performed for each sample, being each extract injected three times.

[3] Parts of the text of this section have been adapted with permission from Lerma-García et al. (2010b). Copyright 2010 WILEY–VCH Verlag GmbH & Co. KGaA,Weinheim.

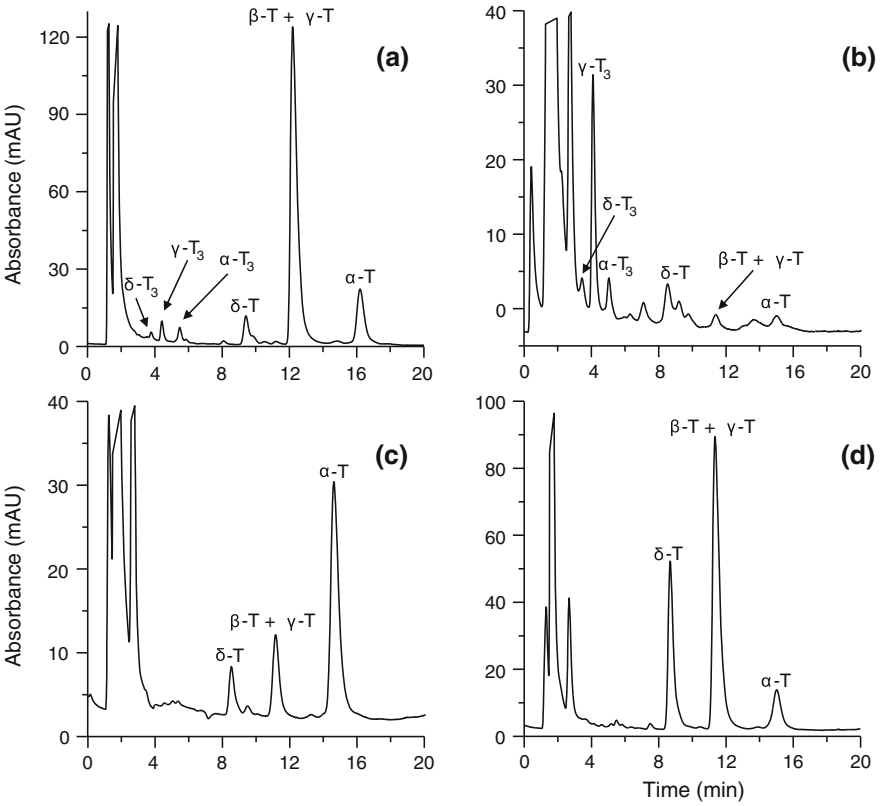

Fig. 4.8 Chromatograms of **a** corn, **b** grapeseed, **c** hazelnut and **d** soybean oil extracts. Mobile phase: 75:8:17 ACN/MeOH/water (v/v/v) with 0.2 % acetic acid. Other experimental conditions as in Fig. 4.6 (Reprinted with permission from Cerretani et al. (2010) . Copyright 2009 American Chemical Society)

Table 4.5 Contents of Ts and T_3s in vegetable oils (mg kg^{-1}) (Reprinted with permission from Cerretani et al. (2010) . Copyright 2009 American Chemical Society)

Oil	δ-T	β-T + γ-T	α-T	δ-T_3	β-T_3 + γ-T_3	α-T_3
Avocado	12.2–23.9	6.3–67.6	34.2–55.1	0–7.9	0–9.3	0–5.3
Corn	11.1–22.3	125.0–237.0	51.7–82.6	4.8–7.1	4.6–7.3	2.3–12.4
EVOO	0–5.6	7.5–10.1	52.1–111.7	ND[a]	ND[a]	ND[a]
Grapeseed	6.0–10.2	6.3–17.2	5.8–54.8	0–8.2	10.3–31.0	2.1–12.3
Hazelnut	7.0–12.1	18.8–32.2	71.5–119.7	ND[a]	ND[a]	ND[a]
Peanut	6.9–31.3	36.7–74.1	42.6–44.5	ND[a]	ND[a]	ND[a]
Red palm	ND[a]	4.2–8.3	6.8–20.8	8.8–11.3	27.0–40.4	15.2–35.1
Soybean	66.9–87.8	95.4–177.1	17.4–52.6	ND[a]	ND[a]	ND[a]

[a] ND = Not detected

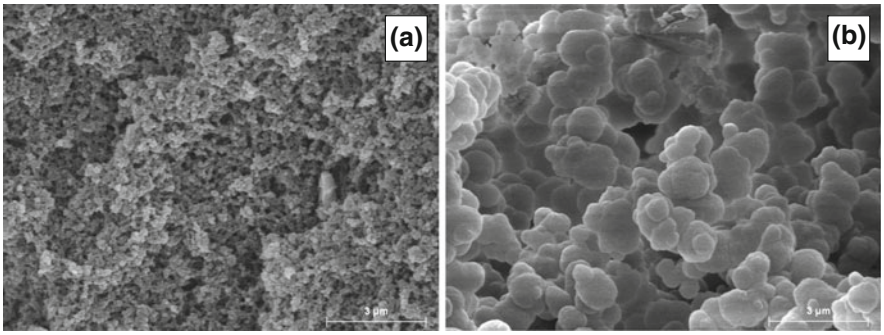

Fig. 4.9 SEM micrograph of the **a** Thermally and **b** Photo-polymerized LMA based monolithic columns prepared with 12 wt % 1,4-butanediol in the polymerization mixture. The bar lengths stand for 3 μm (Reprinted with permission from Lerma-García et al. (2010b). Copyright 2010 WILEY–VCH Verlag GmbH & Co. KGaA,Weinheim)

4.3.1 Influence of Mobile Phase Composition

The initial conditions to prepare the LMA-based monolithic columns were similar than those used in T separation by CEC (Sect. 4.1); however, in this case, the total column length was 20 cm. The first polymerization mixture used to construct columns was composed by a 40 wt % monomers (59.8 wt % LMA, 40.2 wt % EDMA) and 60 wt % porogens (20 wt % 1,4-butanediol and 80 wt % 1-propanol) in the presence of AIBN as initiator (thermal polymerization). However, no META monomer was added in this mixture (since EOF generation is not necessary in nano-LC). With this polymerization mixture, a monolith with poor permeability and small globules and pores (see Fig. 4.9a) was obtained. These features could be attributed to the absence of META in the polymerization mixture.

To solve this problem, the same polymerization mixture indicated above for thermal initiation, was polymerized under UV irradiation, since it has been demonstrated that columns prepared by UV irradiation showed shorter polymerization times and higher permeabilities than those thermally initiated (Bernabé-Zafón 2009; Yu, 2001). As it can be observed in Fig. 4.9b, the photo-polymerized column showed larger pores and globule sizes than that thermally polymerized (Fig. 4.9a).

Next, and using the photo-polymerized column, mobile phase composition (mixtures of ACN and water) for T separation was optimized. For this purpose, a T standard mixture containing ca. 300 μg mL^{-1} of α-, γ- and δ-Ts was employed. To evaluate the quality of T separation, efficiency and resolution values were calculated (Fig. 4.10). It can be seen that both efficiency and resolution are highly dependent on the water content in the mobile phase.

When the water content was increased, efficiency values progressively increased (Fig. 4.10a), reaching a maximum at 24 % water, and decreasing at higher water contents. On the other hand, resolution also improved when the water

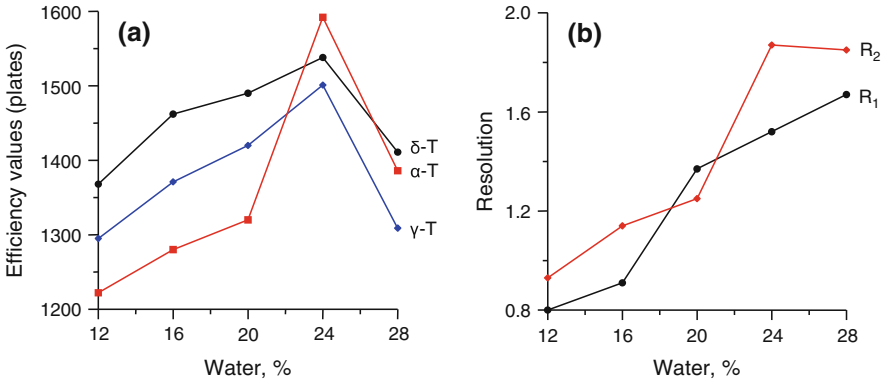

Fig. 4.10 **a** Efficiency and **b** Resolution values of Ts at several water contents in the mobile phase (R_1 = resolution between δ- and γ-T; R_2 = resolution between γ- and α-T) (Reprinted with permission from Lerma-García et al. (2010b). Copyright 2010 WILEY–VCH Verlag GmbH & Co. KGaA,Weinheim)

content increased (Fig. 4.10b). Therefore, a mobile phase containing 76:24 ACN/water (v/v) was selected as the best compromise between efficiency, resolution and analysis time (ca. 23 min, see Fig. 4.11a). Also in this case, column worked under an RP mechanism. This fact could be deduced from analyte retention order (δ-, γ-, α-T). This behaviour agrees with other studies on Ts eluted with RP-HPLC-packed columns (Abidi 2000; Gimeno 2000).

Next, an attempt to improve T separation was made by adding MeOH percentages ranging from 2 to 10 % to the mobile phase (keeping constant the optimal ACN/water ratio). The addition of a 4 % MeOH (see Fig. 4.11b) showed better efficiencies, similar resolutions and shorter analysis times than the mobile phase containing 76:24 ACN/water (v/v) (Fig. 4.11a). Thus, a mobile phase containing 96 % ACN/water (76:24) and 4 % MeOH was selected as the best compromise between efficiency, resolution and analysis time (*ca.* 16 min).

4.3.2 Quantitation Studies and Application to Real Samples

External calibration curves of peak areas were constructed as indicated in Sect. 4.2.2. In all cases, an excellent linearity with $r > 0.998$ was obtained. Other analytical figures of merit of the proposed method, which were calculated as in Sect. 4.2.2., are shown in Table 4.6. The repeatability values for retention times and peak areas were in all cases below 0.15 and 3.1 %, respectively. Similar sensitivities were obtained for δ- and γ-T, being this parameter lower for α-T. Then, a higher LOD was obtained for α-T with respect to the other two Ts. These results are in agreement with other reported data (Fanali 2004) and with our previous studies.

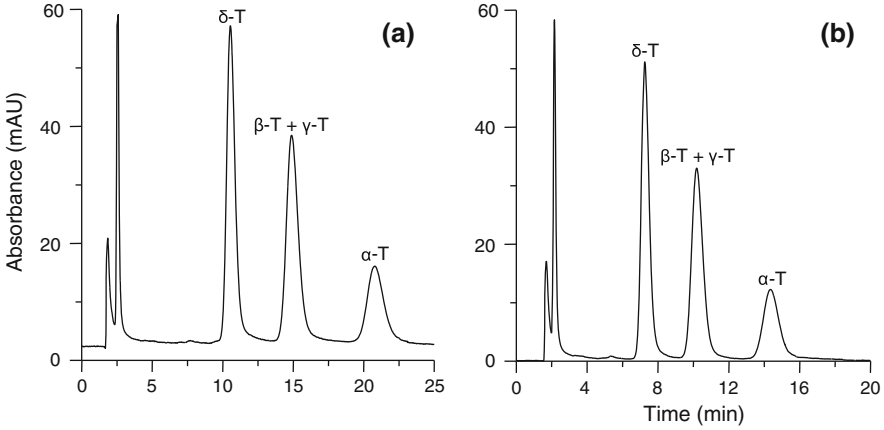

Fig. 4.11 Influence of MeOH content in the mobile phase composition on the separation of T standards: **a** 76:24 % ACN/water and **b** 96 % ACN/water mixture (76:24) and 4 % MeOH. Chromatographic conditions: flow rate, 0.5 μL min^{-1}; wavelength detection, 295 nm (Reprinted with permission from Lerma-García et al. (2010b). Copyright 2010 WILEY–VCH Verlag GmbH & Co. KGaA,Weinheim)

Table 4.6 Analytical figures of merit for the proposed nano-LC method in the determination of Ts (Reprinted with permission from Lerma-García et al. (2010b). Copyright 2010 WILEY–VCH Verlag GmbH & Co. KGaA,Weinheim)

Analyte	Repeatability[a], RSD, %		LOD	LOQ	Relative
	Area	t_R	(μg mL^{-1})	(μg mL^{-1})	sensitivity[b]
δ-T	2.30	0.10	0.12	0.40	1.79
γ-T	2.80	0.10	0.14	0.40	1.88
α-T	3.10	0.15	0.26	0.70	1.00

[a] For a T concentration of 50 μg mL^{-1} (n = 10)
[b] As the ratio of the slopes of calibration curves of Ts (respect to α-T)

The optimized method was applied to the determination of Ts in several oil samples. Representative chromatograms of corn, hazelnut and soybean oil extracts are given in Fig. 4.12. As observed, Different fingerprints of Ts were obtained according to the botanical origin of the oil. The found concentrations of Ts, expressed as mg kg^{-1} oil, are reported in Table 4.7. These data are consistent with those previously reported for oils of the same botanical origins (Dionisi 1995; Jee 2002). Also in this case, β- and γ-Ts are quantified together. As shown in Table 4.7 and Fig. 4.12A, large quantities of β-T + γ-T and small amounts of α-T and δ-T were present in corn oil. Hazelnut oil showed α-T concentrations higher than those of the other Ts (Table 4.7 and Fig. 4.12b). In soybean oil, large quantities of β-T + γ-T and δ-T were observed (Table 4.7 and Fig. 4.12c). Thus, these Ts could be used to detect the presence of soybean oil in adulterated EVOO (Dionisi 1995), in which the most abundant isomer was α-T (Table 4.7).

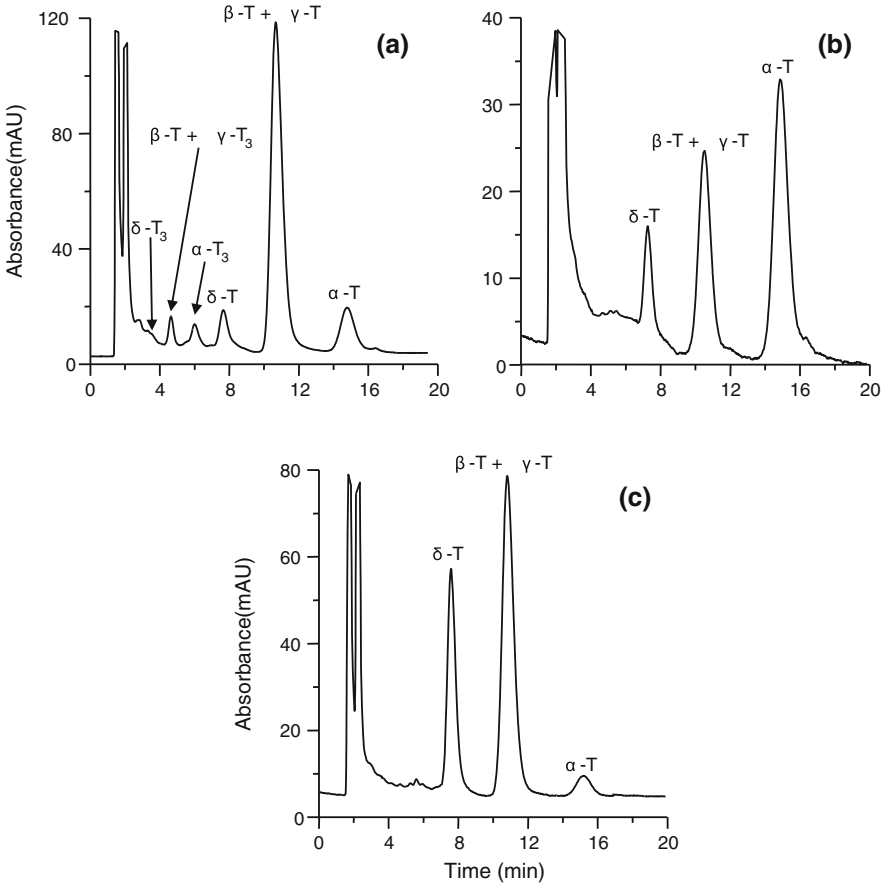

Fig. 4.12 Chromatograms of **a** corn, **b** hazelnut and **c** soybean oil extracts. Mobile phase: 96 % ACN/water mixture (76:24) and 4 % MeOH. Other working conditions as in Fig. 4.11 (Reprinted with permission from Lerma-García et al. (2010b). Copyright 2010 WILEY–VCH Verlag GmbH & Co. KGaA,Weinheim)

Table 4.7 Contents of Ts and T_3s in vegetable oils (mg kg^{-1}) (Reprinted with permission from Lerma-García et al. (2010b). Copyright 2010 WILEY–VCH Verlag GmbH & Co. KGaA, Weinheim)

Oil	δ-T	β-T + γ-T	α-T	δ-T_3	β-T_3 + γ-T_3	α-T_3
Avocado	11.6–25.9	7.8–64.1	27.1–52.7	0.5–6.9	ND[a]–8.1	ND[a]–6.9
Corn	10.0–21.1	120.7–228.3	53.1–86.2	3.9–8.5	3.9–6.7	3.2–14.2
EVOO	ND[a]–4.5	8.0–9.9	50.0–120.5	ND[a]	ND[a]	ND[a]
Grapeseed	6.8–11.0	6.0–18.1	4.9–56.5	ND[a]–9.1	11.9–33.1	2.8–11.9
Hazelnut	6.4–13.2	17.8–33.5	73.5–120.0	ND[a]	ND[a]	ND[a]
Peanut	5.9–32.3	33.3–72.4	41.6–45.8	ND[a]	ND[a]	ND[a]
Red palm	ND[a]	3.9–8.9	6.0–23.1	7.9–12.4	27.0–43.5	16.3–37.1
Soybean	65.4–89.7	94.7–179.1	16.9–55.1	ND[a]	ND[a]	ND[a]

[a] ND = Not detected (below the LOD value)

As in Sects. 4.1.3 and 4.2.2, the presence of other peaks ascribed to T_3s, were also quantified (Table 4.7). As performed in Sect. 4.2.2, T_3 concentrations were obtained using the calibration curve of the corresponding T. The contents found were consistent with those reported in literature (Jee 2002; Watson 2009).

4.4 Determination of Sterols by CEC Using Methacrylate Monolithic Columns[4]

The aim of this study was to develop a fast CEC method to determine sterols in vegetable oils using methacrylate ester-based monolithic columns. The potential of this method to evaluate olive oil adulteration with sunflower and soybean oils was also studied. For these purposes, the following vegetable oils were employed: sunflower (Hacendado), EVOO (Carbonell), soybean (Biolasi), corn, peanut, grapeseed and hazelnut (Guinama).

Standard solutions (ca. 5 mM) of the following sterol standards (ergosterol, cholesterol, stigmasterol and β-sistosterol) were prepared in 2-propanol and stored at −20 °C in amber vials. Working solutions were prepared daily by dilution of these stock solutions with the mobile phase.

4.4.1 Optimization of the Separation Conditions

For sterol separation, the optimal monolithic column obtained for the separation of Ts by CEC was first tried. This column contained 40 wt % of monomers (59.8 wt % of LMA, 39.9 wt % of EDMA and 0.3 wt % of META), 60 wt % of porogens (80 wt % of 1-propanol and 20 wt % of 1,4-butanediol) and AIBN as thermal initiator.

In first place, mobile phase composition was optimized. For this purpose, different ACN/THF/water ternary mixtures containing 5 mM Tris at pH 8.0 were tried (Abidi 2004). Always keeping a constant 5 % water content, THF percentage was varied between 5 and 35 %. When a THF content of 35 % was added, several sterol peaks overlapped. Then, when the THF content was decreased, a large increase in resolution values was observed; however, with a 5 % THF broad peaks were obtained. As a result of this study, a mobile phase containing 85:10:5 (v/v/v) ACN/THF/water was selected for further studies since it provided the best resolution and efficiency values in less than 10 min (see Table 4.8 and Fig. 4.13a).

Different ternary mixtures, containing in this case 2-propanol instead of THF, were also tried as mobile phase (the reason of trying sterol separation with

[4] Parts of the text of this section have been adapted with permission from Lerma-García et al. (2008b). Copyright 2008 WILEY–VCH Verlag GmbH & Co. KGaA,Weinheim.

Table 4.8 Efficiency, resolution and *k*-values obtained with the two optimal mobile phases using an LMA-based monolithic column with 12 wt % 1,4-butanediol (column A3) (Reprinted with permission from Lerma-García et al. (2008b). Copyright 2008 WILEY–VCH Verlag GmbH & Co. KGaA,Weinheim)

Solutes	ACN/THF/Tris (85:10:5)			ACN/2-propanol/Tris (85:10:5)		
	N (plates/m)	R[a]	*k*	N (plates/m)	R[a]	*k*
Ergosterol	28,200	–	3.4	36,300	–	2.2
Cholesterol	34,700	3.4	4.8	46,300	3.3	3.0
Stigmasterol	26,000	1.5	5.7	28,800	1.5	3.4
β-Sitosterol	34,600	1.8	6.7	60,900	2.0	4.1

[a] Resolution (R) was calculated between two adjacent peaks

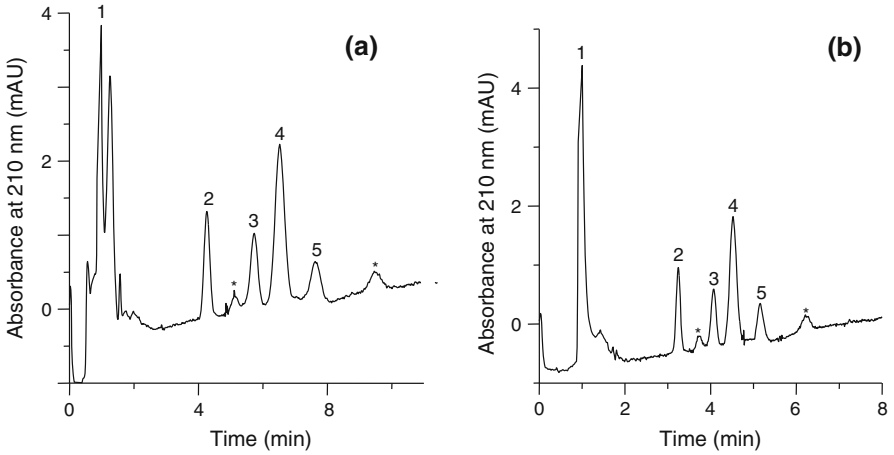

Fig. 4.13 Influence of the mobile phase composition on the separation of sterols: **a** 85:10:5 (v/v/v) ACN/THF/water and **b** 85:10:5 (v/v/v) ACN/2-propanol/water, both containing 5 mM Tris at pH 8.0. CEC conditions: LMA-based monolithic column prepared with 12 wt % 1,4-butanediol in the polymerization mixture (column A3) (Lerma-García et al. 2007); electrokinetic injection, 10 kV for 2 s; separation voltage, 20 kV. Peak identification: *1*, thiourea; *2*, ergosterol; *3*, cholesterol; *4*, stigmasterol; *5*, *β*-sitosterol. Impurities were labeled with an *asterisk* (Reprinted with permission from Lerma-García et al. (2008b). Copyright 2008 WILEY–VCH Verlag GmbH & Co. KGaA,Weinheim)

2-propanol is the higher solubility of sterols in this solvent when compared to that obtained with THF). Also in this case, 2-propanol content was varied within the 5–35 % range. The best results were obtained with a mobile phase constituted by 85:10:5 (v/v/v) ACN/2-propanol/water (see Fig. 4.13b). A comparison between efficiencies, *k*-values and peak pair resolutions obtained with the mobile phases containing either 10 % THF or 10 % 2-propanol is shown in Table 4.8. As deduced from this table, better efficiencies, lower *k*-values and similar resolutions were obtained when the mobile phase containing 2-propanol was compared with the

Table 4.9 Composition of the polymerization mixtures used for the preparation of LMA-based monolithic columns and their efficiency and retention values (Reprinted with permission from Lerma-García et al. (2008b). Copyright 2008 WILEY–VCH Verlag GmbH & Co. KGaA, Weinheim)

Column	Monomers/porogens, (%, wt/wt)	LMA/EDMA, (%, wt/wt)	1-Propanol/ 1,4-butanediol, (%, wt/wt)	$N_{\beta\text{-sitosterol}}$ (plates/m)	$k_{\beta\text{-sitosterol}}$
A1	40:60	60:40	86:14	NM[a]	NM[a]
A2	40:60	60:40	83:17	45,200	6.2
A3	40:60	60:40	80:20	60,900	4.1
A4	40:60	60:40	75:25	53,600	3.9
A5	30:70	60:40	80:20	28,200	2.9
A6	50:50	60:40	80:20	NM[a]	NM[a]
A7	40:60	70:30	80:20	58,700	3.6
A8	40:60	50:50	80:20	NM[a]	NM[a]

[a] Not measured

THF containing one. Thus, this mobile phase (85:10:5 (v/v/v) ACN/2-propanol/ water) was selected for further studies.

Next, under the optimal mobile phase conditions, the effect of porogenic solvent composition on the monolith morphology and on the chromatographic performance was investigated. In all cases, both monomers/porogens and monomers/crosslinker ratios were kept constant at 40:60 and 60:40 % (wt/wt), respectively. For this purpose, the content of 1,4-butanediol in the polymerization mixture was varied from 8 to 15 wt % (14–25 wt % for the porogenic solvents). With less than 10 wt % 1,4-butanediol (Table 4.9, column A1), a column with small pore sizes (<125 nm) (Lerma-García 2007), clearly unsuitable for any flow-through applications, was obtained.

When the content of 1,4-butanediol in the polymerization mixture was 10 wt % (column A2), analytes resolution was similar to that obtained using a 12 wt % 1,4-butanediol (column A3), but an increase in the analysis time ($\approx$15 min) and a decrease in the efficiency values was observed. This increase in the retentivity of solutes was due to a strong decrease of both the pore size of the monolith and the dimension of the globules, also implying an increase in the surface area, as observed for polymerization mixtures containing low 1,4-butanediol contents (Eeltink 2005 and 2007). This behavior can be explained briefly as follows. In a mixture of porogenic solvents with small 1,4-butanediol content (low polarity), phase separation will occur late in the polymerization process, due to the relatively high solubility of the polymer in the solvent. At the time of phase separation, the system contains a large polymer concentration, which precipitates in the form of numerous nuclei. All these nuclei are allowed to grow for only a limited period of time before all the monomers are exhausted. Overall, the globules that are formed in such a system are small and, consequently, the voids between them (pores) are small as well. The result would be a polymer with high surface area, and consequently, more retentivity. The low efficiencies obtained at 10 wt % of 1,4-butanediol (column A2) could be explained by the double-layer overlap,

as suggested by several authors (Eeltink 2005; Peters 1998). Next, a column containing 15 wt % 1,4-butanediol (column A4) was prepared. With this column, analysis time was reduced to 5 min although a coelution between cholesterol and stigmasterol peaks was observed. No improvements in resolution were reached when the mobile phase composition was slightly modified. Then, a content of 12 wt % of butanediol (20 wt % in the porogenic solvent) was selected for further experiments.

Once the optimal 1,4-butanediol content was established, the monomers/porogens ratio was next optimized, since this ratio affects the character of the monolith (Eeltink 2005; Peters 1998) (see Table 4.9, columns A3, A5 and A6). When the monomers/porogens ratio was 30:70 % wt:wt (column A5), cholesterol and stigmasterol peaks overlapped. This overlapping could be attributed to the large globule sizes formed in the monolith (Eeltink 2005; Peters 1998). However, when the ratio was varied up to 50:50 % wt:wt (column A6), the bed permeability was significantly reduced leading to blockage problems of columns. At the sight of these results, a monolithic column constructed using a 40:60 % wt:wt monomer/porogen ratio was selected for the next experiments.

Next, the monomer/crosslinker ratio was optimized by varying the EDMA (crosslinker) content from 30 to 50 % wt (Table 4.9, columns A3, A7 and A8). When the weight content of porogenic solvent (80:20 (wt/wt) 1,4-butanediol/1-propanol) was kept constant at 60 wt %, and the weight content of EDMA in monomer mixture was decreased from 40 (column A3) to 30 wt % (column A7), the efficiency values were similar, although β-sitosterol and cholesterol peaks partially overlapped. At 50 wt % EDMA (column A8), the permeability became so poor that it was impossible to flush the column due to the highly dense polymeric bed formed (Eeltink 2005). Thus, column A3, which provided the best results in terms of efficiency, resolution and analysis time, was selected.

A similar study was next carried out by varying the nature of the alkyl methacrylate monomer. For this purpose, LMA was substituted by ODMA (another methacrylate monomer with a longer alkyl chain). The 1,4-butanediol content in the polymerization mixture was first examined in the 4–15 wt % range (7–25 wt % of the porogenic solvent mixture) (Table 4.10, columns B1–B5). When the content of 1,4-butanediol was 4 % wt (column B1), the monolith permeability was very poor, leading to blockage problems of columns. When the content was increased up to 6 wt % 1,4-butanediol (column B2), poor efficiencies and long analysis times were observed, which could be attributed to the double-layer overlap. With 8 wt % (column B3), an efficiency of 42,000 for β-sitosterol, and resolution values for all the consecutive peak pairs, comprised between 1.2 and 2.9, were obtained. When 12 wt % (column B4) was tried, similar resolution values, higher efficiencies and lower analysis times were obtained if compared with those obtained by the column constructed using an 8 % wt 1,4-butanediol. Finally, when a percentage of 15 wt % 1,4-butanediol was used (column B5), cholesterol and stigmasterol peaks overlapped. As a result of this study, a column constructed using a content of 12 wt % 1,4-butanediol (column B4) was selected for the following research.

Table 4.10 Composition of the polymerization mixtures used for the preparation of ODMA-based monolithic columns and their efficiency and retention values (Reprinted with permission from Lerma-García et al. (2008b). Copyright 2008 WILEY–VCH Verlag GmbH & Co. KGaA,Weinheim)

Column	Monomers/porogens, (%, wt/wt)	ODMA/EDMA, (%, wt/wt)	1-Propanol/ 1,4-butanediol, (%, wt/wt)	$N_{\beta\text{-sitosterol}}$ (plates/m)	$k_{\beta\text{-sitosterol}}$
B1	40:60	60:40	93:7	NM[a]	NM[a]
B2	40:60	60:40	90:10	26,000	7.6
B3	40:60	60:40	86:14	42,000	4.8
B4	40:60	60:40	80:20	46,400	4.6
B5	40:60	60:40	75:25	36,200	3.9
B6	30:70	60:40	80:20	43,800	6.2
B7	50:50	60:40	80:20	NM[a]	NM[a]
B8	40:60	70:30	80:20	NM[a]	NM[a]
B9	40:60	50:50	80:20	34,200	7.1

[a] Not measured

The monomers/porogens ratio for ODMA columns was also optimized by varying it in the range 30:70–50:50 % wt:wt (Table 4.10, columns B4, B6 and B7). When the porogen content was increased from 60 to 70 wt % (column B6), the column efficiency for β-sitosterol decreased from 46,400 to 43,800 plates/m, while the k-value increased from 4.6 to 6.2. However, when the porogen weight fraction was reduced from 60 to 50 wt % (columns B4 and B7, respectively), all solutes co-eluted as a single peak. Thus, monomers/porogens ratio of 40:60 % wt:wt was selected for the next studies.

Next, the effect of the EDMA (crosslinker) content in the polymerization mixture was studied by varying it between 30 and 50 wt % (Table 4.10, columns B4, B8 and B9). When a 30 wt % EDMA was used (column B8), all sterol peaks overlapped in less than 2 min. However, a 50 wt % EDMA gave worse efficiency values (34,200 plates/m for β-sitosterol) and longer retentions times (*ca.* 13 min) than those obtained with 40 wt % EDMA. Thus, a 40 wt % EDMA content (column B4) was selected as the optimal one. The sterol separation provided by this column is shown in Fig. 4.14.

When this electrochromatogram (Fig. 4.14) was compared with that obtained using the optimal LMA column (Fig 4.13b), a slightly longer retention time was observed, although so much longer analysis times could be expected by using the ODMA column (longer alkyl chain than that of LMA). This fact could be explained taking into account that changes in the polymerization mixture (different bulk monomer) induce changes in both monolith hydrophobicity and in its structure. This behaviour has been also observed in literature (Delaunay-Bertoncini 2004; Waguespack 2005). Finally, when the monolithic bed of both columns was examined by SEM (Fig. 4.15), both the ODMA- and the LMA-based columns present voids and globules of similar sizes.

Additionally, the peak efficiencies achieved with the ODMA-based column were lower (26,000–46,400) than those obtained with the LMA-based

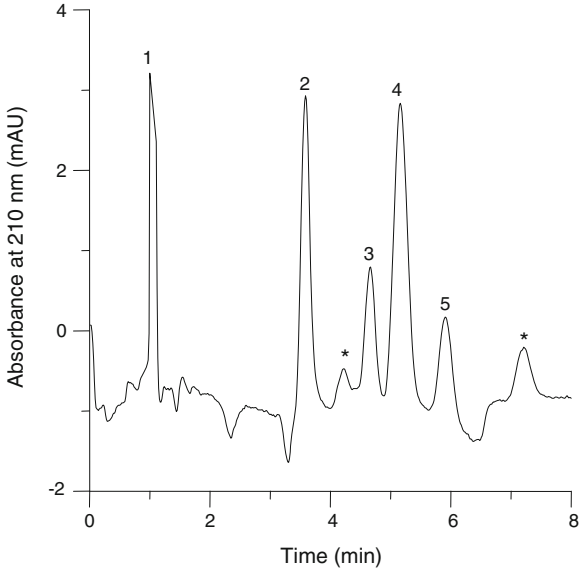

Fig. 4.14 Electrochromatogram obtained with an ODMA-based monolithic column prepared with 12 wt % 1,4-butanediol in the polymerization mixture (column B4). Mobile phase: 85:10:5 (v/v/v) ACN/2-propanol/water containing 5 mM Tris at pH 8.0. Peak identification and other experimental conditions as in Fig. 4.13 (Reprinted with permission from Lerma-García et al. (2008b). Copyright 2008 WILEY–VCH Verlag GmbH & Co. KGaA,Weinheim)

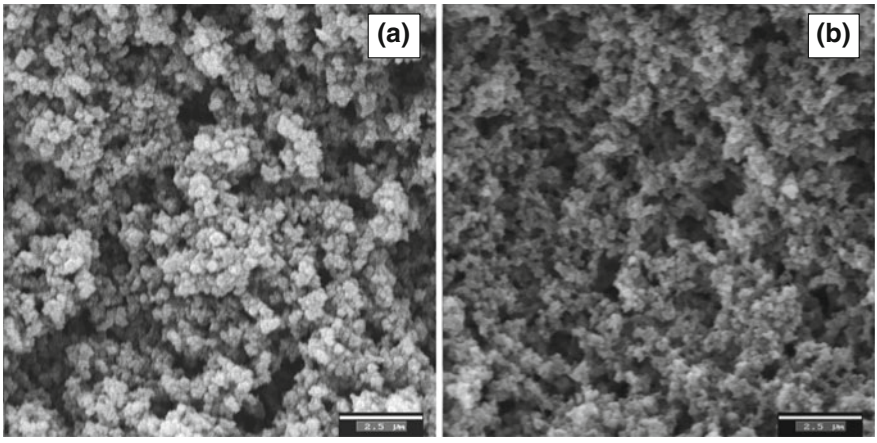

Fig. 4.15 SEM micrographs of the **a** LMA (column A3) and **b** ODMA (column B4) monolithic materials inside the capillary. The bar lengths stand for 2.5 μm (Reprinted with permission from Lerma-García et al. (2008b). Copyright 2008 WILEY–VCH Verlag GmbH & Co. KGaA, Weinheim)

Table 4.11 Analytical figures of merit for the sterol standards (Reprinted with permission from Lerma-García et al. (2008b). Copyright 2008 WILEY–VCH Verlag GmbH & Co. KGaA, Weinheim)

Compounds	Intra-day rep. RSD, %		Inter-day rep. RSD, %		Column-to-column reprod. RSD, %		Sensitivities, mM^{-1}
	t_R	Peak area	t_R	Peak area	t_R	Peak area	
Ergosterol	0.12	2.62	2.15	4.40	3.81	5.20	31.3
Cholesterol	0.34	2.92	2.44	5.22	4.26	6.20	28.5
Stigmasterol	0.27	2.10	2.72	4.92	4.40	5.63	29.6
β-Sitosterol	0.11	2.84	2.91	4.74	3.73	5.44	31.5
EOF	0.43	1.92	1.52	3.52	3.10	4.92	-

column (28,800–60,900 plates/m). As a result of this study, the LMA monolithic column (column A3) was selected as the best compromise between resolution, efficiency and analysis time.

4.4.2 Quantitation Studies and Application to Real Samples

External calibration curves were obtained by injecting six standard solutions of each solute within its linearity range (0.125–5 mM). All curves were linear with r values higher than 0.994. Intra- and inter-day repeatabilities in the selected conditions were obtained by injecting a mixture containing 0.75 mM of each sterol ten times per day during three consecutive days (Table 4.11). The column-to-column reproducibility was also tested by repeating the same number of injections on three different monolithic columns, which were prepared using with the same polymerization mixture. The EOF reproducibility, retention times and peak areas are summarized in Table 4.11.

As observed, the column-to-column reproducibilities of the retention times and peak areas were better than 4.4 and 6.2 %, respectively. About 80 injections of the standard mixture and 50 injections of vegetable oil extracts were performed without the need of replacing the column, therefore, the stability of the columns was satisfactory. On the other hand, all the sterols gave closely similar sensitivities. The LODs, also calculated at a signal-to-noise ratio of 3, ranged from 0.025 to 0.037 mM^{-1} for stigmasterol and ergosterol peaks, respectively.

Next, vegetable oil samples were analyzed. Representative electrochromatograms of EVOO, hazelnut and soybean oil extracts are shown in Fig. 4.16.

Peak identification was performed by comparing the retention times with those of the standards or by spiking the sample extracts with the standards. The assignments of other sample peaks, such as avenasterol and campesterol, were tentatively made taking into account the common occurrence of these sterols in the vegetable oils analyzed (Abidi 2004; Benitez-Sánchez 2003; Bohacenko 2001; Cercaci 2003; Jee 2002; Martínez-Vidal 2007; Matthäus 2008; Parcerisa 2000). Thus, the peak located close to 4 min (no. 6 of Fig. 4.16) was tentatively assigned

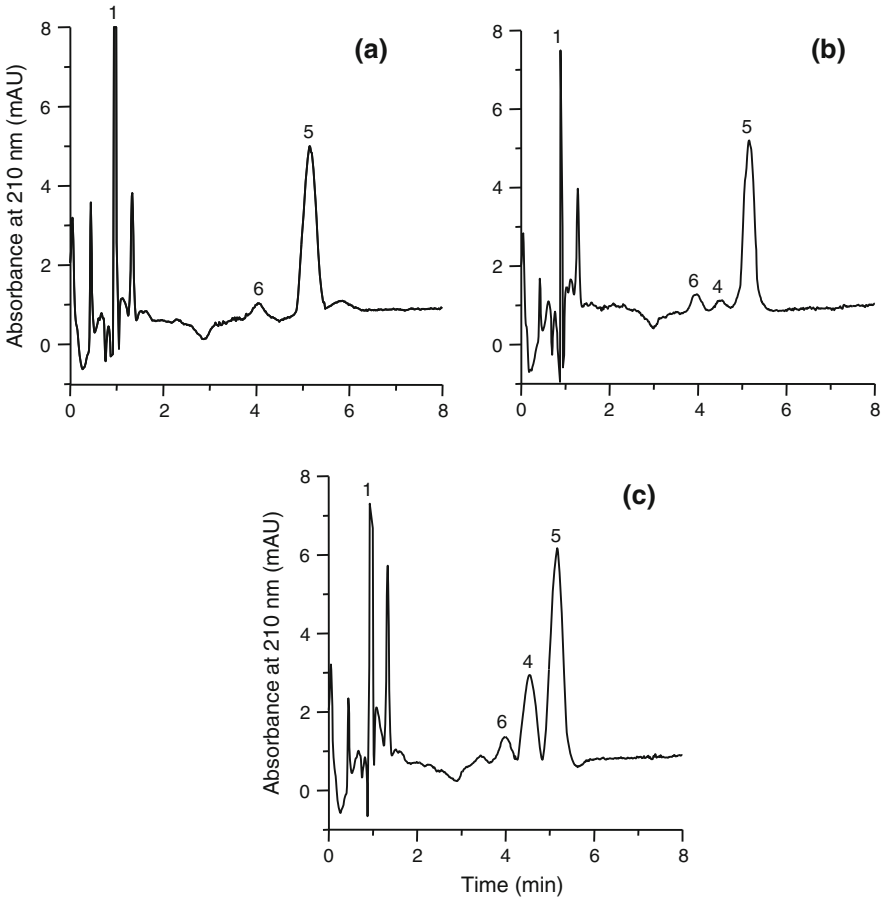

Fig. 4.16 Electrochromatograms of **a** EVOO, **b** hazelnut and **c** soybean oils obtained using an LMA-based monolithic capillary column (column A3). Mobile phase: 85:10:5 (v/v/v) ACN-2-propanol-water containing 5 mM Tris at pH 8.0. Peak identification: 5, β-sitosterol + campesterol; 6, avenasterol. Identification of other peaks and other working conditions as in Fig. 4.13 (Reprinted with permission from Lerma-García et al. (2008b). Copyright 2008 WILEY–VCH Verlag GmbH & Co. KGaA,Weinheim)

to avenasterol. This peak eluted close to cholesterol peak, which is present in vegetable oils in concentrations below the LOD of the proposed method (Bohacenko 2001; Cañabate-Díaz 2007; Cercaci 2003; Martínez-Vidal 2007). The coelution of cholesterol and avenasterol is also consistent with findings reported in literature for RP columns (Martínez-Vidal 2007). On the other hand, the presumably coelution found for β-sitosterol and campesterol was expected taking into account the structural similarity between both sterols, in fact, Mezine et al. (2003) failed to separate both compounds using an RP hexyl-phenyl column. However, Abidi et al. (2004) were able to resolve this pair employing a CEC C_{18} packed

Table 4.12 Percentage of sterols found in vegetable oils [a] (Reprinted with permission from Lerma-García et al. (2008b). Copyright 2008 WILEY–VCH Verlag GmbH & Co. KGaA, Weinheim)

Oil	Avenasterol, %	Stigmasterol, %	β-Sitosterol + campesterol, %
Sunflower	5	10	85
EVOO	9	ND	91
Soybean	3	19	78
Corn	7	6	87
Peanut	7	9	84
Grapeseed	3	12	85
Hazelnut	5	1	94

[a] ND = Not detected

column, but at expenses of long analysis times (<55 min). Then, the percentage of these unresolved peaks was expressed as the sum of both compounds.

Due to the similarity between the sensitivities found for all sterol standards (see Table 4.11), the β-sitosterol + campesterol and avenasterol contents were estimated using β-sitosterol as reference standard. The found percentages of sterols in the vegetable oils are shown in Table 4.12. These results are in agreement with previously reported data (Abidi 2004; Benitez-Sánchez 2003; Bohacenko 2001; Cañabate-Díaz 2007; Cercaci 2003; Jee 2002; Martínez-Vidal 2007, Matthäus 2008; Parcerisa 2000). As it can be observed in Table 4.12, both soybean and sunflower oils showed large quantities of stigmasterol. As this sterol is not found in EVOO (is below the LOD) (Bohacenko 2001; Benitez-Sánchez 2003; Cañabate-Díaz 2007; Cercaci 2003; Jee 2002; Martínez-Vidal 2007, Parcerisa 2000), it could be used as an adulteration marker (Ballesteros 1995; Kamm 2001) of EVOO adulteration with soybean and sunflower oils. Consequently, by injecting a series of mixtures of these two oils with EVOO, and using the stigmasterol peak area as an adulteration marker, the presence of 8 % soybean or sunflower oil in virgin olive oil was clearly evidenced (see Fig. 4.17).

4.5 Determination of Sterols by UPLC-MS[5]

In this work, an UPLC method (using APCI-MS as detection technique) has been developed to identify and determine the main sterols present in vegetable oils with different botanical origins. For this purpose, the vegetable oils employed in this study are shown in Table 4.13.

[5] Parts of the text of this section have been adapted with permission from Lerma-García et al. (2010a). Copyright 2010 American Chemical Society.

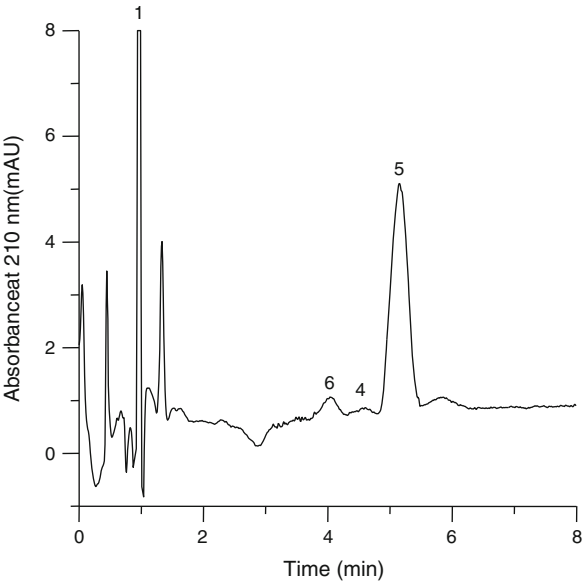

Fig. 4.17 Electrochromatogram of an EVOO containing 8 % soybean oil showing the stigmasterol peak (no. 4). Peak identification and other working conditions as in Fig. 4.16 (Reprinted with permission from Lerma-García et al. (2008b). Copyright 2008 WILEY–VCH Verlag GmbH & Co. KGaA,Weinheim)

4.5.1 Optimization of the Separation Conditions

To optimize sterol separation, a sterol standard mixture containing ca. 50 μg mL^{-1} of ergosterol, stigmasterol, cholesterol and lanosterol, and 38 and 5 μg mL^{-1} for *β*-sitosterol and campesterol, respectively, was used.

The first parameter to be optimized was mobile phase composition. Different mixtures of ACN/water, both containing 0.01 % acetic acid (Cañabate-Díaz 2007) were tried in gradient elution mode, using a constant column temperature (30 °C) and a fixed flow rate (0.5 mL min^{-1}). For each sterol standard, two SIR channels, which corresponded to the $[M + H]^+$ and $[M + H\text{-}H_2O]^+$ ions, were monitored. However, only the $[M + H\text{-}H_2O]^+$ peaks, which showed higher intensities than the respective $[M + H]^+$ peaks, were used for identification and quantification. This fact has been previously reported in literature (Cañabate-Díaz 2007; Lerma-García 2008a; Segura-Carretero 2008). The APCI mass spectra of the six sterol standards showing the $[M + H\text{-}H_2O]^+$ peaks (at *m/z* 379.5, 369.5, 383.5, 395.5, 397.5 and 409.5 for ergosterol, cholesterol, campesterol, stigmasterol, *β*-sitosterol and lanosterol, respectively) are shown in Fig. 4.18. Since stigmasterol and campesterol peaks overlapped in all the

Table 4.13 Botanical origin, number and brand of the vegetable oil samples used in this work

Origin	No. of samples	Brand
Avocado	2	Guinama
	2	Marnys
Corn	2	Guinama
	1	Asua
	1	Cristal
Olive	1	Carbonell
	1	Grupo Hojiblanca
	1	Borges
	1	Torrereal
Hazelnut	2	Guinama
	1	Percheron
	1	Flumen
Grapeseed	1	Guinama
	1	Paul Corcelet
	1	Pons
	1	Coosur
Peanut	1	Guinama
	1	Bellsola
	1	Apsara Vital
	1	Maurel
Soybean	1	Coosur
	1	Guinama
	1	Biolasi
	1	Sojola
Sunflower	2	Koipesol
	1	Hacendado
	1	Coosur

gradient elutions tested, a linear gradient from 80 to 100 % ACN for 0.5 min, followed by an isocratic elution with 100 % ACN was selected as the best compromise between analysis time and resolution (Fig. 4.19b). This peak pair overlapping has been also reported in literature (Lu 2007).

Next, the influence of column temperature, which was varied between 10 and 40 °C, was evaluated. For this purpose, the optimal gradient elution and a flow rate of 0.5 mL min^{-1} were used. When column temperature was 40 °C (Fig. 4.19a), an overlapping between lanosterol and cholesterol peaks was observed. When the temperature was decreased from 30 to 10 °C (Fig. 4.19b–d), a slight decrease in efficiency values jointly with an increase in analysis time was evidenced. However, the global resolution (measured as the geometrical mean of the resolution between the consecutive sterol pairs) slightly improved (from 1.18 to 1.30). For this reason, a column temperature of 10 °C was selected for further studies.

Once optimized gradient elution and column temperature, the influence of the flow rate, which was varied between 0.4 and 1.2 mL min^{-1}, was next evaluated

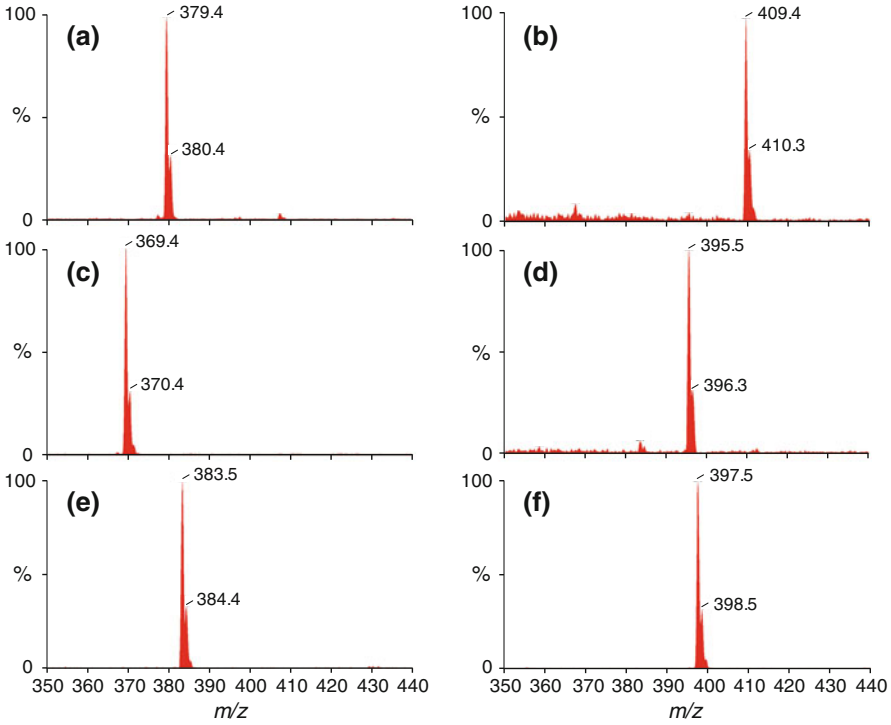

Fig. 4.18 Full scan mass spectra of the six sterol standards used in this study. Peak identification: **a**, ergosterol; **b**, lanosterol; **c**, cholesterol; **d**, stigmasterol; **e**, campesterol; **f**, *β*-sitosterol (Reprinted with permission from Lerma-García et al. (2010a). Copyright 2010 American Chemical Society)

(see Fig. 4.20). When the flow rate was increased from 0.4 to 0.8 mL min^{-1} (Fig. 4.20a, b), higher efficiencies were obtained, whereas the global resolution decreased from 1.47 to 1.28; a decrease of both parameters was observed when the flow rate was increased up to 1.2 mL min^{-1} (Fig. 4.20c). As a result, a flow rate of 0.8 mL min^{-1} was selected as the best compromise between efficiency, resolution and analysis time.

4.5.2 Quantitation Studies and Application to Real Samples

Under the proposed chromatographic conditions, external calibration curves were obtained by injecting six standard solutions of each sterol within its linearity range 0.5–50 μg mL^{-1}, except for *β*-sitosterol that ranged up to 250 μg mL^{-1}). In all

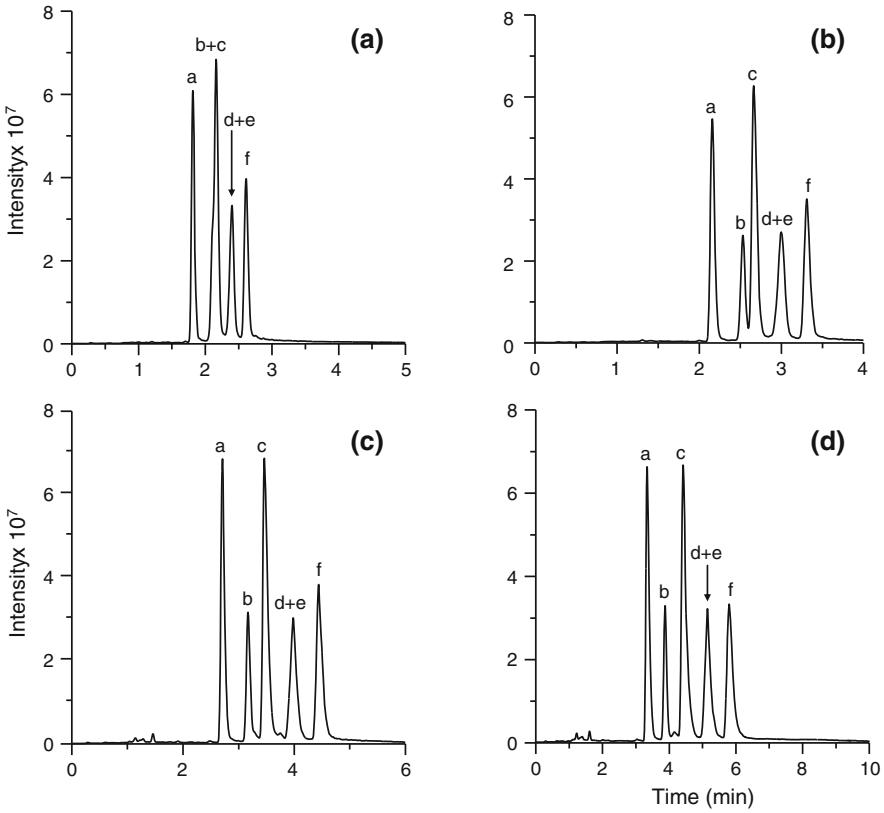

Fig. 4.19 Influence of the column temperature on the separation of sterols: **a** 40 °C, **b** 30 °C, **c** 20 °C and **d** 10 °C. Chromatographic conditions: linear gradient from 80 to 100 % ACN for 0.5 min followed by isocratic elution with 100 % ACN for 4.5 more min using a flow rate of 0.5 mL min^{-1}. Peak identification as in Fig. 4.18 (Reprinted with permission from Lerma-García et al. (2010a). Copyright 2010 American Chemical Society)

cases, an excellent linearity with $r > 0.999$ was obtained. Other analytical figures of merit of the proposed method are shown in Table 4.14. Precision was obtained by testing the repeatabilities of peak areas and retention time obtained by injecting ten times per day during 3 days the same 1 μg mL^{-1} solution. The relative sensitivities of sterols (respect to β-sitosterol) were comprised between 0.9 and 1.2, except for lanosterol, which gave a value of 0.4. This behavior, which was in agreement with previous studies (Lu 2007), was attributed to differences in sterol structures.

The LODs and LOQs of the solutes were obtained for signal-to-noise ratio of 3 and 10, respectively. LODs were comprised between 0.03 and 0.07 μg mL^{-1}, whereas the LOQs ranged from 0.10 to 0.25 μg mL^{-1}. These values were higher

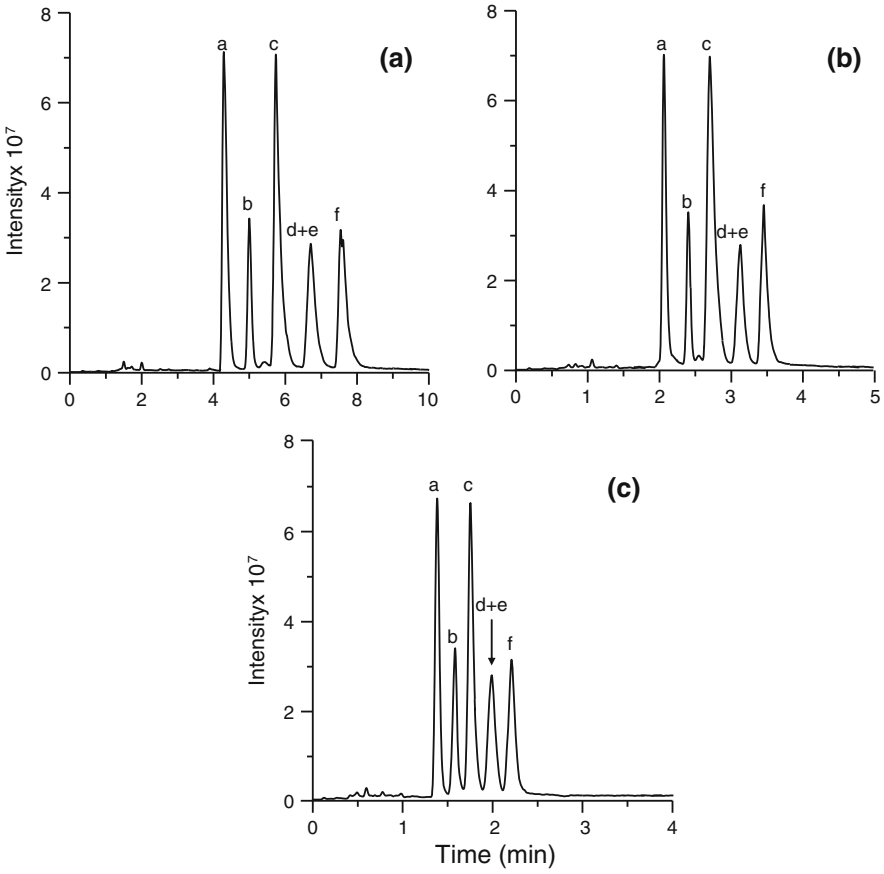

Fig. 4.20 Influence of flow rate on the separation of sterols: **a** 0.4, **b** 0.8 and **c** 1.2 mL min^{-1}. Chromatographic conditions: temperature 10 °C; gradient elution and peak identification as in Fig. 4.19 (Reprinted with permission from Lerma-García et al. (2010a). Copyright 2010 American Chemical Society)

than those reported by Lu (2007) working with the same stationary phase in an UPLC system connected to a triple-quadrupole mass spectrometer. On the other hand, the values obtained in this work were lower than those obtained using a conventional HPLC system connected to a single-quadrupole instrument (Cañabate-Díaz 2007; Martínez-Vidal 2007). In any case, a substantial reduction in the analysis time was achieved with the proposed method (between 4 and 10-fold lower than those found in the literature) (Cañabate-Díaz 2007; Martínez-Vidal 2007; Segura-Carretero 2008).

Table 4.14 Analytical figures of merit of the proposed UPLC-MS method for the determination of sterols (Reprinted with permission from Lerma-García et al. (2010a). Copyright 2010 American Chemical Society)

Analyte	Intra-day rep[a], %		Inter-day rep[b], %		LOD	LOQ	Relative
	Area	t_R	Area	t_R	(μg mL^{-1})	(μg mL^{-1})	Sensitivity[c]
Ergosterol	2.8	0.08	3.6	0.25	0.04	0.13	1.1
Lanosterol	2.7	0.08	3.2	0.27	0.07	0.25	0.4
Cholesterol	2.7	0.10	4.1	0.30	0.03	0.10	1.2
Stigmasterol	2.6	0.11	3.7	0.30	0.04	0.13	0.9
Campesterol	2.9	0.11	3.8	0.31	0.03	0.10	1.2
β-Sitosterol	2.4	0.12	5.0	0.40	0.04	0.13	1.0

[a] Repeatability (as RSD) for a sterol concentration of 1 μg mL^{-1} (n = 10)
[b] Repeatability (as RSD) for a sterol concentration of 1 μg mL^{-1} (3 days)
[c] As the ratio of the slopes of calibration curves of sterols (respect to *β*-sitosterol)

Table 4.15 Ions observed in the APCI mass spectra of the oil samples with their corresponding retention times (t_R) (Reprinted with permission from Lerma-García et al. (2010a). Copyright 2010 American Chemical Society)

Peak no.	Analyte	t_R (min)	Ion $[M + H\text{-}H_2O]^+$ (*m/z*)
1	Erythrodiol	1.4	425.5
2	Uvaol	1.4	425.5
3	Ergosterol	2.1	379.5
4	Brassicasterol	2.2	381.5
5	Δ^5-Avenasterol	2.4	395.5
6	Cholesterol	2.7	369.5
7	Campesterol	3.1	383.5
8	Campestanol	3.1	385.5
9	Stigmasterol	3.1	395.5
10	Clerosterol	3.1	395.5
11	$\Delta^{5,24}$-Stigmastadienol	3.3	395.5
12	*β*-Sitosterol	3.5	397.5
13	Δ^7-Stigmastenol	3.5	397.5
14	Sitostanol	4.5	399.5

When the analytical performance of the proposed method was compared to GC methods using FID or MS detection (Cercaci 2007; Cunha 2006; Galeano Díaz 2005; Parcerisa 2000; Rivera del Álamo 2004; Sanchéz-Casas 2004; Thanh 2006), a low peak resolution was obtained, especially for some peak pairs as *β*-sitosterol/Δ^7-stigmastenol and stigmasterol/clerosterol; however, longer analysis times (25–30 min) than that found with the proposed method (5 min) were obtained. In spite of the overlapping of these peak pairs, satisfactory results were achieved in terms of resolution/analysis time ratio. Besides, an additional advantage of the recommended method is that the derivatization step is avoided, which is time-consuming and could be a source of artefacts (Lu 2007).

Table 4.16 Proportions of sterols found in total sterol fraction (%) (Reprinted with permission from Lerma-García et al. (2010a). Copyright 2010 American Chemical Society)

Sterol	Avocado	Corn	EVOO	Grapeseed	Hazelnut	Peanut	Soybean	Sunflower
Erythrodiol + Uvaol	0.05–0.17	0.27–0.45	0.53–0.90	0.01–0.07	0.16–0.19	0.30–0.35	0.10–0.15	0.25–0.35
Ergosterol	0.01–0.02	0.01–0.02	0.01–0.02	0.00–0.02	0.25–0.34	0.50–0.90	0.01-0.05	0.03–0.05
Brassicasterol	0.25–0.37	0.15–0.18	0.11–0.18	0.10–0.20	0.30–0.40	0.10–0.18	0.28–0.30	0.19–0.23
Δ^5-Avensterol	17.20–18.15	3.95–5.75	11.00-13.00	2.50–2.80	1.90–2.10	9.18–11.32	3.50–4.00	6.45–9.05
Cholesterol	0.22–0.62	0.31–0.53	0.32–0.47	0.54–0.78	0.30–0.40	0.68–2.10	0.80–0.90	0.78–0.83
Campesterol	4.50–6.30	19.00–19.75	2.74–3.13	12.82–13.14	4.50–5.00	16.47–18.20	17.00–19.00	10.20–10.89
Campestanol	0.31–0.41	0.83–0.91	0.24–0.32	0.58–0.62	0.20-0.23	0.50–0.74	0.60–0.80	0.43–0.53
Stigmasterol + clerosterol	0.44–0.75	6.54–8.08	1.51–3.00	13.94–15.54	0.90–1.00	10.30–11.93	18.40–19.10	8.94–9.37
$\Delta^{5.24}$-Stigmastadienol	ND	0.63–0.70	0.80–0.91	ND	0.95–1.03	0.49–0.51	ND	0.62–0.68
β-Sitosterol + Stigmastenol	72.67–76.54	61.33–66.21	77.69–82.44	64.39–67.27	87.01–88.54	53.27–61.03	54.70–58.61	67.56–71.76
Sitostanol	0.48–0.54	2.10–2.30	0.30–0.38	2.24–2.44	2.00–2.30	0.45–0.50	0.70–1.00	0.35–0.46

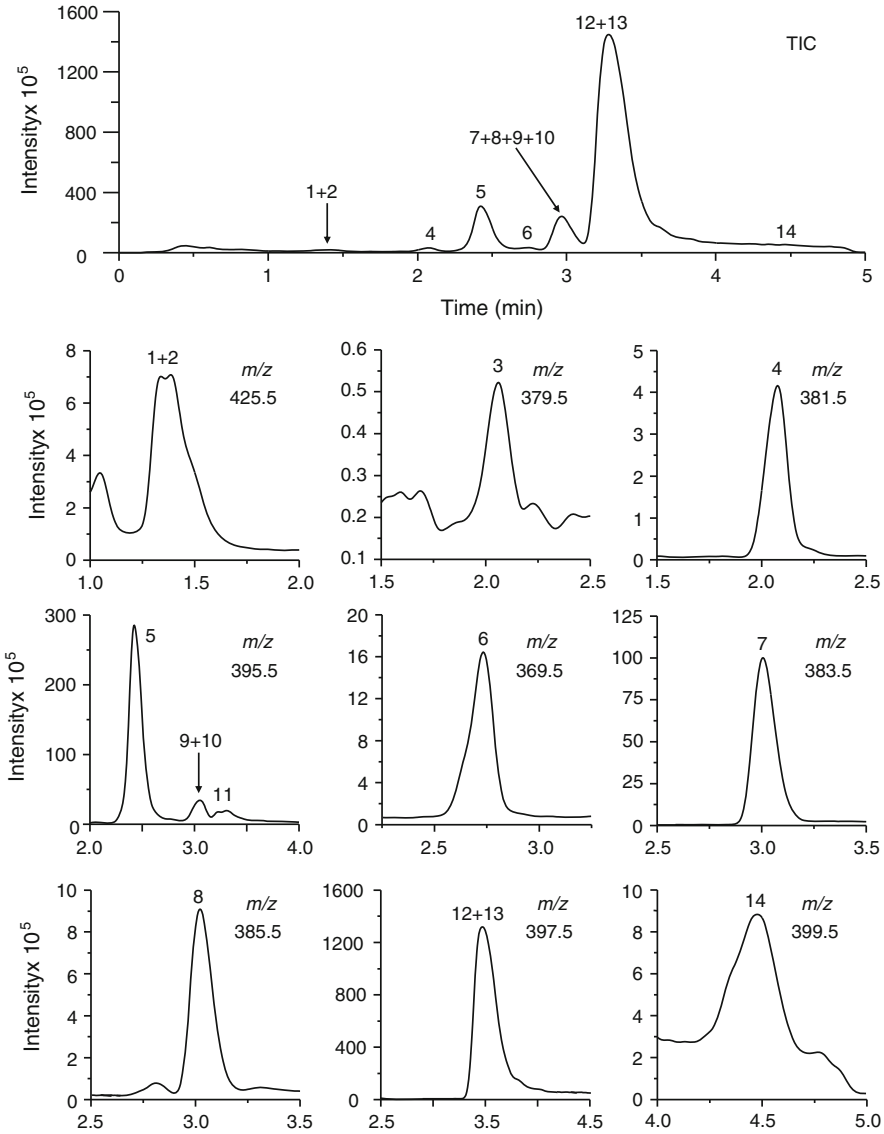

Fig. 4.21 TIC and SIRs of an EVOO extract. Chromatographic conditions: gradient elution as in Fig. 4.19; column temperature, 10 °C; flow rate, 0.8 mL min^{-1}. Peak identification as indicated in Table 4.14 (Reprinted with permission from Lerma-García et al. (2010a). Copyright 2010 American Chemical Society)

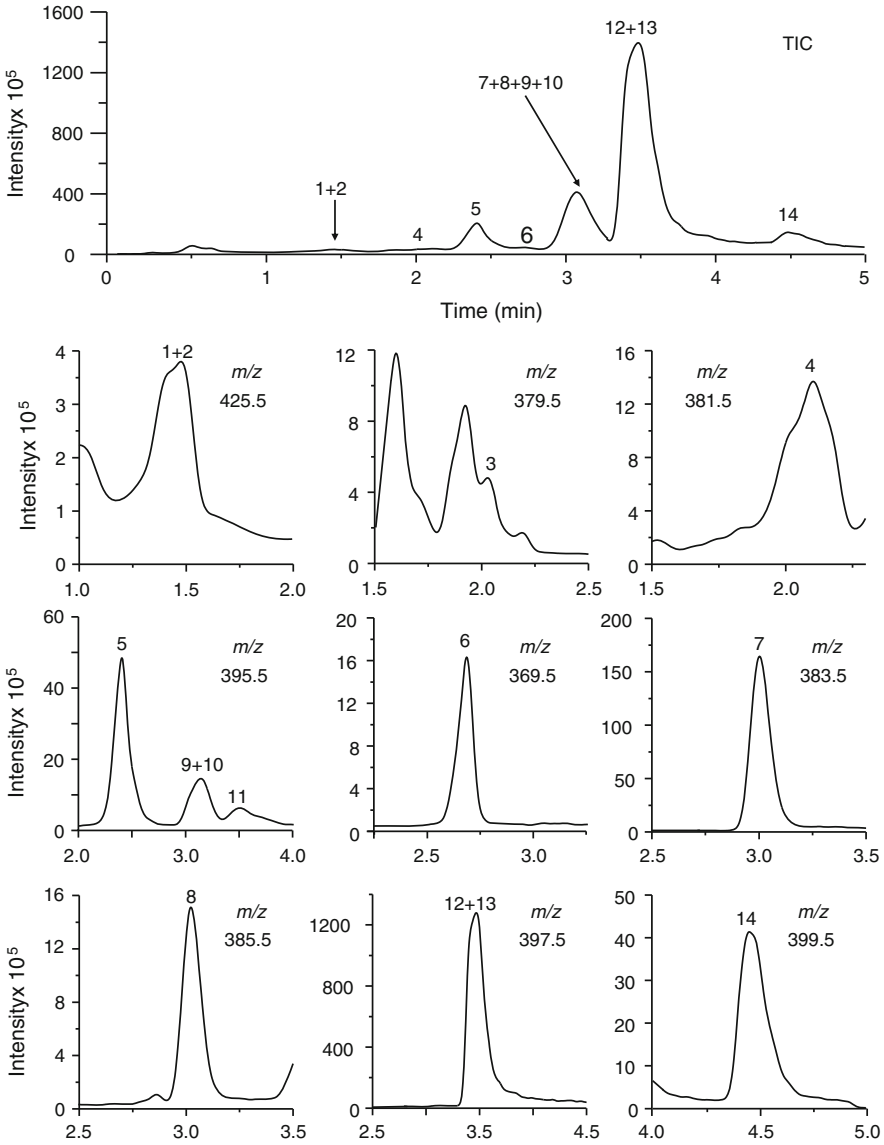

Fig. 4.22 TIC and SIRs of a hazelnut oil extract. Other experimental conditions as in Fig. 4.21 (adapted with permission from Lerma-García et al. (2010a). Copyright 2010 American Chemical Society)

After all these considerations, the optimized method was applied to the analysis of real samples. All the sterol extracts were injected three times. To identify other sterol peaks, which presence in vegetable oils has been previously described in literature (Cañabate-Díaz 2007; Lerma-García 2008a; Segura-Carretero 2008), the *m/z* values corresponding to the $[M + H\text{-}H_2O]^+$ ions of these sterols (see Table 4.15) were also recorded. A total of 11 peaks, which corresponded to individual sterols or combination of sterol peaks were distinguished in less than 5 min.

The TIC and SIRs of EVOO and hazelnut extracts are shown in Figs. 4.21 and 4.22, respectively. To quantify the main sterols found in the samples, peak areas were measured from the SIR chromatograms, which were smoothed using a mean algorithm set at window 3 and number 5. The calibration curves of the sterol standards were used to quantify that sterol and also to estimate the concentrations of those sterols which were not available as standards: lanosterol calibration curve was used to estimate the concentration of the saturated sterols (campestanol and sitostanol), since lanosterol showed a similar sensitivity to that reported in the literature for these compounds (Lu 2007). This curve was also used to estimate erythrodiol + uvaol concentrations due to the structural resemblance between these compounds. Finally, the β-sitosterol calibration curve was used to estimate the rest of sterols (brassicasterol, Δ^5-avenasterol and $\Delta^{5,24}$-stigmastadienol).

The percentages of sterols, calculated as explained before, are shown in Table 4.16. These values found in these samples were in good agreement with data previously reported (Abidi 2004; Cañabate-Díaz 2007; Jee 2002; Martínez-Vidal 2007; Parcerisa 2000). For all vegetable oils, the most abundant sterol was β-sitosterol. Soybean oil contained large quantities of campesterol and stigmasterol + clerosterol, being these contents lower for corn oil, and still lower in EVOO. Thus, stigmaterol could be used as marker of EVOO adulteration with these two cheaper oils. The highest contents of Δ^5-avenasterol were found in avocado followed by EVOO and peanut oils. This sterol was found in much lower amounts in hazelnut than in EVOO; however, sitostanol showed a larger content in hazelnut (see Figs. 4.21 and 4.22). So these peaks could be used to detect EVOO adulteration with hazelnut oil. On the other hand, hazelnut and peanut oils showed large ergosterol contents. These high amounts could indicate a fungal activity in the raw material, which also indicates the quality of these oils (Parsia 2006).

References

Abidi SL (1999) J Chromatogr A 844:67
Abidi SL (2000) J Chromatogr A 881:197
Abidi SL (2004) J Chromatogr A 1059:199
Abidi SL, Mounts TL (1997) J Chromatogr A 782:25
Abidi SL, Rennick KA (2001) J Chromatogr A 913:379

Abidi SL, Thiam S, Warner IM (2002) J Chromatogr A 949:195
Ballesteros E, Gallego M, Valcárcel M (1995) Anal Chim Acta 308:253
Benitez-Sánchez PL, León-Camacho M, Aparicio R (2003) Eur Food Res Technol 218:13
Bernabé-Zafón V, Cantó-Mirapeix A, Simó-Alfonso EF, Ramis-Ramos G, Herrero-Martínez JM (2009) Electrophoresis 30:1929
Bohacenko I, Kopicová Z (2001) Czech J Food Sci 19:97
Cañabate-Díaz B, Segura Carretero A, Fernández-Gutiérrez A, Belmonte Vega A, Garrido Frenich A, Martínez Vidal JL, Duran Martos J (2007) Food Chem 102:593
Cercaci L, Passalacqua G, Poerio A, Rodriguez-Estrada MT, Lercker G (2007) Food Chem 102:66
Cercaci L, Rodríguez-Estrada MT, Lercker G (2003) J Chromatogr A 985:211
Cerretani L, Lerma-García MJ, Herrero-Martínez JM, Gallina-Toschi T, Simó-Alfonso EF (2010) J Agric Food Chem 58:757. Copyright 2009 American Chemical Society
Choo YM, Yap SC, Ooi CK, Ma AN, Goh SH, Ong ASH (1996) J Am Oil Chem Soc 73:599
Cunha SC, Fernandes JO, Beatriz M, Oliveira PP (2006) J Chromatogr A 1128:220
Delaunay-Bertoncini N, Demesmay C, Rocca JL (2004) Electrophoresis 25:3204
Dionisi F, Prodolliet J, Tagliaferri E (1995) J Am Oil Chem Soc 72:1505
Eeltink S, Herrero-Martínez JM, Rozing GP, Schoenmakers PJ, Kok WT (2005) Anal Chem 77:7342
Eeltink S, Svec F (2007) Electrophoresis 28:137
Fanali S, Camera E, Chankvetadze B, D'Orazio G, Quaglia MG (2004) J Pharmaceut Biomed 35:331
Galeano Diaz T, Durán Merás J, Sánchez Casas J, Alexandre Franco ME (2005) Food Control 16:339
Gimeno E, Castellote AI, Lamuela-Raventós RM, De la Torre MC, López-Sabater MC (2000) J Chromatogr A 881:255
Gruszka J, Kruk J (2007) Chromatographia 66:909
Jee M (2002) Oils and fat authentication. CRC Press, Blackwell Publishing, Boca Raton
Kamm W, Dionisi F, Hischenhuber C, Engel KH (2001) Food Rev Int 17:249
Lerma-García MJ, Simó-Alfonso EF, Méndez A, Lliberia JL, Herrero-Martínez JM (2010a) J Agric Food Chem 58:2771. Copyright 2010 American Chemical Society
Lerma-García MJ, Cerretani L, Herrero-Martínez JM, Bendini A, Simó-Alfonso EF (2010b) J Sep Sci 33:2681. Copyright 2010 WILEY-VCH Verlag GmbH & Co. KgaA, Weinheim
Lerma-García MJ, Ramis-Ramos G, Herrero-Martínez JM, Simó-Alfonso EF (2008a) Rapid Commun Mass Spectrom 22:973
Lerma-García MJ, Simó-Alfonso EF, Ramis-Ramos G, Herrero-Martínez JM (2008b). Electrophoresis 29:4603. Copyright 2008 WILEY-VCH Verlag GmbH & Co. KgaA, Weinheim
Lerma-García MJ, Simó-Alfonso EF, Ramis-Ramos G, Herrero-Martínez JM (2007) Electrophoresis 28:4128. Copyright 2007 WILEY-VCH Verlag GmbH & Co. KgaA, Weinheim
Lu B, Zhang Y, Wu X, Shi J (2007) Anal Chim Acta 588:50
Martínez-Vidal JL, Garrido-Frenich A, Escobar-García MA, Romero-González R (2007) Chromatographia 65:695
Matthäus B (2008) Eur J Lipid Sci Technol 110:645
Mezine I, Zhang H, Macku C, Lijana R (2003) J Agric Food Chem 51:563
Parcerisa J, Casals I, Boatella J, Codony R, Rafecas M (2000) J Chromatogr A 881:149
Parsia Z, Górecki TJ (2006) J Chromatogr A 1130:145
Peters EC, Petro M, Svec F, Fréchet JMJ (1998) Anal Chem 70:2288
Rivera del Álamo RM, Fregapane G, Aranda F, Gómez-Alonso S, Salvador MD (2004) Food Chem 84:533
Rovellini P, Azzolini M, Cortesi N (1997) Riv Ital Sost Grasse 74:1
Sánchez-Casas J, Osorio Bueno E, Montaño García AF, Martinez Cano M (2004) Food Chem 87:225
Segura-Carretero A, Carrasco-Pancorbo A, Cortacero S, Gori A, Cerretani L, Fernández-Gutiérrez A (2008) Eur J Lipid Sci Technol 110:1142

Thanh TT, Vergnes MF, Kaloustian J, El-Moselhy TF, Amiot-Carlin MJ, Portugal H (2006) J Sci Food Agric 86:220
Waguespack BL, Hodges SA, Bush ME, Sondergeld LJ, Bushey MM (2005) J Chromatogr A 1078:171
Waseem A, Rishi L, Yaqoob M, Nabi A (2009) Anal Sci 25:407
Watson RR, Preedy VR (2009) Tocotrienols: vitamin E beyond tocopherols. The American Oil Chemist's Society, Urbana
Yu C, Xu M, Svec F, Fréchet JMJ (2001) J Polym Sci Pol Chem 40:755

Chapter 5
Development of Methods for the Classification of Vegetable Oils According to Their Botanical Origin

5.1 Classification Using FTIR Spectroscopy Data[1]

The aim of this work was to construct an LDA model able to classify vegetable oils according to their botanical origin using FTIR spectroscopy data. Also, FTIR data treatment by MLR was used to detect and quantify EVOO adulteration with other low cost edible oils. For these purposes, the vegetable oils shown in Table 5.1 were used. The FTIR spectra of these 30 oil samples were then measured. In all cases, at least two spectra were recorded for each sample. As indicated in this table, four samples of each botanical origin were used to construct a training set in the classification studies, while the remaining samples of each category were employed to evaluate the prediction capability of the classification models.

5.1.1 Data Treatment and Construction of Data Matrices

As indicated in Table 5.2, all the FTIR spectra measured were divided in 26 wavelength regions according to the different peaks or shoulders observed, which represent structural or functional group information. Then, for statistical data treatment, the peak/shoulder area of each region was measured. In this study, both the normalization procedures A and B, previously described in Sect. 3.7, were used. Then, 26 normalized variables to be used as predictors were obtained by normalization procedure A, whereas 325 predictors were obtained by normalization procedure B. Thus, for classification studies, two matrices containing 20 objects each were constructed. Each object corresponded to the mean of the two

[1] Parts of the text of this section have been adapted with permission from Lerma-García et al. (2010). Copyright 2009 Elsevier Ltd.

M. J. Lerma García, *Characterization and Authentication of Olive and Other Vegetable Oils*, Springer Theses, DOI: 10.1007/978-3-642-31418-6_5,

Table 5.1 Botanical origin, number of samples, brand and use during LDA model construction of the oil samples (Reprinted from Lerma-García et al. (2010). Copyright 2009 Elsevier Ltd.)

Origin	No. of samples	Brand	LDA set
Hazelnut	2	Guinama	Training
	2	Percheron	Training
	2	Flumen	Evaluation
Sunflower	2	Koipesol	Training
	2	Hacendado	Training
	1	Capicua	Evaluation
	1	Coosol	Evaluation
Corn	1	Guinama	Training
	1	Asua	Training
	1	Artua	Evaluation
	1	Mazola	Evaluation
Corn germ	1	Guinama	Training
	1	Hacendado	Training
EVOO	1	Carbonell	Training
	1	Grupo Hojiblanca	Training
	1	Borges	Training
	1	Torrereal	Training
	1	Coosur	Evaluation
	1	Hacendado	Evaluation
Soybean	2	Guinama	Training
	2	Biolasi	Training
	2	Sojola	Evaluation

spectra of each training sample of Table 5.1, and either 26 or 325 predictors, according to normalization procedures A and B, respectively. A response column, which contains five categories (one category for each oil botanical origin, since corn and corn germ were considered as a single category), was added to these matrices. These matrices were used as training sets. To construct these training matrices, only the means of the replicates of the samples were included; in this way, the internal dispersion of the categories was reduced, which was important to reduce the number of variables selected during model construction.

Two more matrices were next constructed as evaluation sets. Each matrix contained ten objects which corresponded to the mean of two replicates (Table 5.1), and either 26 or 325 predictors, according to normalization procedures A and B, respectively.

The spectra of five oils, one for each botanical origin, which were tailored at two absorbance units, are shown in Fig. 5.1. As it can be observed, only small differences between the different spectra were evidenced.

In order to enhance these differences, the peak areas at all the wavelength ranges were conveniently handled by multivariate statistical techniques, since band interpretation is not needed to obtain information about oil botanical origin.

Table 5.2 FTIR spectral regions selected as predictor variables for statistical data treatment (Reprinted from Lerma-García et al. (2010). Copyright 2009 Elsevier Ltd.)

Identification No.	Range, cm^{-1}	Functional group	Nominal frequency	Mode of vibration
1	3,029 – 2,989	=C–H (trans)	3,025[a]	Stretching
		=C–H (cis)	3,006[a]	Stretching
2	2,989 – 2,946	–C–H (CH_3)	2,953[a]	Stretching (asym)
3	2,946 – 2,881	–C–H (CH_2)	2,924[a]	Stretching (asym)
4	2,881 – 2,782	–C–H (CH_2)	2,853[a]	Stretching (sym)
5	1,795 – 1,677	–C=O (ester)	1,746[a]	Stretching
		–C=O (acid)	1,711[a]	Stretching
6	1,486 – 1,446	–C–H (CH_2)	1,465[b]	Bending (scissoring)
7	1,446 – 1,425	–C–H (CH_3)	1,450[b]	Bending (asym)
8	1,425 – 1,409	=C–H (cis)	1,417[a]	Bending (rocking)
9	1,409 – 1,396	=C–H	1,400[b]	Bending
10	1,396 – 1,382	=C–H	–[b]	Bending
11	1,382 – 1,371	–C–H (CH_3)	1,377[a]	Bending (sym)
12	1,371 – 1,330	O–H	1,359[b]	Bending (in plane)
13	1,330 – 1,290	Non-assigned	1,319[a]	Bending
14	1,290 – 1,211	–C–O	1,238[a]	Stretching
		$–CH_2–$		Bending
15	1,211 – 1,147	–C–O	1,163[a]	Stretching
		$–CH_2–$		Bending
16	1,147 – 1,128	–C–O	1,138[b]	Stretching
17	1,128 – 1,106	–C–O	1,118[a]	Stretching
18	1,106 – 1,072	–C–O	1,097[a]	Stretching
19	1,072 – 1,043	–C–O	–[b]	Stretching
20	1,043 – 1,006	–C–O	1,033[a]	Stretching
21	1,006 – 929	–HC=CH– (trans)	968[a]	Bending (out of plane)
22	929 – 885	–HC = CH– (cis)?	914[a]	Bending (out of plane)
23	885 – 802	$=CH_2$	850[b]	Wagging
24	802 – 754	–C–H	–[b]	Bending (out of plane)
25	754 – 701	$–(CH_2)_n–$	723[a]	Rocking
		–HC = CH– (cis)		Bending (out of plane)
26	701 – 640	C⋯⋯C	685[b]	Bending (out of plane)
		O–H	650[b]	Bending (out of plane)

[a] According to Guillén and Cabo (1998); [b] according to Silverstein et al. (1981)

5.1.2 Construction of LDA Models

To classify oils according to the five botanical origins, two LDA models were constructed, one for each normalization procedure. The best results according to both, low λ_w values and simple models having a small number of predictors, were obtained using normalization procedure B, which was selected. As it can be observed in Fig. 5.2, an excellent resolution between all category pairs ($\lambda_w = 0.362$) was obtained using normalization procedure B. As a large number of

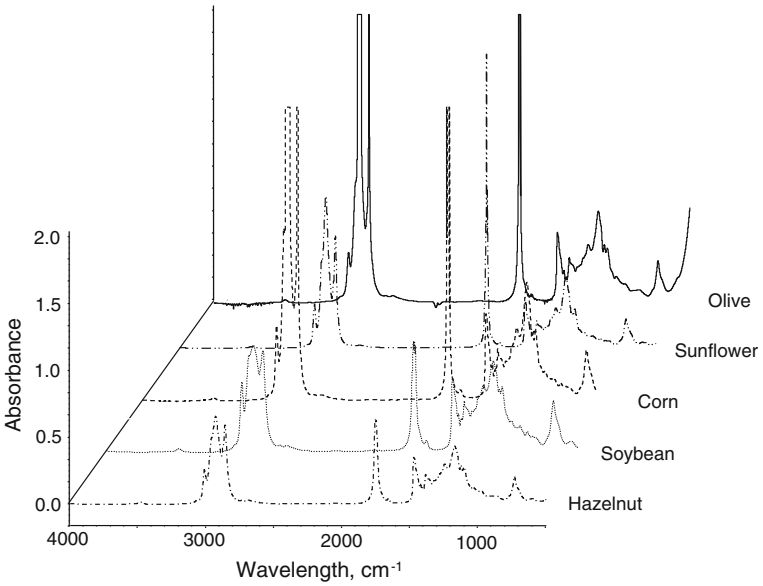

Fig. 5.1 FTIR spectra of representative samples of EVOO, sunflower, corn, soybean and hazelnut oils. Data were tailored at two absorbance units to better show the differences among the small peaks (Reprinted from Lerma-García et al. (2010) Copyright 2009 Elsevier Ltd.)

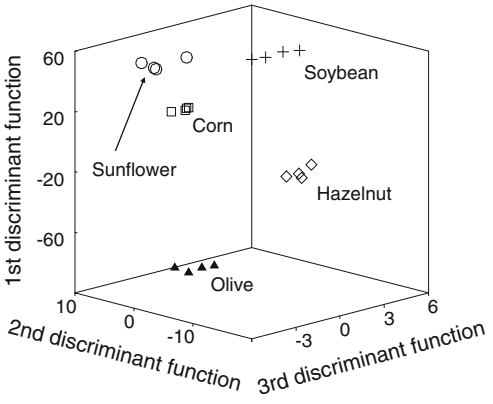

Fig. 5.2 Score plot on an oblique plane of the 3-D space defined by the three first discriminant functions of the LDA model constructed to classify vegetable oils according to their botanical origin (Reprinted from Lerma-García et al. (2010) Copyright 2009 Elsevier Ltd.)

categories were distinguished at the same time, this λ_w value could be considered quite low.

The predictors selected by the SPSS stepwise algorithm and the corresponding standardized coefficients of the model, which indicate which are the predictors with large discriminant capabilities, are given in Table 5.3.

According to Table 5.2, the main wavelength regions selected by the algorithm to construct the LDA model corresponded to =C–H (bending), O–H (bending in plane), –C–H (CH_3, bending sym), –C–O (stretching), –CH_2– (bending),

Table 5.3 Predictors selected and corresponding standardized coefficients of the LDA model constructed to predict the botanical origin of vegetable oils (Reprinted from Lerma-García et al. (2010). Copyright 2009 Elsevier Ltd.)

Predictor[a]	f_1	f_2	f_3	f_4
8/9	19.00	8.20	5.14	3.63
10/12	0.75	9.37	4.03	0.92
11/13	−28.35	5.40	−3.19	−2.13
14/17	16.01	−3.49	−1.50	0.65
15/17	−6.81	5.74	−1.01	1.68
19/25	−13.73	4.33	1.25	0.91
21/26	12.51	−3.76	−0.64	−0.95
22/24	7.84	−5.13	2.26	−1.36

[a] Pairs of wavelength regions identified according to Table 5.2

–HC=CH– (trans, bending out of plane), O–H (bending out of plane) and C⋯C (bending out of plane). When the model was evaluated by leave-one-out validation, all training set objects were correctly classified. In addition to this, all the objects of the evaluation set were also correctly assigned. Thus, using a 95 % probability, the prediction capability of the model was 100 %.

5.1.3 Use of MLR to Determine EVOO Adulteration

In order to quantify EVOO adulteration, binary mixtures containing EVOO and 0, 5, 10, 30, 50, 75 and 100 wt % low cost oil (hazelnut, sunflower, corn or soybean) were prepared (Table 5.1). To improve robustness of MLR models, each point of the calibration curve was prepared using an EVOO from a different geographical origin. The same consideration was also made with the low cost oil samples. Then, using these mixtures, two calibration matrices for each oil pair were constructed. These matrices contained seven objects each, which corresponded to the mean of the duplicated spectra of the mixtures, and 26 or 325 predictors according to normalization procedures A and B, respectively. A response column, which contains the low cost oil percentages of the mixtures, was added to these matrices.

On the other hand, additional mixtures of the sunflower-, corn-, soybean- and hazelnut-EVOO pairs, containing 5, 50 and 80 % low cost oil (a total of 12 more binary mixtures) were also prepared and used as validation set in regression studies.

Thus, MLR models, one for each binary combination of oils, and taking into account both normalization procedures A and B, were constructed. In all cases, the best results were obtained using normalization procedure B, which gave models with higher r values than normalization procedure A. Thus, normalization procedure B was selected. A plot showing the predicted against the nominal oil percentages for each binary mixture is shown in Fig. 5.3. Table 5.4 shows which predictors were selected by the MLR models and which are their corresponding

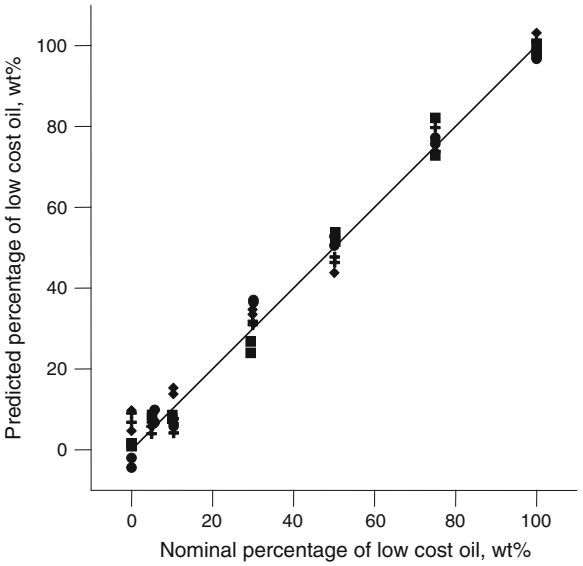

Fig. 5.3 Predicted (MLR) versus nominal oil percentages for binary mixtures of EVOO with sunflower (*filled circle*), corn (*filled square*), soybean (*plus*) and hazelnut (*filled diamond*) oils. The straight-line is y = x (Reprinted from Lerma-García et al. (2010) Copyright 2009 Elsevier Ltd.)

non-standardized coefficients. In all cases, except for the corn-EVOO mixtures, only one predictor was selected by the model to predict oil percentages.

According to Table 5.2, the main wavelength transitions selected to construct the MLR model were $=CH_2$ (wagging), O–H (bending out of plane) and C⋯C (bending out of plane) for the sunflower-EVOO pair, =C–H (trans and cis, stretching), –C–O (stretching) and $–CH_2–$ (bending) for the hazelnut-EVOO pair, $–(CH_2)_n–$ (rocking) and –HC=CH– (cis, bending out of plane) for the soybean-EVOO pair and –C–O (stretching) and =C–H (trans and cis, stretching) for the corn-EVOO pair. In all oil pairs, a transition with a double bond was selected, suggesting that unsaturated fatty acids were important in binary mixture quantification. The *r* values, average prediction errors (calculated as the sum of the absolute differences between expected and predicted oil percentages divided by the number of predictions) and the LODs (calculated as three times the standard deviation of the 5 wt % percentage of low cost oil) are also included in Table 5.15. In all cases, and using leave-one-out validation, the average prediction errors were lower than 2 %, which indicate the quality of the models. When the validation sets were taken into account, the average prediction errors were lower than 5 %. LOD values were also below 5 %. This value was lower than those previously published for the same binary mixtures. Thus, for the sunflower-EVOO mixture, a 4 % was obtained versus the 6 % reported by Vlachos et al. (2006). On the other hand, for soybean-EVOO a 1.7 % versus 6 % was (Vlachos et al. 2006) obtained. A 1.3 versus 9 % (Vlachos et al. 2006) was gained for the corn-EVOO mixture, and finally a 4.8 versus 25 % (Ozen and Mauer 2002) and versus 8 % (Baeten 2005) were obtained for hazelnut-EVOO mixtures.

Table 5.4 Predictors selected and their corresponding non-standarized model coefficients (coef.), *r* values, average prediction errors (av. pred. error) and LODs obtained for the MLR models constructed to predict EVOO adulteration (Reprinted from Lerma-García et al. (2010). Copyright 2009 Elsevier Ltd.)

Binary mixture	Predictor	Coef.	*r*	Av. pred. error, %	LOD, %
Hazelnut-EVOO	1/15	−1,080	0.955	2.0	4.8
	Constant	348			
Sunflower-EVOO	23/26	325	0.992	1.7	4.0
	Constant	−270			
Corn-EVOO	1/17	−353	0.997	1.5	1.3
	1/16	221			
	Constant	309			
Soybean-EVOO	13/25	324	0.990	1.9	1.7
	Constant	−228			

5.2 Classification Using Sterol Profiles Established by Direct Infusion MS[2]

The aim of this work was the construction of LDA models to classify vegetable oils according to their botanical origin, by using sterol profiles obtained by direct infusion MS with two different ion sources: ESI and APPI. The vegetable oils employed in this work are shown in Table 5.5.

To optimize the MS working conditions, the following sterol standards (β-sitosterol, campesterol, ergosterol, stigmasterol and cholesterol) were used. For each sterol standard, and in both ion sources, peaks at two *m/z* values, which corresponded to the $[M + H]^+$ and $[M + H{-}H_2O]^+$ ions, were observed. The $[M + H{-}H_2O]^+$ peaks showed, in all cases except for ergosterol with APPI, higher intensities than the respective $[M + H]^+$ peaks. For this reason, the intensities of the $[M + H{-}H_2O]^+$ peaks were used as the optimization criteria for the working conditions. Under the optimal conditions (see Sect. 3.5.5) and with both ion sources, different relationships between the abundances corresponding to the $[M + H]^+$ and $[M + H{-}H_2O]^+$ peaks for each sterol standard, were observed. Thus, sterols could be distinguished by both the different *m/z* values and by the different intensity ratios of the $[M + H]^+$ and $[M + H{-}H_2O]^+$ peaks. This could be useful to retrieve information even from sterols having peaks at the same *m/z* values. As different vegetable oils also showed different spectral profiles of the sterol fraction, the profiles could be used to distinguish between oils with different botanical origin.

[2] Parts of the text of this section have been adapted with permission from Lerma-García et al. (2008). Copyright 2008 John Wiley & Sons, Ltd.

Table 5.5 Botanical origin, number of samples and brand of the vegetable oil samples used in this work (Reprinted with permission from Lerma-García et al. (2008). Copyright 2008 John Wiley & Sons, Ltd.)

Origin	No. of samples	Brand
Hazelnut	4	Guinama
Sunflower	2	Koipesol
	2	Hacendado
Corn	2	Guinama
Corn germ	1	Guinama
	1	Hacendado
Olive	1	Carbonell
	1	Grupo Hojiblanca
	1	Borges
	1	Torrereal
Soybean	2	Guinama
	2	Biolasi
Avocado	4	Guinama
Peanut	4	Guinama
Grapeseed	4	Guinama

5.2.1 Selection and Normalization of the Variables

The spectra obtained with both the ESI and APPI sources showed peaks at the same *m/z* values, which corresponded to the $[M + H]^+$ and the $[M + H-H_2O]^+$ ions of the sterols indicated in Table 5.6. Since the sterols giving peaks at the same *m/z* values were jointly measured, a total of 16 peaks at different *m/z* values were obtained to be used as variables.

Figure 5.4 shows the spectra obtained with both the ESI and APPI sources for a soybean oil, in which the 16 peaks to be used as variables are marked with an asterisk. As observed, the peaks obtained with the APPI source showed higher intensities than those provided by the ESI source.

In this study, normalized variables obtained by normalization procedure B were used. When this procedure was applied, $(16 \times 15)/2 = 120$ non-redundant peak ratios were obtained.

All vegetable oils listed in Table 5.5 were also subjected to analysis by the official GC-FID method of analysis (Commission Regulation (EEC) No. 2568/91, annex V). A representative chromatogram of a soybean oil samples is shown in Fig. 5.5.

After oil analysis by both techniques, direct infusion MS and GC-FID, a study of the correlation between the relative intensities of the MS peaks and the areas of the GC peaks was performed. Owing to the coincidence of the *m/z* values of the peaks of several sterols, a correlation study by using the MS peak intensities and GC peaks areas of individual sterols was not possible. Thus, the sterols were organized into seven groups according to the coincidence in their *m/z* values. The different groups are indicated in Table 5.6. In order to compare data, both MS and GC peaks were normalized as follows: First, for each mass spectrum, the sum of the MS peak intensities of each group was divided by the sum of the peak intensities of all the sterols. Second, for each gas chromatogram, the sum of the

Table 5.6 Molecular mass (most abundant isotopes) and *m/z* values of the $[M + H]^+$ and $[M + H\text{-}H_2O]^+$ peaks of the sterols employed in this study (Reprinted with permission from Lerma-García et al. (2008). Copyright 2008 John Wiley & Sons, Ltd.)

Sterol	M, Da	$[M + H]^+$	$[M + H\text{-}H_2O]^+$	Group
Cholesterol	386.7	387.7	369.7	1
Ergosterol	396.7	397.7	378.7	2
Brassicasterol	398.7	399.7	381.7	3
24-Methylene cholesterol	398.7	399.7	381.7	3
Δ^7-Campesterol	398.7	399.7	381.7	3
Campesterol	400.7	401.7	383.7	4
Campestanol	402.7	403.7	385.7	5
Clerosterol	412.7	413.7	395.7	6
Stigmasterol	412.7	413.7	395.7	6
Δ^7-Avenasterol	412.7	413.7	395.7	6
Δ^5-Avenasterol	412.7	413.7	395.7	6
$\Delta^{5,24}$-Stigmastadienol	412.7	413.7	395.7	6
$\Delta^{7,25}$-Stigmastadienol	412.7	413.7	395.7	6
Fucosterol	412.7	413.7	395.7	6
Isofucosterol	412.7	413.7	395.7	6
Δ^5-Avenastenol	414.7	415.7	397.7	2
Δ^7-Stigmastenol	414.7	415.7	397.7	2
β-Sitosterol	414.7	415.7	397.7	2
Sitostanol	416.7	417.7	399.7	3
Erythrodiol	442.7	443.7	425.7	7
Uvaol	442.7	443.7	425.7	7

[a] Each group is formed by the sterols having peaks with the same *m/z* values

areas of the GC peaks of each group was divided by the sum of the peak areas of all the sterols. The MS and GC data processed in this way for each group of sterols, and for a representative soybean oil sample, were plotted in Fig. 5.6.

As shown in this figure, the MS peak intensities and GC peak areas were non-linearly correlated, which could be a consequence of the different response factors of the sterols by both techniques; however, Fig. 5.6 clearly shows that sterols having higher concentration in samples give both large MS peak intensities and large GC peak areas. Similar plots were obtained with the other oil samples.

5.2.2 Construction of Data Matrices and LDA Models

Two matrices, one for ESI and another for APPI data, which containing 128 injections (32 samples × 4 replicates) and 120 predictors each, were constructed. A response column, containing the eight categories corresponding to the eight botanical origins of the oils (corn and corn germ were considered as a single category), was added to each matrix. These matrices were used both to construct LDA training matrices and to provide evaluation sets. Only the means of the replicates of the

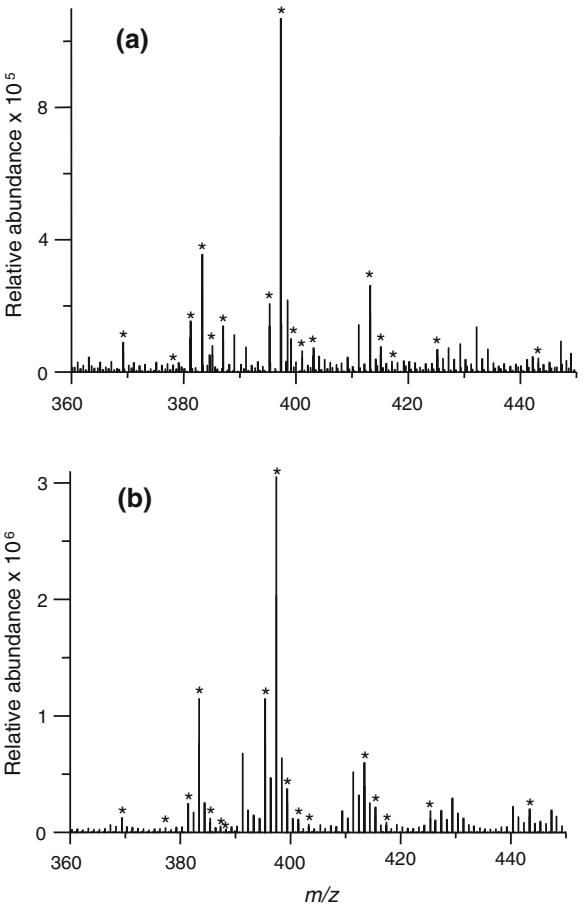

Fig. 5.4 Direct infusion MS spectra of a sterol extract of a soybean oil obtained with the ESI (**a**), and APPI (**b**) ion sources. The *m/z* peaks, which correspond to the sterols of Table 5.6, are indicated by an *asterisk* (Reprinted with permission from Lerma-García et al. (2008). Copyright 2008 John Wiley & Sons, Ltd.)

samples were included in the training matrices; in this way, the internal dispersion of the categories was reduced, which was important to also reduce the number of variables selected by the stepwise algorithm during model construction. In the evaluation set, all the individual injections of the samples were included.

The capability for the classification of the studied oils according to their botanical origin was tested by constructing two LDA models, using both ESI and APPI data. An excellent resolution between the eight categories was achieved using ESI-MS data (see Fig. 5.7, $\lambda_w = 0.294$). Taking into account that a large number of categories were simultaneously distinguished, this λ_w value was rather good. The variables selected by the SPSS stepwise algorithm, and the corresponding standardized coefficients of the model, are given in Table 5.7. An excellent resolution between the avocado and the rest of categories as a whole was observed along the first discriminant function, f_1. This function is mainly constructed with the peak intensity ratios taken at *m/z* 403.7/397.7 and 403.7/399.7

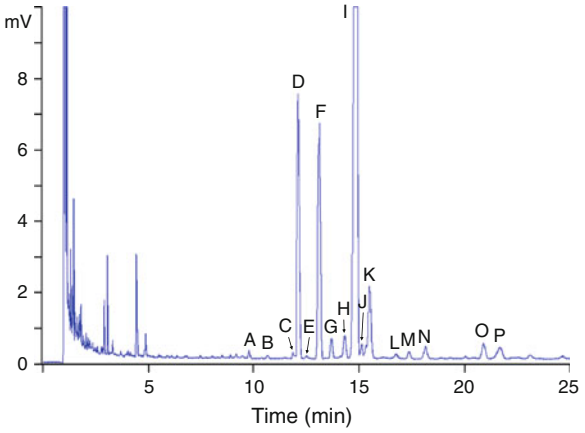

Fig. 5.5 Typical FID gas chromatogram of a sterol extract of a soybean oil. Peak identification: Cholesterol (*A*), brassicasterol (*B*), 24-methylene cholesterol (*C*), campesterol (*D*), campestanol (*E*), stigmasterol (*F*), Δ^7-campesterol (*G*), clerosterol (*H*), β-sitosterol (*I*), sitostanol (*J*), Δ^5-avenasterol (*K*), $\Delta^{5,24}$-stigmastadienol (*L*), Δ^7-stigmastenol (*M*), Δ^7-avenasterol (*N*), erythrodiol (*O*) and uvaol (*P*). β-Sitosterol peak was tailored to better appreciate small peaks (Reprinted with permission from Lerma-García et al. (2008). Copyright 2008 John Wiley & Sons, Ltd.)

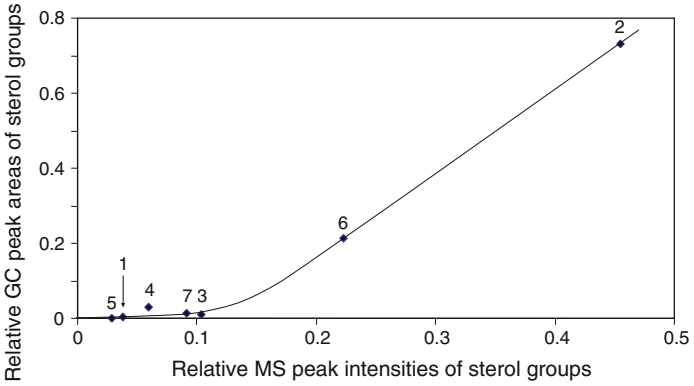

Fig. 5.6 Relative GC peak areas plotted against the relative MS peak intensities of the seven sterol groups indicated in Table 5.6 (Reprinted with permission from Lerma-García et al. (2008). Copyright 2008 John Wiley & Sons, Ltd.)

(see Table 5.7). All the other categories were resolved along the second and third discriminant functions, f_2 and f_3.

On the other hand, when the APPI-MS data was used to construct the LDA model, all oil category pairs were also very well resolved, being the λ_w value similar to that obtained with the ESI-MS data (Fig. 5.8, $\lambda_w = 0.383$).

The variables selected and the corresponding standardized coefficients of the model are given in Table 5.8. In this case, along the first discriminant function, f_1,

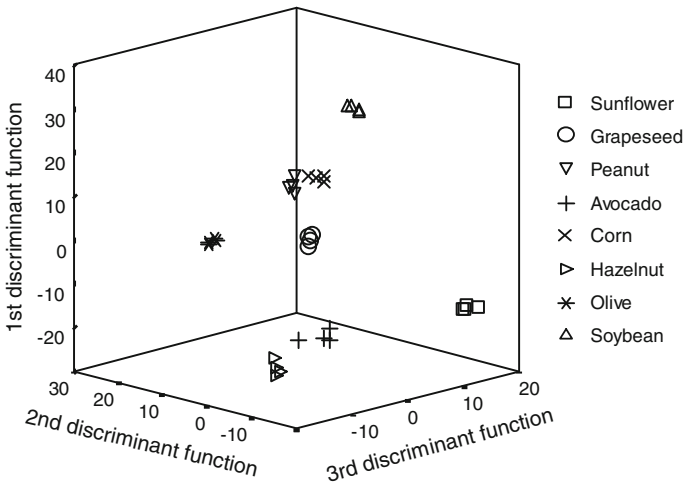

Fig. 5.7 Score plot on an oblique plane of the 3D space defined by the three first discriminant functions of the LDA model constructed with the ESI-MS data (Reprinted with permission from Lerma-García et al. (2008). Copyright 2008 John Wiley & Sons, Ltd.)

Table 5.7 Predictors selected and corresponding standardized coefficients of the LDA model constructed to predict the botanical origin of vegetable oils infused in ESI-MS (reprinted with permission from Lerma-García et al. (2008). Copyright 2008 John Wiley & Sons, Ltd.)

Predictors[a]	f_1	f_2	f_3	f_4	f_5	f_6	f_7
395.7/385.7	3.0	6.9	4.8	−1.5	0.9	−0.5	−0.2
395.7/387.7	0.5	−8.2	−1.0	0.8	1.1	1.7	0.5
399.7/397.7	9.4	2.8	3.3	−2.7	3.4	−0.2	0.8
401.7/383.7	4.6	4.4	1.5	1.3	0.8	−0.9	2.3
403.7/397.7	−16.6	−11.5	−5.5	4.6	−1.7	0.1	−4.3
403.7/399.7	14.6	13.3	9.0	−3.9	1.4	1.4	7.0
413.7/369.7	−1.8	−2.4	−0.8	−0.1	2.2	0.3	−0.3
415.7/397.7	−4.5	8.1	2.1	0.7	−4.1	−0.1	2.0
415.7/403.7	2.7	−5.8	1.2	0.3	0.8	0.4	−0.4
417.7/369.7	−1.6	−1.2	−1.1	−0.1	−2.1	0.7	−0.2
425.7/403.7	0.3	3.7	0.9	0.4	0.1	−1.5	0.6
443.7/399.7	−2.1	−5.8	−3.5	0.1	1.9	0.1	−4.7
443.7/403.7	0.6	5.1	2.2	1.2	−0.8	0.8	2.4

[a] Identified by the *m/z* values of the peak pairs

a satisfactory resolution was obtained for each category pair, except for corn-peanut categories. This function was mainly constructed with the peak intensity ratios taken at *m/z* 397.7/383.7, 413.7/397.7 and 415.7/383.7. Also, along the f_2 and f_3 (constructed mainly by campestanol) the corn—peanut pair appears overlapped, being the rest of categories well resolved. The corn—peanut pair was resolved along f_4. For the two models constructed with both the ESI- and the APPI-MS data, and using leave-one-out validation, all the points of the respective

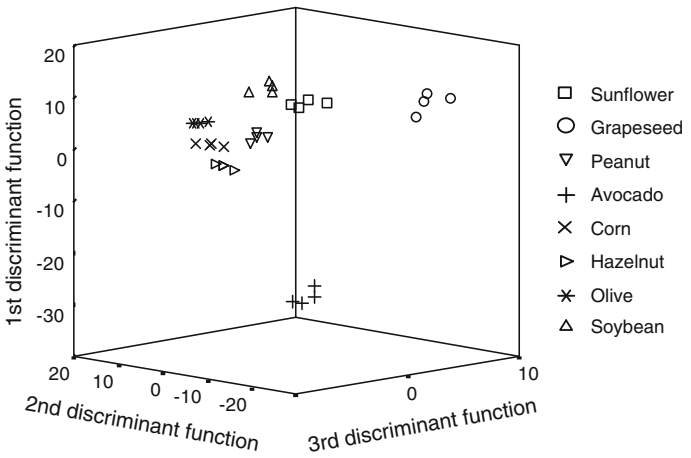

Fig. 5.8 Score plot on an oblique plane of the 3D space defined by the three first discriminant functions of the LDA model constructed with the APPI-MS data (Reprinted with permission from Lerma-García et al. (2008). Copyright 2008 John Wiley & Sons, Ltd.)

training sets were correctly classified. The corresponding evaluation sets, containing 128 original data points each, were used to check the prediction capability of the models. Using a 95 % probability, all the objects were correctly assigned; thus, the prediction capability of both models was 100 %.

5.3 Classification Using Alcoholic Fraction Profiles Established by HPLC-MS[3]

The aim of this work was to develop an RP-HPLC method, using both UV-Vis and MS, to obtain the alcohol profile of oils coming from different botanical origins. For this purpose, prior to HPLC separation, alcohols were esterified with diphenic anhydride. Also, LDA models were constructed to classify oils from seven different botanical origins (see Table 5.9) using alcohols obtained by HPLC-MS as predictors.

5.3.1 Optimization of the Esterification Procedure

Aliphatic alcohols show a poor sensitivity in both, UV-Vis and MS detection (Micó-Tormos et al. 2008a, b). For this reason, and in order to enhance their

[3] Parts of the text of this section have been adapted with permission from Lerma-García et al. (2009). Copyright 2008 Elsevier B.V

Table 5.8 Predictors selected and corresponding standardized coefficients of the LDA model constructed to predict the botanical origin of vegetable oils injected in APPI-MS (Reprinted with permission from Lerma-García et al. (2008). Copyright 2008 John Wiley & Sons, Ltd.)

Predictors[a]	f_1	f_2	f_3	f_4	f_5	f_6	f_7
385.7/383.7	−10.6	1.9	3.6	0.7	−1.2	−0.1	−2.1
397.7/383.7	24.7	15.4	8.0	2.4	5.8	0.8	3.0
401.7/381.7	−9.0	4.7	−4.9	0.2	1.8	2.6	−0.9
413.7/397.7	22.5	4.1	12.9	1.8	4.4	−0.9	2.4
415.7/383.7	−23.6	−12.5	−12.4	−3.1	−1.8	3.3	−1.3
415.7/413.7	16.3	8.5	6.0	0.9	2.0	−2.3	2.3
425.7/369.7	−6.6	−0.8	−2.6	8.7	−0.5	1.7	3.8
425.7/381.7	2.3	−6.9	−4.0	4.1	−4.7	−9.1	1.2
425.7/383.7	10.5	7.5	13.0	−15.0	6.5	9.3	−8.1
425.7/397.7	−15.5	−5.4	−12.9	0.2	0.3	3.2	0.6
443.7/383.7	2.4	2.5	0.7	8.7	−1.7	−8.9	9.6
443.7/399.7	14.5	0.3	3.0	−0.5	−3.2	1.0	−4.0
443.7/401.7	−3.5	2.4	−1.6	−5.2	4.7	2.8	−1.2
443.7/403.7	−1.8	−1.3	0.6	2.0	−0.8	−1.2	−1.6

[a] Identified by the *m/z* values of the peak pairs

Table 5.9 Botanical origin, number of samples and brand of the vegetable oil samples used in this work (Reprinted from Lerma-García et al. (2009). Copyright 2008 Elsevier B.V)

Origin	No. of samples	Brand
Hazelnut	4	Guinama
Sunflower	2	Koipesol
	2	Hacendado
Corn	2	Guinama
Corn germ	1	Guinama
	1	Hacendado
EVOO	1	Carbonell
	1	Grupo Hojiblanca
	1	Borges
	1	Torrereal
Soybean	2	Guinama
	2	Biolasi
Peanut	4	Guinama
Grapeseed	4	Guinama

sensitivity, these compounds were derivatized using diphenic anhydride, as explained in Sect. 3.3.2. The esterification reaction of alcohols with this reagent is illustrated in Fig. 3.2. The hemiester obtained provides both a chromophore with a large molar absorptivity and a negative charge, which facilitates its MS detection. Derivatization was performed by melting the standards of linear alcohols with a large excess of diphenic anhydride. Due to the low solubility of these solutes in polar solvents, the use of THF was necessary to solubilize them. A reaction temperature of 60 °C was selected taking into account THF boiling point (66 °C). 10 mg of each alcohol standard were suspended in 4 mL THF and introduced in a

screw-cap tube. Derivatization was performed with and without the presence of finely grinded urea. Hemiester peaks increased at least two times when urea was present in the reaction medium. This fact was also observed when other derivatization agents (maleic and phthalic anhydrides) were used to derivatize ethoxylated fatty alcohol (Micó-Tormos et al. 2008a, b). The addition of 0.25 g finely grinded urea provided the best reaction in shorter reaction time.

On the other hand, the reaction time and yield were optimized by preparing eight screw-cap tubes (containing 10 mg of each alcohol standard dissolved in 4 mL THF, 0.45 g diphenic anhydride and 0.25 g finely grinded urea). Tubes were removed from the bath at intervals of 15 min and injected into the HPLC system using isocratic elution with a binary mixture of ACN/water 90:10 (v/v) containing 0.1 % acetic acid. It was observed that reaction yield increased when the reaction time increased, and a plateau was observed at 100 min. To assure a complete reaction yield, the derivatization was performed for 120 min. A linear dependence of log k with the number of carbons in the alkyl chain of the alcohols was observed, while the retention times were comprised between 6.7 and 56.5 min for C16 and C26, respectively.

5.3.2 Optimization of the Separation Conditions

The optimization of alcohol separation was performed using an EVOO extract since most aliphatic and triterpene alcohol standards are unavailable or high-cost price. Using the isocration elution conditions described in Sect. 5.3.1 (90:10 (v/v) ACN/water mixtures), the peaks ascribed to C24 and C26 alcohols were identified, although many other peaks were also observed in the EVOO samples. Thus, and in order to identify these peaks, MS detection was coupled in series to the HPLC-UV-Vis system. Using the EICs at the *m/z* values of Table 5.10, peaks corresponding to several triterpene alcohols, phytol and 4-methylsterols were identified in the range comprised between 9 and 25 min, while peaks corresponding to linear alcohols were identified at times higher than 90 min. Thus, gradient elution was tried in order to speed up the analysis. The optimal conditions were found to be an isocratic elution with 90 % ACN for 25 min, by a linear gradient from 90 to 100 % ACN for 10 min, and finally by an isocratic elution with 100 % ACN for ten more minute. The TIC and EICs of an EVOO and sunflower oil extracts are shown in Fig. 5.9 and 5.10, respectively. The assignment of alcohol peaks was performed according to the *m/z* values of Table 5.10. Using the information provided by MS detection, alcohol peaks were also identified in UV-Vis chromatograms. A UV-Vis chromatogram of the EVOO sample (whose mass spectrum is given in Fig. 5.9) is shown in Fig. 5.11. Under these conditions, all the derivatized alcoholic fractions of the vegetable oils were injected. Several differences between the alcohol profiles of oils from different botanical origin were observed (see Figs. 5.9 and 5.10).

Table 5.10 Type, peak labelling, *m/z* value and possible identification of the alcohols studied in this work (Reprinted from Lerma-García et al. (2009). Copyright 2008 Elsevier B.V)

Type	Peak labelling	*m/z*[a]	Possible compound
Linear alcohols	1	493	1-Octadecanol (C18)
	2a	521	1-Eicosanol (C20)
	3	549	1-Docosanol (C22)
	4	563	1-Tricosanol (C23)
	5	577	1-Tetracosanol (C24)
	6	591	1-Pentacosanol (C25)
	7	605	1-Hexacosanol (C26)
	8	619	1-Heptacosanol (C27)
	9	633	1-Octacosanol (C28)
	10	647	1-Nonacosanol (C29)
	11	661	Tricontanol (C30)
4-Methylsterols	12	513	Geranylgeraniol
	13a–d	649	Obtusifoliol, cycloeucalenol, citrostadienol
Diterpene alcohol	14	519	Phytol
Triterpene alcohols	13a–d	649	Cycloartenol, α-amyrin, β-amyrin, taraxerol, dammaradienol, lupeol butyrospermol, parkeol
	15	651	Cycloartanol, lanostenol
	16	661	24-Methylenecycloartanol
	17	663	24-Methylenelanost-9(11)-enol, cyclolaudenol, cyclobranol
Unknown	2b–c	521	Unknown

[a] *m/z* value corresponding to the $[M\text{-}H]^-$ peak of the hemiester of the alcohol

5.3.3 Construction of Data Matrices and LDA Models

In this work, the original variables (which corresponded to the peak area of each alcohol derivative measured from its corresponding EIC, previously smoothed using a filter set at nine points) were normalized by procedure B, in which the area of each peak taken from the corresponding EIC was divided by each one of the areas of the other 27 peaks (also taken from their EICs). With this procedure, a total of 378 predictors were obtained for LDA model construction.

Three different matrices were constructed. All matrices contained 84 objects (28 samples of Table 5.9 × 3 replicates). The first matrix was constructed using only the 55 predictors obtained from linear alcohols. The second one was constructed using 136 predictors, obtained from 4-methylsterols + triterpene alcohols + phytol. Finally, the third matrix contained all the available predictors (a total of 378). A response column, containing the seven categories corresponding to the seven botanical origins of the oils (corn and corn germ were considered as a single category), was added to the three matrices. These matrices were used as evaluation sets. Only the means of the three replicates of the samples (28 objects each) were included in the training matrices. In this way, and as indicated above,

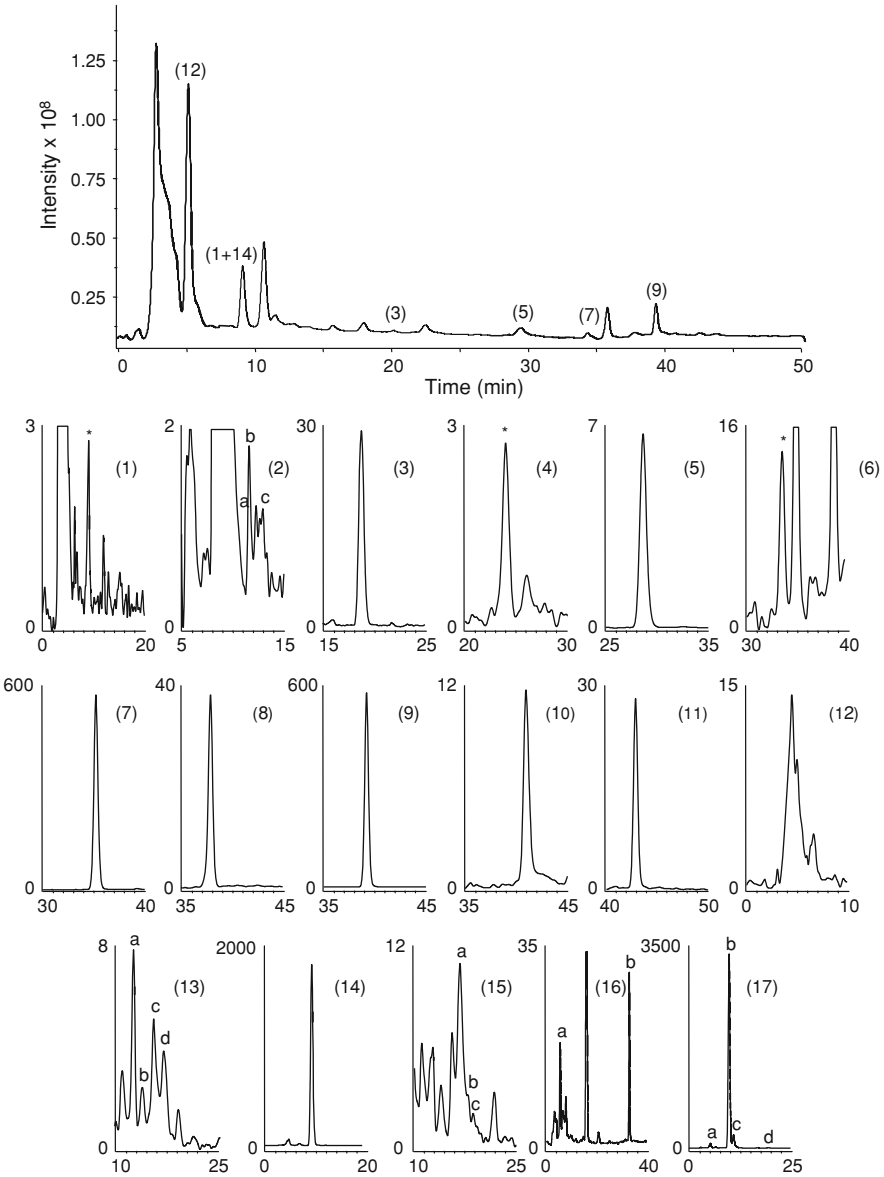

Fig. 5.9 TIC and EICs of an EVOO extract. EIC intensity scales are multiplied by 10^4. Between parenthesis, peak labelling according to Table 5.10. The EICs were obtained at the *m/z* values also indicated in Table 5.10; when the EIC contains more than one peak, the peak used for data analysis is indicated with an *asterisk* or with *low case* characters. Mobile phase: 90 % ACN for 20 min, followed by a linear gradient up to 100 % ACN for 10 min and 100 % ACN for 20 more min (Reprinted from Lerma-García et al. (2009). Copyright 2008 Elsevier B.V)

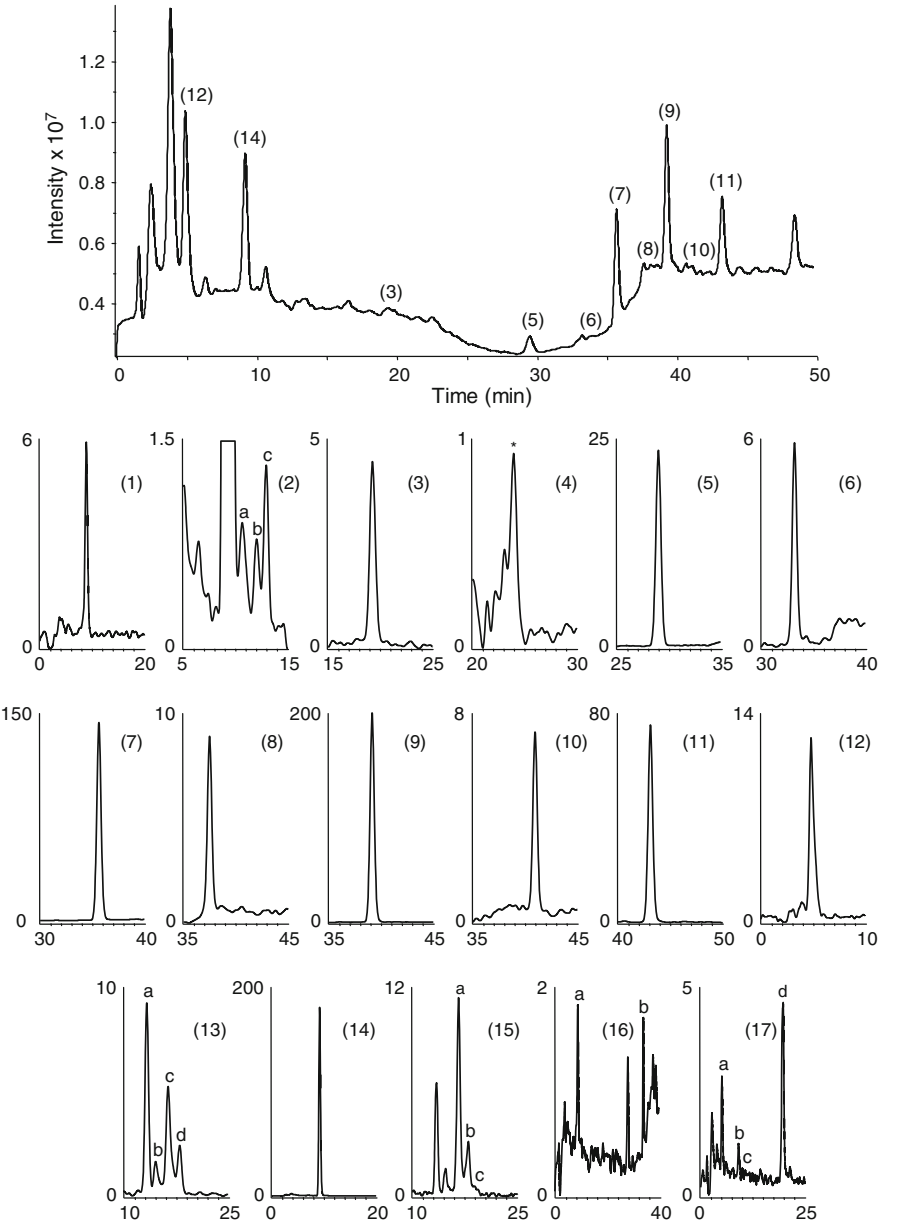

Fig. 5.10 TIC and EICs of a sunflower oil extract. Other details as in Fig. 5.9 (Reprinted from Lerma-García et al. (2009). Copyright 2008 Elsevier B.V)

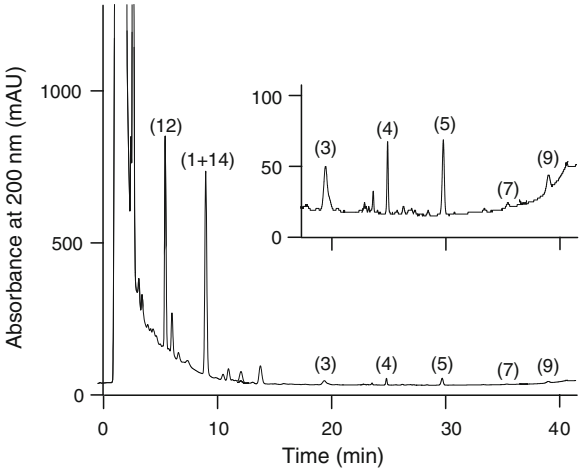

Fig. 5.11 UV-Vis chromatogram of an extract of the same sample of EVOO as in Fig. 5.9. Other details as in (Reprinted from Lerma-García et al. (2009). Copyright 2008 Elsevier B.V)

the internal dispersion of the categories was reduced, also reduce the number of variables selected by the SPSS stepwise algorithm (in this case, the F_{in} and F_{out} values of 3.84 and 2.71, respectively, were adopted).

Next, a first LDA model was constructed using the first matrix (which contained the 55 predictors obtained from the ratios of linear alcohols). With this model, a poor resolution ($\lambda_w = 0.708$) was obtained; moreover, four objects of the evaluation set were not correctly assigned. Then, another LDA model was constructed using the second matrix (which contained the 136 predictors obtained from the ratios of 4-methylsterols + triterpene alcohols + phytol). In this case, a large improved in category resolution was observed, being λ_w value of 0.327. Finally, another LDA model was constructed using all the available predictors. As observed in Fig. 5.12, an excellent resolution between all the category pairs was obtained ($\lambda_w = 0.163$). The variables selected by the SPSS stepwise algorithm, and the corresponding standardized coefficients of this model, are given in Table 5.11. As shown in Fig. 5.12a, an extremely large separation in three groups (corn-hazelnut-grapeseed, olive and soybean-peanut-sunflower categories) was observed along the f_1. This function was mainly constructed with the ratios taken at *m/z* 649d/651b and 649b/513 (see Table 5.11). On the other hand, olive oil was resolved from the other categories along f_2. According to Fig. 5.12b, the variance gathered along f_3 was due to the resolution of peanut, soybean and grapeseed with respect to the other categories. Finally, all the possible category pairs were very well resolved from each other by using an oblique palne of the 3D space defined by the three first discriminant functions (Fig. 5.12c). For this model, all the objects of the training set were correctly classified by leave-one-out validation. Finally, when the prediction capability of the model was checked using the evaluation set (which the 84 original data points), all the objects were correctly assigned to their corresponding category using a 95 % probability; thus, the prediction capability of the model was 100 %.

5.4 Classification Using Amino Acid Profiles Established by Direct Infusion MS[4]

The aim of this work was to develop a simple and quick method for oil classification according to its botanical origin, based on direct infusion of amino acids in a mass spectrometer. For this purpose, the vegetable oils shown in Table 5.12 were employed.

5.4.1 MS Amino Acid Profiles

After protein hydrolysis (see Sect. 3.3.3), the MS spectra of the different oils (Fig. 5.13) showed the $[M + H]^+$ peaks of the following amino acids: Gly (*m/z* 76.1), Ala (*m/z* 90.1), Ser (*m/z* 106.1), Pro (*m/z* 116.1), Val (*m/z* 118.1), Thr (*m/z* 120.1), Cys (*m/z* 122.2), Ile + Leu (*m/z* 132.2), Asp (*m/z* 134.1), Lys (*m/z* 147.2), Glu (*m/z* 148.2), Met (*m/z* 150.2), His (*m/z* 156.2), Phe (*m/z* 166.2), Arg (*m/z* 175.2), and Tyr (*m/z* 182.2). Leu and Ile, due to their identical MW, gave a single common peak. Asn and Gln were excluded from this study, since hydrolysis converts them into Asp and Glu (Gimeno-Adelantado et al. 2002). Glu is also partially converted into pyroglutamic acid during hydrolysis (Gimeno-Adelantado et al. 2002). Hydrolysis also destroys Trp, and thus it is not determined (Gimeno-Adelantado et al. 2002). The different amino acid peaks showed an intermediate/low abundance due to the lower concentration of proteins in oils; however, they were suitable for data analysis in all cases.

The amino acid profiles obtained differ from the ones obtained by Hidalgo et al. (2001), probably due to the different response factors for each amino acid in MS. To confirm this hypothesis, amino acid stock solutions were directly injected into the mass spectrometer. The amino acids with low MW (Gly, Ala, Ser, Cys, Thr and Asp) gave low sensitivities. On the other hand, amino acids with high MW (Lys, Met, His, Phe, Arg and Tyr) gave high sensitivities.

5.4.2 Construction of Data Matrices and LDA Models

In this work, both normalization procedures, A and B, were applied to the original variables, and then, 16 and $(16 \times 15)/2 = 120$ normalized variables were obtained to be used as predictors according to normalization procedure A and B, respectively.

[4] Parts of the text of this section have been adapted with permission from Lerma-García et al. (2007). Copyright 2007 John Wiley & Sons, Ltd.

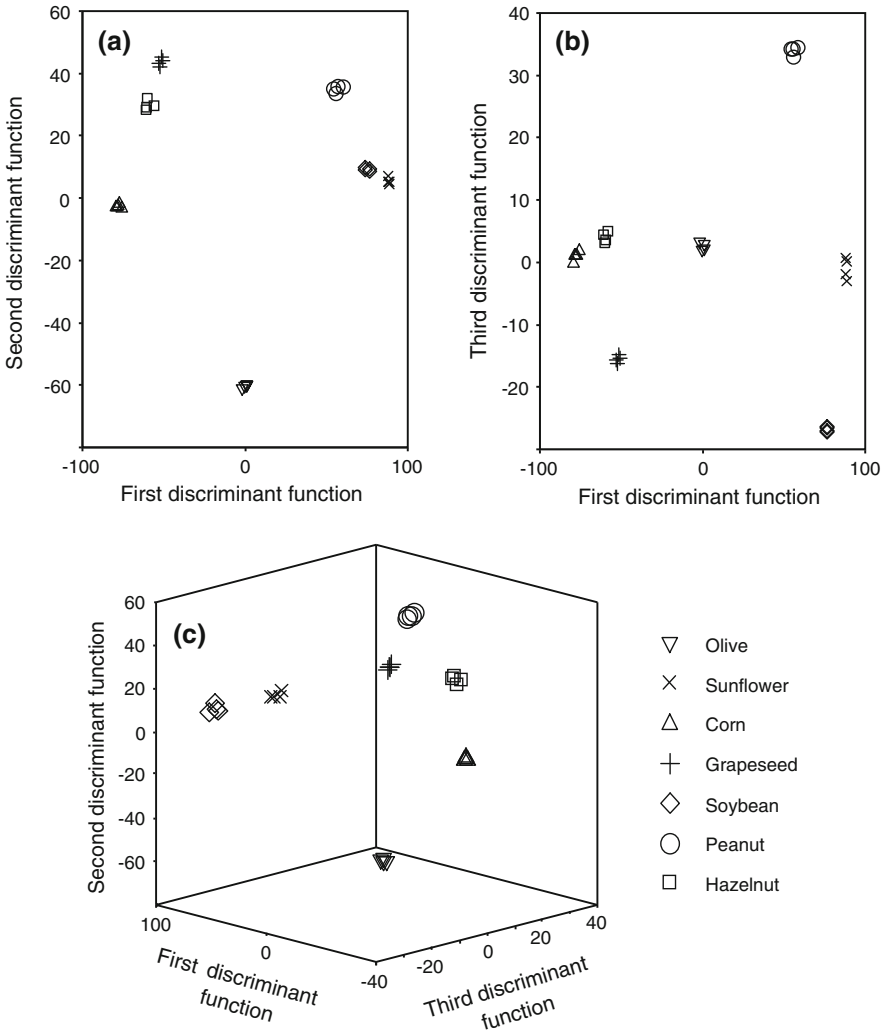

Fig. 5.12 Score plots on the planes of the first and second (**a**), first and third discriminant functions (**b**), on an oblique plane of the 3D space defined by the three first discriminant functions (**c**) of the LDA model constructed to classify vegetable oils according to their botanical origin (Reprinted from Lerma-García et al. (2009). Copyright 2008 Elsevier B.V)

Two matrices containing 272 injections each (68 samples × 4 replicates), and either 16 or 120 predictors (according to normalization procedures A and B, respectively) were constructed. A response column, containing the eight categories corresponding to the eight botanical origins of the oils, was added to the matrices. These matrices constituted the evaluation sets. However, to construct the LDA models, a training set was needed. Each object in the training set was constituted by the mean of the replicates of each sample. This treatment of the data reduced

Table 5.11 Predictors selected and corresponding standardized coefficients of the LDA model constructed to predict the botanical origin of the oil samples (Reprinted from Lerma-García et al. (2009). Copyright 2008 Elsevier B.V)

Predictors[a]	f_1	f_2	f_3	f_4	f_5	f_6
513/651b	−8.22	7.07	4.33	8.21	7.28	3.96
663c/649a	−1.39	−0.48	16.6	−9.75	−5.37	−1.63
663d/649c	−12.2	−1.23	−1.30	−0.39	−1.50	−0.34
649a/649b	−5.21	−2.10	0.51	−0.77	−1.65	−0.74
649b/493	2.45	−7.24	−2.26	−0.63	−0.78	−0.64
649d/651b	30.7	3.45	1.15	0.57	−1.76	−0.75
521b/591	14.9	−0.43	−0.12	2.07	0.79	−0.21
649b/513	−27.6	5.84	0.02	−5.27	0.01	−0.38
649c/513	15.9	−2.78	−2.99	2.51	0.28	−0.86
521b/519	−18.0	2.12	6.00	1.23	1.47	0.69
549/513	−0.69	13.2	−14.4	12.3	9.50	4.13
549/649b	11.6	−2.02	−4.98	−1.54	−1.68	−0.26

[a] *m/z* values of the peak pairs

the dispersion of the objects, which was important to also reduce the number of variables introduced by the stepwise algorithm in model construction. Also, to have similar number of samples within each category, a mean of the replicates of each genetic variety of EVOOs was used; therefore, only three objects in the olive oil category (Arbequina, Hojiblanca, and Picual) were included in the training set, while the other categories were represented by four data points each.

Next, using the training matrices, two LDA models (one for each normalization procedure) capable of classifying the oil samples according to their botanical origin were constructed. The best results in terms of category resolution were obtained using normalization procedure B, which was selected for further studies. With this procedure, the categories hazelnut, EVOO and avocado appeared clearly separated from the other five categories (sunflower, corn, soybean, peanut and grapeseed), which were not resolved from each other. For this reason, a new LDA model was constructed grouping these five categories in a single one. An excellent resolution between this four categories (hazelnut, EVOO, avocado and the one formed by the other oils) was obtained (Fig. 5.14, $\lambda_w = 0.056$).

The variables selected by the SPSS stepwise algorithm, and the corresponding model standardized coefficients, which indicate the predictors with large discriminant capabilities, are given in Table 5.13. All the points of the training set were correctly classified by leave-one-out validation. When the evaluation set was used to check the prediction capability of the model, only twelve objects, which corresponded to replicates of different samples (1 hazelnut, 1 avocado and 10 EVOO) were not correctly assigned using a 95 % probability; thus, the prediction capability was 96 %.

Next, and in order to resolve the five categories previously grouped in a single one, the hazelnut, EVOO and avocado categories were removed from the training set, and a new LDA model was constructed. In this model, soybean and peanut oils

Table 5.12 Botanical origin, genetic variety, number of samples and brand of the vegetable oil samples used in this work (Reprinted with permission from Lerma-García et al. (2007). Copyright 2007 John Wiley & Sons, Ltd.)

Oil sample	Genetic variety	No. of samples	Brand
Hazelnut	Unknown	4	Guinama S.A.
Sunflower	Unknown	2	Koipesol
		2	Hacendado
Corn	Unknown	2	Guinama S.A.
Corn germen	Unknown	1	Guinama S.A.
		1	Hacendado
Soybean	Unknown	2	Guinama S.A.
		2	Biolasi
EVOO	Arbequina	2	Carbonell
		2	Torrereal
		2	Oleastrum
		1	Coosur
		1	Grupo Hojiblanca
		2	Borges
		1	Romanico
		1	Valderrama
		1	Veà
		1	Aubocassa
		1	Rihuelo
	Hojiblanca	2	Carbonell
		2	Coosur
		3	Borges
		7	Grupo Hojiblanca
		1	Columela
	Picual	2	Carbonell
		2	Coosur
		3	Borges
		1	Grupo Hojiblanca
		1	Castillo Tabernas
		1	Castillo Canena
Avocado	Unknown	4	Guinama S.A.
Peanut	Unknown	4	Guinama S.A.
Grapeseed	Unknown	4	Guinama S.A.

were separated with an excellent resolution, while the other three categories (sunflower, corn and grapeseed) still overlapped. Thus, another LDA model was constructed considering these three categories as a single one. To provide equal weights to the resulting categories (soybean, peanut and the one formed by the other three oils), the sunflower, corn and grapeseed categories were plotted by a single point each. For these purpose, the means of the four samples of each category were used. An excellent resolution between the three new categories was obtained ($\lambda_w = 0.042$). A score plot on the plane of the two discriminant functions is shown in Fig. 5.15.

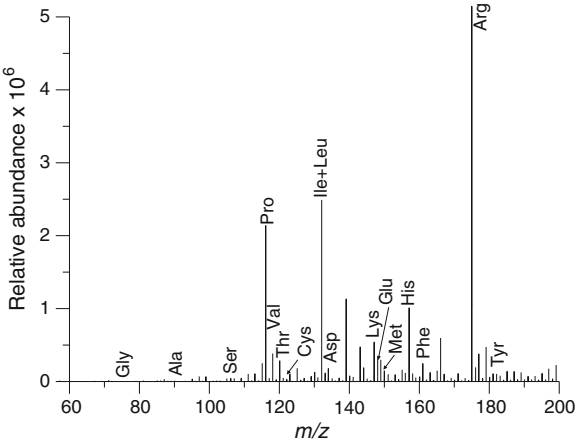

Fig. 5.13 Typical ESI-MS spectrum of an hydrolyzed EVOO oil protein extract. The amino acids studied in this work are indicated (Reprinted with permission from Lerma-García et al. (2007). Copyright 2007 John Wiley & Sons, Ltd.)

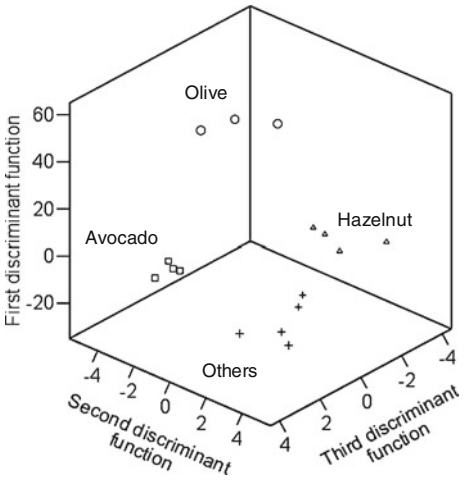

Fig. 5.14 Score plot on an oblique plane of the 3D space defined by the three discriminant functions of the LDA model constructed to resolve the hazelnut, EVOO, avocado and "others" categories. "Others" is the combined category of the sunflower, corn, soybean, peanut and grapeseed oils (Reprinted with permission from Lerma-García et al. (2007). Copyright 2007 John Wiley & Sons, Ltd.)

The variables selected and the corresponding model standardized coefficients are also given in Table 5.13. All the points of the training set were correctly classified by leave-one-out cross-validation. To estimate the prediction capability of the model, the evaluation set, constituted now by 80 original data points, was used. Using a 95 % probability, only three objects, which corresponded to replicates of different samples, were not correctly assigned; thus, the prediction capability was 96 %.

Finally, a third LDA model was now constructed to resolve the sunflower, corn and grapeseed categories. However, a model with a high number of predictors was obtained. Thus, in order to reduce the entrance of predictors in the model, the probability of $F_{in} = 0.02$ was adopted. As shown in Fig. 5.16, a satisfactory resolution among the three categories was achieved ($\lambda_w = 0.279$). The variables selected and the corresponding model standardized coefficients are also given in Table 5.13. All the points of the training set were correctly classified by leave-one-out

Table 5.13 Predictors selected and the corresponding standardized coefficients of the three sequential LDA models constructed to classify vegetable oils according to their botanical origin (Adapted with permission from Lerma-García et al. (2007). Copyright 2007 John Wiley & Sons, Ltd.)

	Hazelnut/EVOO/avocado/others[b]			Soybean/peanut/others[c]		Sunflower/corn/grapeseed	
Predictor[a]	f_1	f_2	f_3	f_1	f_2	f_1	f_2
118.1/76.1	8.07	5.94	0.08	–	–	–	–
150.2/106.1	–	–	–	–	–	−2.18	0.69
148.2/116.1	−1.12	3.85	1.54	–	–	–	–
175.2/116.1	–	–	–	–	–	−3.81	0.26
120.1/118.1	4.56	0.35	0.31	2.93	1.45	–	–
156.2/118.1	–	–	–	−2.17	−1.35	–	–
122.2/120.1	–	–	–	–	–	4.54	−0.87
132.2/122.2	10.42	3.73	3.71	–	–	–	–
175.2/122.2	−13.81	-6.80	−2.72	–	–	–	–
147.2/132.2	–	–	–	−2.17	0.26	–	–
150.2/132.2	7.56	4.88	−0.81	–	–	–	–
156.2/134.1	–	–	–	–	–	2.42	0.46
175.2/156.2	−8.12	−1.18	2.27	–	–	–	–
182.2/156.2	–	–	–	1.43	−0.22	–	–
175.2/166.2	13.09	5.96	−2.42	–	–	–	–

[a] *m/z* values of the ratios of amino acid peaks
[b] Others = sunflower + corn + soybean + peanut + grapeseed
[c] Others = sunflower + corn + grapeseed

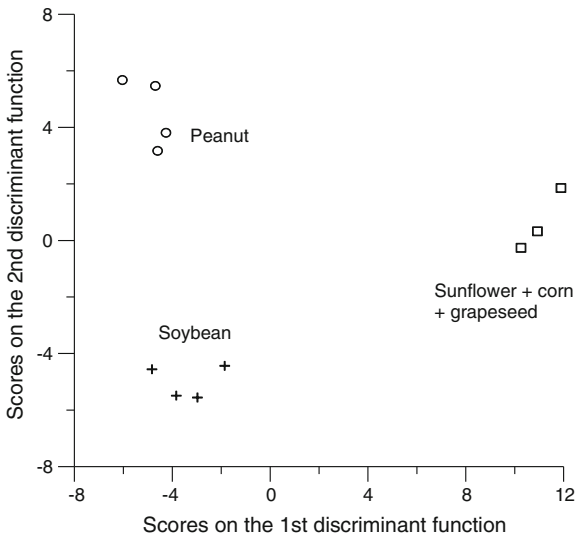

Fig. 5.15 Score plot on the plane of the two discriminant functions of the LDA model constructed to resolve the soybean, peanut and the new combined category (sunflower, corn and grapeseed) (Reprinted with permission from Lerma-García et al. (2007). Copyright 2007 John Wiley & Sons, Ltd.)

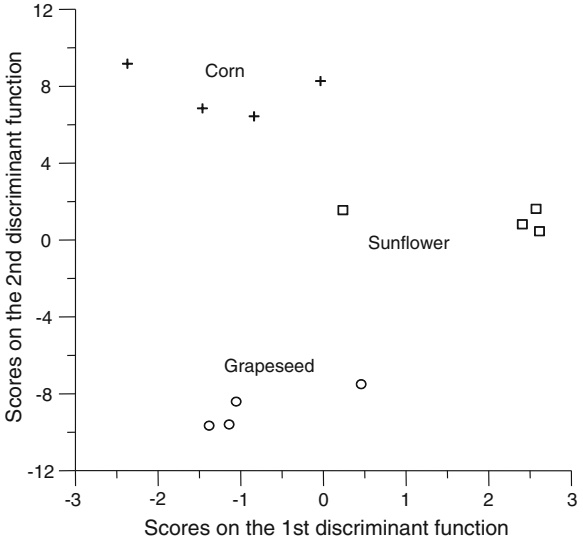

Fig. 5.16 Score plot on the plane of the two discriminant functions of the LDA model constructed to resolve the sunflower, corn and grapeseed categories (Reprinted with permission from Lerma-García et al. (2007). Copyright 2007 John Wiley & Sons, Ltd.)

cross-validation. Using a 95 % probability, only three objects out from a total of 48 original data points of the evaluation set, and corresponding to replicates of different samples, were not correctly assigned; thus, the prediction capability of the model was 94 %. Therefore, the vegetable oils belonging to the eight different botanical origins were correctly classified with a high reliability by the sequential application of three LDA models. In terms of resolution between oil origin categories, the proposed method yields similar results to those reported by using ^{31}P- and ^{1}H-NMR of diglycerides (Vigli et al. 2003).

5.5 Classification Using Amino Acid Profiles Established by HPLC-UV-Vis[5]

The aim of this work was to construct an LDA model capable of classifying vegetable oils according to their botanical origin by using amino acid profiles obtained by HPLC-UV-Vis. For this purpose, two amino acid extractions, performed as indicated in Sect. 3.3.3, were done to each one of the samples described in Table 5.14. These extracts were derivatized with OPA in the presence of NAC before HPLC-UV-Vis analysis (see Sect. 3.3.3).

[5] Parts of the text of this section have been adapted with permission from Concha-Herrera et al. (2010). Copyright 2009 Elsevier Ltd.

Table 5.14 Botanical origin, number of samples and brand of the oil samples used in this work (Reprinted from Concha-Herrera et al. (2010). Copyright 2009 Elsevier Ltd.)

Origin	No. of samples	Brand
Hazelnut	2	Guinama
	2	Percheron
	2	Flumen
Peanut	2	Guinama
	2	Bellsola
	1	Apsara Vital
	1	Maní
Avocado	2	Guinama
	2	Marnys
	2	Serra Vita
Grapeseed	2	Guinama
	1	Coosur
	1	Romulo
	1	Paul Corcelet
	1	Pons
Corn	1	Guinama
	1	Asua
	1	Artua
	1	Mazola
Corn germ	1	Guinama
	1	Hacendado
EVOO	1	Carbonell
	1	Grupo Hojiblanca
	1	Borges
	1	Torrereal
	1	Coosur
	1	Hacendado
Soybean	2	Guinama
	2	Biolasi
	2	Sojola

5.5.1 HPLC-UV-Vis Amino Acid Profiles

Amino acid separation was performed using the experimental conditions indicated in Sect. 3.5.7. Amino acid or mixtures of two or three amino acids solutions of 1,000 μg mL^{-1} were prepared to be derivatized as previously indicated in Sect. 3.3.3. Once derivatized, these solutions were directly injected into the HPLC system or used to spike oil samples when necessary. A chromatogram showing the amino acid peaks of a standard solution is shown in Fig. 5.17. As it can be observed, all amino acid peaks were resolved from each other except Phe/Leu and Asn/Ser pairs, which totally overlapped. This overlappings were not solved by introducing small modifications in the mobile phase composition and/or in the gradient conditions, or by diluting the amino acid extracts (this dilution also led to the loss of information since some minor amino acid peaks were not observed).

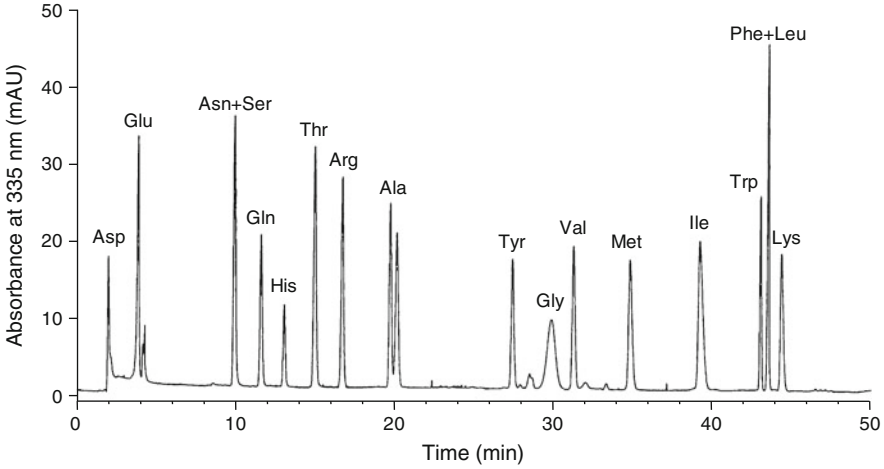

Fig. 5.17 Chromatogram of a standard mixture of derivatized amino acids (Reprinted from Concha-Herrera et al. (2010). Copyright 2009 Elsevier Ltd.)

However, when oil sample extracts were injected (Fig. 5.18), both matrix peaks and a baseline disturbance at long analysis times (40–50 min) were observed. When the chromatograms of Fig. 5.18, which were from different oil extracts (EVOO and hazelnut), were compared, small differences between the amino acid profiles were observed. Then, these differences were enhanced by LDA model construction. For this purpose, 16 peak areas were used as original variables, which corresponded to 18 amino acids (since Phe/Leu and Asn/Ser peaks eluted at the same time).

5.5.2 Construction of Data Matrices and LDA Models

In this work, both normalization procedures, A and B, were applied to the original variables, and then, 16 and $(16 \times 15)/2 = 120$ normalized variables were obtained to be used as predictors according to normalization procedure A and B, respectively. These normalized variables were used to construct LDA models with the aim of classifying oils according to their botanical origin. Two matrices containing 168 injections each (2 extracts *per* sample $\times$ 2 injections), and either 16 or 120 predictors (according to normalization procedures A and B, respectively) were constructed. A response column, which contains seven categories (one category for each oil botanical origin, since corn and corn germ were considered as a single one), was added to these matrices. Both matrices were randomly divided in two equal groups (84 samples each) to be used as training and evaluation sets.

Two LDA models, one for each normalization procedure, were then constructed. Normalization procedure B, which provided low λ_w values and a low

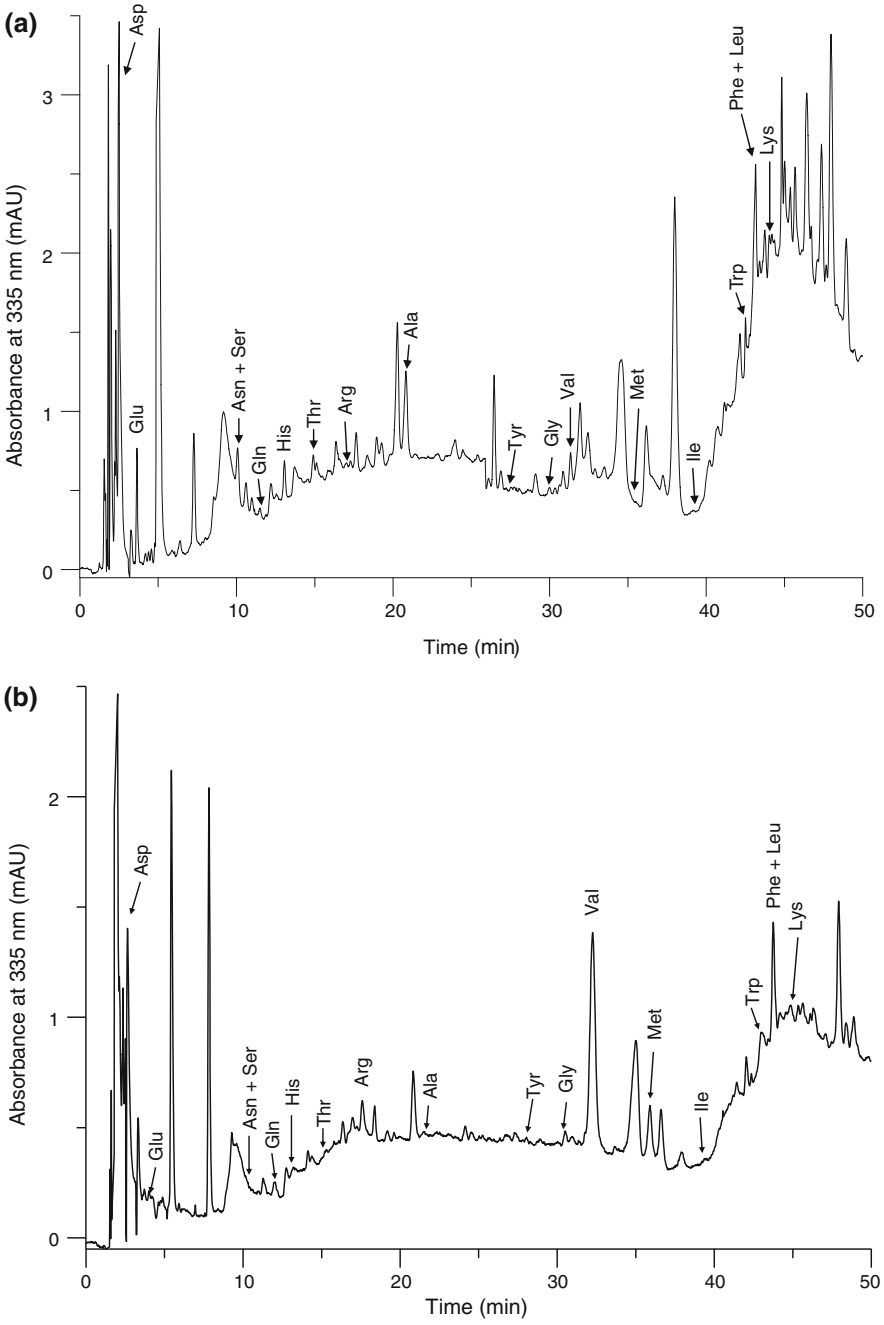

Fig. 5.18 Chromatograms showing the amino acid profiles of an EVOO (**a**), and hazelnut oil (**b**) samples. Other working conditions as in Fig. 5.17 (Reprinted from Concha-Herrera et al. (2010). Copyright 2009 Elsevier Ltd.)

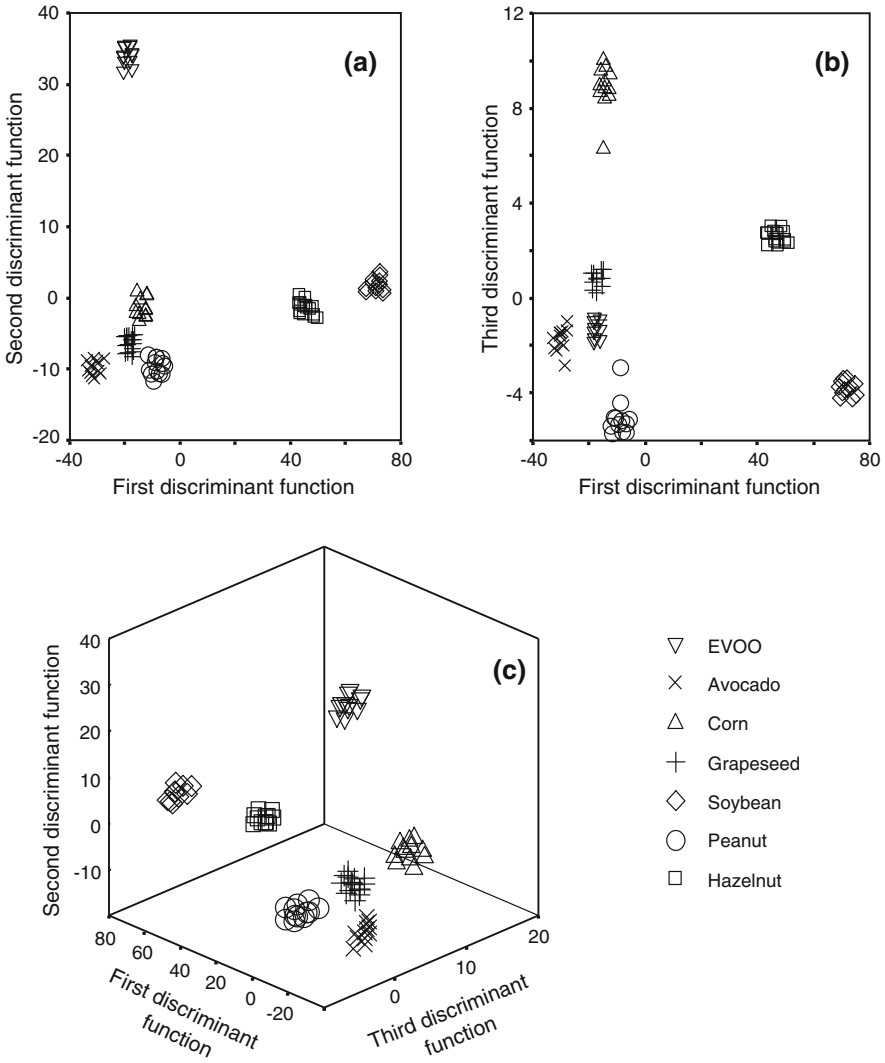

Fig. 5.19 Score plots on the planes of the first and second (**a**), second and third discriminant functions (**b**), on an oblique plane of the 3D space defined by the three discriminant functions (**c**) of the optimal LDA model (Reprinted from Concha-Herrera et al. (2010). Copyright 2009 Elsevier Ltd.)

number of predictors, was selected for further studies. As shown in Fig. 5.19, a good resolution was obtained for all categories ($\lambda_w = 0.393$). As a large number of categories were distinguished at the same time, this λ_w value could be considered quite low.

The variables selected by the SPSS stepwise algorithm, and the corresponding standardized coefficients of the model, are given in Table 5.15.

Table 5.15 Predictors selected and corresponding standardized coefficients of the LDA model constructed to predict the botanical origin of vegetable oils (Reprinted from Concha-Herrera et al. (2010). Copyright 2009 Elsevier Ltd.)

Predictors	f_1	f_2	f_3	f_4	f_5	f_6
Asp/Ala	−7.37	1.40	−1.25	0.01	−2.22	−0.35
(Asn + Ser)/Thr	−10.94	0.70	1.46	2.14	−0.58	−0.74
Gln/Thr	6.46	−1.85	−0.20	−1.84	3.35	1.93
His/Gly	16.16	2.00	1.92	1.18	−0.11	0.68
His/Trp	−16.38	−1.03	1.92	0.84	−0.96	1.00
Arg/Ala	−3.43	12.29	2.89	2.21	9.10	4.01
Arg/Val	7.94	−11.50	−1.17	−0.58	−9.83	−5.49
Ala/Val	−4.93	0.37	−0.04	2.54	0.38	0.83
Ala/Trp	2.67	0.31	0.67	−0.95	2.07	−1.03
Gly/Val	29.30	1.75	0.26	1.50	0.07	0.11
Gly/Ile	−6.20	1.17	0.82	−0.56	−0.98	1.62
Val/Ile	24.08	−0.90	−1.21	1.16	1.64	−1.71
Ile/(Leu + Phe)	16.84	0.46	0.72	1.21	1.10	−0.05

As shown in Fig. 5.19a, an excellent resolution between soybean and hazelnut categories, and also between these and the other categories, was obtained along f_1. This discriminant function was mainly constructed with the peak area ratios Gly/Val and Val/Ile, as observed from the data shown in Table 5.15. The variance gathered by f_2 was mainly associated to the resolution between EVOO and the rest of categories. On the other hand, orn, hazelnut, grapeseed, avocado-EVOO and peanut-soybean categories were resolved along f_3. (see Fig. 5.19b). Finally, as shown in Fig. 5.19c by using a plane oblique to the three first discriminant functions, all category pairs were clearly resolved. When leave-one-out validation was applied, all the objects of the training set were correctly classified. The prediction capability of the model obtained by using the evaluation set, which contained the other 84 original data points not included in the training set, was 100 %, since all the objects were correctly assigned with a probability higher than 95 %.

References

Baeten V, Fernández Pierna JA, Dardenne P, Meurens M, García-González DL, Aparicio-Ruiz R (2005) J Agric Food Chem 53:6201

Commission Regulation (EEC) (1991) No. 2568/91 of 11 July 1991 on the characteristics of olive oil and olive-residue oil and on the relevant methods of analysis. Off J Eur Union L128

Concha-Herrera V, Lerma-García MJ, Herrero-Martínez JM, Simó-Alfonso EF (2010) Food Chem 120:1149. Copyright 2009 Elsevier Ltd

Gimeno-Adelantado JV, Mateo-Castro R, Doménech-Carbó MT, Bosch-Reig F, Doménech-Carbó A, De la Cruz-Cañizares J, Casas-Catalán MJ (2002) Talanta 56:71

Guillén MD, Cabo N (1998) J Agric Food Chem 46:1788

Hidalgo FJ, Alaiz M, Zamora R (2001) Anal Chem 73:698

Lerma-García MJ, Ramis-Ramos G, Herrero-Martínez JM, Simó-Alfonso EF (2007) Rapid Commun Mass Spectrom 21:3751. Copyright 2007 John Wiley & Sons, Ltd
Lerma-García MJ, Ramis-Ramos G, Herrero-Martínez JM, Simó-Alfonso EF (2008) Rapid Commun Mass Spectrom 22:973. Copyright 2008 John Wiley & Sons, Ltd
Lerma-García MJ, Ramis-Ramos G, Herrero-Martínez JM, Gimeno-Adelantado JV, Simó-Alfonso EF (2009) J Chromatogr A 1216:230. Copyright 2008 Elsevier B.V
Lerma-García MJ, Ramis-Ramos G, Herrero-Martínez JM, Simó-Alfonso EF (2010) Food Chem 118:78. Copyright 2009 Elsevier Ltd
Micó-Tormos A, Collado-Soriano C, Torres-Lapasió JR, Simó-Alfonso E, Ramis-Ramos GJ (2008a) J Chromatogr A 1180:32
Micó-Tormos A, Simó-Alfonso E, Ramis-Ramos GJ (2008b) J Chromatogr A 1203:47
Ozen BF, Mauer LJ (2002) J Agric Food Chem 50:3898
Silverstein RM, Bassler GC, Morrill TC (1981) Spectrometric identification of organic compounds. Wiley, Chichester
Vigli G, Philippidis A, Spyros A, Dais P (2003) J Agric Food Chem 51:5715
Vlachos N, Skopelitis Y, Psaroudaki M, Konstantinidou V, Chatzilazarou A, Tegou E (2006) Anal Chim Acta 573–574:459

Chapter 6
Development of Methods for Olive Oil Quality Evaluation

6.1 Classification of Olive Oils According to Their Quality Grade Using Fatty Acid Profiles Obtained by Direct Infusion MS[1]

In this work, a simple and quick method for olive oil classification according to its quality grades, based on direct infusion ESI–MS and LDA, was developed. Moreover, mixtures of EVOO and VOO, and binary mixtures of these two oils with olive oils of lower quality grade have been also evaluated using this methodology and MLR and PLS data treatment. The olive oil samples used for this study are shown in Table 6.1. As explained in Sect. 3.3.4, infusion in the ESI interface of the mass spectrometer was performed after dilution of the sample with a miscible alkaline solvent, followed by direct analysis without any previous extraction step.

6.1.1 Ms Fatty Acid Profiles

A total of seven common peaks, which corresponded to the $[M\text{-}H]^-$ ions of the seven fatty acids, were observed in the MS spectra of all the samples analyzed: The fatty acids identified were: myristic (C14:0, *m/z* 227), palmitoleic (C16:1, *m/z* 253), palmitic (C16:0, *m/z* 255), linolenic (C18:3, *m/z* 277), linoleic (C18:2, *m/z* 279), oleic (C18:1, *m/z* 281) and stearic (C18:0, *m/z* 283). In order to compare the fatty acid profiles obtained for the different oil quality grades, the mass spectra were normalized by dividing each peak abundance by the abundance of the C16:0 peak (see Fig. 6.1).

[1] Parts of the text of this section have been adapted with permission from Lerma-García et al. (2008). Copyright 2007 Elsevier Ltd.

M. J. Lerma García, *Characterization and Authentication of Olive and Other Vegetable Oils*, Springer Theses, DOI: 10.1007/978-3-642-31418-6_6,

Table 6.1 Olive oils used to construct the LDA models (Reprinted from Lerma-García et al. (2008). Copyright 2007 Elsevier Ltd.)

Grade	Brand	Genetic variety	Geographical origin	Set type
EVOO	Coosur	Hojiblanca[a]	Luque (Córdoba)	Training
		Arbequina[a]	Estepa (Sevilla) + La Roda de Andalucía (Sevilla)	Training
		Picual[a]	Villanueva del Arzobispo (Jaén) + Porcuna (Jaén)	Training
	Carbonell	Hojiblanca	Estepa (Sevilla)	Evaluation
		Arbequina	Aguadulce (Sevilla)	Evaluation
		Picual	Martos (Jaén)	Evaluation
	Borges	Hojiblanca[a]	Puente Genil (Córdoba)	Training
		Arbequina[a]	Huelva + Zaragoza + Palma del Río (Córdoba)	Training
		Picual[a]	Quesada (Jaén)	Training
	Torrereal	Arbequina	Vila Franca del Penedés (Barcelona)	Evaluation
	Duc	Arbequina	Vila Franca del Penedés (Barcelona)	Evaluation
	Oleastrum	Arbequina	Les Garrigues (Lleida)	Evaluation
	Hipercor	Hojiblanca	Antequera (Málaga)	Evaluation
	Grupo	Hojiblanca[a]	Fuente de Piedra (Málaga)	Training
	Hojiblanca	Arbequina[a]	Antequera (Málaga)	Training
		Picual[a]	Montoro (Córdoba)	Training
VOO	Coosur	Mixture[b]	Vilches (Jaén)	Training
	Grupo	Hojiblanca[a]	Archidona (Málaga)	Training
	Hojiblanca	Arbequina[a]	Antequera (Málaga)	Training
		Picual[a]	Lucena (Córdoba)	Training
LVOO	Coosur	Mixture[a]	Vilches (Jaén)	Training
	Borges	Mixture[a]	Jódar (Jaén)	Training
	Grupo	Hojiblanca[a]	Archidona (Málaga)	Training
	Hojiblanca	Arbequina[a]	Hinojosa del Duque (Córdoba)	Training
		Picual[a]	La Rembla (Córdoba)	Training
ROPO	Coosur S.A	Mixture[a]	Vilches (Jaén)	Training
	Borges	Mixture[a]	Palma del Río (Córdoba)	Training
OPO	*Confidential*	Mixture	Unknown	Evaluation[b]

[a] Guaranteed quality
[b] Used exclusively to evaluate the MLR model

As observed in this figure, oleic acid peak was the most abundant for all oil quality grades, while the abundance of palmitic, linoleic and stearic acids are intermediate. No significant differences were observed in fatty acid profiles o each quality grade according to the oil genetic variety. The C14:0/C16:0 peak ratio was larger for VOO and LVOO than for the samples of other quality grades. Also, the C18:3/C16:0 peak ratio decreased according to LVOO > EVOO ≈ VOO > ROPO (Fig. 6.1). Thus, to enhance the differences observed between the different profiles, data treatment by different chemometric tools was carried out.

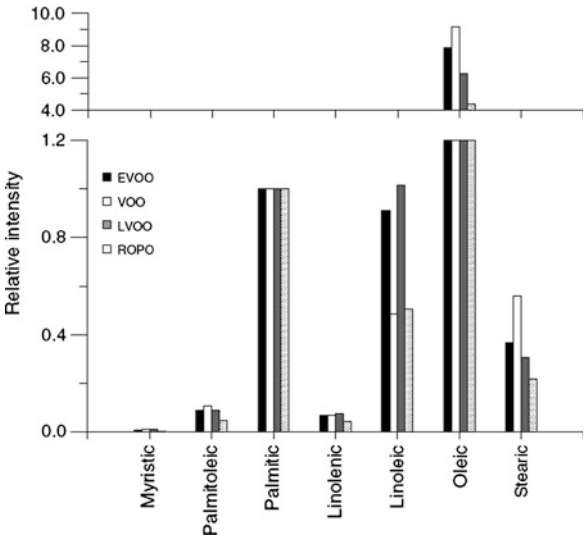

Fig. 6.1 Relative peak intensities of fatty acids observed in the mass spectra of different quality grade olive oils. The palmitic acid peak (*m/z* 255) was used as reference (Reprinted from Lerma-García et al. (2008). Copyright 2007 Elsevier Ltd.)

6.1.2 Construction of Data Matrices and LDA Models

The available olive oil samples (see Table 6.1) were divided to constitute both training and evaluation sets, being the guaranteed samples included in the training set, and those commercially acquired included in the evaluation set, as indicated in this table. The olive oil samples used for each quality grade were selected from different genetic varities (Hojiblanca, Arbequina and Picual), geographical origins (within the Spanish territory) and different climatic conditions in order to assure the robustness of the model. Thus two matrices, one for each normalization procedure, were constructed. Both matrices contained 123 objects (since each samples was injected 4–5 times) and 7 and 21 predictors, according to normalization procedures A and B, respectively.

Then, two LDA models, one for each normalization procedure, were constructed using the SPSS default values of F_{in} and F_{out}, 3.84 and 2.71, respectively. Normalization procedure B, which led to a better category separation, was selected for further studies. When the prediction capability of the model was checked using the evaluation set, all the objects were correctly classified by using a 95 % probability.

Next, all the available samples were jointly used to construct another LDA model in order to achieved a better prediction capability (since samples were obtained from different geographical origins). With this model, EVOO category was very well resolved from the other three categories (LVOO, ROPO and VOO), which were very close to each other (Fig. 6.2, $\lambda_w = 0.52$). The predictors selected by the SPSS stepwise algorithm to construct this model, and the corresponding model standardized coefficients, are given in Table 6.2. As deduced from this table, the C16:0/C16:1, C18:3/C16:1, C18:1/C16:1, C18:0/C16:0 and C18:1/C18:3 peak ratios were relevant to distinguish EVOO from the other three categories.

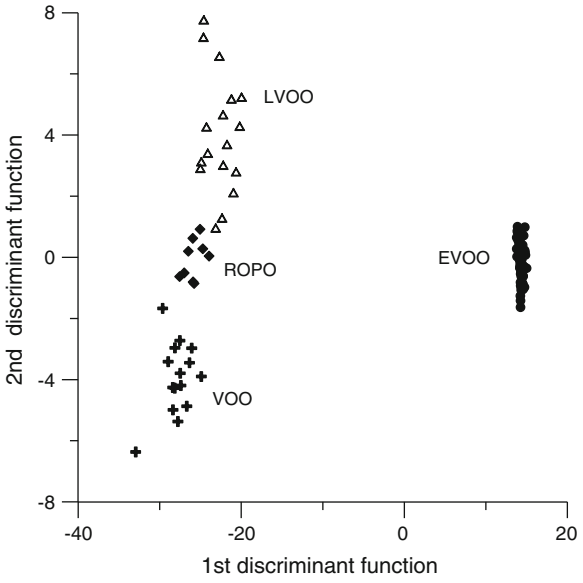

Fig. 6.2 Score plot on the plane of the two first discriminant functions of an LDA model constructed with samples of four different quality grade olive oils using normalization procedure B (Reprinted from Lerma-García et al. (2008). Copyright 2007 Elsevier Ltd.)

Next, EVOO category was removed, and another LDA model was constructed in order to maximize resolution among the VOO, LVOO and ROPO categories. In this case, an excellent resolution between all category pairs was obtained (Fig. 6.3, $\lambda_w = 0.19$). The standardized coefficients of this model are also given in Table 6.2. According to this table, predictors C16:0/C16:1, C18:0/C16:1 and C18:1/C16:0 were important to distinguish the category pairs formed by VOO, LVOO and ROPO. Therefore, all the olive oils could be correctly classify according to their quality grade by the sequential application of two LDA models.

6.1.3 Evaluation of Binary Mixtures of Olive Oils of Different Quality Grade

To estimate the adulteration of EVOO with VOO, or the adulteration of these two oils with the other oils of lower quality by using regression models, a total of five binary mixtures (EVOO-VOO, EVOO-LVOO, EVOO-ROPO, VOO-LVOO and VOO-ROPO) were prepared. For each pair, a total of six mixtures containing ca. 100, 80, 60, 40, 20 and 0 wt % EVOO or VOO, were prepared and infused. Using these mixtures, two matrices, one for each normalization procedure, were constructed. These matrices contained 90 objects each (since each mixture was injected three times), and either 7 or 21 predictors, according to normalization procedures A and B, respectively. A response column containing the percentage of the higher quality grade oil in the mixture (EVOO or VOO) was added to both matrices.

Table 6.2 Standardized coefficients of the discriminant functions obtained to predict the quality grade of olive oils (Reprinted from Lerma-García et al. (2008). Copyright 2007 Elsevier Ltd.)

Predictors	Categories[a]				
	EVOO/VOO/LVOO/ROPO			VOO/LVOO/ROPO	
	f_1	f_2	f_3	f_1	f_2
C16:0/C14:0	–	–	–	3.4	2.5
C18:1/C14:0	0.042	−1.1	0.53	–	–
C18:0/C14:0	–	–	–	−2.3	−2.2
C16:0/C16:1	−8.8	−2.3	−1.2	4.5	−3.5
C18:3/C16:1	6.8	1.3	2.3	–	–
C18:2/C16:1	–	–	–	2.0	−3.3
C18:1/C16:1	15	2.8	4.1	–	–
C18:0/C16:1	−1.7	−0.18	−0.65	−6.1	10
C18:1/C16:0	0.79	−0.71	−1.5	2.5	−7.1
C18:0/C16:0	−7.7	−0.17	−3.7	–	–
C18:2/C18:3	–	–	–	0.17	2.4
C18:1/C18:3	−6.3	0.084	−1.9	–	–
C18:0/C18:3	3.1	0.69	1.7	−0.68	−0.85
C18:1/C18:2	0.71	1.1	1.9	−0.72	3.2
C18:0/C18:1	0.66	−0.38	0.53	2.9	−0.76

[a] Categories included in the training set

To constructed the MLR model, the SPSS backward algorithm was used to select the predictors, by using the default values, $F_{in} = 3.84$ and $F_{out} = 2.71$. Using the matrices described above, two MLR models were constructed, both with and without the inclusion of an independent term (constant). In all cases, the model including the constant provided better linearities than the models without the constant. For this reason, further studies were performed with the inclusion of the constant. The regression coefficient values obtained for the MLR and PLSR1 models are given in Table 6.3. As observed in this table, the predictors with large regression coefficients are common to both MLR and PLSR1 models. To evaluate the quality of the model, the average prediction errors (calculated as the average absolute difference between the expected and predicted oil percentages, divided by the number of predictions), are also given in Table 6.3. As deduced from this table, MLR models showed, in most cases, average prediction errors slightly better than those obtained by the PLSR1 models. Regarding the normalization procedure used to construct the model, for the MLR models normalization procedure B gave better values of the average prediction errors than procedure A. Finally, the MLR model constructed for the binary mixture VOO/ROPO was also evaluated by the analysis of a guaranteed OPO sample (a commercial mixture of ROPO and VOO). As a result of this study, it could be concluded that this model was able to predict the percentage of ROPO in the commercial samples, since the declared and the found percentages of ROPO were 95 ± 3 and 92 ± 5 %, respectively.

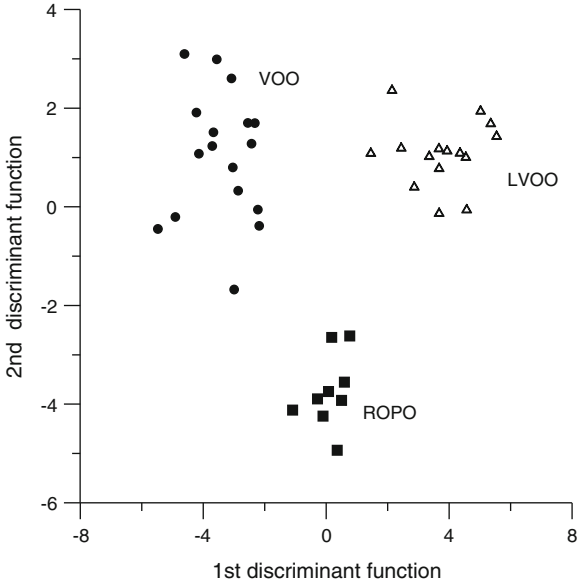

Fig. 6.3 Score plot on the plane of the two discriminant functions of an LDA model constructed with samples of three different quality grade olive oils (EVOO excluded) using normalization procedure B (Reprinted from Lerma-García et al. (2008). Copyright 2007 Elsevier Ltd.)

6.2 Electronic Nose Applied to Defect Detection and Quantitation in Olive Oils and Comparison with Sensory Panel Data[2]

In this work, an electronic nose method, based on the use of MOS sensors, was developed. This method, jointly with LDA and ANN; were applied to the classification of oils containing the typical VOO defects (fusty, mouldy, muddy, rancid and winey) according to their sensory threshold, which has been previously established by a tasting panel. For this purpose, these defects, available as single standards of the IOC, were added to refined sunflower oil. On the other hand, the electronic nose data were also used to quantify the defect percentage added to sunflower oil by the construction of MLR models.

6.2.1 Establishment of the Sensory Threshold by Trained Panelists

As previously explained in Sect. 3.6, ten trained assessors performed eight paired comparison tests between the defected samples and a blank, in order to establish

[2] Parts of the text of this section have been adapted with permission from Lerma-García et al. (2010). Copyright 2010 Elsevier B.V

Table 6.3 Regression coefficient values of the MLR and PLSR1[a] models constructed to predict the composition of binary mixtures of oils of different quality grades (Reprinted from Lerma-García et al. (2008). Copyright 2007 Elsevier Ltd.)

Predictor	EVOO/VOO		EVOO/LVOO		EVOO/ROPO		VOO/LVOO		VOO/ROPO	
	MLR	PLSR1	MLR	PLSR1	MLR	PLSR1	MLR	PLSR1	MLR	PLSR1
C14:0	−0.71	−0.78	0.71	0.63	−0.75	−0.75	−0.32	−0.15	–	0.066
C16:1	−1.2	−0.54	−2.7	−1.3	1.9	0.48	0.45	0.098	–	−0.16
C16:0	1.9	0.31	2.3	0.72	−2.6	−0.48	–	–	–	−0.16
C18:3	2.2	0.67	1.4	0.42	–	0.10	–	0.16	–	–
C18:2	0.41	0.17	0.92	0.061	–	0.11	−1.5	−0.52	1.8	0.465
C18:1	–	−0.20	−1.6	−0.32	2.2	0.078	1.9	0.36	–	−0.23
C18:0	−1.9	−0.23	–	−0.14	–	0.096	–	0.25	−0.94	−0.33
No. of vectors[b]	6	4	6	5	4	4	4	3	2	3
Av. pred. error, %	10	10	9.7	10	9.6	9.0	5.1	5.3	3.4	4.4
C16:1/C14:0	3.0	0.58	–	−0.31	–	0.38	1.4	0.054	−1.1	–
C16:0/C14:0	−5.4	−0.89	–	−0.11	–	−1.2	–	–	–	–
C18:3/C14:0	–	1.8	–	0.15	–	–	2.3	–	–	–
C18:2/C14:0	−0.64	−1.1	−0.35	−0.14	1.4	0.054	−1.7	–	–	–
C18:1/C14:0	3.0	1.1	–	–	–	0.24	–	–	1.3	–
C18:0/C14:0	–	−1.6	–	–	−0.92	−0.85	−1.9	–	–	–
C16:0/C16:1	–	–	–	0.22	−0.44	−0.30	0.82	–	0.54	–
C18:3/C16:1	1.6	0.39	−1.1	−0.20	–	–	−2.9	–	–	0.059
C18:2/C16:1	–	−0.77	2.0	0.39	–	−0.25	1.2	−0.10	–	0.14
C18:1/C16:1	–	0.99	0.77	−0.17	–	−1.2	1.2	0.071	–	–
C18:0/C16:1	−0.69	−0.44	−0.77	−0.14	–	–	–	–	−0.59	–
C18:3/C16:0	−0.69	−0.066	–	−0.17	–	–	0.71	–	0.42	–
C18:2/C16:0	−1.2	−0.80	−0.71	0.28	–	–	–	−0.169	–	0.168

(continued)

Table 6.3 (continued)

Predictor	EVOO/VOO		EVOO/LVOO		EVOO/ROPO		VOO/LVOO		VOO/ROPO	
	MLR	PLSR1	MLR	PLSR1	MLR	PLSR1	MLR	PLSR1	MLR	PLSR1
C18:1/C16:0	–	0.82	–	−0.17	–	0.080	–	0.095	–	–
C18:0/C16:0	–	−1.1	–	−0.097	–	–	–	–	–	−0.051
C18:2/C18:3	2.2	2.0	–	0.20	–	–	−1.2	−0.236	0.95	0.165
C18:1/C18:3	−0.40	−0.41	−1.2	−0.41	–	1.1	–	0.064	−0.48	–
C18:0/C18:3	–	0.091	–	−0.38	0.30	–	−0.40	–	0.71	–
C18:1/C18:2	–	−0.44	–	0.28	0.68	0.19	1.8	0.24	–	−0.14
C18:0/C18:2	–	−0.20	0.68	0.35	–	–	−2.3	0.18	–	–
C18:0/C18:1	–	0.71	–	–	–	–	0.98	–	–	−0.11
No. of vectors[b]	10	10	8	7	5	2	14	4	8	3
Av. pred. error, %	5.3	4.8	4.5	5.8	11	15	2.2	7.1	3.0	5.5

[a] PLSR1 coefficients smaller than 0.05 in absolute values are not given

[b] Number of vectors selected by the forward algorithm of SPSS (MLR), or recommended by The Unscrambler (PLSR1*k*-values)

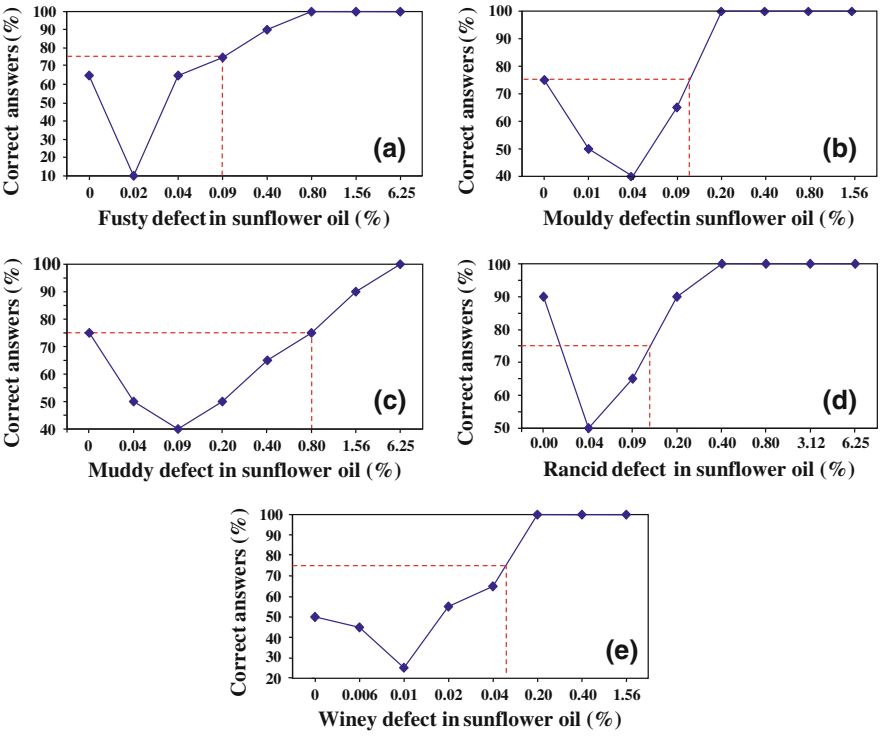

Fig. 6.4 Plots representing the defect [fusty (**a**), mouldy (**b**), muddy (**c**), rancid (**d**), winey (**e**)] against the correct answer percentages, showing the detection threshold (defect % corresponding to 75 % correct answers) (Reprinted from Lerma-García et al. (2010). Copyright 2010 Elsevier B.V)

Table 6.4 λ_w values and predictors selected with their corresponding standardized coefficients of the LDA models constructed for each sensory defect (Reprinted from Lerma-García et al. (2010). Copyright 2010 Elsevier B.V)

	Fusty	Mouldy	Muddy	Rancid	Winey
λ_w					
	0.166	0.167	0.029	0.041	0.184
Predictors[a]					
S1/S2	2.60	–	–	3.99	–
S1/S3	−3.63	7.47	5.76	13.91	2.48
S1/S4	−1.94	10.73	–	–	–
S1/S5	–	−6.62	−7.33	−17.22	–
S1/S6	4.55	−11.29	–	–	–
S2/S3	–	–	−9.82	6.29	–
S3/S5	–	–	–	–	2.96
S4/S5	–	–	11.01	–	–

[a] Ratios of sensor signals

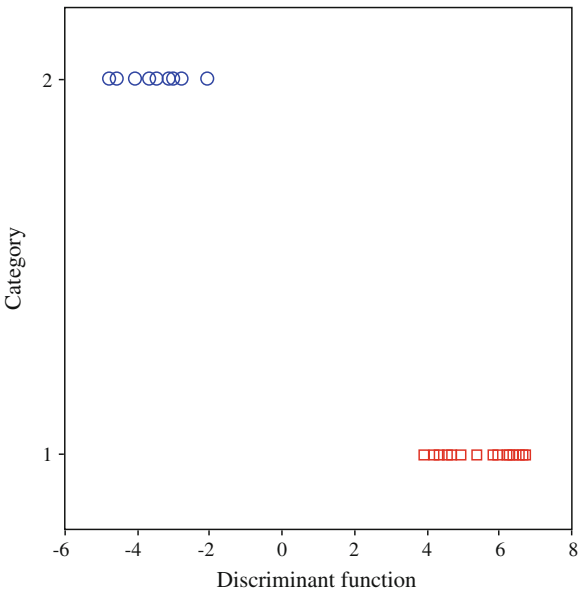

Fig. 6.5 Score plot on the plane of the discriminant function versus the category of the LDA model constructed to classify defected oil samples according to detection threshold of sensory analysis. Samples with a defect higher than detection threshold were grouped as category 1, being the other samples grouped as category 2 (Reprinted from Lerma-García et al. (2010). Copyright 2010 Elsevier B.V)

the mean threshold of the panel. The sensory threshold corresponded to the defect percentage perceived by at least a 75 % of the assessors. The results obtained for the five VOO defects are shown in Fig. 6.4. As observed in this figure, the sensory thresholds of the panel followed the increasing order: winey (0.09 %) = fusty (0.09 %) < mouldy (0.12 %) < rancid (0.13 %) ≪ muddy (0.80 %).

6.2.2 *Classification of Oils Containing VOO Defects According to Their Sensory Threshold as Established by a Sensory Panel*

In order to construct the classification models, two different categories were described. The first category contained the defected samples that have yielded a correct answer percentage higher than 75 % by the tasting panel (samples that were over the sensory threshold), while the rest of samples were included into the second category. For example, for the rancid defect, samples prepared with 0.2, 0.4, 0.8, 3.12 and 6.25 % defect in sunflower oil corresponded to the first category, while those with 0, 0.04 and 0.09 % defect corresponded to the second one.

The responses of the six sensors, which were normalized by normalization procedure B, were used as predictors. Thus, according to this procedure, a total of $(6 \times 5)/2 = 15$ predictors were obtained. These predictors were included in a total of five matrices, one for each sensory defect, which contained 24 objects each (8 samples × 3 replicates). A response column containing the assignments of the samples to one of the two categories described above was added to all the matrices. The λ_w values, the variables selected by the SPSS stepwise algorithm, and the

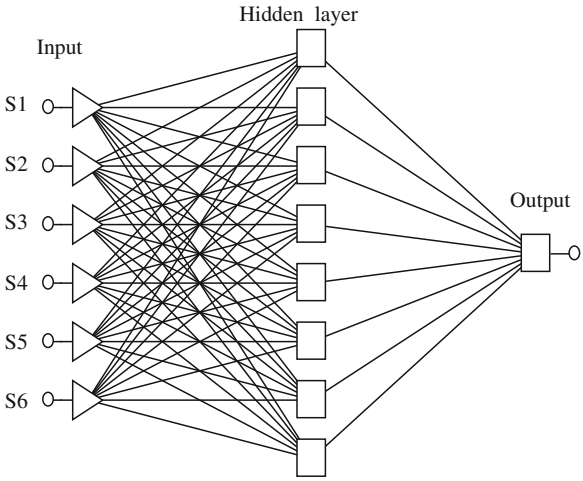

Fig. 6.6 MLP-ANN structures used to classify defected oil samples (Reprinted from Lerma-García et al. (2010). Copyright 2010 Elsevier B.V)

Table 6.5 Results of the MLP-ANN: correctly classified cases (%) for each sensory defect for the training, verification and test sets (Reprinted from Lerma-García et al. (2010). Copyright 2010 Elsevier B.V)

	Correctly classified cases (%)		
	Training	Verification	Test
Rancid	100	100	80
Mouldy	100	85	85
Muddy	100	80	80
Fusty	85	85	85
Winey	75	75	75

corresponding model standardized coefficients of the five LDA models constructed are given in Table 6.4. Since only two categories were used to construct the model, only one discriminant function was obtained.

As observed in this table, the predictor which showed a high discriminant power for all the models was the ratio of sensors 1 and 3 (S1/S3). Regarding λ_w values, they were in all cases lower than 0.2. When the different models were evaluated by leave-one-out validation, all the objects were correctly classified. As an example, a plot showing the LDA model constructed for the rancid defect is given in Fig. 6.5, in which a good resolution between both categories is evidenced.

On the other hand, the potential of MLP-ANN for the classification of the samples according to the two categories described above (samples that were over and under the sensory threshold) was also examined. In order to construct the ANN, the sensor responses represented the inputs, whereas a qualitative variable (containing the two categories) represented the output. Then, the original data set (objects belonging to categories 1 and 2) was randomly divided into training (60 % objects), verification (20 %) and test (20 %) sets. The verification set was used to identify the best ANN on the basis of the network's error performance, and to stop training if over-learning occurred. On the other hand, the test set was used to give an independent assessment of the ANN capability of classifying samples according

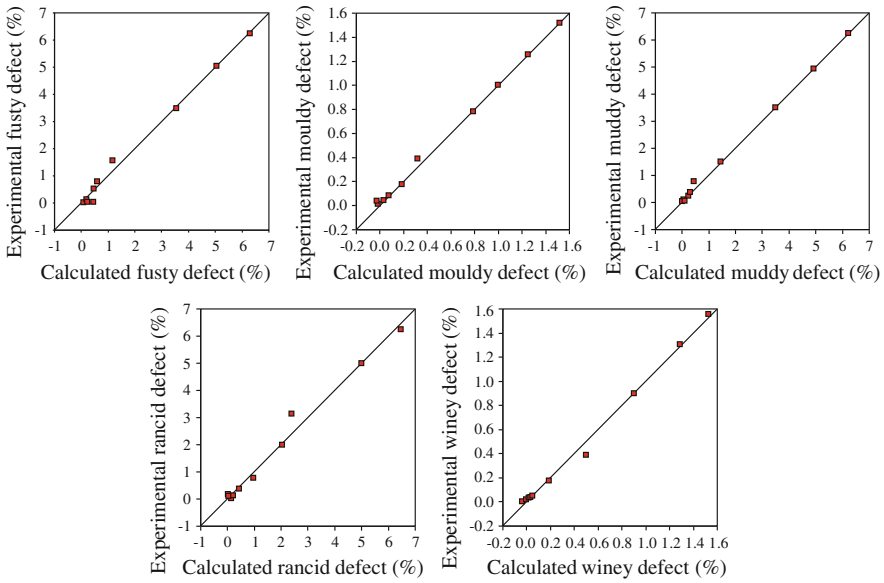

Fig. 6.7 Correlation plots of the calculated versus the experimental defect percentages (Reprinted from Lerma-García et al. (2010). Copyright 2010 Elsevier B.V)

to their sensory threshold. The structure of the best MLP-ANN among all the networks tested to classify the samples is shown in Fig. 6.6. This ANN was characterized by 8 neurons in the hidden layer. For any oil defect considered, the number of iterations needed to achieve a satisfactory result was 50.

The results obtained for the training, verification and test of this MLP-ANN model are shown in Table 6.5. These values were obtained with a momentum value of 0.3 and a learning rate of 0.1. As deduced from Table 6.5, the MLP-ANN showed an acceptable performance. In particular, from test validations, about 100, 85, 85, 80, and 75 % of the data set was correctly classified, for rancid, mouldy, fusty, muddy and winey defects, respectively.

6.2.3 Prediction of Defect Percentage in Sunflower Oil by Electronic Nose Followed by MLR Data Analysis

The possibility of predicting the defect percentage added to the sunflower oil using an electronic nose was also investigated. For this purpose, the 8 samples used in the paired comparison tests (8 for each defect) were used. Two additional samples for each defect were added in order to reduce the weight of the samples with

Table 6.6 *r* values, average prediction errors (*av. err.*) and predictors selected with their corresponding non-standardized coefficients for the MLR models constructed to predict defect percentage (Reprinted from Lerma-García et al. (2010). Copyright 2010 Elsevier B.V)

	Fusty	Mouldy	Muddy	Rancid	Winey
r	0.993	0.997	0.997	0.988	0.996
Av. err.(%)	0.51	0.22	0.43	0.90	0.39
Predictors[a]					
Constant	−651.19	14.74	−440.80	20.18	−66.64
S1/S4	–	–	–	−61.24	–
S3/S4	–	–	–	–	27.25
S3/S6	–	–	–	37.81	–
S4/S5	–	50.46	177.74	–	41.20
S4/S6	657.69	−138.47	–	–	–
S5/S6	–	75.27	271.62	–	–

[a] Ratios of sensor signals

higher defect percentages. To construct MLR matrices, only the means of the replicates of the samples were included (10 objects for each model), which was important to reduce the number of variables selected by the SPSS stepwise algorithm during model construction. The 15 signal ratios described above were also used as predictors to construct the MLR models.

The correlation plots of the calculated versus the experimental defect percentages are shown in Fig. 6.7. The *r* values, average prediction errors (*av. err.*, calculated as the sum of the absolute differences between expected and calculated defect percentages divided by the number of predictions) and the predictors selected for each MLR model with their corresponding non-standardized coefficients are detailed in Table 6.6. As observed, *r* values were in all cases higher than 0.988, being especially higher for fusty, mouldy, muddy and winey defects, were $r > 0.993$. This good correlation is illustrated in Fig. 6.7. On the other hand, and as observed in Table 6.6, the regression models for the fusty defect (which was mainly characterized by the presence of some volatile compounds originated by fermentation processes, i.e. some branched C5 components as 3-methyl butan-1-ol) and mouldy defect (produced by specific mould enzymes that produce volatile compounds such as 1-octen-3-one and 1-octen-3-ol) were mainly constructed with S4/S6 ratio (being S4 and S6 constructed with SnO_2 catalyzed with Au and WO_3, respectively), muddy defect (which was characterized by some volatile compounds originated by fermentation processes of oils stored for a long time on their sediment, i.e. propyl-propionate, ethyl-butanoate, propyl-butanoate and butyl-butanoate) by S5/S6 (SnO_2 catalyzed with Pd and WO_3, respectively), rancid defect (produced by several saturated and unsaturated aldehydes, such as nonanal and E-2-heptenal, respectively) by S1/S4 (SnO_2 and SnO_2 catalyzed with Ag, respectively) and winey defect (produced by acetic acid and ethyl acetate which were formed by sugar fermentation) by S4/S5 ratio (SnO_2 catalyzed with Ag and Pd, respectively).

References

Lerma-García MJ, Herrero-Martínez JM, Ramis-Ramos G, Simó-Alfonso EF (2008) Food Chem 107:1307. Copyright Elsevier Ltd

Lerma-García MJ, Cerretani L, Cevoli C, Simó-Alfonso EF, Bendini A, Gallina-Toschi T (2010) Sensor Actuat. B-Chem 147:283. Copyright 2010 Elsevier B.V

Chapter 7
Development of Methods for the Classification of EVOOs According to Their Genetic Variety

7.1 Classification Using FTIR Spectroscopy Data[1]

The aim of this work was to construct an LDA model able to classify EVOOs according to their genetic variety by using FTIR data. In order to construct this LDA model, the EVOOs shown in Table 7.1 were used. For this purpose, EVOO samples mainly produced at *La Comunitat Valenciana*, Spain, were used. Other samples, such as Hojiblanca and Picual, which were scarcely cultivated at *La Comunitat Valenciana*, were also included in this study because both varieties are, jointly with Arbequina, the main varieties cultivated in Spain.

7.1.1 Data Treatment and Construction of Data Matrices

As indicated in Table 7.2, all the FTIR spectra measured were divided in 20 wavelength regions according to the different peaks or shoulders observed, which represent structural or functional group information. Then, for statistical data treatment, the peak/shoulder area of each region was measured. In this study, only normalization procedure B was applied to the data. Thus, for classification studies, a matrix containing 76 objects (mean of the two replicates of each sample of Table 7.1) and 190 predictors, was constructed. A response column, which contains seven categories, one category for each EVOO genetic variety, was added to this matrix. This matrix was randomly divided in two sets: the training matrix that contained 42 objects (6 samples $\times$ 7 genetic varities) and the evaluation matrix that contained the remaining 34 objects.

[1] Parts of the text of this section have been adapted with permission from Concha-Herrera et al. (2009). Copyright 2009 American Chemical Society.

M. J. Lerma García, *Characterization and Authentication of Olive and Other Vegetable Oils*, Springer Theses, DOI: 10.1007/978-3-642-31418-6_7,

Table 7.1 Genetic variety, number of samples, geographical origin and supplier of the EVOOs employed in this study (Reprinted with permission from Concha-Herrera et al. (2009). Copyright 2009 American Chemical Society)

Genetic variety	No of samples	Geographical origin	Supplier	Crop season
Arbequina	2	Altura (Castellón)	Intercoop	06/07; 07/08
	2	Maestrat *comarca* (Castellón)	Intercoop	06/07; 07/08
	2	Alicante	Intercoop	05/06; 07/08
	2	Palancia *comarca* (Castellón)	Intercoop	06/07; 07/08
Borriolenca	3	Alcalatén *comarca* (Castellón)	Intercoop	05/06; 06/07; 07/08
	4	La Plana *comarca* (Castellón)	Intercoop	05/06; 06/07; 07/08
Canetera	3	Maestrat *comarca* (Castellón)	Intercoop	05/06; 07/08
	2	Adzaneta (Castellón)	Intercoop	06/07; 07/08
	3	La Plana *comarca* (Castellón)	Intercoop	05/06; 06/07; 07/08
Farga	4	Maestrat *comarca* (Castellón)	Intercoop	05/06; 06/07; 07/08
	3	Alcalatén *comarca* (Castellón)	Intercoop	06/07; 07/08
	3	La Plana *comarca* (Castellón)	Intercoop	05/06; 06/07; 07/08
Hojiblanca	2	Estepa (Sevilla)	Carbonell	06/07; 07/08
	2	Luque (Córdoba)	Coosur	06/07; 07/08
	3	Puente Genil (Córdoba)	Borges	06/07; 07/08
	5	Fuente de Piedra (Málaga)	G.Hojiblanca	05/06; 06/07; 07/08
	1	Santaella (Córdoba)	Columela	05/06
Picual	2	Martos (Jaén)	Carbonell	06/07; 07/08
	2	Villanueva del Arzobispo (Jaén) + Porcuna (Jaén)	Coosur	06/07
	3	Quesada (Jaén)	Borges	05/06; 06/07; 07/08
	1	Montoso (Córdoba)	Grupo Hojiblanca	06/07
	1	Tabernas (Almería)	Castillo de Tabernas	06/07
	1	Canena (Jaén)	Castillo de Canena	07/08
Serrana	9	Altura (Castellón)	Cooperativa Altura and Intercoop	05/06; 06/07; 07/08
	3	Artana (Castellón)	Intercoop	06/07; 07/08
	3	Jérica (Castellón)	Intercoop	06/07; 07/08
	5	Viver (Castellón)	Intercoop	05/06; 06/07; 07/08

The spectra of seven EVOOs, one for each genetic variety, are shown in Fig. 7.1. As it can be observed, only small differences between the different spectra were evidenced. In order to enhance these differences that were not appreciated straight away in the spectra, the peak areas at all the wavelength ranges were conveniently

Table 7.2 FTIR spectral regions selected as predictor variables for statistical data treatment (Reprinted with permission from Concha-Herrera et al. (2009). Copyright 2009 American Chemical Society)

Identification no.	Range, cm^{-1}	Functional group	Nominal frequency	Mode of vibration
1	2393–2347	Alcane[2]	–	–
2	2347–2279	Alcane[2]	–	–
3	1870–1712	–C=O (ester)	1746[a]	Stretching
4	1712–1693	–C=O (acid)	1711[a]	Stretching
5	1693–1671	–C=O	–[b]	Stretching
6	1671–1590	–C=C– (cis)	1654[a]	Stretching
7	1467–1426	–C–H (CH_2)	1465[b]	Bending (scissoring)
		–C–H (CH_3)	1450[b]	bending (asym)
8	1426–1407	=C–H (cis)	1417[a]	Bending (rocking)
9	1407–1380	=C–H	1400[b]	Bending
10	1380–1336	–C–H (CH_3)	1377[a]	Bending (sym)
		O–H	1359[b]	bending (in plane)
11	1336–1309	Non-assigned	1319[a]	Bending
12	1309–1292	=C–H (cis)	1294[c]	Bending
13	1292–1257	=C–H	–[c]	Bending
14	1257–1216	–C–O	1238[a]	Stretching
		$–CH_2–$		bending
15	1216–1127	–C–O	1163[a]	Stretching
		$–CH_2–$	1163[a]	bending
		–C–O	1138[b]	stretching
16	1127–1109	–C–O	1118[a]	Stretching
17	1109–1045	–C–O	1097[a]	Stretching
18	1045–998	–C–O	1033[a]	Stretching
19	998–883	–HC=CH– (trans)	968[a]	Bending (out of plane)
		–HC=CH– (cis)?	914[a]	bending (out of plane)
20	883–796	$=CH_2$	850[b]	Wagging

[a] According to Guillén (1998)
[b] according to Silverstein (1981)
[c] according to Yang (2005)

handled by multivariate statistical techniques, since band interpretation is not needed to obtain information about EVOO genetic variety.

7.1.2 Construction of LDA Models

An LDA model was constructed to classify EVOOs according to the seven genetic varieties. A good resolution between all category pairs was obtained (Fig. 7.2, $\lambda_w = 0.576$). As a large number of categories were distinguished at the same time, this λ_w value could be considered quite low.

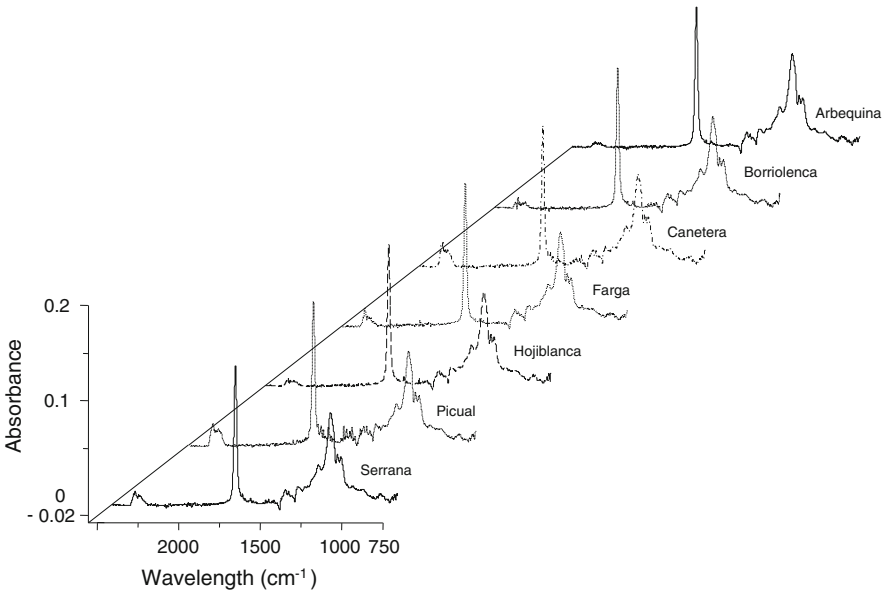

Fig. 7.1 FTIR spectra of EVOO samples of Arbequina from Alicante (crop season 05/06), Borriolenca from Alcalatén *comarca* (crop season 07/08), Canetera from La Plana *comarca* (crop season 06/07), Farga from Maestrat *comarca* (crop season 06/07), Hojiblanca from Luque, Córdoba (crop season 07/08), Picual from Martos, Jaén (crop season 06/07) and Serrana from Altura, Castellón (crop season 05/06) (Reprinted with permission from Concha-Herrera et al. (2009). Copyright 2009 American Chemical Society)

Along f_1, a large resolution between Farga, Picual and the other categories was a whole was observed (see Fig. 7.2a). On the other hand, the variance gathered by f_2 was mainly associated to the resolution between Picual and the rest of categories as a whole. According to Fig. 7.2b, Canetera, Picual and Hojiblanca were resolved from the rest of categories along f_3. Finally, Fig. 7.2c, shows a score plot projected on an oblique plane of the 3-D space defined by the three first discriminant functions. When this 3-D figure was rotated, a good resolution between all the category pairs was evidenced.

The variables selected by the SPSS stepwise algorithm, and the corresponding standardized coefficients of the model, are given in Table 7.3. According to this table, the main IR regions selected by the algorithm to construct the LDA model corresponded to –C=O (acid, stretching), –C–H (CH_2, bending scissoring), –C–H (CH_3, bending sym), =C–H (bending), –C–O (stretching) and –CH_2– (bending).

When the model was evaluated by leave-one-out validation, all training set objects were correctly classified. In addition to this, all the objects of the evaluation set were also correctly assigned with an assignment probability higher than 95 %, except 4 objects, which corresponded to Borriolenca (2 samples), Hojiblanca (1 sample) and Arbequina (1 sample) varieties.

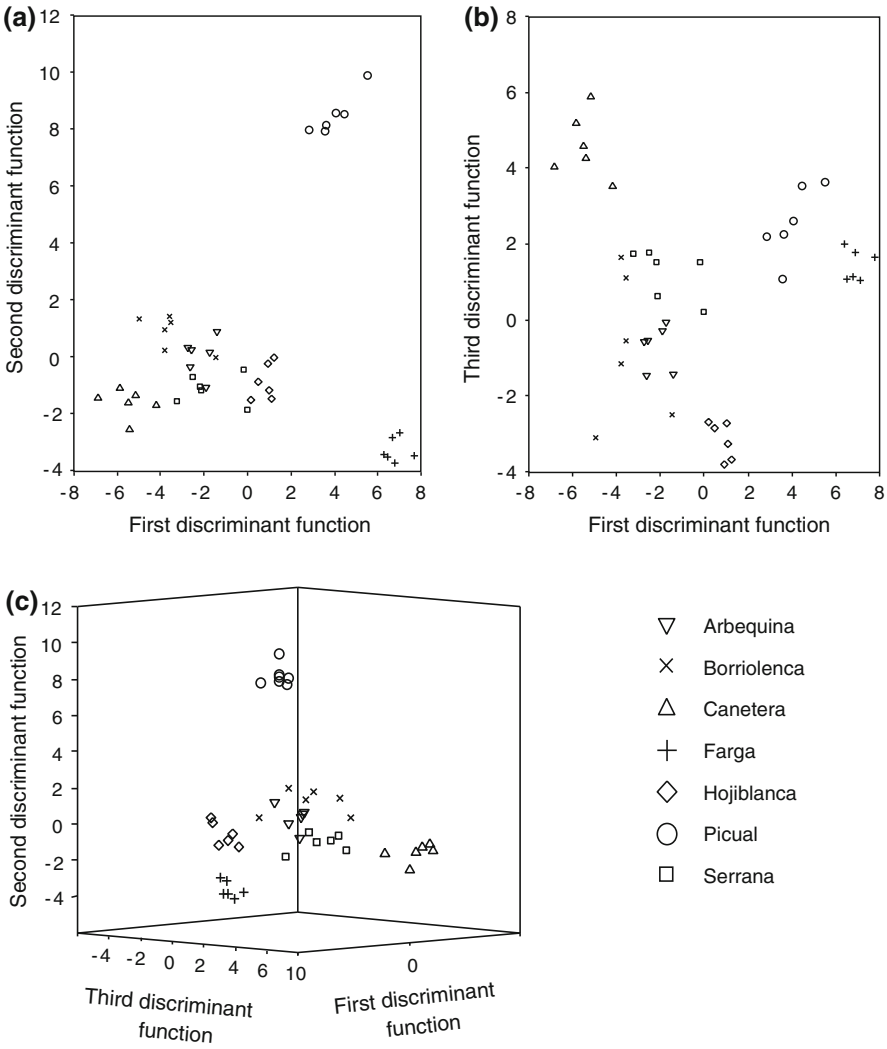

Fig. 7.2 Score plots on the planes of the first and second (**a**), and first and third discriminant functions (**b**), and projected on oblique plane of the 3-D space defined by the three discriminant functions (**c**) of the LDA model constructed to classify EVOOs according to their genetic variety (Reprinted with permission from Concha-Herrera et al. (2009). Copyright 2009 American Chemical Society)

Table 7.3 Predictors selected and corresponding standardized coefficients of the LDA model constructed to predict the genetic variety of EVOOs (Reprinted with permission from Concha-Herrera et al. (2009). Copyright 2009 American Chemical Society)

Predictors[a]	f_1	f_2	f_3	f_4	f_5	f_6
1/5	0.13	−0.91	−0.96	−0.06	−0.60	−2.04
1/7	5.85	4.36	−1.51	4.00	4.07	−2.22
1/9	−6.01	−3.57	3.91	−3.71	−3.11	4.03
3/6	−0.13	0.30	0.47	0.58	0.95	0.76
4/12	9.48	15.43	12.74	16.47	−7.05	−6.22
4/14	−9.00	−14.54	−12.66	−16.58	7.15	6.35
12/15	0.85	1.32	1.25	1.30	−0.89	0.35
13/16	−0.28	−0.55	0.69	−0.11	1.03	−0.48
14/17	1.06	−0.10	−0.37	−0.32	−0.41	0.43

[a] Pairs of wavelength regions identified according to Table 7.2

7.2 Classification Using Fatty Acid and Phenolic Compound Profiles Established by Direct Infusion MS[2]

In this work, the fatty acid and phenolic compound profiles of EVOOs coming from the three most cultivated genetic varieties of Spain (Hojiblanca, Arbequina and Picual), which have been obtained by direct infusion MS, have been used to construct LDA models capable of classifying EVOOs according to their genetic variety. For this purpose, the EVOOs included in Table 7.4 were used.

According to Ríos (2005) and Tripoli (2005), the peaks of seven fatty acids and 28 phenolic compounds were selected as original variables. The *m/z* values of the corresponding $[M\text{-}H]^-$ peaks of the selected fatty acids and phenolic compounds are summarized in Table 7.5. From the 35 compounds indicated in this table, only 20 peaks (to be used as predictors) were observed in the MS spectra. This is due to the fact that several compounds provided ions at the same *m/z* values. The MS spectra showing the peak profiles of three EVOOs, one for each genetic variety, are shown in Fig. 7.3. To make comparison easier, the spectra were standardized by dividing each peak abundance by the abundance of the C16:0 peak; moreover, oleic acid peak (C18:1), which is the most abundant in all the genetic varieties, was tailored at 1.2 to enhanced the differences between the fatty acid profiles. The higher C18:1 peak intensity was obtained for the Hojiblanca variety, followed by Picual and Arbequina. The C18:0 peak intensity (stearic acid) was similar for Hojiblanca and Picual oils, being lower for Arbequina, while the intensities of the C18: 2 peak (linoleic acid) showed the following decreasing order: Arbequina > Hojiblanca > Picual. On the other hand, phenolic compound peaks could not be appreciated in this figure, since their intensity is several orders of magnitude lower than that of the fatty acids. For this reason, to appreciate their profile, a MS

[2] Parts of the text of this section have been adapted with permission from Lerma-García et al. (2008a). Copyright 2007 Elsevier Ltd.

Table 7.4 Genetic variety, number of samples, geographical origin and brand of the EVOO samples (Reprinted from Lerma-García et al. (2008a). Copyright 2007 Elsevier Ltd)

Genetic variety	No of samples	Geographical origin	Brand
Arbequina	2	Aguadulce (Sevilla)	Carbonell
	2	Vila Franca del Penedés (Barcelona)	Torrereal
	2	Les Garrigues (Lleida)	Oleastrum
	1	Estepa (Sevilla) + La Roda de Andalucía (Sevilla)	Coosur
	1	Antequera (Málaga)	Grupo Hojiblanca
	2	Huelva + Zaragoza + Palma del Río (Córdoba)	Borges
	1	Les Garrigues (Lleida)	Romanico
	1	La Puebla Nueva (Toledo)	Valderrama
	1	Sarroca de Lleida (Lleida)	Veá
	1	Mallorca	Aubocassa
	1	La Rioja	Rihuelo
Hojiblanca	2	Estepa (Sevilla)	Carbonell
	2	Luque (Córdoba)	Coosur
	3	Puente Genil (Córdoba)	Borges
	5	Fuente de Piedra (Málaga)	Grupo Hojiblanca
	1	Santaella (Córdoba)	Columela
Picual	2	Martos (Jaén)	Carbonell
	2	Villanueva del Arzobispo (Jaén) + Porcuna (Jaén)	Coosur
	3	Quesada (Jaén)	Borges
	1	Montoso (Córdoba)	Grupo Hojiblanca
	1	Tabernas (Almería)	Castillo de Tabernas
	1	Canena (Jaén)	Castillo de Canena

spectrum with an expanded vertical axis is shown in Fig. 7.4 for a Picual EVOO sample. Similar spectra, showing small differences among the peak profiles, were obtained for the Arbequina and Hojiblanca oils.

7.2.1 Construction of Data Matrices and LDA Models

In this work, both normalization procedure A and B were applied to the data. Regarding predictors, they were divided in two groups: those obtained from the fatty acids and those obtained from the phenolic compounds. This division was performed due to the large differences observed between the peak intensities of both families of compounds. Then, for the fatty acids, 7 and 21 predictors were obtained by normalization procedures A and B, respectively; while the ones obtained for the phenolic compounds were 20 and 190, respectively.

Table 7.5 $[M-H]^-$ peaks of the selected fatty acids and phenolic compounds (Reprinted from Lerma-García et al. (2008a). Copyright 2007 Elsevier Ltd)

Compound (acronym)	*m/z*
Myristic acid (C14:0)	227
Palmitoleic acid (C16:1)	253
Palmitic acid (C16:0)	255
Linolenic acid (C18:3)	277
Linoleic acid (C18:2)	279
Oleic acid (C18:1)	281
Stearic acid (C18:0)	283
TY	137
P-Hydroxybenzoic acid	137
Cinnamic acid	147
p-Hydroxyphenylacetic acid	151
p-Anisic acid	151
HYTY	153
Gentisic acid	153
Protocatechuic acid	153
Coumaric acid	163
Vanillic acid	167
Gallic acid	169
Caffeic acid	179
Homovanillic acid	181
Ferulic acid	193
Syringic acid	197
Sinapic acid	223
EA	241
Dialdehydic form of deacetoxy ligstroside	303
Deacetoxy ligstroside aglycone	303
Dialdehydic form of deacetoxy oleuropein	319
Deacetoxy oleuropein aglycone	319
Pinoresinol	357
Dialdehydic form of ligstroside	361
LAg	361
Dialdehydic form of oleuropein	377
OA	377
10-Hydroxy-oleuropein aglycone	393
AcPIN	415

Taking into account all these considerations, two matrices were constructed for each family of compounds. All matrices contained 304 objects (38 samples of Table 7.4 $\times 2$ days $\times$ 4 replicates) and their corresponding predictors, as explain above. A response column, containing the three categories corresponding to the three genetic varieties, was added to all the matrices. These matrices were used as evaluation sets. To construct LDA training matrices, only the means of the replicates of the samples were included.

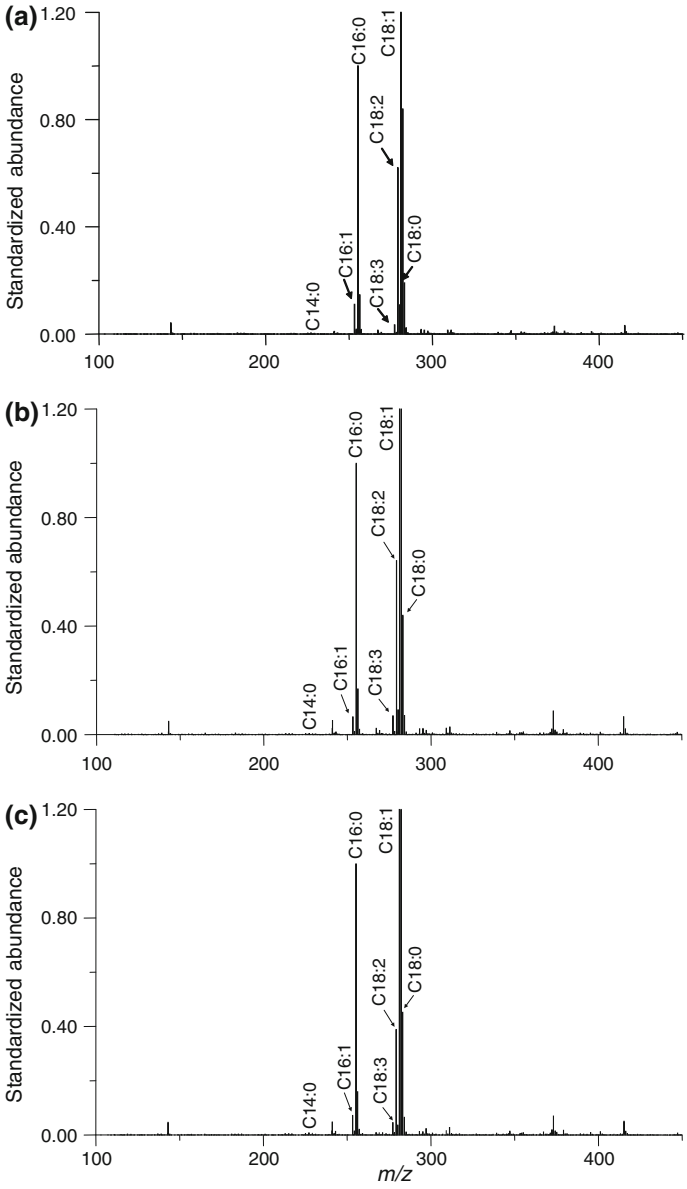

Fig. 7.3 Standardized mass spectra of EVOOs of the three genetic varieties: **a** Arbequina, **b** Hojiblanca and **c** Picual. The intensity of all peaks was divided by the intensity of the C16:0 peak and the C:18:1 peak was tailored at 1.2 (Reprinted from Lerma-García et al. (2008a). Copyright 2007 Elsevier Ltd)

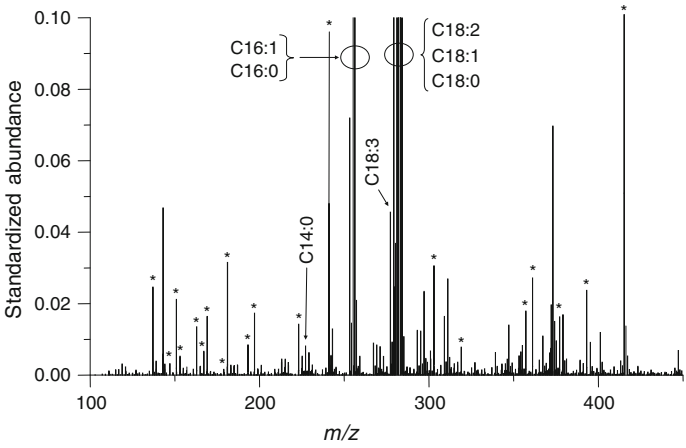

Fig. 7.4 Standardized mass spectrum of a Picual olive oil sample with the vertical axis tailored at 0.1. The peaks of the phenolic compounds of Table 7.5 are indicated with an asterisk (Reprinted from Lerma-García et al. (2008a). Copyright 2007 Elsevier Ltd)

In first place, two LDA models, one for each normalization procedure, were constructed using the data obtained from fatty acid profiles. The best results in terms of category resolution were obtained with normalization procedure B, which was selected for the next studies. With this model, a good resolution between all category pairs was obtained ($\lambda_w = 0.396$). The model was constructed with 7 variables, showing the ratios 279/283 and 279/281 predominant weights. All samples were correctly classified.

Next, another two LDA models (normalization procedures A and B), were constructed using the data obtained from phenolic compound profiles. The best results were also obtained with normalization procedure B, which was selected. In this case, 22 variables were selected ($\lambda_w = 0.236$); however, resolution between the category pairs was slightly worse than that obtained with the fatty acids. The variables showing predominant weights were 303/241, 303/193 and 393/241.

Finally, all the available predictors (fatty acids and phenolic compounds) were jointly used to construct another LDA model. In this case, a high number of predictors (30 variables) were selected to construct the model. Thus, in order to reduce the entrance of predictors in the model, the probability values $F_{in} = 0.01$ and $F_{out}, = 0.20$ were used. Using these values, a model constructed with only 11 predictors was obtained. This model provided an excellent resolution between all category pairs (Fig. 7.5, $\lambda_w = 0.237$).

The predictors selected by the SPSS stepwise algorithm and the corresponding standardized coefficients of the model are given in Table 7.6. Finally, the prediction capability of the model was checked by using the evaluation set. Using a 95 % probability, all the objects were correctly assigned; thus, the prediction capability was 100 %.

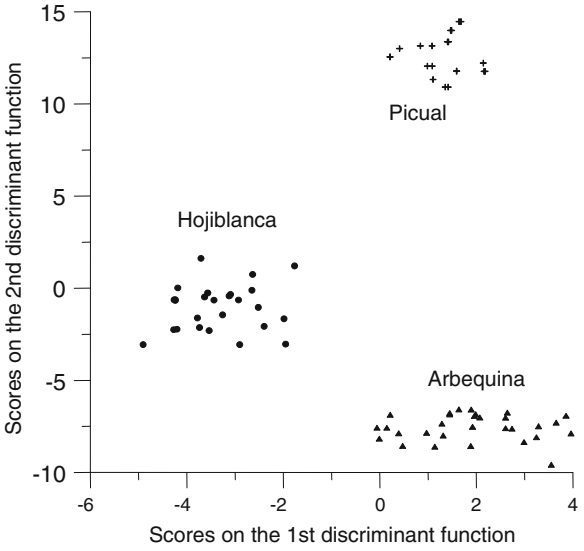

Fig. 7.5 Score plot on the plane of the two LDA discriminant functions obtained to predict EVOO genetic variety after data normalization by procedure B (Reprinted from Lerma-García et al. (2008a). Copyright 2007 Elsevier Ltd)

Table 7.6 Predictors selected and corresponding standardized coefficients of the LDA model constructed to predict the genetic variety of EVOOs (Reprinted from Lerma-García et al. (2008a). Copyright 2007 Elsevier Ltd)

Compounds	Predictors[a]	f_1	f_2
Fatty acids	227/279	−0.40	2.78
	227/281	0.63	−1.98
	255/279	−0.32	0.45
	277/279	−1.21	0.16
	279/281	0.35	0.70
	281/283	0.81	1.08
Phenolic	193/167	0.83	0.22
Compounds	223/181	0.67	−0.02
	303/197	−0.27	−0.82
	415/197	0.87	0.52
	361/223	−0.28	−0.70

[a] *m/z* values of the ratios of abundances of peak pairs

7.3 Classification Using Sterol Profiles Established by HPLC–MS[3]

The aim of this work was to develop an HPLC-MS method that, jointly with LDA, was able to predict the genetic variety of EVOOs according to six different genetic varieties produced at *La Comunitat Valenciana*, Spain. The sterol profiles were used to classify the samples. The EVOO employed in this study, which covered

[3] Parts of the text of this section have been adapted with permission from Lerma-García et al. (2009). Copyright 2009 American Chemical Society.

Table 7.7 Genetic variety, number of samples, geographical origin and crop season of the EVOOs employed in this study (Reprinted with permission from Lerma-García et al. (2009). Copyright 2009 American Chemical Society)

Genetic variety	N° of samples	Geographical origin	Crop season
Arbequina	2	Altura (Castellón)	06/07; 07/08
	2	Maestrat *comarca* (Castellón)	06/07; 07/08
	1	Alicante	05/06
	1	Palancia *comarca* (Castellón)	07/08
Borriolenca	3	Alcalatén *comarca* (Castellón)	05/06; 06/07; 07/08
	3	La Plana *comarca* (Castellón)	05/06; 06/07; 07/08
Canetera	2	Maestrat *comarca* (Castellón)	05/06; 07/08
	2	Adzaneta (Castellón)	06/07; 07/08
	2	La Plana *comarca* (Castellón)	05/06; 07/08
Farga	2	Maestrat *comarca* (Castellón)	05/06; 06/07
	2	Alcalatén *comarca* (Castellón)	06/07; 07/08
	2	La Plana *comarca* (Castellón)	05/06; 07/08
Picual	6	Altura (Castellón)	05/06; 06/07; 07/08
Serrana	2	Altura (Castellón)	06/07; 07/08
	1	Artana (Castellón)	06/07
	1	Jérica (Castellón)	07/08
	2	Viver (Castellón)	05/06; 07/08

different crop seasons and geographical origins in order to assure a correct sampling, are shown in Table 7.7.

7.3.1 Optimization of the Separation Conditions

Although two peaks, corresponding to $[M + H]^+$ and $[M + H-H_2O]^+$ ions, were observed for each sterol standard (erythrodiol, β-sitosterol, campesterol, ergosterol and stigmasterol), only the $[M + H-H_2O]^+$ ions, which showed higher intensities than the respective $[M + H]^+$ peaks (Cañabate-Díaz 2007; Lerma-García 2008b; Segura-Carretero 2008), were used as predictors.

To optimize sterol separation, different ACN/water mixtures, containing in all cases 0.01 % acetic acid, were tried using a gradient elution as mobile phase. For this purpose, a constant flow rate of 1.0 mL min^{-1}, was used. The best results in terms of resolution and analysis time were obtained using a linear gradient from 90 to 100 % ACN for 10 min followed by isocratic elution with 100 % ACN for 2 more min. Thus, this gradient was selected for further studies. A chromatogram showing the peaks corresponding to the different sterol standards using the optimal conditions is shown in Fig. 7.6. As observed, all peaks eluted within 10 min, being this time so much lower than that reported for sterol separation using GC-FID. On the other hand, an overlapping between campesterol and stigmasterol peaks was observed in all the gradient elutions tried. The overlapping of these two peaks was already reported in other HPLC studies (Sanchéz-Machado 2004).

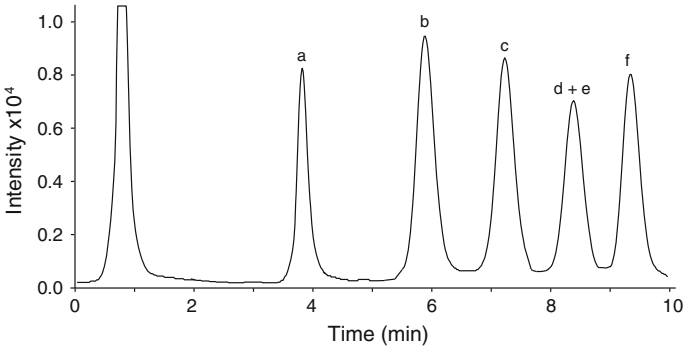

Fig. 7.6 TIC of a standard solution of sterols (*ca.* 100 mg L^{-1}) obtained by using a linear gradient from 90 to 100 % ACN for 10 min followed by isocratic elution with 100 % ACN for 2 more min. Peak identification: **a** erythrodiol, **b** ergosterol, **c** cholesterol, **d** campesterol, **e** stigmasterol and **f** β-sitosterol (Reprinted with permission from Lerma-García et al. (2009). Copyright 2009 American Chemical Society)

Then, the optimized method was applied to the analysis of real samples. To identify other sterol peaks, which presence in vegetable oils has been previously described (Cañabate-Díaz 2007; Lerma-García 2008b; Segura-Carretero 2008), the EICs at the *m/z* values of Table 7.8, were also obtained. A total of 9 peaks, corresponding to 12 possible sterols, were identified in less than 10 min. The TIC and EICs of two EVOO extracts of the genetic varieties Canetera and Serrana are shown in Fig. 7.7a and b, respectively. As it can be observed, several differences between the sterol profiles of both samples could be evidenced. The percentages of sterols found in the EVOOs are shown in Table 7.9. These values found in these samples were in good agreement with data previously reported (Jee 2002). As shown in this table, several differences between the different genetic varieties were found. The sterol separation performance obtained using this method is similar to that previously reported (Segura-Carretero 2008), although the analysis times obtained in literature are higher than the one reported by this methodology (Cañabate-Díaz 2007; Segura-Carretero 2008; Martínez-Vidal 2007).

7.3.2 Construction of Data Matrices and LDA Models

The original variables were measured on the EICs of the samples. The EICs were previously smoothed using a Gaussian filter set at 5 points, and the peak area of each sterol was measured and normalized by procedure B. In this way, a total of 36 normalized variables were obtained to be used as predictors.

Thus, a matrix containing 72 objects (36 samples of Table 7.7 $\times$ 2 replicates) and the 36 predictors, was first constructed. A response column, which contains six categories, one category for each EVOO genetic variety, was added to this matrix, which constituted the evaluation set. The training matrix was constructed using the

Table 7.8 Peak labelling, retention time (t_R) and *m/z* value of the sterols studied in this work (Reprinted with permission from Lerma-García et al. (2009). Copyright 2009 American Chemical Society)

Peak no	Analytes	t_R (min)	*m/z*[a]
1	Erythrodiol	3.90	425
2	Uvaol	3.90	425
3	Brassicasterol	6.10	381
4	Cholesterol	7.25	369
5	Δ^7-Avenasterol	7.25	395
6	Δ^5-Avenasterol	7.25	395
7	Campesterol	8.30	383
8	Campestanol	8.30	385
9	Stigmasterol	8.40	395
10	$\Delta^{5,24}$-Stigmastadienol	9.30	395
11	Δ^7-Stigmastenol	9.40	397
12	β-Sitosterol	9.40	397

[a] *m/z* value corresponding to the $[M + H-H_2O]^+$ peak

mean of the replicates of the samples; thus, a total of 36 objects were included in this matrix.

The capability for the classification of the studied oils according to their genetic variety was tested by constructing an LDA model. In this case, the SPSS default values of F_{in} and F_{out}, 3.84 and 2.71, respectively, were used. With this model, an overlapping between Canetera, Farga and Serrana varieties was evidenced (data not shown), although all the other categories appeared clearly resolved. For this reason, a new LDA model was constructed grouping the three overlapped categories into a single one. With this model, an excellent resolution between the Arbequina, Borriolenca, Picual and the category formed by the grouped categories was obtained (Fig. 7.8, $\lambda_w = 0.290$).

The variables selected by the SPSS stepwise algorithm and the corresponding model standardized coefficients are given in Table 7.10. When leave-one-out cross-validation was applied to the training set data, all the objects were correctly classified. On the other hand, when the prediction capability of the model was checked using the evaluation set, only three objects corresponding to replicates of different samples (1 Borriolenca, 1 Canetera and 1 Farga) were not correctly assigned using a 95 % probability; thus, the prediction capability was higher than 95 %.

Next, a second LDA model was constructed to separate the three categories that have been previously grouped (Canetera, Farga and Serrana). With this LDA model, an excellent resolution among all categories was achieved (Fig. 7.9, $\lambda_w = 0.209$). The variables selected and the corresponding model standardized coefficients are also given in Table 7.10. Also in this case, all the objects of the training set were correctly classified by leave-one-out cross-validation. On the

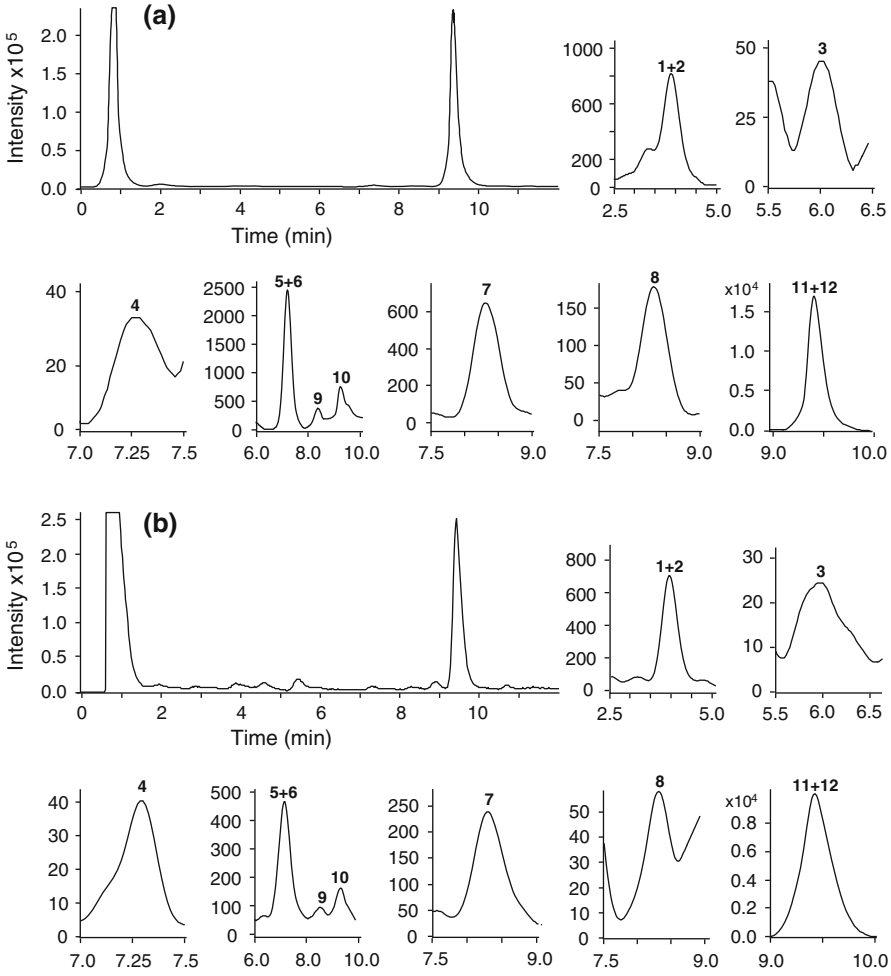

Fig. 7.7 TIC and EICs of Canetera (**a**) and Serrana (**b**) EVOO sterol extracts. The EICs were obtained at the *m/z* values indicated in Table 7.8. Peak labelling as indicated in Table 7.8. Other experimental conditions as in Fig. 7.6 (Reprinted with permission from Lerma-García et al. (2009). Copyright 2009 American Chemical Society)

other hand, when the prediction capability of the model was checked using the evaluation set, constituted now by 36 original data points, only only 2 objects, which corresponded to replicates of different samples (1 Canetera and 1 Farga), were not correctly assigned; thus, the prediction capability was higher than 88 %.

Table 7.9 Proportions of sterols found in the total sterol fraction of EVOOs of different genetic varieties (Reprinted with permission from Lerma-García et al. (2009). Copyright 2009 American Chemical Society)

Sterol	Arbequina	Borriolenca	Canetera	Farga	Picual	Serrana
Erythrodiol + uvaol	0.1–0.3	0.0–0.09	2.0–4.0	0.0–0.4	0.2–0.6	5.0–7.7
Brassicasterol	0.08–0.11	0.06–0.09	0.06–0.12	0.09–0.12	0.1–0.2	0.08–0.15
Cholesterol	0.3–0.6	0.3–0.5	0.1–0.2	0.1–0.5	0.4–0.5	0.2–0.4
Δ^7- + Δ^5-Avenasterol	12.1–14.9	7.0–9.9	11.5–12.3	7.8–9.5	4.3–13.2	5.1–6.4
Campesterol	3.7–4.0	3.2–3.7	3.0–3.5	3.2–3.6	2.5–3.1	1.8–2.4
Campestanol	0.2–0.4	0.2–0.3	0.5–0.9	0.2–0.3	0.2–0.3	0.3–0.6
Stigmasterol	0.7–1.5	1.2–2.8	1.5–2.0	1.1–1.9	0.9–1.5	1.0–2.5
$\Delta^{5,24}$-Stigmastadienol	0.7–1.9	0.6–1.0	3.0–3.7	0.8–1.0	0.9–1.3	1.0–1.5
Δ^7-Stigmastenol + β-Sitosterol	76.0–80.0	79.0–82.3	75.0–77.8	78.7–90.8	77.3–90	81.0–82.7

[a] *ND* not detected

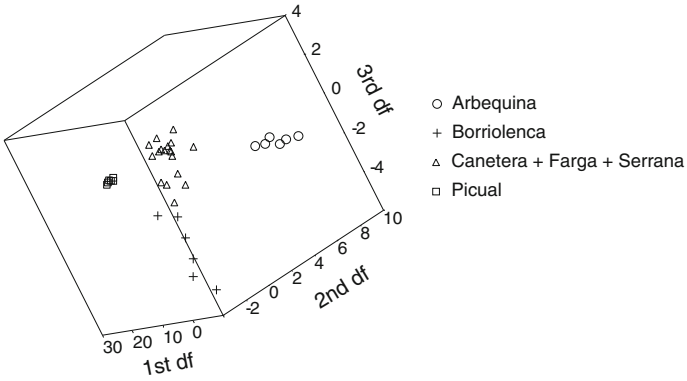

Fig. 7.8 Score plot on an oblique plane of the 3-D space defined by the three discriminant functions of the LDA model constructed to resolve the arbequina, borriolenca, picual and canetera + farga + serrana categories (Reprinted with permission from Lerma-García et al. (2009). Copyright 2009 American Chemical Society)

7.4 Classification Using Sterol Profiles Established by UPLC-MS[4]

In this work, sterol profiles, established by the UPLC-MS method developed in Sect. 4.5, were used to construct an LDA model capable of classifying EVOOs produced at *La Comunitat Valenciana*, Spain, according to their genetic variety. For this purpose, the samples listed in Table 7.7, were used.

[4] Parts of the text of this section have been adapted with permission from Lerma-García et al. (2011). Copyright 2010 Elsevier Ltd.

Table 7.10 Predictors selected and the corresponding standardized coefficients of the two sequential LDA models constructed to predict the genetic variety of EVOOs (Reprinted with permission from Lerma-García et al. (2009). Copy right 2009 American Chemical Society)

	Arbequina/Borriolenca/Picual/ Canetera + Farga + Serrana			*Canetera/Farga/ Serrana*	
Predictor[a]	f_1	f_2	f_3	f_1	f_2
(1 + 2)/3	−1.65	0.48	0.02	−2.08	1.32
(1 + 2)/(5 + 6)	2.62	−1.12	−0.95	3.86	−3.08
(1 + 2)/7	3.82	7.47	−0.12	2.13	−1.44
(1 + 2)/9	−3.30	5.65	−1.29	−5.16	11.45
(1 + 2)/10	−12.61	−5.83	6.49	12.83	−0.58
(1 + 2)/(11 + 12)	24.16	2.47	−5.37	−15.50	1.49
(11 + 12)/3	−0.80	1.44	2.45	3.60	−1.00
(11 + 12)/(5 + 6)	−2.08	0.74	−0.36	−3.59	0.99
(11 + 12)/7	−4.47	−1.08	−0.13	–	–
(11 + 12)/9	6.36	−2.86	5.84	4.63	−11.39
(11 + 12)/10	2.00	0.06	−1.84	3.18	4.81
3/(5 + 6)	3.27	−2.38	7.39	–	–
3/7	0.83	−7.68	0.54	–	–
3/9	0.93	−0.36	−3.68	–	–
3/10	−20.81	6.40	−6.09	–	–
(5 + 6)/9	−4.79	−1.77	−0.78	–	–
(5 + 6)/10	2.79	1.58	0.40	–	–
9/10	4.19	1.25	−0.39	6.51	1.91

[a] *m/z* values of the ratios of sterol peaks labelled as in Table 7.8

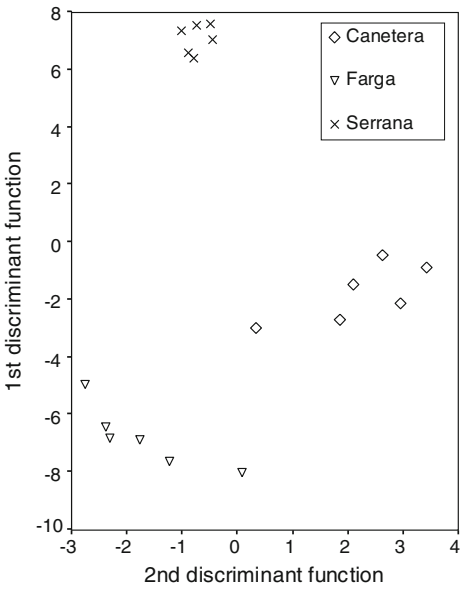

Fig. 7.9 Score plot on the plane of the two discriminant functions of the LDA model constructed to resolve the canetera, farga and serrana categories (Reprinted with permission from Lerma-García et al. (2009). Copyright 2009 American Chemical Society)

The optimal separation of a sterol standard mixture of ca. 50 mg L^{-1} is shown in Fig. 4.20b. As it can be observed in this figure, a satisfactory efficiency and resolution within 5 min, is observed for all sterol peak pairs.

Under these optimal conditions, all the EVOO extracts, coming from seven different genetic varieties, were injected. As indicated in Sect. 4.5, the signals of other sterols different from those used as standards, which were expected in the samples, were also recorded (see Table 4.15). As can be deduced from this table, only 11 sterols or combination of sterol peaks could be distinguished, and then measured. The TIC and SIR chromatograms of two EVOO extracts of the genetic varieties Borriolenca and Farga are shown in Figs. 7.10 and 7.11, respectively. As observed, sterol profiles of both varieties were quite different. These differences in peak profiles were also observed between these varieties and the other five varieties analyzed (data not shown).

7.4.1 Construction of Data Matrices and LDA Models

As indicated above, the 11 peaks were measured and used as original variables. These variables were normalized by normalization procedure B, giving a total of 55 predictors to be used in LDA model construction. Then, a matrix containing these 55 predictors and a total of 126 objects (42 samples of Table 7.7 × 3 replicates) was constructed, and used as evaluation set. To construct LDA training matrix, only the means of the replicates of the samples (a total of 42 objects) were used. A response column, containing the seven categories corresponding to the seven genetic varieties of the EVOOs was added to both matrices.

Next, an LDA model was constructed using the training set. This model was able to separate Arbequina, Borriolenca and Canetera categories among them, being also well resolved from the other four categories (Farga, Hojiblanca, Picual and Serrana), which overlapped (data not shown). To solve this overlapping problem, a new LDA model was constructed by grouping the categories that overlapped into a single one. In this case, an excellent resolution between Arbequina, Borriolenca, Canetera and the category formed by grouping Farga, Hojiblanca, Picual and Serrana categories was obtained (Fig. 7.12, $\lambda_w = 0.319$). The variables selected by the SPSS stepwise algorithm, and the corresponding model standardized coefficients, are given in Table 7.12. For this model, and using leave-one-out cross-validation, all the points of the training set were correctly classified. When the evaluation set was used to check the prediction capability of the model, only three objects corresponding to replicates of different samples (1 Arbequina, 1 Borriolenca and 1 Canetera) were not correctly assigned using a 95 % probability; thus, the prediction capability was higher than 97 %.

Next, the Arbequina, Borriolenca and Canetera categories were removed from the training set, and the remaining categories (Farga, Hojiblanca, Picual and

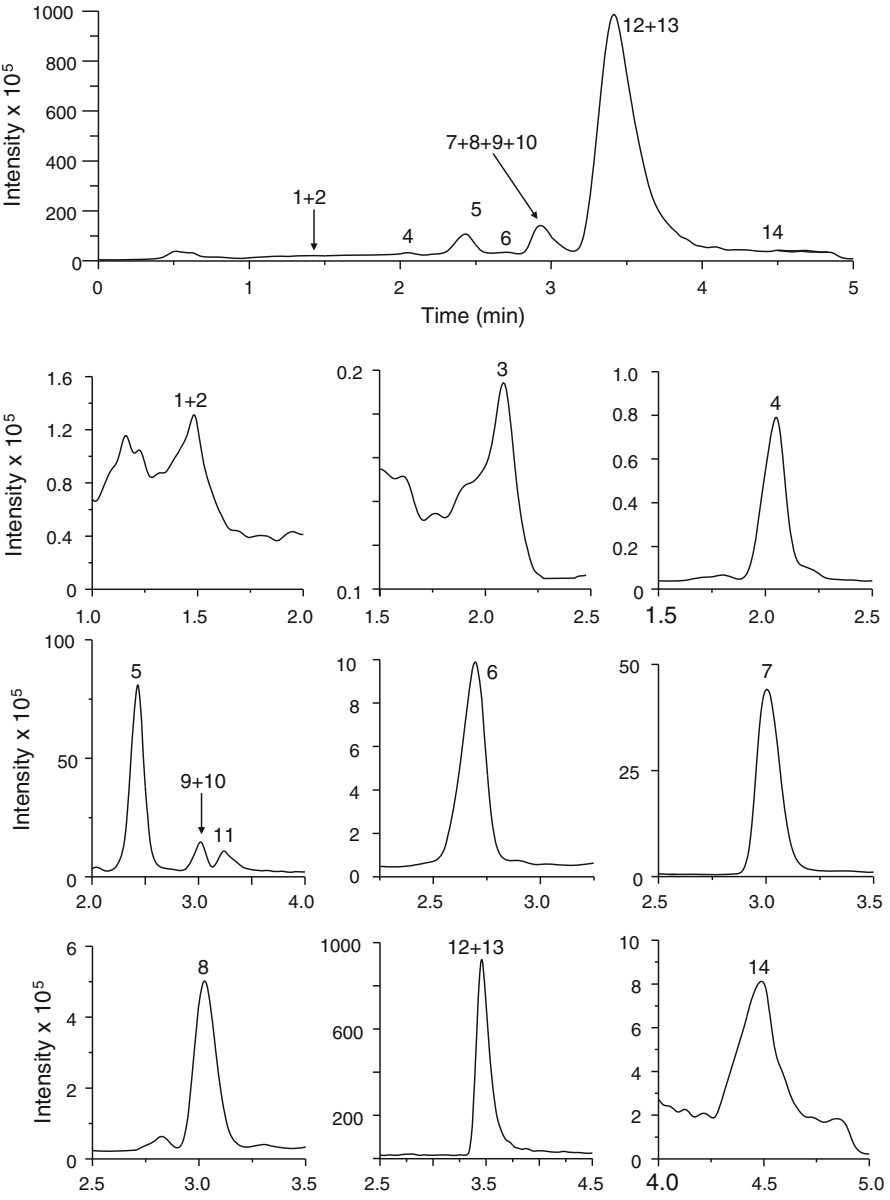

Fig. 7.10 TIC and SIR chromatograms of a Borriolenca EVOO extract. Chromatographic conditions: linear gradient from 80 to 100 % ACN for 0.5 min, followed by isocratic elution with 100 % ACN for 4.5 more min; flow rate, 0.8 mL min^{-1}; column temperature, 10 °C. Peak identification as indicated in Table 4.15 (Reprinted from Lerma-García et al. (2011). Copyright 2010 Elsevier Ltd)

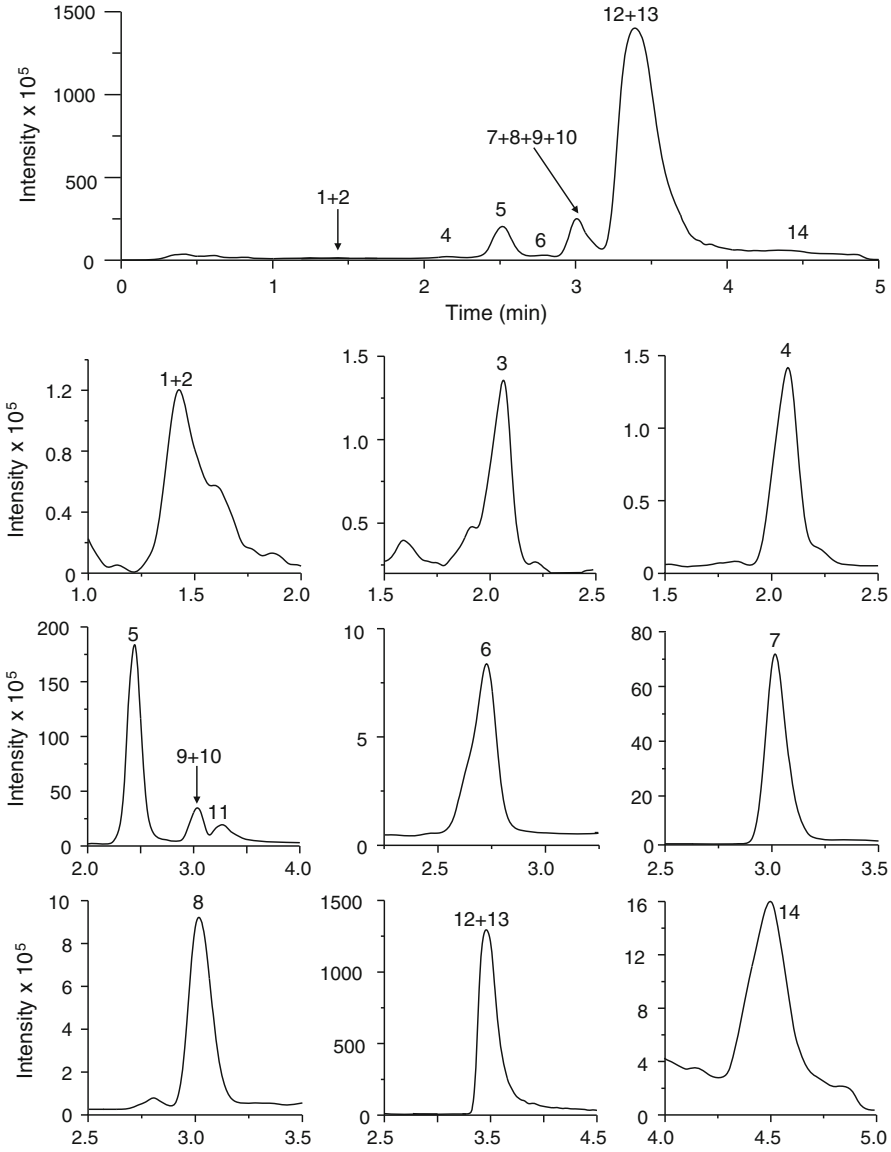

Fig. 7.11 TIC and SIR chromatograms of a Farga EVOO extract. Other experimental conditions as in Fig. 7.10 (Reprinted from Lerma-García et al. (2011). Copyright 2010 Elsevier Ltd)

Serrana) were used to construct another LDA model. In this case, all category pairs were resolved with an excellent resolution (Fig. 7.13, $\lambda_w = 0.368$). The variables selected and the corresponding model standardized coefficients are also given in Table 7.11. For this model, and using leave-one-out cross-validation, all the points

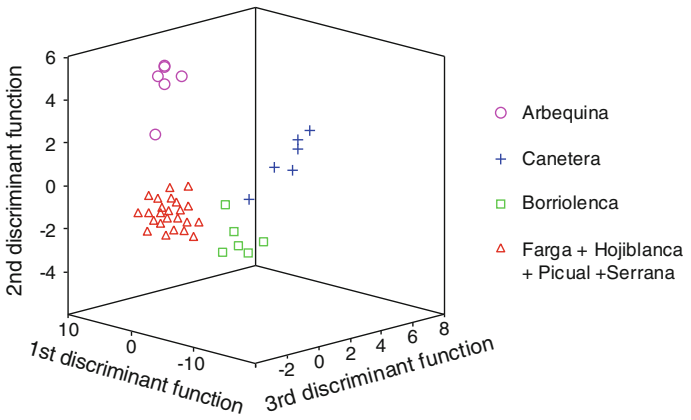

Fig. 7.12 Score plot on an oblique plane of the 3-D space defined by the three discriminant functions of the LDA model constructed to resolve the arbequina, borriolenca, canetera and farga + hojiblanca + picual + serrana categories (Reprinted from Lerma-García et al. (2011). Copyright 2010 Elsevier Ltd)

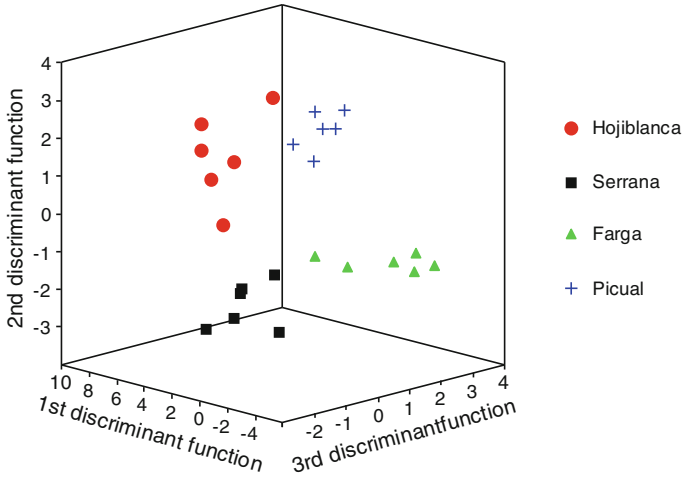

Fig. 7.13 Score plot on an oblique plane of the 3-D space defined by the three discriminant functions of the LDA model constructed to resolve the Farga, Hojiblanca, Picual and Serrana categories (Reprinted from Lerma-García et al. (2011). Copyright 2010 Elsevier Ltd)

of the training set were correctly classified. Moreover, when the evaluation set (which was now constituted by 72 original data points) was used to check the prediction capability of the model, only 1 object, which corresponded to a replicate of a Picual sample, was not correctly assigned using a 95 % probability; thus, the prediction capability was in this case higher than 98 %.

Table 7.11 Predictors selected and the corresponding standardized coefficients of the two sequential LDA models constructed to predict the genetic variety of EVOOs (Reprinted from Lerma-García et al. (2011). Copyright 2010 Elsevier Ltd)

	Arbequina/borriolenca/canetera/ farga + hojiblanca + picual + serrana			Farga/hojiblanca/picual/ serrana		
Predictor[a]	f_1	f_2	f_3	f_1	f_2	f_3
(1 + 2)/3	0.06	1.09	0.46	0.20	−0.74	-0.91
(1 + 2)/4	–	–	–	1.37	−1.22	2.45
(1 + 2)/5	–	–	–	−2.37	2.71	−0.25
(1 + 2)/6	–	–	–	−2.65	0.06	0.82
(1 + 2)/7	–	–	–	0.79	1.42	11.66
(1 + 2)/8	–	–	–	−8.55	3.04	−11.12
(1 + 2)/(9 + 10)	–	–	–	1.62	−1.36	−4.23
(1 + 2)/11	–	–	–	−0.96	10.60	4.14
(1 + 2)/(12 + 13)	–	–	–	10.21	−13.67	−0.60
(1 + 2)/14	–	–	–	−2.60	−0.43	−2.20
¾	2.36	−1.26	1.07	9.50	0.81	2.88
3/6	3.77	−0.39	3.38	–	–	–
3/7	9.57	0.83	1.17	−9.32	−0.83	−3.33
3/11	-21.37	3.31	−5.92	–	–	–
3/14	6.40	−2.06	1.02	–	–	–
4/7	–	–	–	4.72	1.66	1.45
4/(9 + 10)	1.56	0.85	0.13	–	–	–
4/(12 + 13)	−3.66	−1.25	1.27	–	–	–
5/6	1.39	0.21	−1.45	–	–	–
(9 + 10)/11	1.64	1.06	0.65	–	–	–

[a] *m/z* values of the ratios of sterol peaks labelled as in Table 4.15

Table 7.12 Proportions[a] of sterols found in the total sterol fraction of EVOOs of different genetic varieties (Adapted from Lerma-García et al. (2011). Copyright 2010 Elsevier Ltd)

Sterol	Arbequina	Borriolenca	Canetera	Farga	Picual	Serrana
Erythrodiol + Uvaol	0.1–0.3	0.0–0.13	1.9–4.2	0.05–0.3	0.2–0.7	5.0–6.1
Ergosterol	0.01–0.05	0.01–0.02	0.0–0.08	0.03–0.09	0.01–0.02	0.0–0.02
Brassicasterol	0.05–0.10	0.05–0.09	0.05–0.10	0.08–0.10	0.08–0.11	0.08–0.11
Δ^5-Avenasterol	11.1–14.1	7.3–9.1	11.9–12.7	8.0–10.9	4.0–12.2	5.3–6.9
Cholesterol	0.2–0.5	0.3–0.6	0.1–0.2	0.2–0.6	0.3–0.5	0.2–0.4
Campesterol	3.9–4.5	3.2–4.7	3.2–3.8	3.6–4.7	2.7–3.3	2.1–3.0
Campestanol	0.1–0.4	0.3–0.5	0.4–1.0	0.3–0.7	0.2–0.3	0.2–0.5
Stigmasterol + clerosterol	0.9–1.3	1.6–2.7	1.6–1.9	1.2–1.9	1.0–1.4	1.0–2.4
$\Delta^{5,24}$-Stigmastadienol	0.8–1.9	0.5–1.0	3.2–3.8	0.8–2.0	0.8–1.5	1.0–1.6
β-Sitosterol + Δ^7-Stigmastenol	77–82	79.3–83.5	76.0–77.6	77.1–91.1	77.9–91.0	80.8–82.1
Sitostanol	0.5–0.9	0.6–0.8	0.5–1.2	0.9–1.1	0.5–2.5	0.8–1.6

[a] The range values were obtained from the mean value of the three replicates of each sample belonging to each genetic variety

7.4.2 Determination of Sterols in Real Samples

The sterol content present in the EVOO samples of different genetic varieties was also established in this work. For this purpose, the external calibration curves described in Sect. 4.5.2 were used. As explain in this section, and in order to quantify the sterols which were not available as standards, the calibration curves of lanosterol and β-sitosterol were used. The percentages of sterols, calculated as explained in Sect. 4.5.2, are shown in Table 7.12. As it can be observed, the most abundant sterol for all vegetable oils was β-sitosterol. Among the differences between the different genetic varieties that could be evidenced from Table 7.12, it could be highlighted that Canetera and Serrana oils showed larger quantities of erythrodiol and uvaol than the other genetic varieties, and that the highest contents of Δ^5-avenasterol were found in Arbequina variety, followed by the Canetera one (which was also characterized by the highest content of $\Delta^{5,24}$-stigmastadienol).

References

Cañabate-Díaz B, Segura Carretero A, Fernández-Gutiérrez A, Belmonte Vega A, Garrido Frenich A, Martínez Vidal JL, Duran Martos J (2007). Food Chem 102:593

Concha-Herrera V, Lerma-García MJ, Herrero-Martínez JM, Simó-Alfonso EF (2009) J Agric Food Chem 57:9985. Copyright 2009 American Chemical Society

Guillén MD, Cabo N (1998) J Agric Food Chem 46:1788

Jee M (2002) Oils and fat authentication. Blackwell Publishing, CRC Press, Boca Raton

Lerma-García MJ, Herrero-Martínez JM, Ramis-Ramos G, Simó-Alfonso EF (2008a) Food Chem 108:1142. Copyright 2007 Elsevier Ltd

Lerma-García MJ, Ramis-Ramos G, Herrero-Martínez JM, Simó-Alfonso EF (2008b) Rapid Commun Mass Spectrom 22:973

Lerma-García MJ, Concha-Herrera V, Herrero-Martínez JM, Simó-Alfonso EF (2009) J Agric Food Chem 57:10512. Copyright 2009 American Chemical Society

Lerma-García MJ, Simó-Alfonso EF, Méndez A, Lliberia JL, Herrero-Martínez JM (2011) Food Res Int 44:103. Copyright 2010 Elsevier Ltd

Martínez-Vidal JL, Garrido-Frenich A, Escobar-García MA, Romero-González R (2007) Chromatographia 65:695

Ríos JJ, Gil MJ, Gutiérrez-Rosales F (2005) J Chromatogr. A 1903:167

Sánchez-Machado DI, López-Hernández J, Paseiro-Losada P, López-Cervantes J (2004) Biomed Chromatogr 18(3):183–190

Segura-Carretero A, Carrasco-Pancorbo A, Cortacero S, Gori A, Cerretani L, Fernández-Gutiérrez A (2008). Eur J Lipid Sci Technol 110:1142

Silverstein RM, Bassler GC, Morrill TC (1981) Spectrometric identification of organic compounds. Wiley, Chichester

Tripoli E, Giammanco M, Tabacchi G, Di Majo D, Giammanco S, La Guardia M (2005) Nutr Res Rev 18:98

Yang H, Irudayaraj J, Paradkar MM (2005) Food Chem 93:25

Chapter 8
Development of Methods for the Classification of EVOOs According to Their Geographical Origin

8.1 Classification Using Phenolic Compound Profiles Obtained by CEC[1]

The aim of this work was to obtain the phenolic profiles of EVOOs by using a CEC method, and to evaluate the use of these profiles in the prediction of the geographical origin of these EVOO samples. For this purpose, monolithic columns containing LA and BDDA monomers were constructed. The EVOO samples employed in this study are summarized in Table 8.1. The oils employed in this study were collected from different cultivars at different degrees of ripening. Moreover, they also differ in the area of growth, production system and storage time.

8.1.1 Construction of the Monolithic Columns and Optimization of the Separation Conditions

Photo-polymerized LA-based monoliths were prepared by adapting the experimental conditions of a previous work, in which monoliths were chemically polymerized using LPO (Cantó-Mirapeix et al. 2009). The first polymerization mixture tried contained 40 wt % monomers (69.8 wt % LA, 29.9 wt % BDDA and 0.3 wt % META) and 60 wt % porogens (17 wt % 1, 4-butanediol and 83 wt % 1-propanol) with wt % LPO as initiator. A 30:70 (v/v) ACN-water mixture containing 5 mM formic acid at pH 3.0 was firstly used as mobile phase (Aturki et al. 2008). However, when this monolith was tried (10 wt % 1, 4-butanediol in the polymerization mixture), the column exhibited poor permeability, leading to blockage

[1] Parts of the text of this section have been adapted with permission from Lerma-García et al. (2009). Copyright 2009 Elsevier Ltd

M. J. Lerma García, *Characterization and Authentication of Olive and Other Vegetable Oils*, Springer Theses, DOI: 10.1007/978-3-642-31418-6_8,

Table 8.1 Geographical origin, number of samples, genetic variety and suppliers of the EVOOs (Reprinted from Lerma-García et al. (2009). Copyright 2009 Elsevier Ltd)

Geographical origin	N° of samples	Genetic variety	Supplier
Croatia	1	Mastrinka	OLEA
	1	Lastovka	OLEA
	1	Drobnica	OLEA
	3	Oblica	OLEA
	4	Varietal blend	OLEA SMS d.o.o Zvijezda
Italy	1	Brugnola	OLEA
	1	Ascolana Tenera	OLEA
	1	Correggiolo	OLEA
	1	Raggia	OLEA
	1	Frantoio	OLEA
	1	Brisighella	OLEA
	1	Nocellara	OLEA
	1	Ogliarola	OLEA
	1	Ghiacciola	OLEA
	1	Coratina	OLEA
Spain	1	Serrana	Intercoop
	1	Blanquilla	Intercoop
	1	Canetera	Intercoop
	1	Borriolenca	Intercoop
	1	Farga	Intercoop
	2	Hojiblanca	Coosur Carbonell
	2	Arbequina	Carbonell Olearum
	1	Picual	Castillo de Taberna

problems. This fact could be confirmed by the SEM picture (Fig. 8.1a), where small pores and globule sizes were clearly observed.

Then, in order to solve this problem, new polymerization mixtures containing higher contents of 1, 4-butanediol, which ranged between 12 and 18 wt %, were next prepared. When a 12 wt % 1, 4-butanediol was used, larger globules (see Fig. 8.1b) and thus a better permeability were obtained in comparison to those previously obtained by the column constructed with 10 wt % 1, 4-butanediol. However, the 12 wt % column showed a tendency to get blocked when attempting to analyze oil samples. Thus, to solve this problem, 1, 4-butanediol in the polymerization mixture was increased up to 15 wt %. In this case, higher globule sizes where obtained (see Fig. 8.1c), which provided the column with a satisfactory permeability. However, when a phenolic extract (Serrana EVOO variety) was injected in this column, a poor resolution between phenolic compound peaks was obtained (Fig. 8.2a). Then, mobile phase composition was varied to overcome this lack of resolution. The results obtained are shown in Fig. 8.2b–d. As it can be observed in this figure, resolution clearly improved when the ACN content was decreased from 20 to 15 %. However, a decrease in efficiency, an increase in analysis time and a drift in the baseline were observed

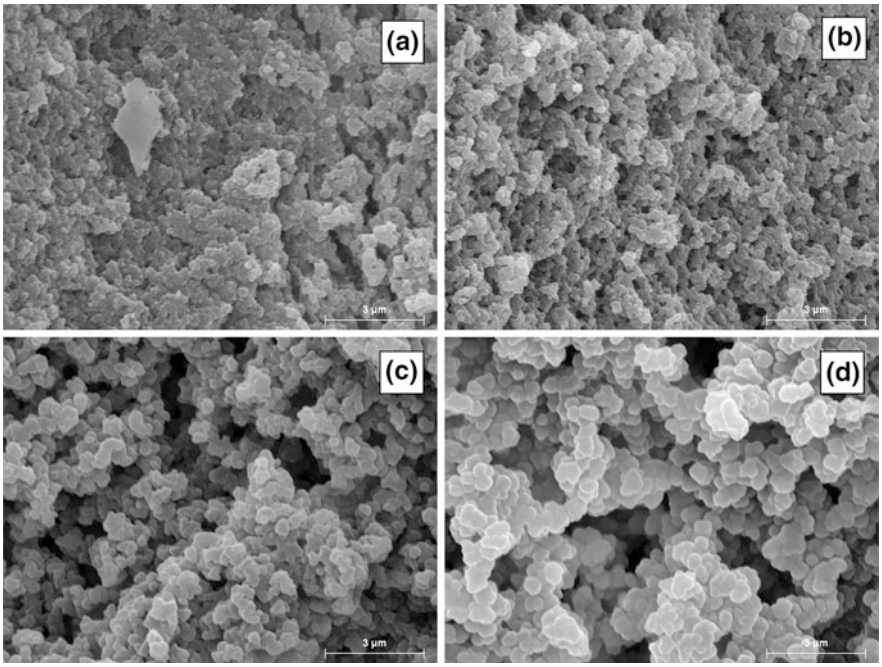

Fig. 8.1 SEM micrographs of LA-based monolithic columns prepared with **a** 10 wt %, **b** 12 wt %, **c** 15 wt % and **d** 18 wt % 1, 4-butanediol in the polymerization mixture. The bar lengths stand for 3 μm (Reprinted from Lerma-García et al. (2009). Copyright 2009 Elsevier Ltd)

when ACN content was decreased to 10 % (Fig. 8.2d). Thus, a mobile phase containing a mixture of 15:85 (v/v) ACN-aqueous buffer of 5 mM formic acid at pH 3.0 was selected as the best compromise between resolution and analysis time (less than 25 min).

Next, using this mobile phase, and to reduce analysis time, a column with 18 wt % 1, 4-butanediol was constructed. With this column, both peak resolution and efficiency decreased (data not shown), which could be attributed to the larger globules (Fig. 8.1d) of this monolithic bed compared with those obtained with a 15 wt % 1, 4-butanediol monolith. Small changes in mobile phase did not lead to a significant separation improvement. Thus, a column prepared with 15 wt % 1, 4-butanediol in the polymerization mixture was selected for the following studies.

8.1.2 Characterization of the Phenolic Compound Profiles

EVOO samples were next analyzed using the optimal conditions. Representative electrochromatograms of EVOO from Croatia (A), Italy (B) and Spain (C, D) are shown in Fig. 8.3. As it can be observed, a total of 17 common peaks were

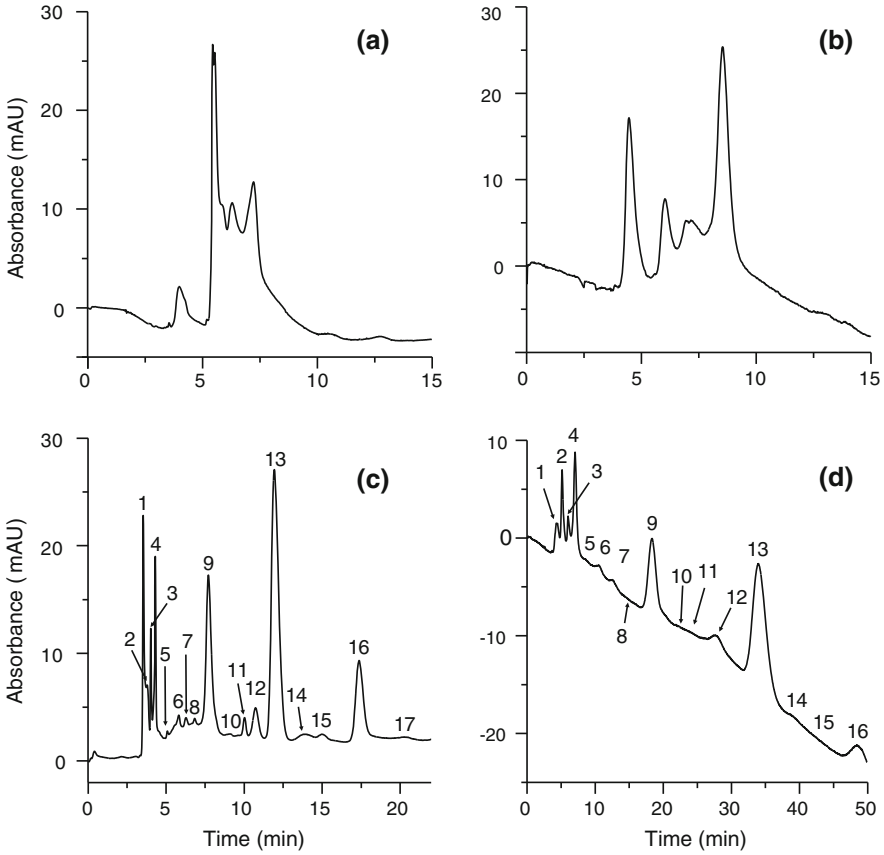

Fig. 8.2 Influence of the mobile phase composition on the separation of phenolic compounds: **a** 30:70, **b** 20:80, **c** 15:85 and **d** 10:90 (v/v) ACN-water mixtures containing 5 mM formic acid at pH 3.0. CEC conditions: LA-based monolithic column prepared with 15 wt % 1, 4-butanediol in the polymerization mixture; electrokinetic injection, −20 kV for 3 s; separation voltage, −10 kV; wavelength detection: 280 nm. The 17 peaks labeled were selected as variables (Reprinted from Lerma-García et al. (2009). Copyright 2009 Elsevier Ltd)

obtained in all cases in less than 25 min. These peaks, which correspond to different phenolic compounds, were related to the genetic variety and geographical origin of the EVOOs, as previously stated by other authors (Brenes et al. 2002; Carrasco-Pancorbo et al. 2006). However, the phenolic compound profiles of EVOOs coming from the same geographical origin (C and D) were closely similar. Thus, the little differences observed between EVOO fingerprints will be enhanced by treating data with chemometric tools.

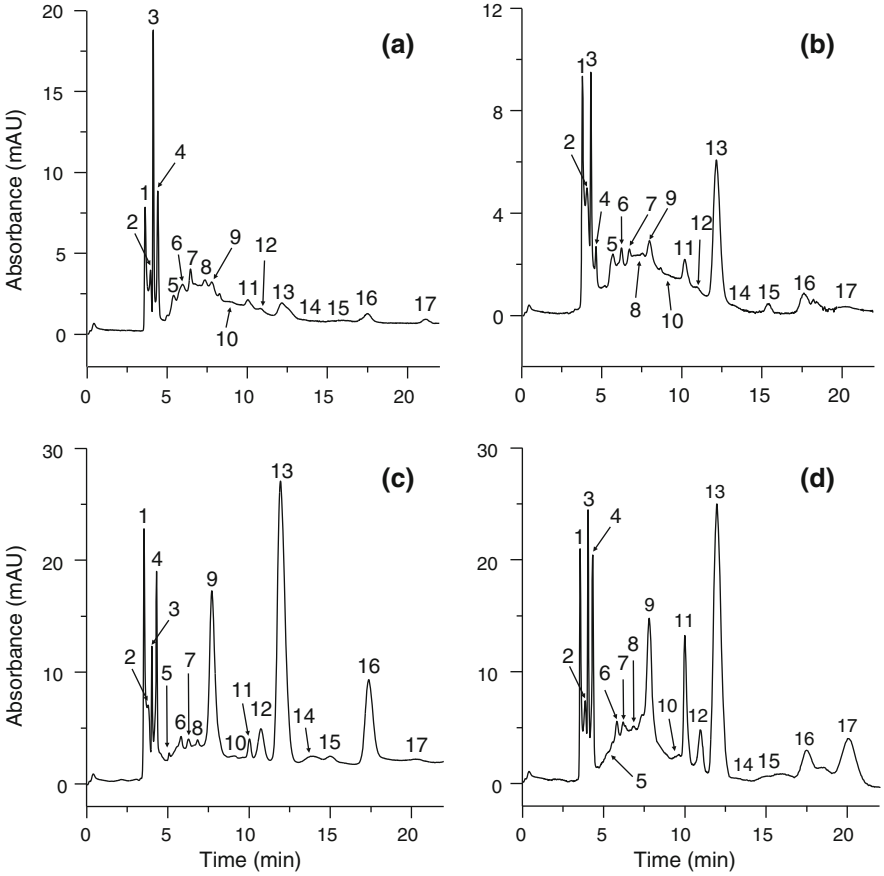

Fig. 8.3 Electrochromatograms of EVOOs from **a** Croatia (Lavstoska), **b** Italy (Frantoio), **c** Spain (Serrana) and **d** Spain (Arbequina) obtained on an LA-based monolithic capillary column under the optimal conditions. CEC conditions: Mobile phase: 15:85 (v/v) ACN-water containing 5 mM formic acid at pH 3.0. Other experimental conditions as in Fig. 8.2 (Reprinted from Lerma-García et al. (2009). Copyright 2009 Elsevier Ltd)

8.1.3 Construction of Data Matrices and LDA Models

The 17 original variables, which corresponded to the 17 peaks labelled in the Fig. 8.3, were processed according to normalization procedure B. A total of 136 predictors were obtained. Then, using these normalized variables and the 30 samples of Table 8.1, a matrix containing 60 injections (all samples were injected by duplicate), as well as the 136 predictors, was constructed and used as evaluation set. A matrix containing the means of sample replicates (30 objects) was that used

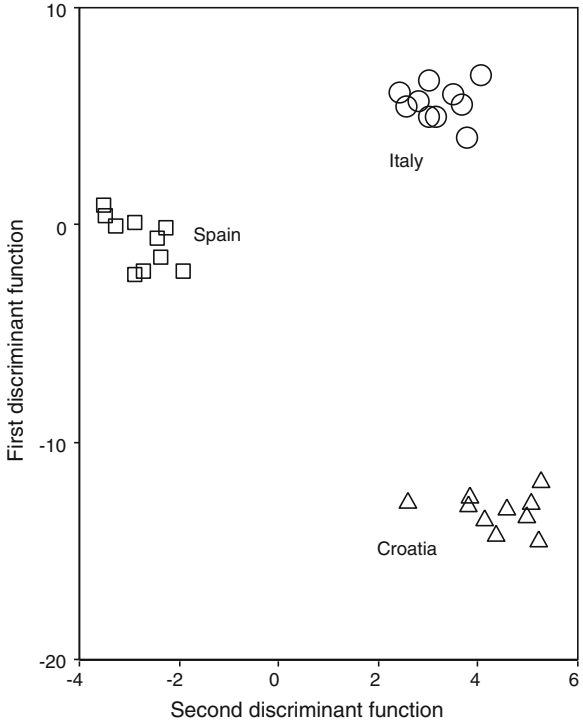

Fig. 8.4 Score plot on the plane of the two LDA discriminant functions obtained to predict the geographical origin of EVOOs (Reprinted from Lerma-García et al. (2009). Copyright 2009 Elsevier Ltd)

Table 8.2 Predictors selected and their corresponding standardized coefficients of the LDA model constructed to predict the geographical origin of the EVOOs (Reprinted from Lerma-García et al. (2009). Copyright 2009 Elsevier Ltd)

Predictor[a]	f_1	f_2
1/4	3.50	1.91
1/15	-4.51	1.37
2/15	8.02	-2.43
7/13	2.22	2.71
7/14	1.64	-1.04
10/13	-0.97	-1.55
11/17	0.98	1.09
12/14	-4.25	2.19
12/17	-2.90	-2.06
15/17	2.04	1.04

[a] Pairs of peak areas identified according to labels in Fig. 8.3

as training set. A response column, which contains the three categories that corresponded to the three EVOO geographical origins, was added to both training and evaluation matrices.

When the LDA model was constructed (using the probability values of $F_{in} = 0.01$ and $F_{out} = 0.10$), an excellent resolution ($\lambda_w = 0.09$) between the three categories was obtained (see Fig. 8.4). The variables selected by the SPSS stepwise algorithm and the corresponding standardized coefficients of this LDA model are shown in Table 8.2. When leave-one-out validation was applied, all the objects of the training set were correctly classified. Concerning the prediction capability of the model, and using a 95 % probability, all the objects of the evaluation set (which contained the 60 original data points) were correctly assigned; thus, the prediction capability was 100 %.

Finally, a validation with blind samples was also performed. For this purpose, a new LDA model constructed with 24 objects (8 samples × 3 geographical origins), which were randomly selected, was constructed. The predictors selected by this model were mainly the same than those selected in the previous model although the values of the coefficients obtained were slightly different. When the prediction capability was evaluated with the new evaluation set (composed by the means of the duplicates of the remaining 6 samples), all the samples were correctly classified with a probability higher than 95 %.

References

Aturki Z, Fanali S, D′Orazio G, Rocco A, Rosati C (2008) Electrophoresis 29:1643

Brenes M, García A, Rios JJ, García P, Garrido A (2002) Int J Food Sci Technol 37:615

Cantó-Mirapeix A, Herrero-Martínez JM, Mongay-Fernández C, Simó-Alfonso EF (2009) Electrophoresis 30:599

Carrasco-Pancorbo A, Gómez-Caravaca AM, Cerretani L, Bendini A, Segura-Carretero A, Fernández-Gutiérrez A (2006) J Agric Food Chem 54:7984

Lerma-García MJ, Lantano C, Chiavaro E, Cerretani L, Herrero-Martínez JM, Simó-Alfonso EF (2009) Food Res Int 42:1446. Copyright 2009 Elsevier Ltd

Chapter 9
Development of Methods for the Evaluation of Olive Oil Oxidation

9.1 Study of Chemical Changes Produced in VOOs with Different Phenolic Content During an Accelerated Ageing Treatment[1]

In this work, the chemical changes produced in an EVOO sample, both in the presence and absence of its phenolic fraction during an accelerated ageing treatment have been studied. The changes produced in phenolic compound concentrations, jointly with the changes observed in free acidity, peroxide value, UV absorbance, fatty acid composition, OSI and T content, were monitored. In addition, transformation of phenolic compounds during the accelerated ageing treatment in EVOO samples with phenolic fraction was also studied. For this purpose, an EVOO sample, which was obtained using olives picked on October 2008 at San Marino from the Brugnola genetic variety, was used. EVOO oxidation was evaluated on two aliquots of this oil sample: EVOO with phenols (EV1) and EVOO without phenols (EV2). This latter was obtained by removing the phenolic compounds as indicated in Sect. 3.3.6. The accelerated ageing treatment was performed as follows (Bendini et al. 2006; Bonoli-Carbognin et al. 2008; Lerma-García et al. 2009a): both samples, EV1 and EV2, were divided in eight aliquots each, stored in glass bottles and kept in the dark at 60 °C for 7 weeks. Two bottles, one of EV1 and the other of EV2, were removed every week from the oven and stored at −20 °C (samples t_0–t_7). Triplicate analyses were carried out in at each storage time on both EV1 and EV2 samples.

[1] Parts of the text of this section have been adapted with permission from Lerma-García MJ et al. (2009c). Copyright 2009 American Chemical Society.

M. J. Lerma García, *Characterization and Authentication of Olive and Other Vegetable Oils*, Springer Theses, DOI: 10.1007/978-3-642-31418-6_9,

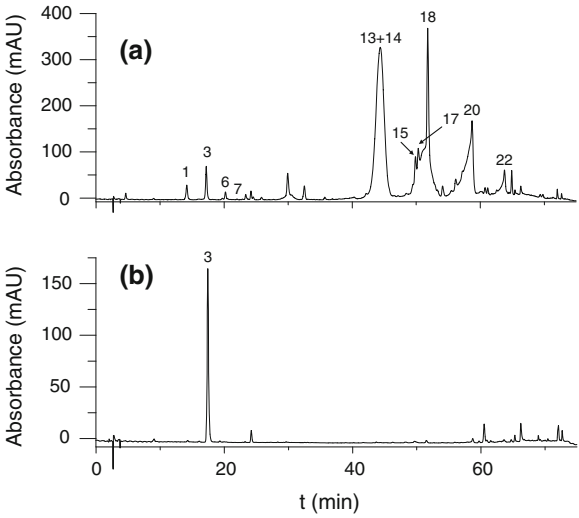

Fig. 9.1 UV-chromatograms of **a** EV1 and **b** EV2 samples at t_0. Peak identification: 1, HYTY; 3, 3,4-DHPAA; 6, Unk; 7, Unk; 13, OxDOA; 14, DOA; 15, OxDLA; 17, DLA; 18, AcPIN; 20, OA and 22, LAg. Detection wavelength: 280 nm (Reprinted with permission from Lerma-García et al. (2009c). Copyright 2009 American Chemical Society)

9.1.1 Evaluation of the Phenolic Content

In first place, both EV1 and EV2 phenolic fractions were analyzed to verify the efficiency of phenolic compound elimination in EV2. The quantification of the different phenolic compounds was performed by constructing calibration curves of 3, 4-DHPAA for the compounds detected at 280 nm ($r = 0.999$) and at 240 nm ($r = 0.998$), whereas the compounds detected at 330 nm were quantified by calibrations curves of API ($r = 0.995$) and LUT ($r = 0.988$). The efficiency of the process was verified when a concentration of 164 mg kg^{-1} oil was obtained in the EV1 sample at zero storage time (t_0), being the concentration of the phenolic compounds in EV2 sample of 0.70 mg kg^{-1} oil at the same storage time. These concentration values were obtained by considering the sum of all quantified phenolic compounds (a total of 22 individual phenols). Thus, phenol content decreased a 99.6 %, as observed in Fig. 9.1. A similar extraction yield was reported by Bonoli-Carbognin et al. (2008) using the same extraction procedure.

The differences produced in the free acidity, peroxide value and fatty acid composition of the EV1 and EV2 samples at t_0 are reported in Table 9.1. As observed in this table, the values of the free acidity percentage were 0.24 and 0.18 % for EV1 and EV2, respectively, being the peroxide values varied between 11.96 and 12.44 meq O_2 kg^{-1} oil. All these values were within the limits set by the EC Regulation for EVOO (Commission Regulation (EC) No. 1989/2003). Regarding fatty acid composition, both samples showed very similar values, which demonstrated that the phenol-removing procedure did not affect this fraction. The high oleic content of both samples was reported to largely contribute to the oxidative stability of EVOOs (Aparicio et al. 1999).

Table 9.1 Chemical parameters of the EV1 and EV2 samples at t_0 (Adapted with permission from Lerma-García et al. (2009c). Copyright 2009 American Chemical Society)

Parameter	EV1	EV2
Free acidity (%)	0.24	0.18
PV[a] (meq O_2 kg^{-1})	11.96	12.44
Myristic acid (%)	0.01	0.01
Palmitic acid (%)	13.07	13.10
Palmitoleic acid (%)	0.60	0.60
Stearic acid (%)	2.46	2.46
Oleic acid (%)	72.88	72.83
Linoleic acid (%)	9.26	9.28
Linolenic acid (%)	0.41	0.41

[a] PV = peroxide value

Next, the changes producing during storage in the oxidative status of EV1 and EV2 samples were studied by measuring the absortivity of the conjugated dienes (k_{232}) and trienes (k_{270}), the OSI time and by establishing T content. Ts were quantified by constructing calibration curves of standard solutions of α-T ($r = 0.999$) after their determination by HPLC-UV-Vis after a dilution of 1 g oil in 10 mL *n*-hexane. The results obtained are shown in Table 9.2.

The k_{232} and k_{270} values for both samples at t_0 were lower than 2.50 and 0.22, respectively, which were the legal limits established by the EC Regulation for EVOO category (Commission Regulation (EC) No. 1989/2003). However, the legal limit for k_{232} was surpassed by both samples after only 1 week of storage (t_1). Regarding k_{270}, only the EV1 sample exceeded the EC limit at t_1, although 1 week later (t_2), EV2 also surpassed this value. These trends were also found by Bendini et al. under similar experimental conditions (Bendini et al. 2006).

Regarding OSI time, the EV2 sample at t_0 showed a lower value than the EV1 sample, which was probably due to the different amounts of phenolic compounds present in these samples. In fact, EV2 showed a reduction of the OSI time to one-third of its initial value (from 33.7 to 10.8 h). The EV2 OSI value of 10.8 h could be only attributed to the high oleic acid content and to the low amounts of polyunsaturated fatty acids (Aparicio et al. 1999). Both EV1 and EV2 samples showed a significant decrease of OSI time during the ageing process, being faster for EV2 (in fact after 4 weeks the OSI time was 100 % reduced), which confirmed the role of the phenolic fraction against the oxidative stability of EV1.

With regard to T content, it was quite similar for both EV1 and EV2 samples at t_0. This fact demonstrated that the alkaline procedure used to wash polar phenols did not affect T fraction. This content remained substantially unvaried for EV1 from t_0 to t_3; then, a strong decrease was observed until the end of the storage time. The constant loss of oxidative stability (Table 9.2) is probably related to the decrease of polar phenols, which during the first 3 weeks, may act as antioxidant molecules also protecting Ts against oxidation (Baldioli et al. 1996; Bendini et al. 2006). On the other hand, Ts started to decrease after 2 weeks of storage for EV2; however, an oscillating trend was evidenced at higher storage times. This trend

Table 9.2 Chemical parameters for EV1 and EV2 samples at different storage times[a] (Reprinted with permission from Lerma-García et al. (2009c). Copyright 2009 American Chemical Society)

Storage time, t_i (weeks)	k_{232}		k_{270}		OSI time (h)		Ts (mg kg^{-1})	
	EV1	EV2	EV1	EV2	EV1	EV2	EV1	EV2
0	2.24 f	2.45 d	0.19 g*	0.16 f	33.65 a*	10.8 a	181.9 a	148.4 a
1	3.51 e	3.67 cd	0.24 f*	0.17 f	22.23 b*	9.03 b	191.1 a	170.6 a
2	4.52 d	5.43 bc	0.26 f	0.23 ef	19.20 c*	6.2 c	195.5 a*	140.8 a
3	5.42 c	6.43 b*	0.34 e	0.29 e	15.78 d*	3.8 d	181.9 a*	90.6 b
4	7.48 b	8.41 a	0.40 d	0.39 d	10.55 e*	1.3 e	139.6 b*	42.0 c
5	9.69 a*	8.48 a	0.51 c	0.47 c	7.28 f*	0 f	85.4 c*	46.9 c
6	7.48 b	8.93 a	0.59 b	0.59 b	5.83 g*	0 f	55.3 d	70.3 bc*
7	7.71 b	9.74 a*	0.68 a	0.67 a	3.43 h*	0 f	25.9 e	97.2 b*

[a] Mean values ($n = 3$). Means with different letters within the same column were significantly different ($p < 0.05$). Means with an asterisk for the same parameter and at a given storage time were significantly different ($p < 0.05$)

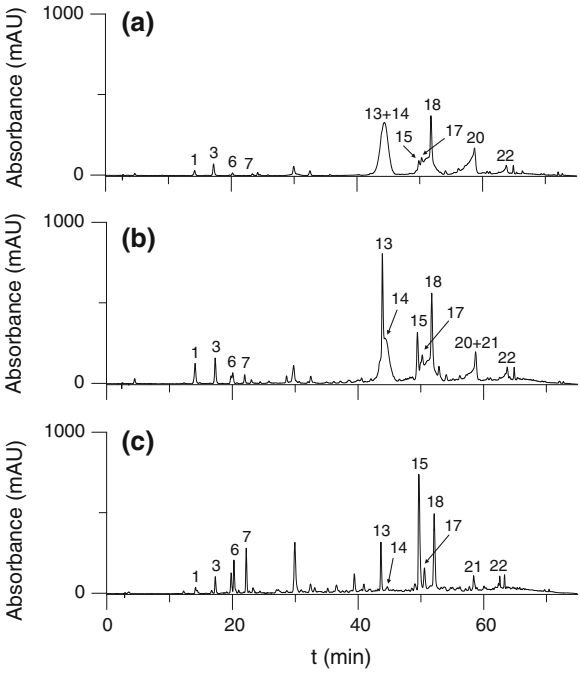

Fig. 9.2 Chromatograms showing the evolution of the EV1 phenolic profile after ageing treatment at 60 °C: **a** t_0, **b** t_3 and **c** t_7. Peak identification: 21, OxLAg; other peaks as in Fig. 9.1. Detection wavelength: 280 nm (Reprinted with permission from Lerma-García et al. (2009c). Copyright 2009 American Chemical Society)

could be explained taking into account a synergic effect between α-T and phospholipids (Bandarra et al. 1999), and the formation of T oxidized derivatives. These latter compounds could overlap with T peaks during HPLC elution, interfering in T determination.

9.1.2 Phenolic Compound Transformation in EV1 Samples During the Accelerated Ageing Treatment

The UV-chromatograms obtained at 280, 240 and 330 nm showing 22 phenolic compounds at three storage times (t_0, t_3 and t_7) are shown in Figs. 9.2, 9.3 and 9.4. A decrease in the content of DOA (peak 14), DLA (peak 17) and LAg (peak 22) when the storage time was increased was evidenced at 280 nm (Fig. 9.2), jointly with the disappearance of OA (peak 20) and the formation of their possible oxidized derivatives (peaks 13, 15, 21 and traces of OxOA). On the other hand, the changes produced in the content of EA (peak 12) and the appearances of several hypothetical oxidized compounds that absorb only at 240 nm (4, 9, 10 and 11) are evidenced in Fig. 9.3. Finally, Fig. 9.4 evidences the trend of the loss of LUT (peak 16), and the slightly decreased of API (peak 19), during storage.

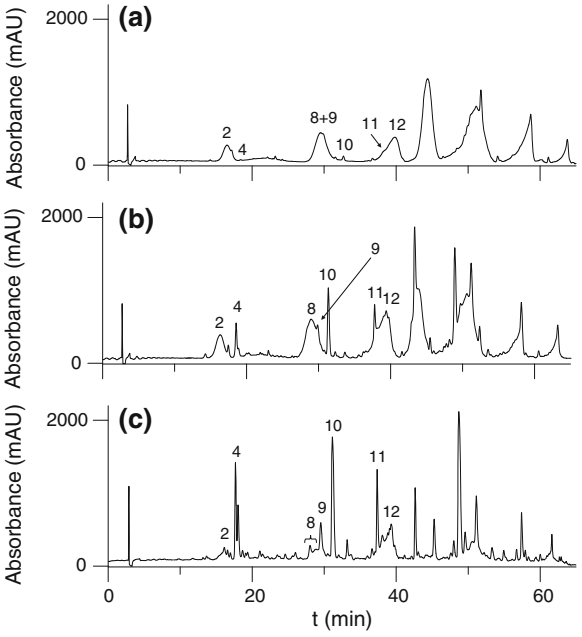

Fig. 9.3 Chromatograms showing the evolution of the EV1 phenolic profile after ageing treatment at 60°C: **a** t_0, **b** t_3 and **c** t_7. Peak identification: 2, DEA; 4, OxDEA; 8, 9 and 10, Unknown; 11, OxEA and 12, EA. Detection wavelength: 240 nm (Reprinted with permission from Lerma-García et al. (2009c). Copyright 2009 American Chemical Society)

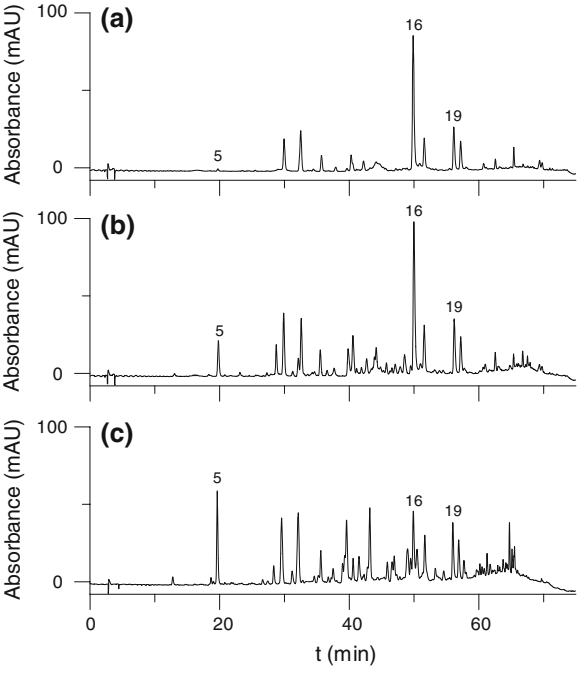

Fig. 9.4 Chromatograms showing the evolution of the EV1 phenolic profile after ageing treatment at 60°C: **a** t_0, **b** t_3 and **c** t_7. Peak identification: 5, Unknown; 16, LUT and 19, API. Detection wavelength: 330 nm (Reprinted with permission from Lerma-García et al. (2009c). Copyright 2009 American Chemical Society)

A list containing the 22 phenolic compounds studied in this work, jointly with their retention times, wavelengths of maxima UV absortivity, MW and MS fragmentation patterns are shown in Table 9.3.

From the results summarized in Table 9.3, it is possible to conclude that:

1. The absorbing band near to 240 nm is typical of a carboxymethyl enol-ether group. Thus, for example, EA (peak 12) is characterized by this band. On the other hand, the bands at 277 and 282 nm are due to a mono-hydroxyphenyl group and to an *ortho*-hydroxyphenyl group, respectively; thus, for example, HYTY (peak 1) and secoiridoid derivatives containing HYTY (OxDOA (peak 13), DOA (peak 14), OxOA (tr), OA (peak 20) and the peaks of unknown compounds 3, 6 and 7) exhibit a secondary UV maximum in the vicinity of 280 nm, whereas those molecules having an mono-hydroxyphenyl group such as TY (OxDLA (peak 15), DLA (peak 17), OxLAg (peak 21) and LAg (peak 22)) show a secondary maximum in the vicinity of 277 nm.
2. HYTY exhibits only an $[M + H\text{-}H_2O]^+$ ion. The presence of an initial high percentage of water inhibits a good electrospray ionization of molecules having acidic properties, such as HYTY and TY. As suggested by Rovellini et al. (2002), it is not possible to reveal the pseudo molecular ion for HYTY due to its difficulty to give protonated adducts.
3. Some authors (Ríos et al. 2005; Rovellini et al. 2002) have indicated that the oxidation of secoiridoid structures involves the acidic portion (EA) and not the aromatic alcoholic moiety (HYTY and TY); for this reason, the oxidized forms shown in Table 9.3 maintain the UV specific absorbance of their non oxidized forms.
4. The oxidation involves the conversion of the aldehydic group of EA to a carboxylic group (according to the scheme reported in Fig. 9.5).
5. The oxidized forms of secoiridoids, which are more polar than their respective non oxidized derivatives, elute before these latter. In the case of the couple DEA-OxDEA (peaks 2 and 4 peaks, respectively), the presence of a second carboxylic group in the molecule does not cause an anticipated elution.
6. Under the ESI conditions applied in this study, both the oxidized and non oxidized forms of secoiridoids are characterized by the presence of the sodium adduct $[M + Na]^+$, the loss of the phenolic group (*m/z* 241 and *m/z* 225 for the oxidized and non oxidized forms of secoiridoids, respectively; *m/z* 183 and *m/z* 167 for the oxidized and non oxidized forms of the decarboxymethyl structures of secoiridoids, respectively), and the loss of the acidic group (*m/z* 137 and *m/z* 121 for molecules having HYTY and TY, respectively). A general scheme of the evolution of secoiridoids during storage is shown in Fig. 9.5.
7. The peaks related to the oxidized forms of secoiridoids are narrower than those related to molecules having one or two aldehydic groups.

The evolution of the content of the main phenolic compounds during storage for the EV1 sample is shown in Fig. 9.6a. To correctly appreciated the disappearance of the phenolic compounds, all areas have been divided by the 3, 4-DHPAA area

Table 9.3 Retention times, wavelengths of maxima UV absortivity, MW and MS fragmentation patterns of the phenolic compounds (Reprinted with permission from Lerma-García et al. (2009c). Copyright 2009 American Chemical Soiety)

Analyte	Peak no.	t_R (rnin)	^max (mn)	MW	$[M + H]^+$	[M + Na]~	$[M\text{-}H_20 + H]$~	Loss of PG[b]	Loss of AG[C]	Other fragments
HYTY	1	11.6	232/280	154	–	–	137.1	–	–	–
DEA	2	16.8	230	184	185.1	207.1	–	–	–	–
Unk	3	18.0	232/280	260	–	283.2	–	–	–	299.0 $[M + K]^+$
OxDEA	4	18.5	236	200	–	223.1	–	–	–	123.1/165.0
Unknown	5	20.0	290/310	–	–	–	–	-	–	338.4/321.8/191.1/185.8
Unknown	6	20.1	232/280	–	–	–	–	–	–	177.0/235.1/668.1
Unknown	7	22.0	232/280	–	–	–	–	–	–	113.1/157.1/349.2
Unknown	8	29.5	234	–	–	–	–	–	–	297.1/239.1/221.1/181.1/165.1
Unknown	9	30.4	234	336	–	359.0	–	–	–	375.1 $[M + K]^+$
Unknown	10	36.1	240	–	–	–	–	–	–	237.1/197.1/165.1
OxEA	11	38.9	240	258	259.1	281.1	–	–	–	185.1/227.1/241.1 $[M\text{-}OH]^-$
EA	12	39.9	240	242	243.1	265.1	–	–	–	211.1 $[M\text{-}OCH_3]^-$
OxDOA	13	44.0	234/282	336	337.1	359.1	–	183.1	137.1	375.1 $[M + K]^+$
DOA	14	45.0	234/282	320	–	343.1	–	–	137.1	361.1
OxDLA	15	49.8	242/276	320	–	343.1	–	183.1	121.1	359.1 $[M + K]^+$
LUT	16	50.0	254/348	286	287.1	309.1	–	–	–	-
DLA	17	51.5	236/276	304	–	327.1	–	–	121.1	-
AcPIN	18	53.8	236/280	416	417.1	439.1	–	–	–	455.1 $[M + K]^+$/357 $[M\text{-}CH_3COOH + H]^+$/233 $[M\text{-}CH3COOH\text{-}phenylOCH_3 + H]^+$
API	19	56.1	268/338	270	271.1	–	–	–	–	–
OxOA	tr[a]	56.1	236/280	394	395.1	417.1	–	241.1	137.1	439.1
OA	20	58.7	236/282	378	379.1	401.1	–	225.1	137.1	419.1
OxLA	21	60.1	232/276	378	379.1	401.1	–	241.1	121.1	-
LA	22	63.9	230/276	362	363.1	385.1	–	225.1	121.1	–

[a] *tr* = trace; [b] *PG* = phenolic group; [c] *AG* = acidic group

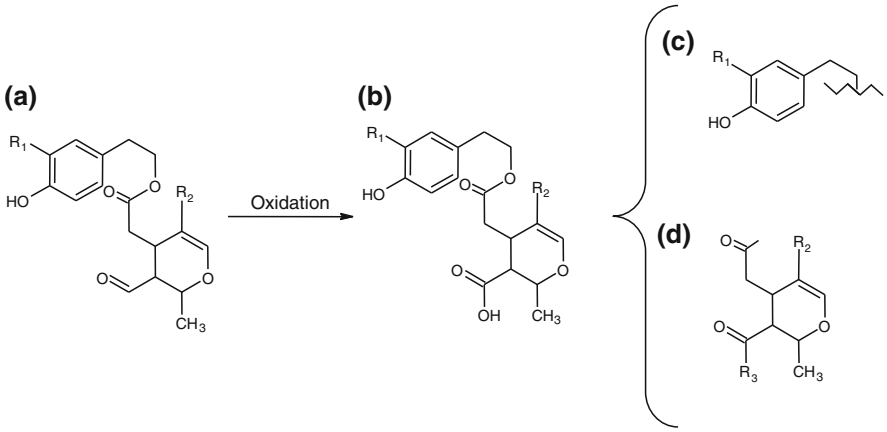

Fig. 9.5 General scheme of the evolution of secoiridoids during ageing treatment. **a** structure of secoiridoids: LAg (R_1 = H and R_2 = $-COOCH_3$); OA (R_1 = OH and R_2 = $-COOCH_3$); DLA (R_1 = H and R_2 = −H); DOA (R_1 = OH and R_2 = −H). **b** oxidized forms of secoiridoids: OxLAg (R_1 = H and R_2 = $-COOCH_3$); OxOA (R_1 = OH and R_2 = $-COOCH_3$); OxDLA (R_1 = H and R_2 = −H); OxDOA (R_1 = OH and R_2 = −H). **c** loss of acidic group during mass fragmentation: R_1 = H fragment with m/z = 121; R_1 = OH fragment with m/z = 137. **d** loss of phenolic group during mass fragmentation: R_2 = $-COOCH_3$ and R_3 = OH fragment with m/z = 241; R_2 = $-COOCH_3$ and R_3 = H fragment with m/z = 225; R_2 = H and R_3 = OH fragment with m/z = 183; R_2 = H and R_3 = H fragment with m/z = 167 (Reprinted with permission from Lerma-García et al. (2009c). Copyright 2009 American Chemical Society)

(to estimate the extraction recovery), being data expressed as the natural logarithm of the ratios of areas. Generally, a decrease of the more abundant compounds (secoiridoids) was observed. Peaks 21 and 22 were jointly evaluated: peak 21 appeared overlapped with peak 22 from t_3 to t_7. At t_7, peak 22 was absent. As previously observed at room temperature (Boselli et al. 2009; Di Lecce et al. 2006), transformations of secoiridoids to more simple compounds (for example decarboxymethyl structures), followed by a further conversion to phenyl ethyl alcohols (such as TY and HYTY), occurred. In this work, TY was not found in the EV1 sample at t_0, whereas the concentration of HYTY, which was initially low, increased from t_0 to t_4. This trend was also observed for oils stored at room temperature (Boselli et al. 2009; Di Lecce et al. 2006). Concerning lignans, AcPIN (peak 18 of Fig. 9.2c) slightly decreased exhibiting a high content also at the end of storage process (t_7). This tendency for lignans has been also observed when oils were heated with conventional or microwave oven (Carrasco-Pancorbo et al. 2007; Cerretani et al. 2009).

On the other hand, the evolution of the neo-formation compounds during storage is shown in Fig. 9.6b (area values were also divided by the 3, 4-DHPAA area and expressed as natural logarithms). The most important neo-formation compounds are peaks 4 (oxidation form of decarboxymethyl elenolic acid, OxDEA) and 15 (oxidized form of decarboxymethyl ligstroside aglycon, OxDLA),

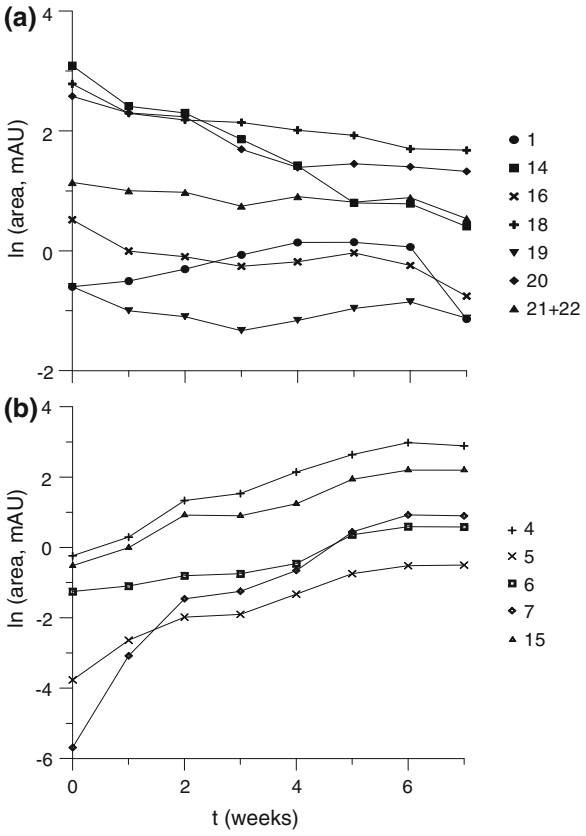

Fig. 9.6 Plots showing the trends of phenolic (**a**) and neo-formation compounds (**b**) during storage (from t_0 to t_7) of EV1. Area values were divided by the 3, 4-DHPAA area (internal standard). Peak identification as reported in Table 9.3 (Reprinted with permission from Lerma-García et al. (2009c). Copyright 2009 American Chemical Society)

respectively, followed by peaks 5, 6 and 7 (unknown compounds). Peak 13 (data not reported in Fig. 9.6b) was probably due to an oxidized secoiridoid, being tentatively assigned as an oxidized form of DOA (OxDOA).

9.2 Evaluation of the Oxidative Status of VOOs with Different Phenolic Content by Direct Infusion MS[2]

The aim of this work was to evaluate the oxidative status of VOOs using direct infusion APCI-MS assisted by LDA. For this purpose, samples at eight oxidation levels, with and without phenolic compounds, were used. These samples were the

[2] Parts of the text of this section have been adapted with permission from Lerma-García et al. (2009d). Copyright 2009 Springer-Verlag

EV1 and EV2 described in Sect. 9.1, whose qualitative parameters have been previously described.

9.2.1 MS Analysis and Selection of the Variables

According to a series of recent articles, the oxidation status of VOOs can be monitored using different oxidation markers (Armaforte et al. 2007; Bendini et al. 2006; Del Carlo et al. 2004; Lerma-García et al. 2009b; Rovellini et al. 1998; Verardo et al. 2009), such as OFAs, which have been used as an oxidation marker in several areas of applied research (Armaforte et al. 2007; Bendini et al. 2006; Del Carlo et al. 2004; Rovellini et al. 1998) and for the determination of lipid extracts obtained from other matrices, such as spaghetti pasta (Verardo et al. 2009). Another marker used to identify the oxidation status of VOOs has been the determination of the oxidized forms of phenolic compounds by HPLC–MS (Armaforte et al. 2007; Lerma-García et al. 2009b). Thus, the use of the profiles of free fatty acids, OFAs, phenols and their oxidized forms, jointly with α-T, have been selected as oxidation markers to monitor the oxidative status of VOOs in this work. Then, the abundances of the $[M\text{-}H]^-$ peaks of these compounds (see Table 9.4) were measured in the 4 replicates performed for each sample. As observed in Table 9.4, owing to the coincidence of the *m/z* values of three peak pairs (hydroxy-linoleic acid/keto-oleic acid, DOA/OxDLA and OA/OxLAg), these peaks were measured as the sum of the abundances of the two compounds of each pair; then, a total of 27 peaks was obtained to be used as predictors for LDA construction.

The fatty acid and OFA profiles obtained for EV1 at t_0 and t_3 are shown in Fig. 9.7. As it can be observed in this figure, the peak intensities of OFAs (peaks 8–12) increased from t_0 to t_3. This trend was also observed at the other storage times.

On the other hand, the peak profiles of α-T, phenolic compounds and their oxidized forms (only those whose *m/z* range was between 280 and 450) for the EV1 at t_0 and t_3 are shown in Fig. 9.8.

As it can be observed in this figure, the intensity of peaks 19 and 21 increased, which was attributed to the transformation of *ortho*-diphenolic forms to mono oxydrilic forms. In addition to this, a decrease of the intensity of peak 24 (α-T) is evidenced, while the intensities of peaks 28 and 30 (oxidized forms of phenolic compounds) and the pairs 20/27 and 21/29 increased. The intensity increase of both 20/27 and 21/29 peak pairs could be related with the contribution of the oxidized form peaks 27 and 29. These trends are in agreement with previous reports (Bendini et al. 2006; Verardo et al. 2009).

Table 9.4 $[M-H]^-$ peaks of selected fatty acids and antioxidant compounds (Reprinted with permission from Lerma-García et al. (2009d). Copyright 2009 Springer-Verlag)

Peak no.	Compound (acronym)	*m/z*
Fatty acids		
1	Myristic acid (C14:0)	227
2	Palmitoleic acid (C16:1)	253
3	Palmitic acid (C16:0)	255
4	Linolenic acid (C18:3)	277
5	Linoleic acid (C18:2)	279
6	Oleic acid (C18:1)	281
7	Stearic acid (C18:0)	283
OFAs		
8	Keto-linolenic acid	291
9	Keto-linoleic acid	293
10	Hydroxy-linoleic acid	295
11	Keto-oleic acid	295
12	Hydroxy-oleic acid	297
Phenolic and T compounds		
13	TY	137
14	HYTY	153
15	DEA	183
16	EA	241
17	API	269
18	LUT	285
19	DLA	303
20	DOA	319
21	LAg	361
22	OA	377
23	AcPIN	415
24	α-T	443
Oxidized phenols		
25	OxDEA	199
26	OxEA	257
27	OxDLA	319
28	OxDOA	335
29	OxLAg	377
30	OxOA	393

9.2.2 Construction of Data Matrices and LDA Models

After normalization of the 27 original variables by normalization procedure B, which led to a total of 351 predictors, two matrices were constructed. The first matrix, composed by EV1 samples, contained a total of 32 objects (8 samples × 4 replicates) and the 351 predictors. The second matrix comprised both EV1 and EV2 samples, and contained 64 objects (8 EV1 samples × 8 EV2 samples × 4

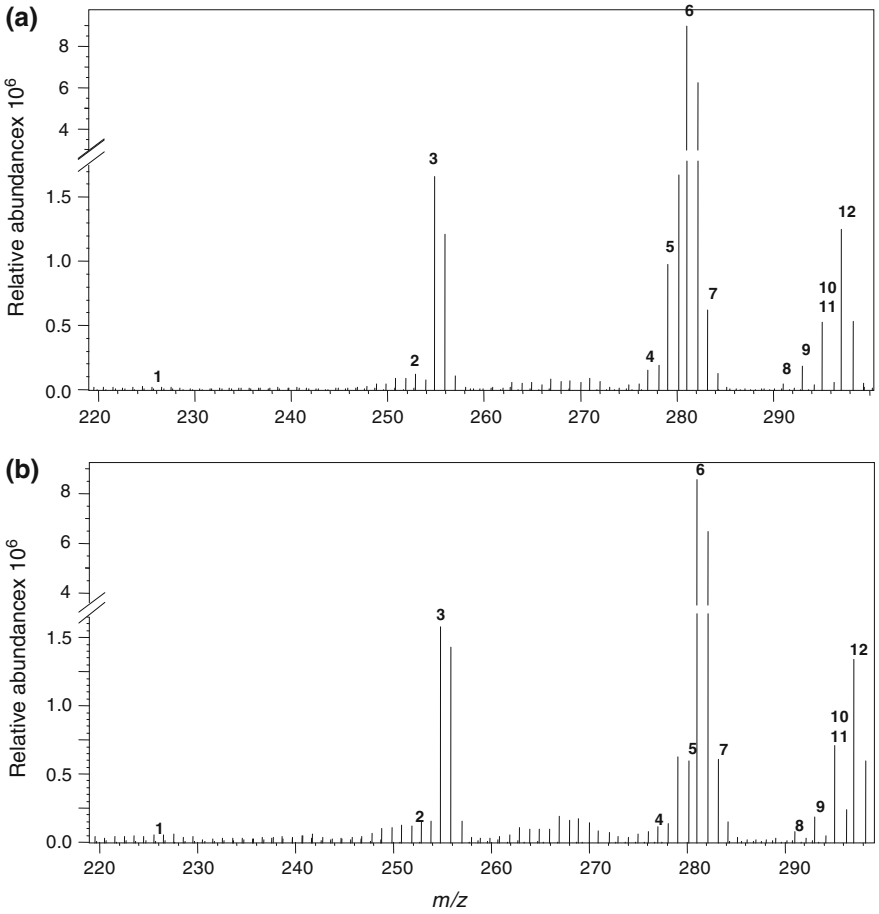

Fig. 9.7 MS spectra showing the peak profiles of fatty acids and their oxidized forms for EV1 at storage times t_0 (**a**) and t_3 (**b**). The $[M\text{-}H]^-$ peaks are labelled as indicated in Table 9.4 (Reprinted with permission from Lerma-García et al. (2009d). Copyright 2009 Springer-Verlag)

replicates) and 66 predictors (which corresponded to the α-T, fatty acid and OFA peaks). Only 66 predictors were selected since phenolic compounds were removed by the previous treatment in EV2 samples, and consequently their oxidized forms were not present in the MS spectra. A response column, which contained the eight categories corresponding to the eight storage times, was added to both matrices.

Then, two LDA models, one for each matrix, were constructed in order to classify oil samples according to their oxidative status. When the LDA model was constructed using the matrix that contained EV1 samples, an excellent resolution between the eight category pairs was observed (Fig. 9.9, $\lambda_w = 0.229$). The

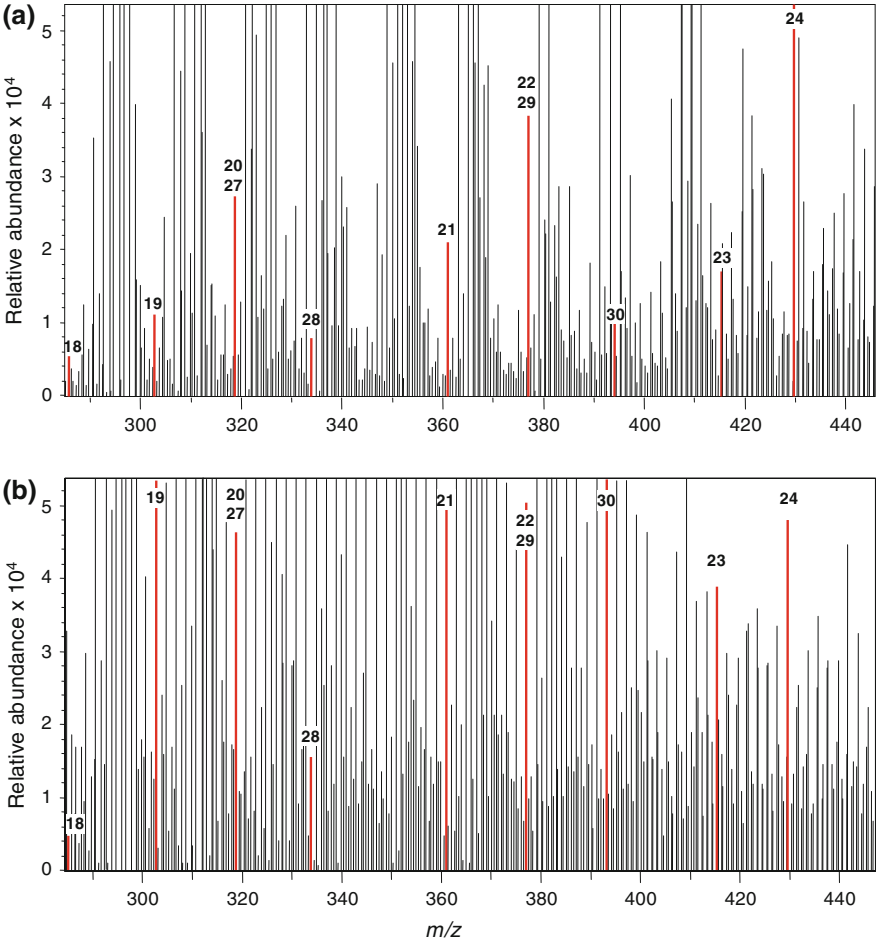

Fig. 9.8 MS spectra showing the peak profiles of tocopherol, phenolic compounds and their oxidized forms for the EV1 at storage times t_0 (**a**) and t_3 (**b**). The $[M\text{-}H]^-$ peaks are labelled as indicated in Table 9.4 (Reprinted with permission from Lerma-García et al. (2009d). Copyright 2009 Springer-Verlag)

variables selected by the SPSS stepwise algorithm, showing the predictors with large discriminant capabilities, are given in Table 9.5.

Next, a second LDA model was constructed using the matrix that contained both EV1 and EV2 samples. A good resolution between all category pairs was also obtained in this case (see Fig. 9.10), being λ_w value of 0.928. Although this value could seemed quite high, it could be considered an optimal one since a large number of categories were simultaneously distinguished. As observed in Fig. 9.10a, the t_0 and t_1 categories appeared well resolved from the other six categories along f_1, while t_0 and t_5 were resolved along f_2. As observed in

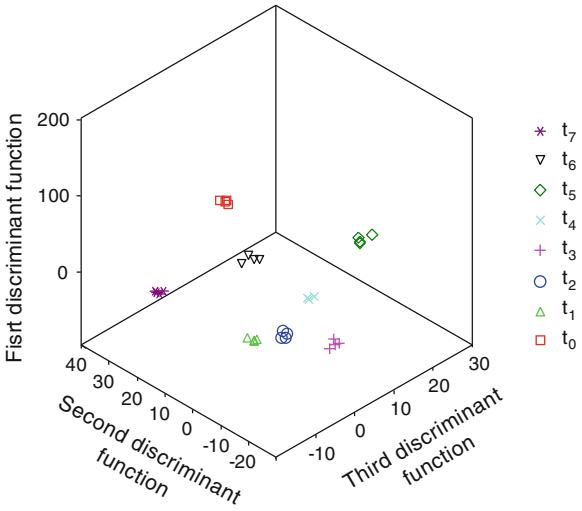

Fig. 9.9 Score plot on an oblique plane of the 3-D space defined by the three first discriminant functions of the LDA model constructed with the EV1 samples (Reprinted with permission from Lerma-García et al. (2009d). Copyright 2009 Springer-Verlag)

Table 9.5 Predictors selected and corresponding standardized coefficients of the LDA model constructed with the EV1 samples to predict the oxidative status (Reprinted with permission from M.J. Lerma-García et al. (2009d) . Copyright 2009 Springer-Verlag)

Predictors[a]	f_1	f_2	f_3	f_4	f_5	f_6	f_7
227/277	−0.17	−0.45	−0.64	1.48	1.19	0.64	0.61
227/303	5.81	0.24	0.20	0.03	0.01	−0.35	0.06
255/279	9.83	1.70	2.87	2.25	1.79	0.80	−0.96
255/281	−4.33	1.60	−0.98	−1.96	−0.58	−0.36	0.83
255/361	−0.97	−3.79	−0.10	0.33	−0.20	−0.80	−2.27
277/283	4.65	1.00	−1.09	1.26	1.35	−0.96	−0.14
277/183	−5.48	−1.48	−0.52	0.35	−0.85	2.21	0.76
279/281	5.62	2.82	2.25	0.46	0.72	0.40	−1.72
281/361	4.94	3.66	0.40	−0.62	0.63	0.23	2.13
283/183	8.30	1.51	−0.05	0.22	0.96	−1.71	−0.87
269/257	−0.29	−2.13	−0.07	0.21	0.73	−0.01	0.68
377/335	−0.38	0.32	0.20	0.47	−1.04	0.01	0.20
199/393	−1.89	0.04	−0.09	0.16	0.17	0.27	0.74

[a] *m/z* values of the ratios of abundances of peak pairs

Fig 9.10b, f_3 was able to resolve t_7 from the other categories, while f_4 resolved the pair t_1/t_6. Finally, a score plot on an oblique plane of the 3-D space defined by the three first discriminant functions is shown in Fig. 9.10c. Although it is difficult to appreciate the separation between all categories when represented in a plane, all category pairs were clearly resolved when this 3-D figure was rotated. The variables selected and the corresponding standardized coefficients of the model are given in Table 9.6. For both LDA models, and using leave-one-out cross-validation, all the points of the respective matrices were correctly classified.

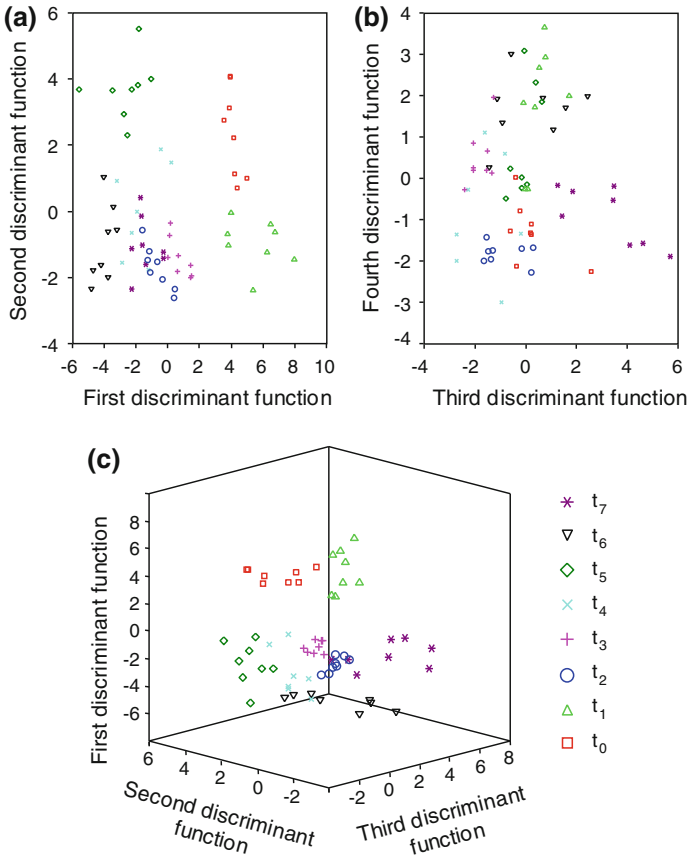

Fig. 9.10 Score plots on the planes of the first and second (**a**), and third and fourth discriminant functions (**b**), and on an oblique plane of the 3-D space defined by the three first discriminant functions (**c**) of the LDA model constructed with the EV1 and EV2 samples (Reprinted with permission from Lerma-García et al. (2009d). Copyright 2009 Springer-Verlag)

9.3 MOS Sensors for Monitoring of Oxidative Status Evolution and Sensory Analysis of VOOs with Different Phenolic Contents[3]

In this work, a method based on MOS sensors, jointly with the application of LDA, was used to VOOs according to their oxidative level. For this purpose, the EV1 and EV2 samples, previously described in Sect. 9.1, were used. These samples were

[3] Parts of the text of this section have been adapted with permission from Lerma-García et al. (2009e). Copyright 2009 Elsevier Ltd

Table 9.6 Predictors selected and corresponding standardized coefficients of the LDA model constructed with the EV1 and EV2 samples to predict the oxidative status (Reprinted with permission from Lerma-García et al. (2009d). Copyright 2009 Springer-Verlag)

Predictors[a]	f_1	f_2	f_3	f_4	f_5	f_6	f_7
255/277	−0.36	−0.33	0.54	1.85	−0.91	0.83	−0.35
255/281	−0.11	−0.34	0.99	1.97	0.84	−1.34	0.55
255/291	−1.17	3.02	−2.94	−8.05	−2.68	−1.73	0.41
277/279	−0.96	−0.02	1.57	0.01	0.85	1.85	0.78
281/283	1.71	−0.18	1.81	2.76	1.26	0.10	0.37
283/291	0.81	−1.90	3.10	7.22	2.96	1.20	−0.17
443/277	−1.38	0.69	0.27	−1.37	3.45	1.23	1.30
443/279	2.91	0.19	−0.22	0.90	−3.26	−1.60	−2.49

[a] *m/z* values of the ratios of abundances of peak pairs

also evaluated by a testing panel. A set of 25 additional VOO samples, which were also subjected to the panel test assessment, was used to evaluate the LDA model in order to verify if they were well assigned according to sensory data. In order to assure the robustness of the model, these samples were collected by covering different geographical origins and genetic varieties, as well as different years.

9.3.1 Construction of Data Matrices and LDA Models

The signals of the 6 MOS sensors, extracted in this case using the feature extraction algorithm "classical feature" (see Sect. 3.5.8), were used as predictors for LDA model construction. Three matrices containing 6 predictors each were constructed. The two first matrices, composed by EV1 and EV2 samples, respectively, contained a total of 16 objects each (8 samples × 2 replicates), while the third matrix comprised both EV1 and EV2 samples, and contained 32 objects (8 EV1 samples × 8 EV2 samples × 2 replicates). A response column, which contained the eight categories corresponding to the eight storage times, was added to the three matrices.

Then, a first LDA model was constructed using the matrix constructed with the EV1 samples. As observed in Fig. 9.11, an excellent resolution was obtained for all categories. A λ_w value of 0.049, which could be considered very low due to the fact that a large number of categories were simultaneously distinguished, was obtained for this model.

Next, another LDA model was constructed using the matrix containing the EV2 samples. An excellent resolution for all categories (see Fig. 9.12) was also obtained with this model, being $\lambda_w = 0.068$.

Finally, a third LDA model was constructed using all, EV1 and EV2 samples. Again, a satisfactory resolution between all the category pairs was achieved ($\lambda_w = 0.892$).The high λ_w value obtained could be due to the fact that 2 different

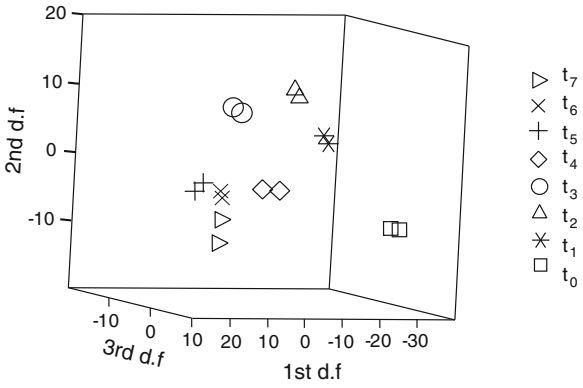

Fig. 9.11 Score plot on an oblique plane of the 3-D space defined by the three first discriminant functions of the LDA model constructed with EV1 samples (d.f., discriminant function) (Reprinted from Lerma-García et al. (2009e). Copyright 2009 Elsevier Ltd.)

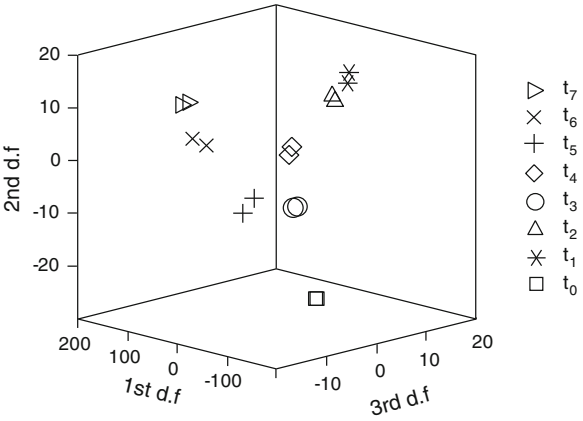

Fig. 9.12 Score plot on an oblique plane of the 3-D space defined by the three first discriminant functions of the LDA model constructed with the EV2 samples. For other comments, see Fig. 9.11 (Reprinted from Lerma-García et al. (2009e). Copyright 2009 Elsevier Ltd.)

groups, one for EV1 and the other for EV2 samples, were observed at any given storage time category (data not shown). Thus, it is possible to conclude that electronic nose data could discriminate between samples with and without phenolic compounds at any stage of storage time. The variables selected by the three models, and their corresponding standardized coefficients, are shown in Table 9.7. Since the model constructed with the EV1 samples was the only one that uses sensor 3 as a predictor, this sensor was supposed to respond to the volatile compounds formed after oxidation in the presence of phenolic compounds. For the three models, all the objects were correctly classified by leave-one-out cross-validation.

9.3.2 Sensory Analysis and Evaluation of the Constructed LDA Model

Both EV1 and EV2 samples were subjected to an organoleptic assessment by a testing panel. The positive attributes green fruity, and leaf and grass were only

Table 9.7 Predictors selected and corresponding standardized coefficients for the three models constructed to predict the storage time (Reprinted from Lerma-García et al. (2009e). Copyright 2009 Elsevier Ltd.)

	Pred.	Sensor 1	Sensor 2	Sensor 3	Sensor 4	Sensor 5
EV1	f_1	1.75	−1.01	0.53	−1.22	–
	f_2	0.50	−0.00	−0.56	1.06	–
	f_3	−1.46	1.27	2.90	−2.39	–
	f_4	3.58	1.47	−3.62	−1.30	–
EV2	f_1	−2.36	−14.51	–	10.73	6.40
	f_2	1.99	0.74	–	−2.30	−0.12
	f_3	0.50	−1.62	–	2.35	−0.30
	f_4	−2.58	0.03	–	0.03	2.93
EV1 and EV2	f_1	−2.83	−5.80	–	4.50	4.16
	f_2	−4.84	−0.90	–	0.96	5.45
	f_3	−2.15	−1.31	–	2.77	1.01
	f_4	4.06	0.33	–	−0.36	−3.25

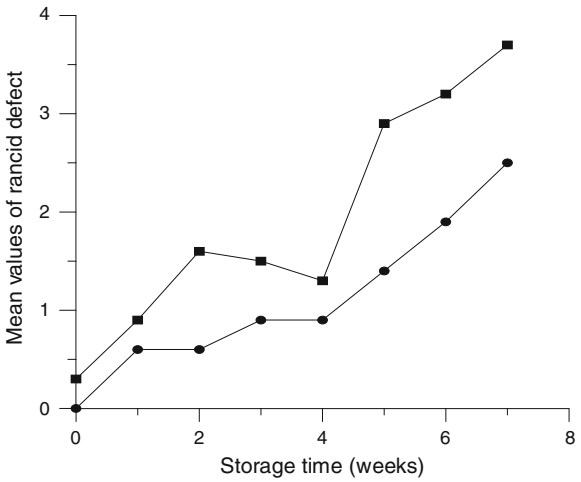

Fig. 9.13 Evolution of the rancid defect expressed as the mean values of the sensory analysis as a function of storage time for EV1 (*filled circle*) and EV2 (*filled square*) samples (Reprinted from Lerma-García et al. (2009e). Copyright 2009 Elsevier Ltd.)

detected in the EV1 sample at t_0. All other samples were characterized by a ripe fruity and any pleasant attributes. Regarding negative attributes, two different defects were detected. Winey defect, which was only detected in the EV1 sample at t_1, and rancid defect, which was detected in all samples at the different storage times (see Fig. 9.13, where mean values were used instead of median to better show inter-sample variations). As it can be observed in this figure, rancidity was more pronounced for the EV2 samples, which could be indirectly attributed to the absence of phenolic compounds. Therefore, the model clearly responded to the rancid defect.

Table 9.8 Median values for the sensory attributes and predicted category for the 25 samples used to evaluate the LDA model (Reprinted from Lerma-García et al. (2009e). Copyright 2009 Elsevier Ltd.)

Sample	Fruity (type)	Other pleasant attributes	Defects	Predicted category
N1	3 (green)	2 (grass, tomato)	0	t_0
N2	2 (green)	2 (grass, artichoke, almond)	0	t_0
N3	2 (green)	2 (grass, artichoke)	0	t_0
N4	2 (green)	2 (leaf, almond)	0	t_0
N5	2 (green)	2 (leaf, grass, tomato, almond)	0	t_0
N6	3 (green)	2 (grass, artichoke, tomato)	0	t_0
N7	3 (green)	3 (grass, artichoke, tomato)	0	t_0
N8	3 (green)	2 (grass, artichoke, tomato)	0	t_0
N9	2 (ripe)	2 (other)	0	t_0
N10	2 (ripe)	2 (tomato)	0	t_0
N11	1 (ripe)	0	1.5 (fusty)	t_1
N12	1 (ripe)	0	1 (winey)	t_1
N13	1 (ripe)	0	2 (rancid)	t_1
N14	1 (ripe)	0	5 (3 of muddy, 2 of rancid)	t_2
N15	1 (ripe)	0	2 (rancid)	t_1
N16[a]	0	0	2 (winey)	t_0
N17[a]	0	0	3 (winey)	t_0
N18[a]	0	0	3 (rancid)	t_3
N19[a]	0	0	5 (rancid)	t_7
N20[a]	0	0	1 (fusty)	t_1
N21[a]	0	0	3 (fusty)	t_3
N22[a]	0	0	1 (muddy)	t_1
N23[a]	0	0	2 (muddy)	t_1
N24[a]	0	0	1 (mouldy)	t_1
N25[a]	0	0	2 (mouldy)	t_1

[a] Official defects provided by IOC

The additional set of 25 VOOs was also subjected to the organoleptic assessment by the panel, being the results of this evaluation used to validate the model. The most important sensory attributes of these samples, and the model predicted category, are shown in Table 9.8. As observed, the model is able to distinguish the non-defected samples from the others (non-defected samples were in all cases included into the t_0 category). In addition to this, the model was able to correctly identify 13 defective samples, with the exception of samples N16 and N17, which were characterized by a winey defect and fruity absence. Specifically, the model responded linearly for the rancid defect (samples N13, N15, N18 and N19), quite well for samples N11, N20, and N21 (which were characterized by different intensities of fusty), but less for oils with other defects, such as mouldy and muddy.

Finally, it is interesting to highlight that slight differences were observed between the genuinely defected samples (N13 to N15), and between those provided by IOC to recognize the rancid defect (N18 and N19). This could be attributed to the differences in total volatile compounds present in real samples and in the rancid standard (Aparicio et al. 2000). In this respect, the near total absence of volatile components responsible for pleasant fruity note (from the LOX pathway), and the presence of high concentrations of several saturated and unsaturated aldehydes in the IOC samples, could have influenced the MOS response.

9.4 Prediction of OFA Concentration in VOOs Using MOS Sensors and MLR[4]

In this work, an electronic nose method, jointly with the application of MLR models, is used to evaluate OFA concentration in VOOs characterised by different oxidative status. For this purpose, a total of 72 VOOs, coming from different Italian regions (Abruzzo, Emilia-Romagna, Puglia, Sicily and Toscana) and from different harvest seasons (2006-07, 2007-08 and 2008-09) were used. Moreover, the oils were obtained from olives coming from different genetic variety, degree of ripening, production system (type, productive capacity and manufacturer) and storage time.

9.4.1 OFA Content

Different OFA contents were obtained according to the different storage time of the oil samples time (2 weeks, 16 months and 34 months after oil production), as it can be observed in Fig. 9.14. Based on the study of MS spectra, OFAs could be grouped as follows: isomeric forms of keto-linolenic acid (*m/z* 383, 1), isomeric forms of keto-linoleic acid (*m/z* 385, 2) and isomeric forms of keto-oleic acid (*m/z* 387, 3). All these *m/z* values corresponded to the $[M + H]^+$ ions (Rovellini et al. 1998, 2004).

When the 72 VOOs were analyzed, a wide range of OFA values, which were comprised between 0.3 and 6.5 %, were obtained. These differences could be attributed to the fact that the oil samples came from different harvest seasons and were analyzed at times ranging from 1 week to 36 months after production. Rovellini et al. (2004), which have determined the OFA content in several VOOs, have stated that OFA percentages ranging from 2 to 4 % are typical for EVOOs stored at room temperature from 2 to 18 months, while oil samples characterized by a total OFA higher than 4 % must be considered as "expired". Thus, taking into

[4] Parts of the text of this section have been adapted with permission from Lerma-García et al. (2009f). Copyright 2009 American Chemical Society.

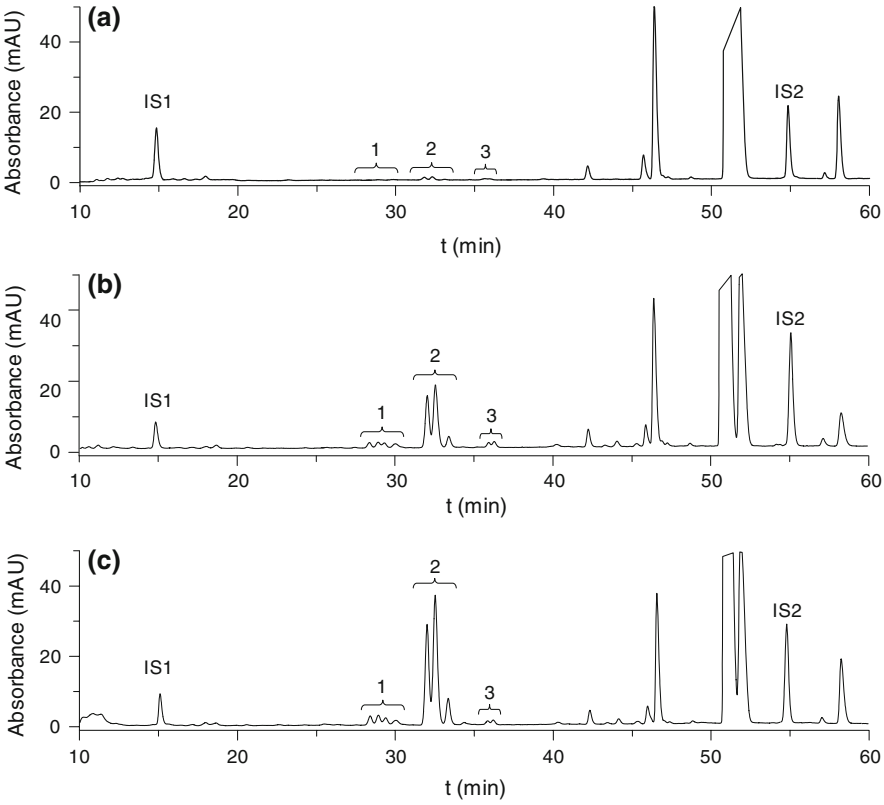

Fig. 9.14 Cromatograms of OFAs in VOOs analyzed after **a** 2 weeks, **b** 16 months and **c** 34 months of oil production. Detection was performed at 255 nm. Peak identification (as benzyl-ester derivatives): 1, group of isomeric forms of keto-linolenic acid; 2 group of isomeric forms of keto-linoleic acid; 3, group of isomeric forms of keto-oleic acid. IS1 and IS2 (internal standards) are benzyl caproate and benzyl heptadecanoate, respectively (Reprinted with permission from Lerma-García et al. (2009f). Copyright 2009 American Chemical Society)

these considerations, the 72 VOOs analyzed in this study were divided in 4 groups (Fig. 9.15a–d):

- Group 1, that contained all samples having an OFA value < 1.0 % (see Fig. 9.15a). A total of 23 samples, with a mean of 0.6 % OFA, were included in this group.
- Group 2, which contained a total of 15 samples with a mean of 1.8 %. In this group, OFA contents are equal or higher than 1.0 %, and lower than 2.5 % (Fig. 9.15b).
- Group 3, constituted by 23 samples with a mean of 3.0 % OFA. These samples corresponded to that with OFA values equal or higher than 2.5 %, and lower than 4 % (Fig. 9.15c).

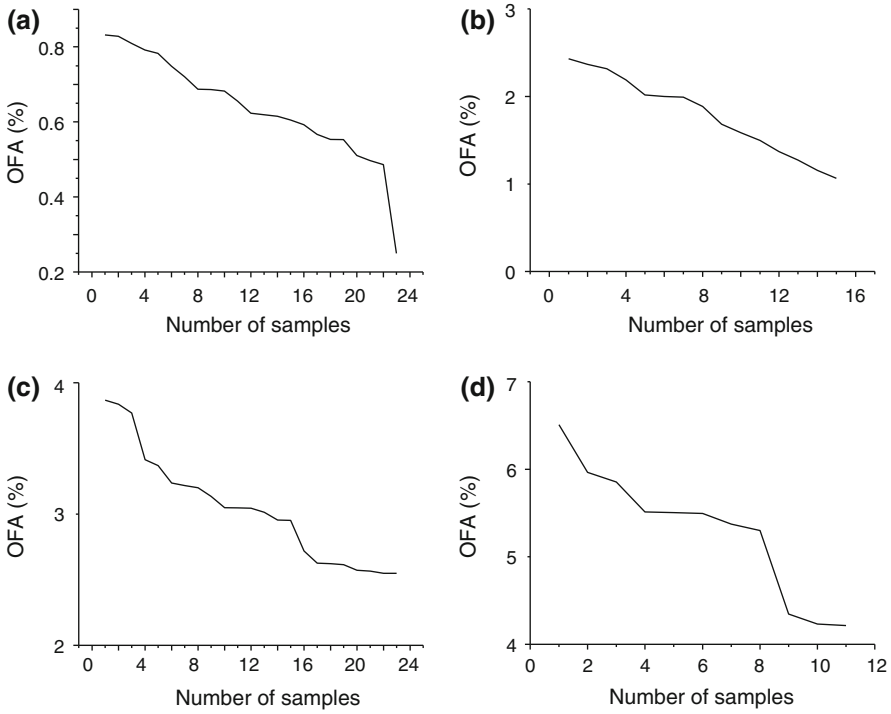

Fig. 9.15 Plots representing the OFA values of the 72 VOOs employed in this study. **a** OFA < 1.0 %; **b** 1.0 % $\leq$ OFA < 2.5 %; **c** 2.5 % $\leq$ OFA < 4 % and **d** OFA ≥ 4 % (Reprinted with permission from Lerma-García et al. (2009f). Copyright 2009 American Chemical Society)

- Group 4, that contained all samples having an OFA value ≥ 4 % (Fig. 9.15d). A total of 11 samples, with a mean of 5.3 % OFA, were included in this group.

All the samples produced within 1 month before analysis belonged to group 1. Their OFA values were comprised between a very narrow range (0.3 to 0.8 %). On the other hand, group 4 showed higher OFA percentages and a wider range of variability (from 4.2 to 6.5 %). As a result of this study, it could be concluded that the freshness of VOOs could be evaluated with a simple OFA assay, which reduce the number of other analyses, such as peroxide values or k_{232} for primary oxidation products, and *p*-anisidine value or volatile content for secondary oxidation products.

9.4.2 Construction of Data Matrices and MLR Models

Two data matrices, which corresponded to the calibration and external validation sets, were constructed. The calibration matrix contained 60 randomly selected

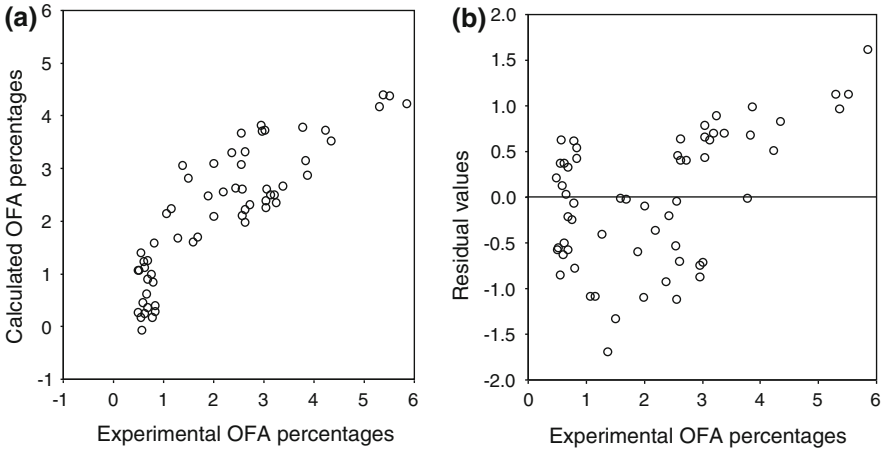

Fig. 9.16 **a** Correlation plot of the calculated versus the experimental OFA percentages. **b** Plot of the residual values versus the experimental OFA percentages (Reprinted with permission from Lerma-García et al. (2009f). Copyright 2009 American Chemical Society)

objects (which corresponded to the mean of 60 samples), while the external validation matrix was constructed with the remaining 12 objects (mean of 12 samples). The signals of the 6 MOS sensors, extracted using the extraction algorithm "classical feature" (see Sect. 3.5.8), were used as predictors. A response column, containing the OFA concentrations obtained by HPLC, was also added to these matrices.

Using the calibration matrix, two MLR models were constructed, which corresponded to the exclusion and inclusion of an independent term or constant. A better linearity was obtained when the model was constructed without the inclusion of the constant ($r = 0.961$). Thus, further studies were performed without the constant. The correlation plot of the predicted versus the experimental OFA percentages obtained without the inclusion of the constant is shown in Fig. 9.16a. When leave-one-out validation was applied, the average prediction error (calculated as the sum of the absolute differences between expected and calculated OFA percentages divided by the number of predictions) was 30 %. The quality of this model was evaluated by examining the residual values and/or the relative errors. Then, residual values were plotted against experimental OFA percentages (see Fig. 9.16b).

A heteroscedasticity (non-constant variance) of data was evidenced as a result of the dependence of the residuals with the experimental values. This problem can be solved by applying a transformation of the variables or by using weighted least-squares (Vandeginste, 1998). For this reason, different transformations were applied to the experimental OFA percentages: natural logarithm and square and cube roots. When the cube root transformation was applied to the data, homocedasticity was finally obtained (see Fig. 9.17b). In addition to this, an improvement in model linearity was also observed ($r = 0.995$). The correlation plot of the

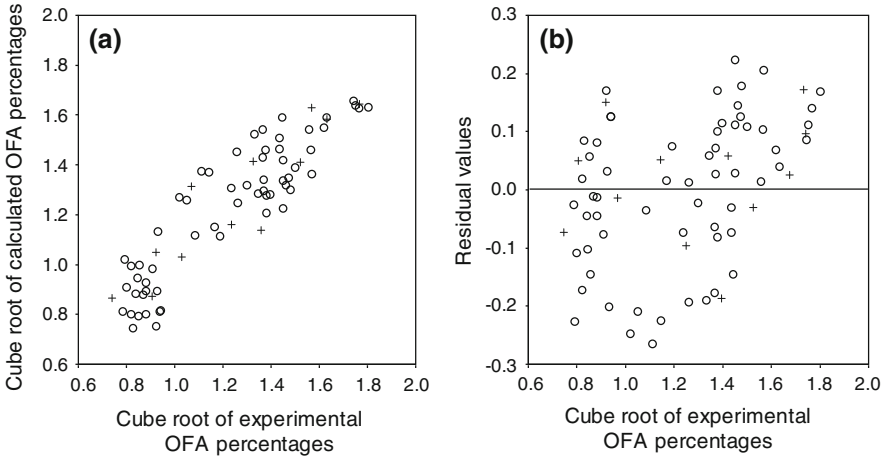

Fig. 9.17 **a** Correlation plot of the calculated versus the experimental OFA percentages obtained after cube root transformation. **b** Plot of the residual values versus the experimental OFA percentages obtained after cube root transformation. For both, a and b, samples were marked as calibration (*circle*) and validation (*plus*) (Reprinted with permission from Lerma-García et al. (2009f). Copyright 2009 American Chemical Society)

Table 9.9 Predictors selected and their corresponding non-standardized coefficients (coef.), and confidence limits for the MLR model constructed after a cube root transformation of the variable (Reprinted with permission Lerma-García et al. (2009f). Copyright 2009 American Chemical Society)

Predictor	Coef.	Confidence limits[a]
Sensor 2	3.18	2.42, 3.94
Sensor 3	10.12	7.67, 12.57
Sensor 4	−8.61	−10.63, −6.58
Sensor 5	−7.98	−10.12, −5.84
Sensor 6	6.16	4.63, 7.69

[a] For a 95 % confidence interval

calculated versus the experimental OFA percentages obtained after data cube root transformation is shown in Fig. 9.17a.

The predictors selected during model construction, and their corresponding non-standardized coefficients and confidence limits, are listed in Table 9.9. According to this table, sensors 2–6 were selected, which corresponded to $SnO_2 + SiO_2$–SnO_2 catalyzed with three different metals and to WO_3. When leave-one-out validation was applied, the average prediction error was 8 %. When the model was applied to the validation set, a good prediction capability was observed (see Fig. 9.17a), being the average validation error 9 %.

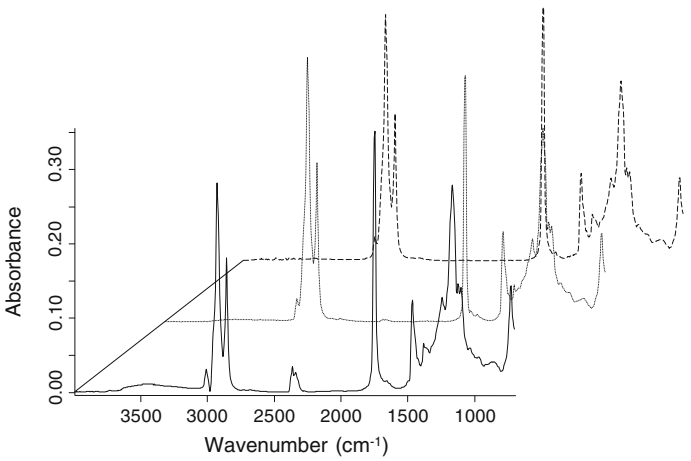

Fig. 9.18 FTIR spectra of VOOs after 2 weeks (*continuous line*), 16 months (*dotted line*) and 34 months (*dashed line*) of oil production (Reprinted from Lerma-García et al. (2011). Copyright 2010 Elsevier Ltd.)

9.5 Prediction of OFA Concentration in VOOs Using FTIR and MLR[5]

The aim of this work was to develop an FTIR method capable of predicting, jointly with the use of MLR models, the OFA concentration found in VOOs characterized by different oxidative statuses. For this purpose, the 72 VOO samples employed in Sect. 9.4 were also used.

9.5.1 Description of FTIR Spectra and Construction of Data Matrices and MLR Models

The FTIR spectra of the same 3 VOO samples presented in Sect. 9.4.1, which were characterized by different storage times, and thus having different OFA content (see the chromatograms of Fig. 9.14), are shown in Fig. 9.18.

In order to obtain the variables to be used in MLR model construction, the FTIR spectra were divided in 25 wavelength regions. These regions were described in Table 5.2. For each region, the peak or shoulder area was measured and used as original variable. After application of normalization procedure B, a total of 300 normalized variables to be used as predictors were obtained.

[5] Parts of the text of this section have been adapted with permission from Lerma-García et al.(2011). Copyright 2010 Elsevier Ltd.

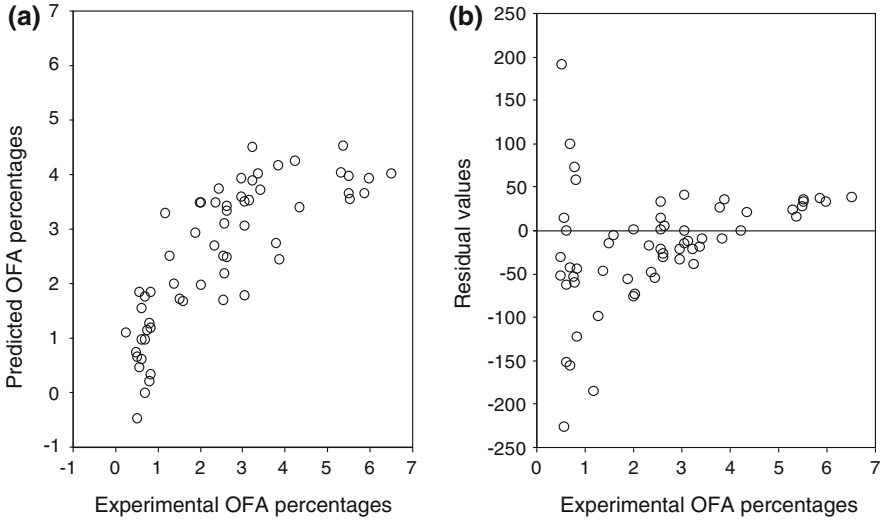

Fig. 9.19 **a** Correlation plot of the predicted versus the experimental OFA percentages. **b** Plot of the residual values versus the experimental OFA percentages (Reprinted from Lerma-García et al. (2011). Copyright 2010 Elsevier Ltd.)

Then, for MLR studies, two data matrices, which corresponded to the calibration and external validation sets, were constructed. The calibration matrix contained 60 randomly selected objects (which corresponded to the mean of 60 samples), while the external validation matrix was constructed with the remaining 12 objects (mean of 12 samples). Both matrices contained the 300 predictors previously described. A response column, containing the OFA concentrations obtained by HPLC, was also added to these matrices.

As indicated in Sect. 9.4.2, the calibration matrix was used to construct two MLR models, which were obtained either with or without the inclusion of a constant. Also in this case, a better linearity was obtained when the model was constructed without the inclusion of the constant ($r = 0.944$). Thus, further studies were performed without the constant. The correlation plot of the predicted versus the experimental OFA percentages obtained without the inclusion of the constant is shown in Fig. 9.19a.

When leave-one-out validation was applied, the average prediction error (calculated as previously described in Sect. 9.4.) was 52 %. Next, the residual values were plotted against the experimental OFA percentages (Fig. 9.19b) to obtain information regarding the quality of the model. Also in this case, the data showed a pronounced heteroscedasticity. Thus, different variable transformations, such as natural logarithm and square and cube roots were applied to the experimental OFA percentages. An acceptable homoscedasticity was achieved when the cube root transformation was used (see Fig. 9.20b). Using the cube root transformation, linearity also improved ($r = 0.996$). The correlation plot of the predicted versus the experimental OFA percentages obtained using the cube root

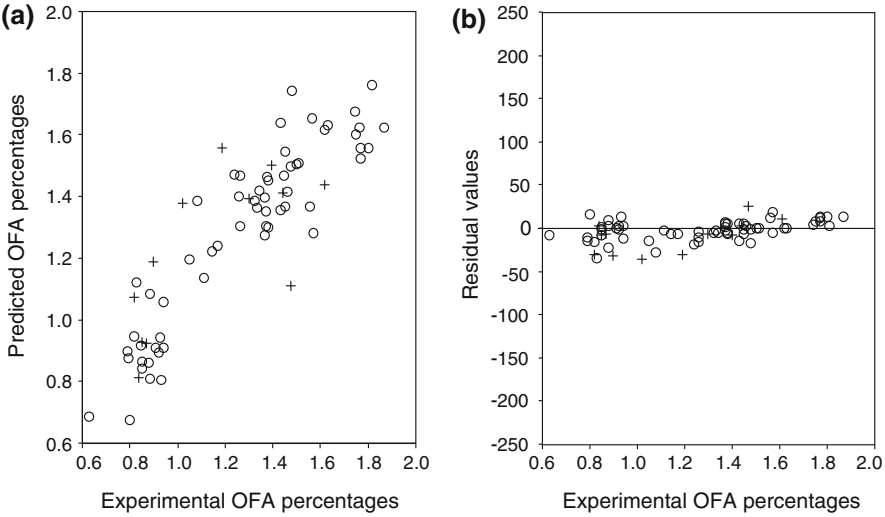

Fig. 9.20 **a** Correlation plot of the predicted versus the experimental OFA percentages obtained after cube root transformation. **b** Plot of the residual values versus the experimental OFA percentages obtained after cube root transformation. For both, a and b, samples were marked as calibration (*circle*) and validation (+) (Reprinted from Lerma-García et al. (2011). Copyright 2010 Elsevier Ltd.)

Table 9.10 Predictors selected and their corresponding non-standardized coefficients (coef.) for the MLR model constructed after the cubic root transformation of the variable (Reprinted from Lerma-García et al. (2011). Copyright 2010 Elsevier Ltd.)

Predictor	Coef.
3/17	0.056
3/20	−0.020
1/23	−0.068
19/22	−0.041
6/7	−0.001
14/22	−0.001
5/24	0.003
12/17	0.261

transformation is shown in Fig. 9.20a. The predictors selected for this model and their corresponding non-standardized coefficients are detailed in Table 9.10. According to this table, the wavelength regions with a predominant weight in the construction of the MLR model corresponded to = C–H (trans and cis, stretching), –C–H (CH_2, stretching asym), O–H (bending in plane), C–O (stretching), –H–C = C–H– (cis?) and = CH_2 (wagging). These regions were those more affected by oxidation, since they were characterized by a functional group with oxygen or a double bond. When leave-one-out validation was applied, the average prediction error was 8 %. When the model was applied to the validation set, an excellent prediction capability was observed (see Fig. 9.20a), being the average validation error 17 %.

References

Aparicio R, Rocha SM, Delgadillo I, Morales MT (2000) J Agric Food Chem 48:853
Aparicio R, Roda L, Albi MA, Gutiérrez F (1999) J Agric Food Chem 47:4150
Armaforte E, Mancebo-Campos V, Bendini A, Salvador MD, Fregapane G, Cerretani L (2007) J Sep Sci 30:2401
Baldioli M, Servili M, Perretti G, Montedoro GF (1996) J Am Oil Chem Soc 73:1589
Bandarra NM, Campos RM, Batista I, Nunes ML, Empis JM (1999) J Am Oil Chem Soc 76:905
Bendini A, Cerretani L, Vecchi S, Carrasco-Pancorbo A, Lercker G (2006) J Agric Food Chem 54:4880
Bonoli-Carbognin M, Cerretani L, Bendini A, Almajano MP, Gordon MH (2008) J Agric Food Chem 56:7076
Boselli E, Di Lecce G, Strabbioli R, Pieralisi G, Frega NG (2009) LWT Food Sci Technol 42:748
Carrasco-Pancorbo A, Cerretani L, Bendini A, Segura-Carretero A, Lercker G, Fernández-Gutiérrez A (2007) J Agric Food Chem 55:4771
Cerretani L, Bendini A, Rodriguez-Estrada MT, Vittadini E, Chiavaro E (2009) Food Chem 115:1381
Commission regulation (EC) No. 1989/2003 of 6 Nov 2003 amending regulation (ECC) No. 2568/91 on the characteristics of olive oil and olive-residue oil and on the relevant methods of analysis. Off. J Eur Commun L295 (2003) pp 57–77
Del Carlo M, Sacchetti G, Di Mattia C, Compagnone D, Mastrocola D, Liberatore L, Cichelli A (2004) J Agric Food Chem 52:4072
Di Lecce G, Bendini A, Cerretani L, Bonoli-Carbognin M, Lercker G (2006) Ind Aliment-Italy 46(1):873
Lerma-García MJ, Simó-Alfonso EF, Bendini A, Cerretani L (2009a) Food Chem 117:608
Lerma-García MJ, Simó-Alfonso EF, Chiavaro E, Bendini A, Lercker G, Cerretani L (2009b) J Agric Food Chem 57:7834
Lerma-García MJ, Simó-Alfonso EF, Chiavaro E, Bendini A, Lercker G, Cerretani L (2009c) J Agric Food Chem 57:7834. Copyright 2009 American Chemical Society
Lerma-García MJ, Herrero-Martínez JM, Simó-Alfonso EF, Lercker G, Cerretani L (2009d) Anal Bional Chem 395:1543. Copyright 2009 Springer-Verlag
Lerma-García MJ, Simó-Alfonso EF, Bendini A, Cerretani L (2009e) Food Chem 117:608. Copyright 2009 Elsevier Ltd
Lerma-García MJ, Simó-Alfonso EF, Bendini A, Cerretani L (2009f) J Agric Food Chem 57:9365. Copyright 2009 American Chemical Society
Lerma-García MJ, Simó-Alfonso EF, Bendini A, Cerretani L (2011) Food Chem 124:679. Copyright 2010 Elsevier Ltd
Ríos JJ, Gil MJ, Gutiérrez-Rosales F (2005) J Chromatogr A 1903:167
Rovellini P, Cortesi N (2002) Riv Ital Sost Grasse 69:1
Rovellini P, Cortesi N (2004) Ital J Food Sci 16: 333
Rovellini P, Cortesi N, Fedeli E (1998) Riv Ital Sost Grasse 75: 57
Vandeginste BGM, Massart DL, Buydens LMC, De Jong S, Lewi PJ, Smeyers-Verbeke J (1998) Data handling in science and technology part B. Elsevier Science B. V, Amsterdam
Verardo V, Ferioli F, Riciputi Y, Infelice G, Marconi E, Caboni MF (2009) Food Chem 114:472

Chapter 10
General Conclusions

Different fast and sensitive methods for the characterization of vegetable oils according to their botanical origin, and for the characterization and authentication of olive oils in relation to their quality, genetic variety and geographical origin have been developed. For this purpose, different oil components profiles, such as Ts and T_3s, sterols, alcohols, amino acids, fatty acids and phenolic compounds, have been used. These profiles have been established using different analytical techniques, including CEC, direct infusion MS, HPLC coupled to both UV-Vis and MS detectors, nano-LC, UPLC-MS, FTIR, electronic nose, etc.

The concrete objectives obtained through the entire thesis are summarized below, grouped by chapters.

10.1 Development of Methods for the Determination of Ts and T_3s in Vegetable Oils

Different methods have been developed for the determination of Ts and T_3s in vegetable oils.

A CEC method using laboratory-made LMA monolithic columns was first developed. The best resolution was obtained with a content of 12 wt % 1,4-butanediol in the polymerization mixture, which yielded a small pore size (250 nm). For T separation, the best compromise between resolution and analysis time (less than 10 min) was achieved with a mobile phase containing 99:1 (v/v) MeOH–aqueous buffer at pH 8. On the other hand, to analyze T_3-containing oils, a 93:7 (v/v) MeOH–aqueous buffer mobile phase is recommended.

A nano-LC method for the determination of Ts and T_3s was next developed. Analytes separation was evaluated using two different monolithic columns, a commercial silica column and a laboratory-made LMA column. Using the monolithic silica column, the best compromise between efficiency, resolution and

M. J. Lerma García, *Characterization and Authentication of Olive and Other Vegetable Oils*, Springer Theses, DOI: 10.1007/978-3-642-31418-6_10,

short analysis time (less than 18 min) was achieved with a mobile phase containing ACN/MeOH/water 75:8:17 (v/v/v) containing 0.2 % acetic acid. When the LMA monolithic column was used, the best results were obtained using a mobile phase containing 96 % ACN/water (76:24) mixture and 4 % MeOH. With this mobile phase, analysis time was similar to that obtained with the silica column. Among the advantages of the nano-LC methods developed, the low consumption of solvents and sample (10 nL) is highlighted.

Both methods, CEC and nano-LC, allowed the detection and evaluation of olive oil adulteration with other vegetable oils of different botanical origin, also allowing the identification of adulteration with oils rich in T_3s in a short analysis time.

Due to these characteristics, these methods provide an alternative to the traditional HPLC methods. Furthermore, it has been demonstrated the potential of monolithic columns, which represent a competitive alternative to packed columns.

10.2 Development of Methods for the Determination of Sterols in Vegetable Oils

Different methods have been developed for the determination of sterols in vegetable oils.

A CEC method using laboratory-made methacrylate monolithic columns has been first developed. The composition of the polymerization mixture was optimized using two different monomers, LMA and ODMA, and varying the monomer/porogen, monomer/crosslinker and porogenic solvent ratios. The best results in terms of resolution, efficiency and short analysis times (less than 7 min) were obtained with an LMA column prepared with a ratio LMA/EDMA of 60:40 and 60 % of porogens with a 20 % 1,4-butanediol (12 % in the polymerization mixture). The best mobile phase was an ACN/2-propanol/water mixture containing 5 mM Tris at pH 8. Compared to other CEC methods, this method significantly reduced analysis time, giving also low LOD values.

On the other hand, an UPLC-MS method has been also developed for the determination of sterols. With this method, the separation of sterols could be achieved in less than 5 min, providing narrow peaks with good symmetry. Although several sample peaks were not completely resolved, the high selectivity provided by the SIR acquisition of MS instrument made it possible to separate most of analytes.

The methods based on the determination of sterols by UPLC-MS and CEC also allowed the rapid detection and assessment of the adulteration of olive oil with other vegetable oils of different botanical origin.

10.3 Development of Methods for the Classification of Vegetable Oils According to Their Botanical Origin

Different fast and simple methods, capable of classifying vegetable oils according to their botanical origin, have been developed using LDA as chemometric tool.

For this purpose, the data obtained by FTIR spectroscopy has been firstly used. Once the IR spectrum was divided into 26 regions, an LDA model capable of classifying vegetable oil samples of five different botanical origins by using only eight spectral regions was constructed. On the other hand, the potential of FTIR spectroscopy for the prediction of EVOO adulteration with sunflower, soybean, hazelnut or corn oils has been also demonstrated. MLR models constructed with a single predictor were obtained, except for the EVOO-corn mixture, in which the model was constructed with two predictors. All these models were able to detect at least 5 % of the adulterant oil in EVOO.

On the other hand, the possibility of classifying vegetable oils according to their botanical origin by using sterol profiles established by direct infusion MS has been also demonstrated. The potential of ESI and APPI ion sources for this purpose have been compared, giving APPI higher sensitivities and better signal-to-noise ratios for all the ions that ESI. However, using both the ESI-MS and the APPI-MS data, all oil samples belonging to eight different botanical origins were perfectly classified with excellent resolution among the categories. Excellent correlation between the sterol profiles obtained by the proposed method and those obtained by GC-FID was found. Thus, the proposed method is a good alternative to the official method (GC-FID), with the added advantage that prior chromatographic separation is not required.

Next, the profiles of aliphatic and triterpene alcohols, obtained by HPLC-MS, were also used for the same purpose. An LDA model capable of correctly classifying oils with a prediction probability higher than 95 % was obtained.

Finally, protein information present in the oils was also employed to classify oils according to their botanical origin. Proteins were isolated by precipitation and hydrolyzed. The resulting amino acids were determined by direct infusion MS and HPLC-UV-Vis after derivatization with OPA-NAC. In the case of MS, and by the successive application of three LDA models, it was possible to correctly classify oils from eight different botanical origins. Moreover, using the profiles obtained by HPLC-UV-Vis, a good resolution between seven botanical origins was obtained using only an LDA model.

10.4 Development of Methods for Olive Oil Quality Evaluation

A rapid and simple method based on direct infusion of oils into a mass spectrometer, capable of predicting olive oil quality grade, has been developed. After a simple sample dilution (1:50), oils were infused into the mass spectrometer, and

the peak abundances of the fatty acids were measured. Using LDA, the oils were unequivocally classified according to European Union marketing standards. Using MLR, binary mixtures of different quality grade oils can be evaluated with average prediction errors within the 3–5 % range; however, errors of the order of 11 % should be expected for EVOO/ROPO mixtures.

On the other hand, the ability of the electronic nose to evaluate the presence of the most common defects of VOO when tested in different concentrations has been demonstrated. The sensory analysis performed by a panel of trained assessors could be made more robust by the jointly use of an electronic nose, which was able to test singular defects one-by-one and to classify the defected oils according to their sensory threshold. On the other hand, excellent predictions of the defect percentage were obtained using MLR models. Then, the electronic nose, if correctly trained, could be considered an useful tool to work in parallel to panellists, for example to realize a rapid screening of large set of samples with the aim to discriminate defective oils. Under this point of view it could be helpful to test the panel performance.

10.5 Development of Methods for the Classification of EVOOs According to Their Genetic Variety

Different fast and simple methods, capable of classifying EVOOs according to their genetic variety, have been developed using LDA as chemometric tool.

First, the data obtained by FTIR spectroscopy has been used. Once the IR spectrum was divided into 26 regions, an LDA model capable of classifying EVOO from seven genetic varieties, mainly grown in the *Comunitat Valenciana*, Spain, was constructed by using only nine predictors. With this model, an excellent resolution was achieved between all category pairs.

Second, direct infusion MS data was used for the same purpose. EVOO samples were 1:50 diluted without any previous extraction and injected into a mass spectrometer, measuring both fatty acid and phenolic compound profiles. Using LDA models constructed with both profiles, EVOOs are perfectly classified according to their genetic variety.

Finally, the possibility of classifying EVOOs using their sterol profiles established by HPLC-MS and UPLC-MS has been also studied. In both cases, two sequential LDA models were necessary to correctly classify all samples, with prediction capabilities higher than 88 % in all cases.

All this methods are of interest from the industrial point of view because they provide rapid identification of genetic variety in EVOOs.

10.6 Development of Methods for the Classification of EVOOs According to Their Geographical Origin

A CEC method using laboratory-made LA monolithic columns, which allows the prediction of EVOO geographical origin by using phenolic compound profiles, has been developed. The best resolution between the analytes was achieved using a column with 15 % of 1,4-butanediol in the polymerization mixture, and a mobile phase containing ACN/water 15:85 (v/v) with 5 mM formic acid at pH 3. Using CEC data and LDA, an excellent resolution was achieved between the three categories considered (EVOOs from Spain, Italy and Croatia).

10.7 Development of Methods for the Evaluation of Olive Oil Oxidation

First, the chemical changes produced in VOO samples containing different contents of phenolic compounds during an accelerated aging process have been studied. In this work, the importance of the role of phenolic compounds in oil stability against oxidation has been demonstrated. The differences observed between both types of samples enforced this agreement due to the different OSI values obtained that demonstrated a high contribution of polar phenolic compounds to oil shelf life. During the storage treatment, a decrease of the major secoiridoids and the formation of some of their oxidized forms were observed for the phenol rich EVOO sample. For this reason, these latter compounds could be considered as potential markers of the loss of extra VOO freshness.

Next, the same samples subjected to an accelerated aging process were analyzed by direct infusion MS and by a MOS sensor array in order to construct LDA models capable of predicting sample oxidative status. In MS, the abundances of fatty acids and phenolic compounds, OFAs and the abundances of their oxidation products were used as predictors. These abundances, which were measured after a simple dilution of samples with an alkaline mixture of solvents, made possible a rapid analysis of samples, thus avoiding the conventional extraction methods for this type of compounds. An excellent LDA model capable of correctly classifying all category pairs was obtained. On the other hand, when the analysis was carried out with the electronic nose, sensor signals were used as predictors. The LDA model constructed also resulted in an excellent resolution between all category pairs. Furthermore, this model was evaluated by analysis of various aged samples whose status was previously determined by sensory analysis. A good correlation was obtained between the model and sensory analysis. In particular, the model distinguished all VOOs without defects from the others, and responded linearly for the samples characterized by a rancid defect.

Finally, by constructing MLR models, methods capable of predicting the concentration of OFAs in different VOO samples naturally oxidized have been

developed. These samples were analyzed by electronic nose and FTIR spectroscopy. Using both techniques, it was necessary to apply the cube root transformation to OFA experimental data to obtain homoscedasticity in the residuals. Using data from the electronic nose, the MLR model was constructed with five predictors with an average error of 9 %, while using the data obtained by FTIR spectroscopy, MLR model was constructed with eight predictors, being its average error of 17 %.

The two proposed methods, based on electronic nose and FTIR spectroscopy, are a good alternative to HPLC methods since they avoid OFA extraction and provided shorter analysis times.